Complex roles ankyrin-1 plays in malaria infections

Hong Ming Huang, BBiotech (Hons)

A thesis submitted for the degree of Doctor of Philosophy

Australian National University

The John Curtin School of Medical Research

The College of Biology, Medicine and Environment

December 2016

Declaration

I declare that the experimental work presented in this thesis is the original work by myself, unless otherwise stated in the text. Dr Gaetan Burgio and Dr Denis Bauer carried out ENU mutagenesis and the associated bioinformatics analysis of the whole exome sequencing results. Dr Gaetan Burgio, Ms Ning Huang and Ms Emmaline Brown performed CRISPR/Cas9 genome editing on mouse models. Ms Emmaline Brown performed splenectomy on mice presented in Figure 4.10. Dr Ante Jerkovic examined the binding kinetics of ankyrin-1 and β-spectrin through the use of Biacore 2000 (Supplementary Figure 5.1). The proteomic analysis of erythrocyte membrane, as presented in Figure 4.5, was performed by Dr Matthew McKay from the Australian Proteome Analysis Facility (APAF).

This thesis has not been submitted before for any examination in this or any other universities, and conforms to the Australian National University guidelines and regulations.

Hong Ming Huang

(Author, PhD candidate)

Gaetan Burgio

(Supervisor)

Genome Editing and Genetics of Host-Pathogen Interactions Group

Department of Immunology and Infectious Diseases

The John Curtin School of Medical Research

The Australian National University

Simon Foote

(Co-supervisor)

Word count: 30691

Acknowledgements

First, I would like to praise God for His blessings and for providing me this opportunity to work with all the wonderful people during my PhD study. I would also like to thank God for granting me the capability and perseverance to complete these four years of study.

I am also forever indebted to my supervisors, Dr Gaetan Burgio, A/Prof Brendan McMorran and Prof Simon Foote, for their advices and guidance throughout the PhD project. Thank you for being there every step of the way from Hobart to Canberra; without your tireless support, this thesis would not have come to fruition. I would particularly like to thank Gaetan, for his patience and encouragement throughout these years, which have helped to build up my confidence, with both my research and personally.

I would also like to express my gratitude to the awesome past and present lab members – Andy Greth, Clare Smith, Patrick Lelliott, Elinor Hortle, Bernardette Schnider, Tony Jerkovic, Nazneen Adenwalla, Bernadette Pederson, Ning Huang, Emmaline Brown, Shelley Lampkin, Lora Jensen, Anna Ehmann, Hao Yang and Nay Chi Khin, for their tremendous support during these four years of PhD. I would especially like to thank Tony Jerkovic and Patrick Lelliott, for their assistance and advice in protein and mouse work respectively; Lora Jensen and Nazneen Adenwalla, for putting up with my English, and for their meticulous attention to detail in proofreading my thesis; and Ceri Flowers, for assisting all of us in settling in as we moved interstate and all the paperwork-related tasks during my research.

I am also grateful to Prof Leann Tilley, Dr Matt Dixon and Oliver Looker, for the collaboration opportunity, as well as providing technical assistance on the RBC deformability experiments as well as Matthew McKay for the proteomic analysis and expertise in LC/MS. I would also like to thank Dr David Rabbolini from the Royal North Shore Hospital for assisting with the collection of human blood samples, and Dr Peter Milburn for assisting with protein purification in Biomolecular Resource Facility (BRF).

I also acknowledge the funding sources from National Health and Medical Research Council, Australian Research Council, the National Collaborative Research Infrastructure Strategy, the Education Investment Fund, the Howard Hughes Medical Institute, as well as the scholarship and travel grants provided by Macquarie University and The Australian National University. Without them, this work would not be possible.

Last but not least, I would like thank my family and friends, for being understanding and caring through periods of stress and my brothers and sisters in Christ, for their continual prayers and life advice throughout these years.

Abstract

Despite the numerous interventions employed in the past few decades, malaria remains one of the most lethal diseases affecting millions of people worldwide. This is partly due to the emergence of resistance to the current parasite-targeted antimalarials. In contrast, erythrocytic genetic mutations have been conferring malaria protection in humans for thousands of years without losing their effectiveness. This presents a new therapeutic approach to mimic these genetic mutations to treat malaria, known as host-directed therapy (HDT), which requires further understanding of host-parasite interactions to identify potential HDT drug targets.

One such HDT target is the erythrocytic cytoskeleton, which parasites rely on for their survival. Ankyrin-1 (*Ank-1*) is one of erythrocytic cytoskeleton proteins, which has been associated with hereditary spherocytosis (HS) in humans. This thesis investigates the roles of *Ank-1* in malaria infections using mouse models and blood from HS patients. Mice with *Ank-1* mutations were found to exhibit phenotypes similar to human HS patients and are protected against malaria via multiple mechanisms, suggesting that *Ank-1* plays a complex role in malaria infections. These mechanisms are heavily influenced by the nature of *Ank-1* mutations, which is further confirmed in human HS erythrocytes. This thesis also explores the possibility of using the ankyrin-spectrin interaction as a HDT target. Results show that the disruption of this interaction has little effect on the health of the mice, while conferring significant resistance towards malaria, thus enabling the use of high throughput screening (HTS) for drug discovery.

To summarise, this thesis highlights the complex interactions between the erythrocyte cytoskeleton and malarial parasites, as well as providing insights into the heterogeneous protective role of *Ank-1* in mediating malaria resistance. It also raises the possibility of using erythrocytic cytoskeletal proteins as HDT drug targets, which could potentially yield novel therapies for malaria in the future.

Contents

List of Figures

List of Supplementary Figures

List of Tables

CHAPTER 1

LITERATURE REVIEW

1.1 Introduction to Malaria

Malaria remains one of the most lethal diseases in the world, with more than 200 million cases and approximately 400,000 deaths each year [1], with the majority of the victims being young children and pregnant women. Although the number of cases has decreased considerably with improvements in socio-economic status, the introduction of bednets and insecticides, as well as artemisinin combination therapies [2-4], malaria still poses a major threat to people in developing countries and areas with limited access to healthcare [5]. This is due to several factors which significantly impede the eradication of malaria from these countries, such as the development of drug resistant malarial parasites, insecticide-resistant mosquito vectors and the low socioeconomic status of these countries.

Malaria is caused by a parasitic protozoa, *Plasmodium*, of which there are currently five major species of Plasmodium that infect people – *Plasmodium falciparum, P. vivax, P. ovale, P. malariae and P. knowlesi. P. falciparum* is endemic to many countries and is responsible for the majority of the deaths associated with malaria; whereas *P. vivax* is also widespread but has lower mortality. Transmission of *Plasmodium* is dependent on *Anopheles* mosquitoes, and is therefore limited to areas where *Anopheles* thrive [6]. This includes tropical and sub-tropical regions in Africa, South-east Asia, South America and the Middle East [7]. Malaria incidence usually increases during wet seasons, where humidity and temperature are ideal for the mosquitoes.

1.1.1 Parasite lifecycle and pathogenesis

As illustrated in Figure 1.1, the *Plasmodium* lifecycle involves two hosts – the *Anopheles* mosquitoes and humans. The sexual stage occurs in the mosquitoes, where sporozoites accumulated in the salivary glands ready to be injected into the human host during blood meals. Following injection, the sporozoites travel to the liver where they infect the hepatocytes [8] and

the host remains asymptomatic. After 6-8 days, the parasites differentiate into thousands of merozoites [9]. These merozoites then invade red blood cells (RBCs) and begin another round of asexual replication. The intra-erythrocytic parasites are classified into three different growth stages, starting with the ring stage, then trophozoite stage and finally the schizont stage, which is followed by egress of new merozoites to invade more RBCs. After 10-12 days [10], some parasites will instead differentiate into sexual gametocytes and be ingested by the mosquitoes, completing the lifecycle. Blood stage parasites are responsible for the clinical symptoms associated with malaria, including but not limited to fever, severe anaemia, cerebral malaria, coma and even death [11]. The presentation of these symptoms greatly dependent on the gender, age and genetics of the host, as well as the parasite species [12]. It is important that these characteristics are considered as we develop effective tactics to combat malaria.

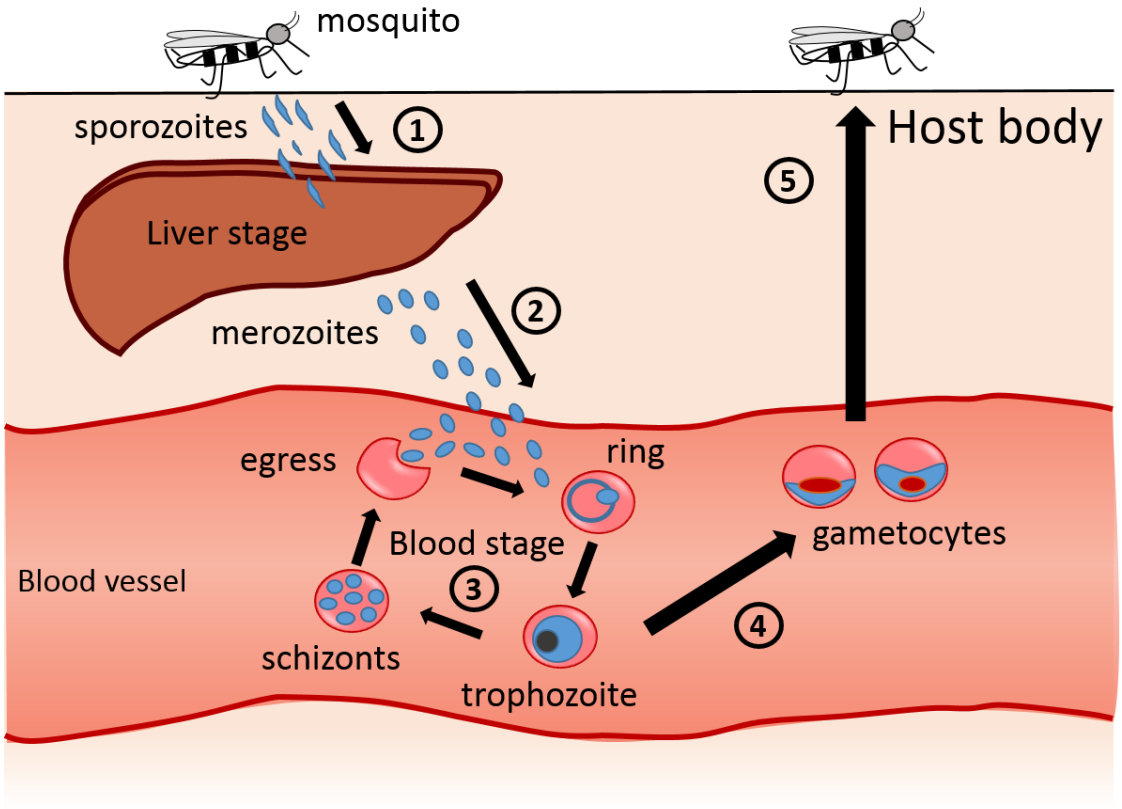

Figure 1.1: The asexual lifecycle of *Plasmodium falciparum*. 1) The sporozoites are first injected by Anopheles mosquito during a blood meal, which then travel to the liver and infect hepatocytes. 2) After few cycles of asexual replication, the merozoites emerge from liver and start invading erythrocytes. 3) During the blood stage, the parasites mature from ring, to trophozoite and finally replicate into schizonts before egress. The newly released merozoites invade more erythrocytes and the cycle continues again. 4) After 10-12days, merozoites are able to differentiate into male or female gametocytes. 5) These gametocytes are then taken up into mosquito during blood meal and the sexual cycle occurs in the mosquito.

1.1.2 Malaria preventative strategies

1.1.2.1 Vector control

As the *Plasmodium* requires insect hosts for their survival, many malaria preventative strategies often target the mosquito vectors to control the spread of malaria. One such intervention is the long lasting insecticide-treated bednets (ITN), which have been a major contributor to the decline of malaria cases since their introduction in the 2000s [13]. The financial support from the World Health Organisation (WHO) in the implementation of ITNs has accounted for an approximately 50% reduction in parasite prevalence over 15 years in sub-Saharan Africa [14]. Indoor residual spraying (IRS) of insecticides also contributes towards reduction of malarial incidence, although not as much as ITNs [14]. Despite this success, there have been some concerns about the emergence of insecticide-resistant mosquitoes as the current interventions rely heavily on one class of insecticides – the pyrethroids [15]. Also, the effectiveness of these approaches appeared to vary with mosquito species, as it was observed that ITNs were not as effective when employed in Southeast Asia, likely due to these mosquitoes having blood meals during early evening, when ITNs were not in use [16,17].

1.1.2.2 Malaria vaccine

Apart from vector control, there has been a lot of effort invested in the development of a potential vaccine for malaria in the past few decades, especially against the most lethal *Plasmodium* parasite species, *P. falciparum*, which is the main focus of this section. Although several vaccine candidates were developed, such as SPf66 and SE36 [18-21], only one is commercially available. This is partly due to the fact that *Plasmodium* often have a high genetic mutation rate, making them genetically diverse, and hence, difficult to target. Coupled with the lack of cross-species protection, vaccine development for *Plasmodium* has been very challenging.

RTS, S is currently the most advanced malaria vaccine candidate available. It targets the parasite circumsporozoite surface protein (CSP), one of the important proteins involved in the invasion of sporozoites into the hepatocytes [22]. In the phase 3 of the clinical trial, however, it was reported that it only reduced about 30% of malaria cases [23]. The vaccine also did not provide long lasting protection, with only modest protection after 18 months, and required booster injections [24]. Others have suggested using radiation-attenuated sporozoites to achieve malarial immunity [25], which was shown to have excellent protection, although the feasibility of this approach is questionable as it is greatly dependent on the dosage of radiation and on vaccine delivery methods [26-28]. From these examples, it is apparent that the development of a malaria vaccines requires substantial amount of time and resources, which is unlikely to alleviate the malaria burden in the near future. As a result, it is reasonable to consider alternative approaches to combat malaria more effectively.

1.1.3 Current treatments and antimalarial resistance

In addition to various preventative measures, malaria treatment also plays a crucial role in the control of this disease. Indeed, treatments for malaria can be found as early as 200BC in China, indicative of the long treatment history between humans and *Plasmodium* [29]. Since then, a lot of treatments for malaria have been developed, particularly in the last century, with the majority of them falling into one of four classes: quinoline derivatives, anti-folates, artemisinin derivatives and antimicrobials, each with different mechanisms of action, although most target the erythrocytic parasite stage. However, all antimalarials face the issue of drug resistant parasites (reviewed in [30]). This is attributed to the limited number of drug classes which all the current antimalarials are derived from and the widespread use of antimalarial treatment without proper controls [31]. Therefore, the WHO recommends malaria treatments in regions with reported drug resistance to combine at least two drug classes, one of which must be an

artemisinin derivative, and the other one usually consist of a slow-acting antimalarial drug of another class [32]. Although drug resistance is a worldwide socio-economic burden, drug resistance in *Plasmodium* allows us to understand the complex genetics and biology of *Plasmodium* parasites, which will be useful for future drug design and development, hopefully leading to the discovery of new classes of antimalarials. Examples from each of the current classes of antimalarial drugs and their mechanisms of action are discussed below.

1.1.3.1 Quinoline derivatives

Quinoline derivatives in malaria treatment include chloroquine, mefloquine, quinine, primaquine and lumefantrine. Starting from the 1940s, chloroquine was used extensively to treat malaria as a monotherapy [33]. Resistance was reported by the end of 1950s in both Colombia and the Cambodia-Thailand border [34]. It then spread to Africa in the 1970s, and now it is no longer effective as a monotherapy for treating erythrocytic stage malaria [34,35]. During the development of the intra-erythrocytic parasite, haemoglobin is the major food source for the parasites, the digestion of which produces toxic free haem as a by-product. Under native conditions, parasites are able to detoxify the free haem into inert haemozoin crystals [36]. Chloroquine acts by inhibiting the haem detoxification process following haemoglobin digestion [37,38]. It is thought that chloroquine binds to the haematin μ-dimer and adsorbs to the haemozoin crystal, resulting in interruption to the detoxification process [39,40]. Chloroquine-resistant parasites, however, were found to have less accumulation of chloroquine in their food vacuole [41]. Further investigation revealed two important transporter proteins that are responsible for the resistance, *P. falciparum* chloroquine resistance transporter (*Pf*CRT) and *P. falciparum* multidrug resistance transporter 1 (*Pf*MDR1) [42,43]. *Pf*CRT was thought to be responsible for the efflux of chloroquine out of the digestive vacuoles (DV), with more than 15 candidate mutations described [35,44,45]. The predominant *Pf*CRT mutation is lysine to threonine at amino acid residue

76 (K76T), suggesting that it might be responsible for chloroquine resistance [45]. PfMDR1, a member of ATP-binding cassette protein, was proposed to be involved in the import of chloroquine and other antimalarials [46-48]. This is supported by a knockdown study where down-regulation of PfMDR1 showed decreased sensitivity to chloroquine [43]. Further studies have revealed five PfMDR1 mutations (N86Y, Y184F, S1034C, N1042D, and D1246Y) to be associated with increased resistance to chloroquine, possibly by reducing its influx to the DV [49].

1.1.3.2 Folate metabolism inhibitors

Anti-folate drugs such as sulfonamides, pyrimethamine, proguanil, and dapsone, have become a predominant treatment in countries with widespread chloroquine resistance [50]. They are often used in combinations or with drugs from other classes, including sulfadoxine-pyrimethamine (SP) or atovaquone-proguanil. The main function of the folate pathway is to produce folate co-factors which are used for DNA and amino acid synthesis [51]. In particular, pyrimethamine competitively inhibits dihydrofolate reductase (*Pf*DHFR), whereas sulfadoxine targets dihydropteroate synthase (*Pf*DHPS). Resistance to SP emerged at the end of the 1980s [52], first in Southeast Asia before rapidly spreading to Africa [53], rendering the drug ineffective to treat malaria [54,55]. Four *Pf*DHFR point mutations have been described to be associated with pyrimethamine resistance – N51I, C59R, S108N and I164L [56,57], all of which decrease the binding affinity with pyrimethamine [58]. Similarly, amino acid change such as 437G, 581G and 613S in *Pf*DHPS gene are associated with resistance to sulfadoxine [56].

1.1.3.3 Antibiotics

Antibiotics such as doxycycline and clindamycin are a class of drugs which inhibit protein synthesis of microorganisms. They are occasionally used in combination therapy to treat malaria.

Both are slow-acting drugs, which have longer-lasting protective effects. As a result, they are usually used in complement with other fast-acting antimalarials such as chloroquine or quinine, especially in areas with suspected chloroquine resistance [59]. Doxycycline (as reviewed in [60]), in particular, was initially thought to inhibit mitochondrial protein synthesis of *Plasmodium* [61,62], but more recent studies seemed to suggest that the apicoplasts are the drug target [63,64]. Doxycycline is active against both erythrocytic and pre-erythrocytic stage of *Plasmodium falciparum* [65,66]. As such, it is proposed that doxycycline be used as an adjuvant in prophylactics for malaria, as well as a slow-acting schizontocidal drug [67]. Resistance to doxycycline is not well established, although a study inferred *P. falciparum tetQ* GTPase (*PfTetQ*), to be associated with doxycycline resistance based on previous work on other organisms [68,69].

1.1.3.4 Artemisinin derivatives

Artemisinin and its derivatives have become the first line of treatment for malaria infections since the emergence of multidrug resistant *Plasmodium falciparum* in Southeast Asia. It was first purified in the 1970s and started to be widely used in the 1980s [70]. It is a fast acting drug with short half-life, and as such, it is often paired with slower acting drugs, which are known as artemisinin combination therapies (ACTs) [32]. Although it was observed that artemisinin affects all stages of the parasites [71-73], the exact mechanisms of action still remains unknown. It was initially thought to cause oxidative stress by producing reactive oxygen species (ROS) when activated by either haem iron or non-haem iron during haemoglobin breakdown [74,75]. However, the fact that ring-stage *Plasmodium falciparum* parasite and *Toxoplasma gondii*, which produce little to none haemozoin, are also susceptible to artemisinin seem to contradict the theory [72,76]. It has also been suggested that artemisinin might also prevent the formation of haemozoin [77,78], though this was not observed *in vivo* [79]. More recently, it was proposed that artemisinin targets parasite ATPase *Pf*ATP6, based on its structural similarities with thapsigargin, an ATPase

inhibitor [80,81], again, contradicting findings have also been reported [82]. While the mechanism of action for artemisinin is still largely unknown, the rapid ability of *Plasmodium* species to develop resistance and overcome these drug pressures is well established, with clinical resistance to artemisinin being observed in Southeast Asia [83,84] since the early 2000s. Kelch13 gene was believed to be responsible for this resistance [85,86]. *Pf*Kelch13 is involved in ubiquitination and oxidative stress adaptation in *Plasmodium*. Artemisinin-resistant parasites with *Pf*Kelch13 mutations are thought have reduced proteolysis of phosphatidylinositol-3-kinase (*Pf*PI3K), leading to the accumulation of *Pf*PI3K [87]. It is thought that increased PI3P-dependent signalling, as the result of elevated *Pf*PI3K, mediates artemisinin resistance [87]. Another proposed mechanism involves the up-regulation of unfolded protein response pathways, which is thought to alleviate the protein damage caused by artemisinin [88], although further studies are required to support this hypothesis.

1.1.4 Summary

With the rapid emergence of parasite resistance to the current drugs and limited progress in vaccine development, new antimalarials are urgently needed. However, careful considerations must be taken in order to minimise drug resistance - which requires better understanding of parasite biology as well as host environments. In fact, natural resistance to malaria in endemic regions have existed for thousands of years [89], suggesting the importance of the host genetic background in determining malaria susceptibility. Therefore, studying host genetic and host-parasite interactions would prove to be beneficial for developing theoretically resistance-proof therapies in the future.

1.2 Host Genetic Resistance to Malaria

Host genetics plays a significant role in determining malaria susceptibility. For instance, many RBC-related mutations were found to be associated with malaria resistance [90-93]. This is evidenced by the higher-than-usual allele frequency of these RBC mutations in malaria endemic areas (reviewed in [94]). This phenomenon was first described and proposed by Haldane, suggesting that mutations which might otherwise be deleterious actually provide selective advantages against malaria [95]. Since then, many mutations have been characterised, ranging from mutations in RBC membrane proteins, haemoglobin, enzymes and the immune system. Some of these mutations are examined below.

1.2.1 Haemoglobin polymorphisms

Haemoglobin is the most abundant protein in erythrocytes. It usually exists as a heterodimer comprise of two α-globin and two β-globin subunits, and allows the transportation of oxygen and carbon dioxide through the blood. Haemoglobin polymorphisms have long been associated with malaria resistance, including haemoglobin (Hb) S, E and C, which have abnormal β-globins, and α- and β-thalassaemia, which affect the amount of α- and β-globin produced.

The haemoglobin polymorphism, HbS, is associated with sickle cell disease in homozygous individuals [96] and is also one of the well-known polymorphisms to influence malaria susceptibility [97,98]. It is prominent in Middle East populations, as well as sub-Saharan African populations, where the frequency of HbS allele was predicted to be up to 18% in certain regions [97]. Its prevalence is largely influenced by the protection it confers against malaria and the morbidity associated with sickle cell disease. It is caused by a glutamic acid to valine substitution at position 6 of the β-globin chain, resulting in unstable haemoglobin, which polymerises under a low oxygen environment. HbS heterozygosity was shown to have a 10-fold reduced malaria

risk [99], and increased protection towards cerebral malaria and severe malaria [100]. HbS homozygosity, however, is usually associated with higher mortality and morbidity. On the other hand, the HbC allele is far less common than the HbS allele, and it is usually found in parts of West Africa. It is caused by a glutamic acid to lysine substitution at position 6 in β-globin gene. Unlike HbS, HbC homozygosity only causes mild haemolytic anaemia, and provides significant protection against malaria, with up to 90% for homozygotes, and 30% for heterozygotes [101-105]. HbE allele is widely distributed in Southeast Asia and neighbouring regions, with up to 60% allele frequency in certain areas [106,107]. It is caused by a glutamic acid to lysine substitution at position 26 of β-globin chain. It is thought to effect the expression of β-globin gene by creating an alternative splice site, which decreases the production of functional β-globin, thus resulting in β-thalassaemia-like symptoms. However, only homozygotes present a mild haemolytic anaemia, whereas heterozygotes are asymptomatic. It is shown to confer resistance against malaria in several studies [108,109], although increased susceptibility was also implicated as patients with HbE beta thalassemia appeared to have more severe clinical symptoms from malaria infection [110].

Thalassaemias are defined as the loss or reduction in haemoglobin production, typically via deletion or inactivation of the gene. Both α- and β-thalassaemia are found throughout Southeast Asia, Africa and the Middle East [111]. The symptoms of the disorder can range from asymptomatic to severe anaemia, depending on the number of affected alleles. Also, it is not uncommon for α-thalassaemia to be co-inherited with β-thalassaemia, which further complicates the clinical diagnosis. Nevertheless, both thalassaemias are associated with malaria resistance [112-114].

1.2.2 Enzyme-related polymorphisms

Defects in certain enzymes involved in RBC maintenance, or *Plasmodium* development, have been shown to provide increased resistance towards malaria. One notable polymorphism is the X-linked glucose-6-phosphate dehydrogenase (G6PD) deficiency (reviewed in [115,116]). It is

involved in maintaining the oxidative stress environment of RBCs. Increased prevalence of G6PD deficiency is found in all malaria endemic regions, including Africa, Southeast Asia and South America [117-120]. However, it is unclear if the protection only affects hemizygous and homozygous individuals [121-123].

Pyruvate kinase (PK) deficiency is another well-known enzymopathies affecting susceptibility to malaria. It is found worldwide, but with slight increased prevalence in African populations [124,125]. It is a crucial enzyme involved in ATP production. This observation is further supported by *in vitro* and *in vivo* studies, which show significant malaria resistance in both tissue cultured and mouse models [126-128].

1.2.3 Immune-related polymorphisms

In addition to erythrocytes, malaria applies a large selective pressure on the human immune system. One particular aspect is the major histocompatibility complex (MHC) proteins which are encoded by the human leukocyte antigen (HLA) gene complex. High MHC polymorphic rate in African population compared to other populations suggests the possible selection by various environmental pathogens including malaria [129-131]. Many studies have indicated that certain variants of HLA can either confer resistance or susceptibility towards severe malaria or cerebral malaria [132-135]. However, the exact roles of these HLA polymorphisms are still elusive. In addition, cytokines including TNF-alpha [136-138], IFN-gamma[139,140] and interleukins (specifically IL-1[141,142], IL-4[143] and IL-10 [144]) have been implicated to play various roles during malaria infection.

Several studies have indicated that another polymorphisms, complement receptor 1 (CR1), is associated with malaria resistance in endemic areas (reviewed in [145,146]). CR1 is a membrane-bound glycoprotein involved in the activation of the complement of the immune system. These polymorphisms often cause reduction in CR1 levels and it is thought to confer malaria protection [147,148]. Further studies have revealed that erythrocyte CR1 is involved in merozoite invasion and

cytoadherence [148,149], therefore it is likely individuals with CR1 polymorphisms are protected from cerebral malaria which improves their survival.

One further immune-related polymorphism which has been sown to influence susceptibility to malaria is a range of polymorphisms in nitric oxide genes. Nitic oxide is a free radical that mediate host resistance during various infections, and is produced by three different nitric oxide synthases (NOS) [150]. One of the NOS, NOS-2 gene, along with increased NO, have been associated with increased resistance against malaria [151-153]. Specifically, individuals with certain polymorphisms in the promoter region of NOS2 were reported to have less severe malaria [154-156].

1.2.4 Erythrocyte membrane-associated protein polymorphisms

During malaria infections, *Plasmodium* requires specific interactions with erythrocyte surface receptors and cytoskeletal proteins for invasion, protein export and egress. As a result, mutations affecting these proteins are often associated with increased resistance to malaria. Several polymorphisms are described as below.

One of the most notable RBC surface proteins involved in malaria infections is the Duffy antigen receptor for chemokine (DARC), which is a chemokine receptor involved in inflammatory regulation, and is required for effective *P. vivax* invasion into RBCs [157]. Duffy negativity, the absence of Duffy antigen receptor on RBC surface, is common in African populations and in parts of Papua New Guinea [158-160]. Studies have repeatedly suggested that co-evolution between Duffy negative African populations and *Plasmodium* species has resulted in a lack of *P. vivax* distribution across Africa [91,158,161], as well as resistance to *P. knowlesi* in other populations [162-164]. However, this hypothesis was recently challenged due to reports of *P. vivax* infections in Duffy-negative individuals in Madagascar [165-168]. It is thought that *P. vivax* are subjected to large

selective pressure to be able utilise cryptic pathways to invade RBCs in this Madagascan population [166,169,170].

Another polymorphism that has also been associated with malaria susceptibility is ABO blood antigens. These blood groups were thought to emerge during co-evolution with *Plasmodium* millions of years ago, suggesting selective advantage offered by group O allele [171,172]. Although several studies have indicated that individuals with non-O blood group have higher risk of severe malaria, they appear to not have accounted for other confounding factors [173-175].

Glycophorins (GYP) are another major glycoprotein family found on the RBC membrane which facilitates RBCs circulating with less resistance by providing a hydrophilic surface. Polymorphisms such as Glycophorin B-null and Gerbich (Glycophorin C) negativity were found at high frequency in certain malaria endemic regions [176,177], although contradicting findings regarding their roles in malaria have been reported [178-180]. Recent studies have also revealed basigin to be involved in facilitating erythrocyte invasion. Erythrocytes lacking basigin were found to be significantly resistant to merozoite invasion *in vitro* [181]. Although several polymorphisms have been described for basigin, no association has been implied between basigin polymorphisms and malaria protection at the population level [181].

Southeast Asian ovalocytosis (SAO), as the name implies, is a hereditary condition found exclusively in Southeast Asia [182], and certain parts of Papua New Guinea, with up to 35% prevalence [183]. It is commonly caused by mutations in the transmembrane protein band 3 on the RBC surface. This results in more rigid and elliptical shaped RBCs [184]. It has been reported to protect against cerebral form of *P. falciparum* and more importantly, *P. vivax*, which is more common in these regions [185-187].

Hereditary spherocytosis (HS) and elliptocytosis (HE) are disorders caused by disruptions to the RBC cytoskeletal structure vertically and horizontally, respectively. Both disorders have been hypothesised to confer resistance towards malaria, demonstrated though *in vitro* and *in vivo*

studies with mouse models [188-193]. HE has increased prevalence in African populations, with 0.6 to 3% incidence [188,194,195], while on the other hand, HS appeared to be more common in Northern European populations [196-198], with only rare cases have been reported in other populations [199,200]. HS is typically caused by mutations in ankyrin-1, spectrins, band 3 or protein 4.2, with the majority of cases arising from ankyrin-1 mutations [201]. HS patients often exhibit deficiency in ankyrin and spectrin and, less commonly, band 3 [202,203]. One particular study examined the RBCs from HS patients and found that they significantly impaired the growth of parasites [191]. This is consistent with various mouse models carrying ankyrin-1 mutations, including *(nb/nb)*, *Ank-1^{MRI23420}* and *Ank-1^{1674}* mice. All of these mutations exhibit HS-like phenotypes and were found to be significantly resistant to murine malarial parasites, *P. chabaudi* infection [189,190,204]. When compiled, it is evident that HS confers protection against malaria despite the lack of evidence from population studies.

1.2.5 Summary

From the studies reviewed above, there is no doubt that host genetics play a significant role in malaria infections. These genetic polymorphisms that arise as humans and *Plasmodium* co-evolve are likely to reveal crucial weaknesses in parasites that can be exploited for future therapeutics. However, many mechanisms behind these polymorphisms are not well-established. As a result, it would be of great interest to the malaria community to investigate how these polymorphisms contribute towards malaria resistance, as we combat the issue of antimalarial drug resistance.

1.3 Effects of Genetic Polymorphisms on Host-parasite Interactions

It is well-established that certain genetic polymorphisms confer protection against malaria, although their exact roles are not always clear. Understanding how these polymorphisms give rise to malaria resistance would not only provide useful insight on host-parasite interactions, but also reveal new drug targets. Since these drug targets are not under the influence of parasite genetics, they are consequently thought to be resilient to development of drug resistance. This is the basis of host-directed therapy, and its major strength.

During the blood stage of malaria infection, parasites undergo several distinct phases of development – from RBC invasion to egress. During each phase, merozoites interact with different host proteins in order to thrive. As a result, genetic polymorphisms of these proteins are thought to impair parasite development, as summarised in Table 1.1. This review will focus on the protective effects of these genetic polymorphisms in various aspects of blood-stage malaria.

Table 1.1: Resistance mechanisms of common RBC genetic polymorphisms

Genetic Polymorphisms	Possible mechanisms of resistance				Reference
	Erythrocyte invasion	Intra-erythrocytic growth	Cytoadherence ability	Susceptibility to phagocytosis	
Haemoglobin S	Reduced	Reduced	Reduced	Increased	205-209
Haemoglobin C	Normal	Reduced	Reduced	Unknown	209-212
Haemoglobin E	Reduced	Reduced	Unknown	Increased	109,213
α- and β-thalassaemia	Reduced	Reduced	Reduced	Increased	114,205,214-217
Glucose-6-Phosphate Dehydrogenase (G6PD) Deficiency	Normal	Reduced	Unknown	Increased	218-221
Pyruvate Kinase (PK) Deficiency	Reduced	Normal	Unknown	Increased	128,222
Complement Receptor 1 (CR1) polymorphisms	Reduced	Unknown	Reduced	Unknown	148,149,223,224
Duffy negativity	Reduced (*P. vivax*)	Normal	Unknown	Unknown	91,225,226
O blood group	Normal	Normal	Reduced	Unknown	172,227
Glycophorin A (GYPA) deficiency	Reduced	Unknown	Unknown	Unknown	228,229
Glycophorin B (GYPB) deficiency	Reduced	Unknown	Unknown	Unknown	179,230
Glycophorin C (GYPC) deficiency	Reduced	Unknown	Unknown	Unknown	178,231
Southeast Asian Ovalocytosis (SAO)	Reduced	Normal	Reduced	Unknown	186,232
Hereditary elliptocytosis (HE)	Reduced or Normal	Reduced	Unknown	Unknown	191-193
Hereditary spherocytosis (HS)	Reduced or Normal	Reduced or Normal	Unknown	Unknown	189-191,204

1.3.1 Merozoite invasion

Blood stage of malaria infection begins with the invasion of merozoites into RBCs, which has been extensively studied. Merozoites are propelled into the bloodstream following their egress from RBCs or in vesicles known as merosomes, to allow safe passage into the bloodstream [233,234]. The merozoites first reversibly attach at any location on the RBC membrane, followed by the reorientation of merozoites to align their apical end towards the RBCs [235]. This allows specific receptors to interact and bind to various RBC receptors. Additional proteins are then released from the apical organelle to modify RBC cytoskeleton in preparation for invasion [236]. Tight junctions are formed between the RBC and the merozoite and are powered by actin-myosin motor to move from the anterior to posterior end of merozoite while surrounding the it with RBC membrane, thus forming parasitophorous vacuole [237]. The RBC membrane is then resealed and returned to normal in 10 minutes [238]. This process is illustrated as below (Figure 1.2).

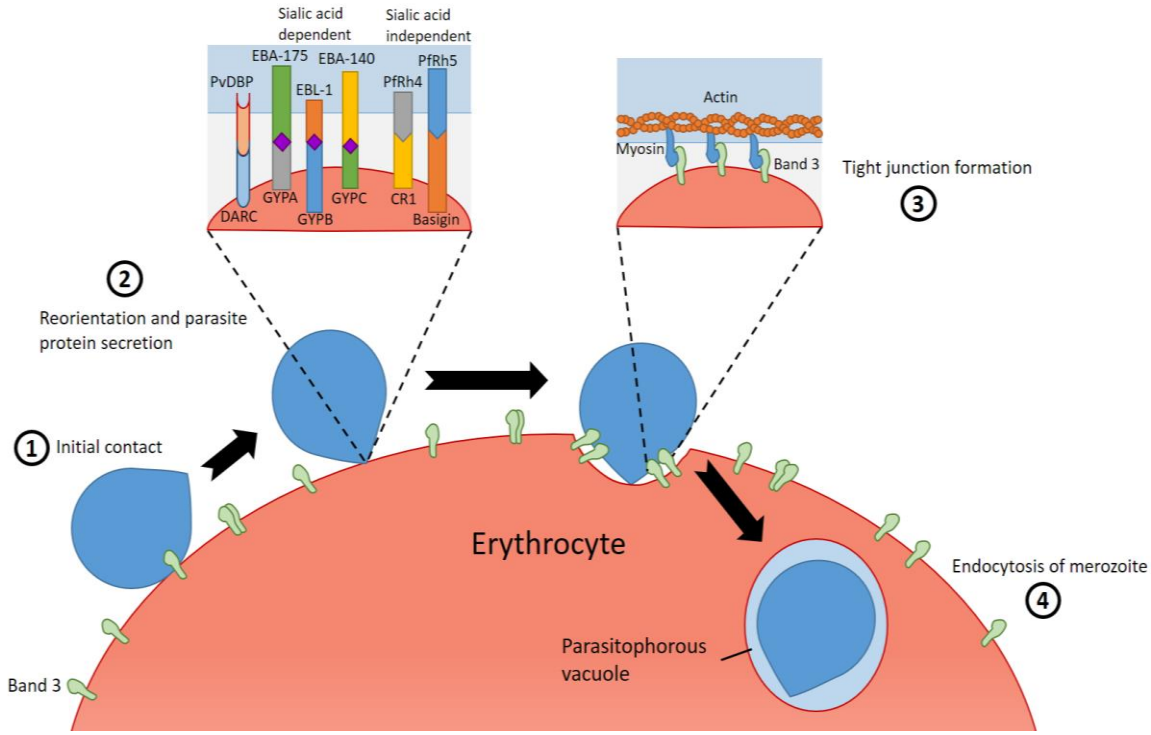

Figure 1.2: The erythrocyte invasion process by a merozoite. 1) Merozoite first binds reversibly onto erythrocyte surface. 2) Merozoite then reorients to align its apical end with erythrocyte surface, and binding with various host ligands occurs. Parasite proteins are secreted to remodel erythrocyte cytoskeleton. 3) Tight junctions are formed and merozoite is propelled into the erythrocyte through actin-myosin motor. 4) Resealing of erythrocyte membrane occurs to give rise to parasitophorous vacuole. The erythrocyte plasma membrane then returns to normal.

The RBC invasion process has been an area of interest due to the direct exposure of parasite antigens to the host immune system as well as its dependence on host RBC receptors and cytoskeleton. Over the past decades, several RBC receptors have been implicated to facilitate the invasion process, and mutations in these receptors are often associated with malaria resistance.

Perhaps one of the most prominent examples of such receptors is the Duffy antigen receptor for chemokine (DARC) on the erythrocyte surface. As previously mentioned, Duffy negativity has been thought to be responsible for eradication of *Plasmodium vivax* from the majority of Africa [158]. The inhibition of erythrocyte invasion was further supported by *in vitro* studies where antibodies raised against *Plasmodium vivax* Duffy binding protein (PvDBP) prevents the invasion of *P. vivax* into Duffy-positive erythrocytes [91,225]. It is well-established that PvDBP binds to DARC irreversibly during erythrocyte invasion [226]. Further studies revealed that the binding motif is localised to 170 amino acids in domain II of PvDBP [239,240], which made it one of the promising targets for vaccine development [241].

On the other hand, two families of *Plasmodium falciparum* proteins have been discovered to be involved in the apical interaction with erythrocytes: the Duffy or erythrocyte binding-like (DBL or EBL) proteins and the reticulocyte binding-like (RBL) proteins [242]. Both families were thought to have redundant roles during merozoite invasion, as seen in a knockout study showing no significant invasion impairment when several invasion proteins were disrupted [243-246]. EBL proteins are involved in the sialic acid-dependent invasion pathway, which recognise and bind specifically to erythrocyte receptors containing sialic acid residues. Furthermore, studies in murine malaria models such as *Plasmodium yoelii*, revealed that EBL proteins might determine the parasite's preference for erythrocyte type [247], emphasising the importance of understanding interactions with host proteins. Several EBL proteins and their binding partners have previously been identified: erythrocyte-binding antigen 175 (EBA-175) binds to Glycophorin A [248,249]; EBL-1 binds to Glycophorin B [179]; and EBA-140 (or BAEBL) binds to Glycophorin C [178]. Deficiency in

Glycophorin A was reported to have reduced *P. falciparum* erythrocyte invasion [228], whilst antibodies against EBL-1 and EBA-140 were found to inhibit interaction with Glycophorin B and C respectively [178,230,231], and they were thought to be the basis behind the increased resistance to malaria in population with Glycophorin B-null and Gerbich (Glycophorin C) negativity.

Examples of RBL protein family members include *P. falciparum* reticulocyte-binding homolog 4 (PfRh4) and PfRh5, which are involved in sialic acid-independent invasion pathways. PfRh4 was found to interact with CR1 during erythrocyte invasion, and treatment with antibodies and soluble CR1 inhibits the merozoite-RBC binding [149,223,250]. Recently, it was discovered that PfRh5 interacts with CD147 or basigin on the erythrocyte surface during invasion [181,251]. The correlations of basigin polymorphisms with malaria protection in human populations are still unclear, despite the fact that some of these polymorphisms were found to have reduced binding with PfRh5 *in vitro*. Nevertheless, with the characterisation of the blocking epitope, PfRh5 was considered to be a candidate for vaccine development, whereas basigin might be a druggable target for host-oriented therapy for malaria [252,253]. Other RBC receptors such as CD55 have recently been proposed to be essential for merozoite invasion, based on genetic screening [254], although its implications in human populations remain to be investigated [255].

Modification of the erythrocyte cytoskeleton is also essential in establishing a successful merozoite invasion. As a result, polymorphisms in various cytoskeletal proteins have been associated with increased resistance towards merozoite invasion. One of the major component of RBC cytoskeleton, the protein band 3, is necessary for merozoite invasion into RBC. Band 3 mutations have been shown to give rise to Southeast Asian Ovalocytosis (SAO), which is thought to impair the invasion of *P. falciparum* and *P. knowlesi* merozoites into RBCs [256-258]. While the mechanisms remain elusive, some researchers have suggested that reduced deformability of erythrocytes to be the primary mechanism behind this resistance [259,260]. However, band 3 could also be involved in the primary contact of the merozoites with RBCs, forming a complex with

merozoite surface proteins-1 (MSP-1) and Glycophorin A [261]. This might suggest a more complex mechanism apart from RBC deformability.

Invasion inhibition has also been reported for other cytoskeletal proteins. Hereditary elliptocytosis (HE), a genetic disorder caused by mutations in a single, or multiple, RBC cytoskeletal proteins including alpha-spectrin, beta-spectrin and protein 4.1, was thought to confer malaria resistance [192,193]. Although HE is more commonly reported in malaria endemic countries [188], the mechanisms behind its resistance are not well-defined. Some *in vitro* studies reported increased resistance to invasion [192,193], while others reported no differences [191]. It is possible that contradicting results might be due to the heterogeneity of the manifestation of HE, where different causative mutations would give rise to different phenotypes, which consequently affect malaria susceptibility, a phenomenon known as allelic heterogeneity.

Other genetic disorders such as pyruvate kinase deficiency (PKD) were also reported to affect erythrocyte invasion, with RBCs from PKD patients being more resistant to merozoite invasion [128,222], possibly due to ATP depletion [127]. Similarly, several haemoglobin variants including HbAE, beta-thalassemia/HbE and alpha-thalassemia have been shown to experience less erythrocyte invasion *in vitro* [109]. Despite the evidence, the exact mechanisms behind these polymorphisms have not yet been dissected.

1.3.2 Parasite intra-erythrocytic growth and egress

In order to grow and replicate following erythrocyte invasion, parasites remodel the erythrocytes to better suit their requirements. They export proteins for nutrient acquisition, immune evasion and for egress from the erythrocyte, as well as importing host proteins for food and to carry out certain enzymatic reactions. These processes heavily rely on the RBC environments in order to provide the necessary conditions for optimal parasite growth.

Therefore, disruptions to any of these pathways are likely to give rise to impaired parasite growth.

The primary food source of intra-erythrocytic parasites is thought to be the haemoglobin. Numerous studies have discovered an acidic vacuole in parasites responsible for haemoglobin degradation, and detoxification of the toxic haem into haemozoin crystals [262,263]. The parasites also employ new permeation pathway (NPP) to import other nutrients including amino acids, carbohydrates and various ions [264,265]. Parasite protein export is facilitated by the *Plasmodium* translocon of exported proteins (PTEX), which is essential for growth in blood stage [266,267]. PTEX is responsible for exportation of proteins containing PEXEL-motif as well as several PEXEL-negative exported proteins (PNEPs) into the RBC cytosol [268-270]. Further protein trafficking is mediated by a Golgi-like membranous structure known as the Maurer's cleft which interacts with cytoskeletal actin and plays a crucial role in remodelling the RBCs by transferring membrane-associated proteins to the RBC surface. One of which is *Plasmodium falciparum* erythrocyte membrane protein 1 (*Pf*EMP1), which involved in immune evasion by mediating cytoadherence to the endothelium [209,271,272]. In addition, parasites are also known to utilise host proteins for their survival. Host kinases – specifically MEK-1 and PAK-1, have been proposed to be used by the blood-stage parasites [273]. Other examples include haem synthesis enzymes such as delta-aminolevulinate dehydratase (ALAD) [274] and ferrochelatase [275], as well as enzymes involved in anti-oxidation – superoxide dismutase [276] and peroxiredoxin 2 [277].

During the egress of merozoites from the RBCs, the parasites have to modify RBC cytoskeletons in order to destabilise the erythrocyte membrane. This involves the loss of adaptor proteins such as adducin and tropomycin, as well as phosphorylation of Band 3 to weaken the cytoskeletal network [278,279]. Further degradation of the cytoskeletal structure is mediated through the parasite cysteine protease falcipain-2 and the aspartic protease plasmepsin II [280-282]. Chandramohanadas, et al. [283] have also proposed that host erythrocyte-derived calpain-1 is hijacked during egress, and the absence of this protein prevented egress.

Many genetic polymorphisms affecting RBCs have been associated with intra-erythrocytic parasite growth inhibition, such as those that give rise to abnormal haemoglobin. HbAS was reported to impair *P. falciparum* growth due to RBC sickling under low oxygen conditions [206,207]. LaMonte, et al. [284], on the other hand, proposed that growth inhibition is due to the translocation of sickle erythrocyte miRNAs to the parasites, impairing ribosome functions and thus protein translation machinery. Abnormal parasite growth was also observed in HbCC erythrocytes, where a high percentage of the parasites die as they mature [211,285]. Both HbS and HbC were also thought to impair host cell remodelling, possibly as a result of high oxidative stress from abnormal haemoglobin, which is thought to impair the polymerisation of actin filament, thereby weaken the interaction of Maurer's cleft and RBC cytoskeleton [209]. Presence of free-haem and oxidised haemoglobin can also damage and destabilise the actin filament, which is unfavourable for the maturing parasites[208,286]. In addition, alpha- and HbE/beta-thalassemia were also reported to retard parasite growth *in vitro* [214,217,287], though the exact mechanisms were not clear. Vernes and colleagues proposed that HbE impair parasite growth under high oxygen conditions suggesting oxidative stress-related mechanisms [213]. However, these hypotheses were challenged when normal parasite development was often observed in these cells *in vitro* and in field studies [110,207,288,289].

G6PD deficiency has also been associated with reduced parasite growth [218,290,291], despite numerous contradictory findings [219]. Although the exact mechanisms are still being investigated, two possible explanations have been proposed. First, as with the haemoglobinopathies, parasite deaths occur due to high oxidative damage in both the host cells and the parasites as the result of low glutathione levels [292,293]. Another possibility is that parasites are unable to acquire sufficient ribose derivatives for nucleic acid synthesis due to the low glutathione level [294].

Reduced intra-erythrocytic growth is also reported in erythrocytes with abnormal cytoskeletal structure. Both Schulman, et al. [191] and Chishti, et al. [192] have reported a reduction in parasite growth in erythrocytes deficient in the RBC cytoskeletal proteins ankyrin and spectrins. A more

recent study on mice with *Ank-1* mutation has also reported an increased number of apoptotic parasites in erythrocytes, in agreement with the previous findings [189].

Indeed, blood stage *Plasmodium* have been found to interact with erythrocytic ANK-1 during RBC remodelling. One of the exported proteins, knob-associated histidine-rich protein (KAHRP), has been found to interact strongly with ANK-1 [295,296], and is required for the formation of knob-like structure on infected RBC surface [297], as well as facilitating proper presentation of PfEMP1 [298]. Parasite acyl-CoA synthetases, PfACS1 and PfACS3, have also been reported to bind to ANK-1 [299]. These enzymes are involved in converting fatty acids scavenged from the extracellular matrix into CoA derivatives for further lipid biogenesis [300], and their interactions with ANK-1 are thought to facilitate their functions. ANK-1 was also proposed to be one of the target proteins for cleavage by falcipain-2 during parasite egress [282]. Further research has shown that inhibition of ANK-1 cleavage impaired the development of late-stage parasites [301]. It is possible that *ANK-1* mutations might cause parasite deaths through impairment to RBC remodelling, parasite growth, or egress, which could be explored through further studies.

1.3.3 Splenic filtration and parasite cytoadherence

Another challenge blood-stage *Plasmodium* parasites have to overcome is the constant threat of being removed from blood circulation, either by splenic filtration or the host immune system. The spleen is an important organ responsible for removing old and damaged RBCs, inducing the adaptive immune system and recycling iron [302]. In the context of malaria, the spleen is responsible for three functions: First, the spleen traps the less deformable parasitised erythrocytes thus removing them from circulation [303]; second, development of the immune response through phagocytosis [304]; and third, it acts as a secondary erythropoietic and haematopoietic organ during infections [305]. However, parasites have evolved behaviours and pathways to avoid detection. One such process to evade detection is cytoadherence, a process

where parasites adhere to the endothelium, against the blood flow, which is observed specifically in *P. falciparum*. This provides a safe haven for the late-stage parasites, which would have reduced RBC deformability [306], to escape splenic clearance and avoid recognition by complements and antibodies [307]. Cytoadherence of the parasites often lead to the formation of "rosettes", where clusters of infected and uninfected RBCs aggregate together mediated by parasite proteins of the parasitised erythrocyte surface, as shown in Figure 1.3. This causes obstruction to the blood flow and often manifests as cerebral malaria.

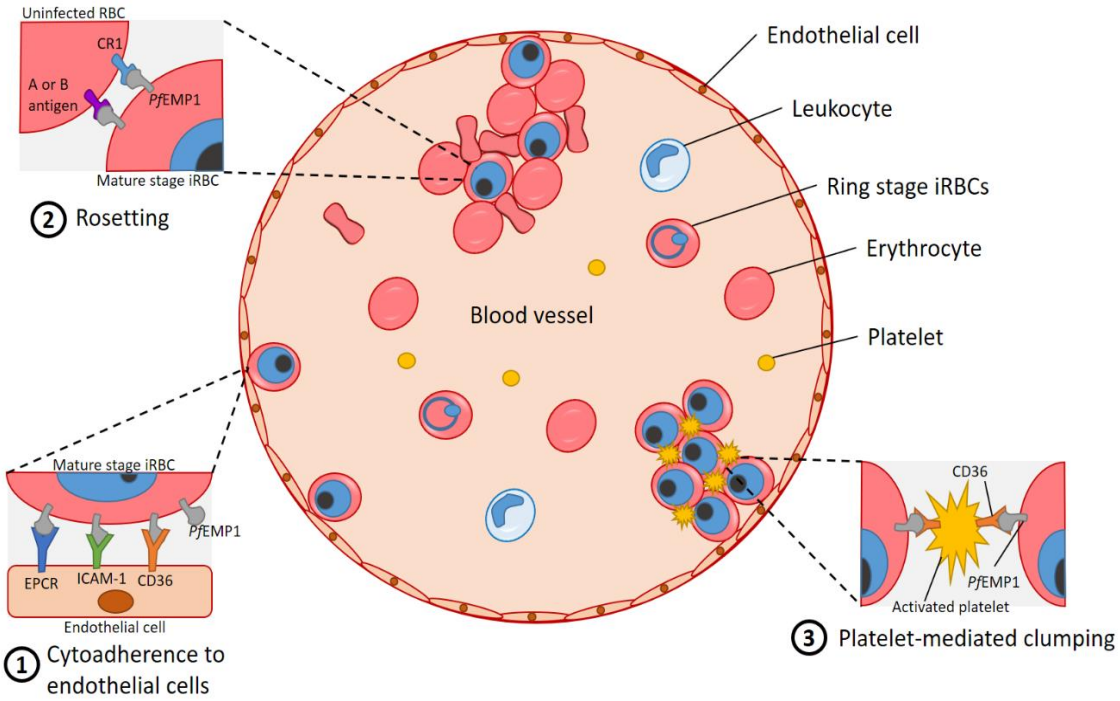

Figure 1.3: Various mechanisms of parasite cytoadherence. 1) Mature stage infected RBC (iRBC) express *Pf*EMP1, which binds to various endothelial receptors, including CD36, ICAM-1 and EPCR. 2) Aggregation of infected and uninfected RBC, known as rosetting, occurs through binding of *Pf*EMP1 with CR1 and A/B antigen on RBC surface. 3) Platelets can also mediate clumping of iRBCs through binding of *Pf*EMP1 with platelet CD36.

Cytoadherence of the parasites depends on two important factors: the presence of parasite antigens on the surface of iRBCs, and the presence of host receptors on other host cells. Similar to other parasite processes, host genetics is a major determinant to the outcome during this

process. As mentioned earlier, previous studies have discovered that polymorphisms in CR1 effect malaria pathogenesis [148,308]. *Pf*EMP1 on the surface of parasitised RBCs has been shown to bind with CR1 on other uninfected RBCs, leading to the formation of rosettes [309,310]. Reduced CR1 levels have been implicated in reducing rosette formation, both in field studies and *in vitro* [148,224]. Soluble CR1 reduces rosette formation, further supporting the interaction [309]. Furthermore, polymorphisms that affect *Pf*EMP1 binding site, such as S1 (a^-), were found in higher frequency in malaria endemic regions [311], and individuals with this phenotype were found to have reduced rosette formations and less likely to have cerebral malaria [148], thus providing a survival advantage [312]. Similar explanation was also proposed for SAO patients, as evidenced from the protection it confers against cerebral malaria [186,232]. Reduced rosetting was also proposed for individuals with O blood group [313], since it is thought that non-O blood groups have trisaccharides which act as receptors for rosetting [227]. Rosettes formed with O blood group more easily disrupted [227], which might contribute to malaria protection.

Receptors on other host cells such as CD36 and ICAM-1 (CD54) are also implicated in mediating cytoadherence. CD36 is a host cell receptor found on endothelial cells, platelets, erythroblasts and macrophages, and it plays a role in a wide range of cellular processes, including lipid metabolism, angiogenesis and promoting inflammation [314,315]. In the context of malaria pathogenesis, *Pf*EMP1 associates with endothelial CD36, leading to sequestration of parasitised erythrocytes from the circulation to evade detection by the spleen [302,316]. *Pf*EMP1 also binds to CD36 on platelets, leading to platelet-mediated clumping and promoting cytoadhesion by acting as a bridge between the endothelium and iRBCs [317,318]. Similarly, ICAM-1 is also found on endothelial cells and has also been implicated to bind to *Pf*EMP1 [319], and is often thought to enhance the adhesion of iRBCs to endothelium, acting synergistically with CD36 [320,321]. Despite evidence from field isolates and *in vitro* studies, associations between CD36 and ICAM-1 polymorphisms and protection towards severe malaria have been unclear. Many studies failed to report an increased malaria protection in populations with CD36 and ICAM-1 variants [322-326],

even though some studies seem to suggest otherwise [327-330]. It is possible that confounding factors might be responsible for the severity of malaria, and thus makes these association studies challenging [331]. More recently, endothelial protein C receptor (EPCR) was discovered to have a role in cerebral malaria pathogenesis [332]. Brain endothelium EPCR is thought to bind to *Pf*EMP1, activating coagulation and promoting obstruction, which leads to cerebral malaria [333,334]. However, contradictory findings regarding associations of EPCR polymorphisms and severe malaria risk have also been reported [335-337].

A proper presentation of various parasite proteins on erythrocyte surface is also crucial for parasite survival. As such, disruptions to the parasite's ability to remodel and export proteins may also contribute towards easier detection of iRBCs. Indeed, impaired cytoadherence was reported in infected erythrocytes with certain haemoglobin variants, including HbS, HbC and alpha-thalassaemia [210,212,215,338]. HbC and HbS erythrocytes were shown to have slower export and reduced amount of parasite proteins to host cell cytoplasm, Maurer's cleft and erythrocyte membrane [339], suggesting impairment to host cell remodelling [209]. This also resulted in abnormal expression of *Pf*EMP1 on iRBC surface, which explained the reduced cytoadherence and rosetting [212,288]. Similar mechanism was also proposed for alpha-thalassaemic erythrocytes [212].

1.3.4 RBC senescence and parasite detection

In addition to splenic filtration, erythrocytes also have their own senescence indicators, which signal the clearance of these erythrocytes from circulation (as shown in Figure 1.4), which poses a challenge for the parasites. One of these mechanisms is through erythrocyte apoptotic pathways, also known as eryptosis. Rise in intracellular calcium levels has been implicated as a stimulator for eryptosis, likely due to oxidative damage and cell shrinkage as the erythrocytes age [340]. It also eventually leads to membrane scrambling which exposes phosphatidylserine (PS) extracellularly, and it has been linked with increased RBC clearance [341]. It is believed that

exposed PS is recognised by various receptors on macrophages, thus facilitates phagocytosis of the erythrocytes [342-344].

Another RBC clearance mechanism, which is non-eryptotic, involves oxidative damage to haemoglobin which produces hemichromes, a product of haemoglobin denaturation [345]. Hemichromes are known to interact with various cytoskeletal proteins, including band 3, ankyrin-1, protein 4.1 and glycophorins [346], causing them to cross-link and aggregate [347,348]. This aggregation is further facilitated by the phosphorylation of band 3 proteins, which reduces their binding affinity for ankyrin-1, making them more mobile to traverse across membrane [349]. Aggregated band 3 has been shown to have increased affinity for naturally occurring autoantibodies IgG and complement C3, making the erythrocytes more likely to be phagocytosed by macrophages [350,351]. Another erythrocyte membrane protein, CD47, has also been implicated in mediating phagocytosis. It has long been believed that presence of CD47 on the erythrocyte surface inhibits phagocytosis through interaction with SIRP-alpha on macrophages [352,353]. The absence or gradual loss of CD47 has also been shown to accelerate RBC clearance in mice [354,355], although some studies have reported otherwise [356]. Upon further investigation, it was discovered that oxidative damage induces CD47 conformational changes, which alters its interaction with SIRP-alpha, switching from inhibitory to activating signal and enabling phagocytosis during malaria infections [357].

Interestingly, parasites have developed several strategies to avoid being phagocytosed. As the parasites grow inside the erythrocytes, they develop new permeation pathways (NPP) to dispose of wastes and obtain nutrients from extracellular space, which causes oxidative damage and makes erythrocytes more permeable to calcium, a stimulator of eryptosis [358]. However, parasites counter this by sequestering intracellular calcium in their organelles to possibly delay eryptosis [359]. Even if membrane scrambling and PS exposure eventually occurs, parasites have been shown to utilise PS to mediate cytoadhesion to endothelium through thrombospondin and CD36 receptors [360,361], thus evading splenic clearance altogether.

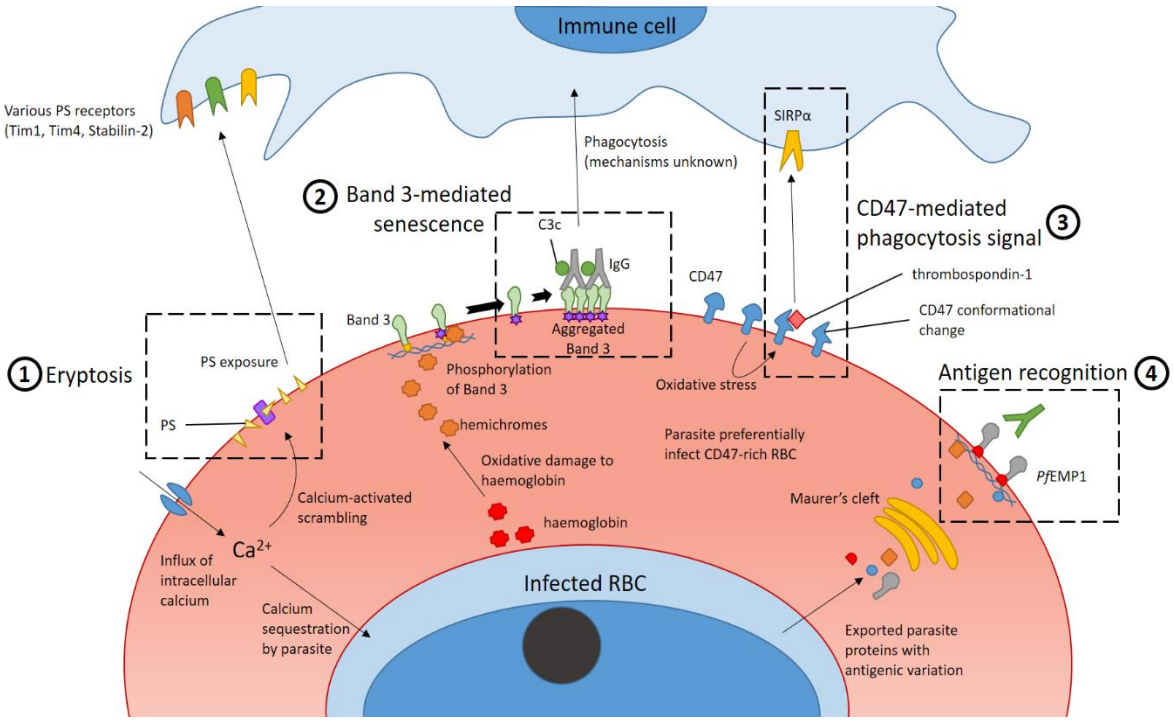

Figure 1.4: Various mechanisms of infected RBC detection. 1) Infected RBC have increased permeability to calcium, which leads to calcium-mediated scrambling of PS, thus exposing PS on RBC surface. Exposed PS is recognised by various PS receptors on the macrophage and facilitates phagocytosis. Parasites counteract by sequestering intracellular calcium to keep RBC calcium level low. 2) Oxidative damage to haemoglobin produces hemichromes, which bind to RBC cytoskeletal proteins and phosphorylate band 3, increasing its mobility. Aggregation of band 3 eventually occurs and allows the binding of autoantibodies IgG and complement C3, leading to phagocytosis. 3) CD47 undergoes conformational change due to oxidative damage from aging, which activates signals for phagocytosis. However, parasites preferentially invade CD47-rich young RBC to avoid this. 4) Direct immune recognition of parasite antigens can activate host immune systems, although high antigenic variation prevents effective recognition.

Another strategy parasites employ to avoid clearance is by invading erythrocytes selectively. Recent studies revealed that some parasite species preferentially invade young RBCs which are rich in CD47 [362]. Infected erythrocytes from mice lacking in CD47 are more likely to be phagocytosed, suggesting an evolutionary adaptation to invade CD47 rich RBCs to evade phagocytosis [362]. In addition, direct immune recognition of parasite proteins has also been challenging due to the high genetic variation of *Pf*EMP1, which is encoded by *var* genes. Parasites contain around 60 *var* genes but each parasite only express one gene at a time, making antibody-mediated clearance difficult [363,364].

With the long co-evolutionary history with malaria, certain genetic polymorphisms in humans have been implicated to promote parasite detection and clearance. Both G6PD deficiency and pyruvate kinase deficiency are associated with increased phagocytosis of infected RBCs [128,220,221]. It is currently thought that these deficiencies cause high oxidative stress, causing accelerating aging, which in turns promote PS exposure [216]. Increased phagocytosis is also observed for infected thalassaemic and sickle cells [205], and several mechanisms have been hypothesised. These include increased PS exposure due to translocase impairment and scramblase activation [365,366] and increased permeability to certain cations, making RBCs more likely to undergo eryptosis [367]. Increased oxidation of haemoglobin in these haemoglobinopathies also promotes the formation of hemichromes, enhancing the aggregation of band 3 [348]. As a result, these cells also exhibit increased binding of naturally occurring antibodies [205,368], indicating possible phagocytosis-mediated parasite clearance.

1.3.5 Summary

As evidenced in this section of the review, *Plasmodium* parasites have developed strategies to exploit various host pathways and processes to their own benefit, including immune evasion and host cell remodelling, as the result of co-evolution with humans. On the flip side, genetic polymorphisms in humans such as the ones that were described above, have proven effective at impairing parasite lifecycle. This constant struggle between host and parasites is a perfect example of "The Red Queen hypothesis", where both species have to constantly evolve and adapt to gain an upper hand in survival. This also demonstrates the importance of host genetics in understanding various parasite processes, as many of these mechanisms would still be unclear if not for these genetic polymorphisms.

This section not only summarises resistance mechanisms of various genetic polymorphisms, but also highlights the complex interactions between hosts and parasites. This is demonstrated by

the fact that mutations in a single gene often affect various processes of parasite lifecycle, giving rise to multiple mechanisms of protection, such as mutations affecting RBC cytoskeletons, haemoglobins and surface receptors. These examples provide a basis for the development of a new host-directed therapy for malaria, which will be discussed in the following section.

1.4 Host-directed Therapies

As discussed in the previous sections, it is evident that *Plasmodium* parasites are highly reliant on the host cell microenvironment for their survival. As such it presents an attractive opportunity for drug interventions to combat malaria. In the past, many antimalarial drugs have been designed to target parasite proteins and processes, rather than the host. With the inevitable emergence of parasite resistance against these antimalarials, it might be more reasonable to turn our attention to the opportunities presented by targeting the host. Such approaches of targeting host proteins and processes are known as "host-directed therapies" (HDT), which have become a popular approach to treat diseases in the past few years [369]. Since it only relies on the host proteins, it is often regarded as a theoretically resistance-proof approach to treat infections. This section of the review will discuss and examine examples of HDT in various infections, and explore the possibility of applying HDT for malaria.

1.4.1 Advantages and disadvantages of HDT

HDT provide some distinctive advantages over the conventional pathogen-directed treatments. Pathogen-directed approaches, although offer more specificity towards pathogens as the result of evolutionary divergence, often face the development of drug resistance. This is especially ineffective in the case of multidrug resistant pathogens, such as *Acinetobacter* [370], tuberculosis [371] and malaria [372]. One explanation for this is that the pathogen-directed drugs impose selective pressure and therefore subjected to changes in pathogen genetics, where mutations in drug targets are likely to cause resistance to the treatments. On the other hand, HDT target the host proteins, which is outside of parasite genetic control. The pathogens would not have control over the availability of various host resources to the pathogens. It is also unlikely for the pathogens to develop a parallel but independent pathways through mutations alone. As the result, HDT are thought to be more resilient to drug resistance, thus providing a possible way

out of the never-ending cycle of drug development. However, one major weakness of HDT is the potential side effects related with targeting the host. It is possible that inhibiting host proteins would affect normal functions of these proteins, which might be deleterious to the host. As an example, imatinib, a tyrosine kinase inhibitor, has been shown to be a potential treatment for vaccinia virus or microbes that rely on host tyrosine kinase [373]. However, it is also associated with skin toxicity, oedema, and potentially cardiac toxicity [374,375]. As the result, it is important to have full understanding on the mechanisms of action and the safety of these drugs. Nevertheless, with proper drug delivery and administration, HDT can still be an invaluable tool to combat multidrug resistant pathogens [376].

1.4.2 Applications of HDT

With a better understanding of host-pathogen interactions, increasingly more research has been aimed at discovering host-directed treatments. HDT typically involves utilising agents such as repurposed drugs, antibodies, recombinant proteins and cellular therapies to improve host defences against pathogen, either by augmenting host immune responses, or by preventing the hijacking of host factors by pathogens [369]. Development of HDT has been applied to wide range of infections and their diseases, including *Mycobacterium tuberculosis* (tuberculosis) [377], HIV [378], Dengue virus [379], Ebola virus [380] and *Leishmania* protozoans (Leishmaniasis) [381]. A few of these are discussed below.

1.4.2.1 Tuberculosis

HDT development for tuberculosis is a trending area of research in recent years. Studies have shown that elevated levels of interleukin-1 (IL-1) are able to inhibit excessive type 1 interferon production, preventing eicosanoid imbalance and thus pathogenesis [382]. Immunotherapy treatment with drugs to increase prostaglandin E2 have been shown to reduce mortality in infected mice [382]. Similarly, another potential HDT for tuberculosis involves the use of a

glucocorticoid receptor inhibitor, Prednisone, to increase the expression of inducible nitric oxide synthase (iNOS) and inducible cyclooxygenase (COX-2) [383], which improves patient survival [384]. Studies have also shown the potential of using Metformin as an adjuvant for antituberculosis treatment. The mechanism of killing *Mycobacterium tuberculosis* by Metformin adjuvants is thought to be via induction of oxidative damage to the bacteria, and improved T-cell responses [385,386].

1.4.2.2 Ebola virus

Ebola virus has received substantial attention in treatment development due to the recent outbreaks and subsequent high mortality [387]. Recent HDT in development for Ebola virus include using repurposed drugs such as Irbesartan and Atorvastatin, to improve tissue repair and reduce pro-inflammatory responses that occur during infection [388]. These are currently in the early phase of clinical trials for improving survival of patients [389]. It is also possible to use a recombinant inhibitor, rNAPc2, to reduce blood coagulation and the release of pro-inflammatory cytokines, which has been shown to work in rhesus monkeys [390].

1.4.3 Discovery of ANK-1 as a candidate HDT target for malaria

Currently, little research has been done on the application of HDT for malaria. It is possible to develop HDT that mimic the protective effect of various genetic polymorphisms, since they are generally well-characterised and effective at conferring resistance. However, most of them are associated with deleterious effects to the host, prompting the need to discover novel, safe, HDT targets for malaria.

Previously, an N-ethyl-N-nitrosourea (ENU) mutagenesis study performed in our lab has discovered ankyrin-1 (ANK-1) to be a potential HDT target for malaria, as described by Greth, et al. [189]. Ankyrin-1 is a 210kDa protein and a major component in RBC cytoskeletal structure. It is

made up of 3 large domains: the amino terminal ankyrin repeats, the middle spectrin-binding domain, and the regulatory domain towards the carboxyl terminus. It has 3 major binding partners: band 3, protein 4.2, and beta-spectrin [391-393], thus functioning as a vertical connector between the RBC membrane and the cytoskeleton structure, as shown in Figure 1.5. Mutations in ANK-1 in humans are often associated with hereditary spherocytosis (HS), a genetic disorder that results in reduced RBC volume and increased osmotic fragility. Symptoms can range from asymptomatic to severe haemolytic anaemia depending on the nature and position of mutations [195,394].

Greth, et al. [189] described an ENU-induced *Ank-1* mutation, MRI23420, which gives rise to a HS-like phenotype, with reduced RBC volume, elevated RBC count but normal total haemoglobin levels. When challenged with a mouse malarial parasite, *P. chabaudi*, heterozygous mice showed significant resistance compared to wild-type, which was consistent with other previously described mice carrying *Ank-1* mutations – namely the *Ank-1$^{(nb/nb)}$* and *Ank-1^{1674}* mice. In terms of resistance mechanisms, both *Ank-1$^{(MRI23420/+)}$* and *Ank-1$^{(nb/nb)}$* were thought to impair parasite intra-erythrocytic growth [189,204], whereas the mechanisms are unclear for *Ank-1^{1674}* mice [190]. For *(nb/nb)* mice, the authors proposed spectrin deficiency to be the cause of reduced parasite growth [204]. However, *Ank-1$^{(MRI23420/+)}$* and *Ank-1^{1674}* heterozygotes have normal levels of spectrins and yet they were significantly resistant to *P. chabaudi*. This conflicting evidence suggests that ANK-1 might mediate resistance through multiple mechanisms. Therefore, a more detailed study is required to elucidate the exact roles ANK-1 has during malaria infection.

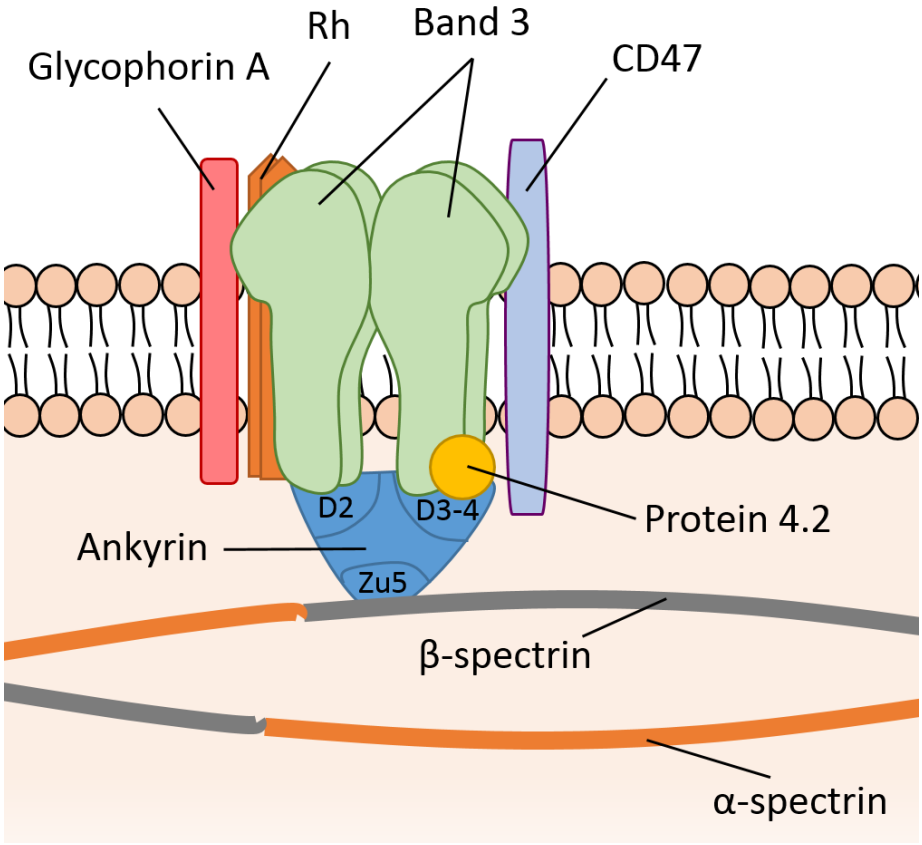

Figure 1.5: Schematic diagram of RBC cytoskeletal structure showing major cytoskeletal proteins of ankyrin complex. Ankyrin is responsible for connecting the spectrin networks to the RBC membrane via binding with protein 4.2 and band 3 on the RBC membrane. The N-terminal ankyrin repeats (D2-D4) are involved in ankyrin-band 3-protein 4.2 binding, whereas Zu5 domain binds to repeat 14-15 of β-spectrin.

Several *in vitro* studies have also recently revealed the binding site of ankyrin-1 and β-spectrin [391,395,396]. It appears to be localised to the Zu5 domain of ANK-1 and repeat 14 and 15 of β-spectrin [396,397]. Mutagenesis studies have indicated several crucial residues that facilitate ankyrin-spectrin binding on beta-spectrin, such as D1781, E1784, T1788 and Y1866 of β-spectrin [398]. Given that mutations in ankyrin-1 or spectrins often result in RBC abnormalities, it is likely that mutations in these residues might also give rise to similar phenotypes as HS patients. This raises the possibility to further investigate this interaction in the context of malaria using a reverse genetics approach in an *in vivo* setting.

1.4.4 Hypotheses of this study

In order to elucidate the exact roles ANK-1 has during malaria infection, several mouse strains carrying various ENU-induced *Ank-1* mutations were examined in this study, namely *Ank-1*$^{(MRI61689)}$, *Ank-1*$^{(MRI95845)}$ and *Ank-1*$^{(MRI96570)}$. These mice were identified by significantly lower RBC volume, similar to *Ank-1*$^{(MRI23420)}$. Their response to malaria infection, as well as their mechanisms of resistance were further explored. We hypothesise that the location of the mutations will give rise to different degrees of malaria resistance, and possibly through different mechanisms.

Another aspect of this study is to determine if ANK-1 is a suitable HDT target. This was done by examining another strain of mouse, TAR3.5, which was generated through CRISPR/Cas9 technique to carry a mutation, D1781R, on the ankyrin binding site of β-spectrin. We hypothesised that the ankyrin-spectrin interaction would be disrupted in the mice, similar to the *in vitro* studies, and consequently conferring resistance to malaria. The RBC phenotypic characteristics of these mice and their response to malaria infections were investigated in this study. This would not only give us insight into the host-parasite interactions, but also raise the possibility of disrupting this interaction pharmacologically as the first step towards HDT development for malaria. High throughput drug screening (HTS) could then be used to identify drug candidates that disrupt the binding of recombinant proteins *in vitro*, which is explored in this study.

1.5 Project Aims

The goals of this project were to investigate the roles ankyrin plays in malaria infections through the use of mouse models with various *Ank-1* mutations, as well as to determine if ANK-1 is a suitable candidate for HDT development for malaria. This is achieved through the following specific aims:

1. Characterise and compare the phenotypes of mice carrying *Ank-1*^{MRI61689}, *Ank-1*^{MRI95845} or *Ank-1*^{MRI96570}.
2. Examine their response towards malaria infection and determine the underlying mechanisms of their resistance.
3. Determine if ANK-1 is a suitable HDT target by characterising TAR3.5 mice and developing an *in vitro* binding assay for HTS to look for drug candidates for disrupting ankyrin-spectrin binding.

CHAPTER 2

MATERIALS AND METHODS

2.1 Mouse Husbandry and Maintenance

2.1.1 ENU mutagenesis screen and ethics statement

SJL/J or B6.BKS (D)-Lepr^{db}/J male mice (G0) were injected with 150 mg/kg and 100 mg/kg of N-ethyl-N-nitrosourea (ENU) (Sigma-Aldrich, St Louis, MO), respectively, at seven weeks old and crossed to females from the isogenic background to produce the first generation progeny (G1). The seven-week-old G1 progeny were bled and analysed on an Advia 120 Automated Haematology Analyser (Siemens, Berlin, Germany) to identify abnormal red blood cell parameters. The G1 MRI61689, MRI95845, MRI96570 mice were identified due to their significantly low mean red cell volume (MCV) – three standard deviation lower than other G1s. These mice were crossed again with mice from the isogenic background to generate G2 progeny and to assess the heritability and the dominance mode of inheritance. Mice that exhibited low MCV (<48 fl) were subjected to whole exome sequencing to identify the causative mutations. Mutant mice were identified via haematological analysis, osmotic fragility test or Amplifuor SNP genotyping assay, which is carried out by the Australian Phenomics Facility (APF). The mice were maintained according to the NHMRC code of practice for experimentation using laboratory animals and all experiments were carried out under the ethics agreements ARA2012/019 and A2014/54 and the NLRD 15.03.

2.1.2 CRISPR/Cas9 system to introduce D1781R mutation in TAR3.5 mouse strain

The CRISPR/Cas9 (Clustered Regularly Interspaced Short Palindromic Repeats/CRISPR-associated 9) system was used to introduce D1781R mutation in SJL/J mice to generate TAR3.5 mouse strain, and was conducted by Dr Gaetan Burgio and Ms. Emmaline Brown. Briefly, guide RNA (gRNA) was first designed as indicated below and cloned into a Px461 plasmid containing a Cas9-D10 as described in published protocol [399].

ACCATCGCTGAGTGGAAGGATGGACTCAATGACATGTGGGCGGACCTGCTGGAGCTCATTGACACCCG

CATGCAGCTGCTGGCTGCCTCCTACGACCTGCACCGCTATTTCTACACAGGC

The highlighted section indicates the gRNA sequence, with the underlined nucleotide being the targeted mutation site.

Embryo donor SJL/J mice were first injected intraperitoneally with 5 IU Pregnant Mare Serum Gonadotrophin, followed by 5 IU of Human Chorionic Gonadotrophin 48 hours later to induced superovulation. They were then immediately placed with fertile a stud male and embryos were collected 12 hours post-conception. 5 ng/µl of cloned Px461 plasmid as above and 25 ng/µl of 150 bp single stranded oligonucleotides containing the nucleotide to be integrated (Integrated Device Technology, San Jose, California) were co-injected into the pronucleus of the fertilised zygotes, followed by transferring into pseudo-pregnant females. The newborn pups were genotyped by Sanger sequencing using primers listed in Section 2.3.2 and the mice positive for the mutation were bred for the maintenance of TAR3.5 mouse strain.

2.2 Phenotypic Characterisation of Mice

2.2.1 Complete blood count analysis

Peripheral blood was collected from at least seven week old uninfected mice via mandibular puncture or retro-orbital bleeding with EDTA lined-CAPIJECT® Micro Collection Tubes (Terumo Medical Corporation, NJ). Blood samples were analysed using an ADVIA® 2120 haematology system (Siemens, Berlin, Germany) on CBC/DIFF settings and species Mouse C57BL/6.

2.2.2 Osmotic fragility measurement

To assess the susceptibility of the RBC membrane to osmotic stress, whole mouse blood was diluted 100-fold with hypotonic mouse tonicity phosphate buffered saline (MT-PBS) containing 0 to 10 g/L of sodium chloride, and incubated for at least 10 minutes at room temperature. The cells were centrifuged at 800 g for 3 minutes, and the supernatant, which contains free haemoglobin, was measured at 540 nm to assess the degree of haemolysis. The absorbance values were expressed as percentage of haemolysis, with haemolysis at 0 g/L sodium considered as 100% lysis.

2.2.3 Scanning electron microscopy

Fresh blood was fixed overnight at 4°C, in 3% EM-grade glutaraldehyde (Sigma-Aldrich, St Louis, MO) immediately upon collection. The samples were washed with MT-PBS 3 times, 10 minutes soak each. The cells were then adhered to the coverslips with 0.1% polyethylenimine (PEI) for 10 minutes, before washing off with MT-PBS. The cells were then dried serially using 30%, 50%, 70%, 80%, 90%, 100%, 100% ethanol, each with a 10 minutes soak. The cells were then soaked in 1:1 ethanol: hexamethyldisilazane solution for 10 minutes, followed by 2 washes with 100%

hexamethyldisilazane (Sigma-Aldrich, St Louis, MO), each 10 minutes. The coverslips were then air-dried overnight and coated with gold and examined under JEOL JSM-6480LV scanning electron microscope, with the assistance from the staff in the Microscopy Unit of Macquarie University, Sydney.

2.2.4 RBC lifetime assay

Each uninfected mouse was injected with 1 mg of EZ-link® Sulfo-NHS- LC Biotin (Biotin) (Thermo Scientific, Waltham, MA) in MT-PBS intravenously. 2 µl of blood was collected on day 1, 7, 14, 21 and 28 from the day of injection. Samples were stained and analysed using a flow cytometer (details described in method 2.4.5). The proportion of Biotin-labelled mature RBCs on day 1 was considered as the "starting point" of 100% of labelled cells. For subsequent timepoints, the remaining number of biotin-labelled RBCs were expressed as a percentage of the starting number as the indication of RBC turnover rate.

For infected mice (according to method 2.4.1), 1 mg of Biotin was injected intravenously as soon as parasitaemia was detectable on flow cytometry (approximately 0.05-0.3%). Samples were collected daily and analysed as above. In addition, the production of reticulocytes (reticulocytosis), parasite load and relative levels of anaemia were also tracked.

2.2.5 RBC deformability assays

2.2.5.1 Ektacytometry

10-15 µl of uninfected RBCs were first resuspended in 500 µl of pre-warmed polyvinylpyrrolidone (PVP) solution at a viscosity of 30 mPa/second at 37 °C until needed. Samples were analyzed according to the manufacturer's instructions with a RheoScan Ektacytometer (Rheo Meditech, Seoul, South Korea) and the elongation index measured across

a range of pressures from 0-20 Pa. Each sample was measured three times to account for technical variabilities. The values were normalized against the wild-type samples.

2.2.5.2 In vitro splenic retention assay

Another method used to indicate RBC deformability is through an *in vitro* splenic retention assay, modified from the method as described by Deplaine, et al. [400]. The unstained cell solution was first prepared by diluting 100 µl wild-type whole blood with mouse-tonicity Ringer's complete solution (MTRC). Separately, 50 µl of whole blood was first labelled with 0.1 µg of either hydroxysulfosuccinimide Atto 633, Atto 565 or Atto 495 (Sigma-Aldrich, US) on ice for 45 minutes. They were then washed two times with MTRC and resuspended in 500 µl of MTRC. Each sample mixture was prepared by adding 40 µl of each labelled blood and made up to 200 µl with MTRC, followed by adding 500 µl of the unstained cell solution, making up to 700 µl in total. Replicates of samples were also prepared with different combination of labelled RBCs to account for dye effects.

The bead layers were prepared by mixing 1 g of each 5-15 µm and 15-25 µm beads, and resuspending these in 4 ml of MTRC. 500 µl of the well-mixed bead mixture was added into a 1 ml filter pipette tip with a trimmed tip. More beads mixture was added to the tip if necessary to make up an approximately 2 mm thickness of bead layer in the tip. The tip was filled with MTRC to the brim of the tip.

These prepared tips were first briefly flushed with MTRC before injecting 500 µl of the sample mixture into the system, followed by flushing the tip with at least 6 ml of MTRC. The leftover sample mixtures were kept as the "pre-filtered" samples. The flow through from the tips were centrifuged and resuspended in 500 µl of MTRC, as the "post-filtered" samples. They were then analysed on BD LSRFortessa flow cytometer (BD Biosciences, Franklin Lakes, NJ) to determine the proportion of each labelled blood pre- and post-filtration (as described in Section 2.4.5). The

percentage of retention is calculated by dividing the difference in labelled blood population pre- and post-filtration by the pre-filtered population to obtain the percentage retained. They were then normalized to the unlabeled population.

2.2.6 Fluorescence Recovery after Photobleaching (FRAP) analysis

To determine the mobility of Band 3 on the erythrocyte membrane, 15 µl of uninfected whole blood was washed once with PBS and subsequently stained with 0.2 mg/ml of Eosin-5-maleimide (EMA) (Biotium, Hayward, CA) in pH8.0 PBS (from a pre-made EMA stock of 50 mg/ml in DMF or DMSO). Cells were stained for 1 hour on ice, followed by washing with PBS at least twice until the supernatant was clear. Cells were then incubated at room temperature for 6 minutes with approximately 7000 U/ml of Streptolysin-O (Sigma-Aldrich, St Louis, MO) which was pre-activated with 100 mM DTT for 15 minutes at room temperature. Cells were then washed twice with PBS and spread on a glass slide. They were then covered with cover slips and pressed upside-down to remove excess liquid and sealed. The samples were then examined on Leica SP5 confocal microscope (Leica Microsystems, Wetzlar, Germany) with the help of Dr Matthew Dixon using the settings below:

FRAP settings on SP5:

- 80% Argon laser power
- 10% opened shutter except during bleaching
- Pinhole fully opened (600 microns)
- 128x128 pixels during FRAP
- 2 line averages
- Zoom factor: 5
- 1µm diameter circular bleach area
- 3 pre-bleached images each at 0.6 seconds interval
- 1 bleach image at 0.6 seconds with 100% opened shutter
- 2 post-bleached images with 0.6 seconds interval
- 10 post-bleached images with 30 seconds interval

2.2.7 Band 3 solubility assay

To determine the proportion of un-bound band 3 in the RBC membrane, 100 µl of mouse whole blood was lysed with ice-cold 5mM phosphate buffer (ph7.4) with cOmplete Protease Inhibitor Cocktail Tablets (protease inhibitor) (Roche, Basel, Switzerland), and centrifuged at 20,000 g for 20 minutes followed by removal of the supernatant. The pellet (RBC ghosts) was further washed with the 5 mM phosphate buffer until the supernatant became clear. 20 µl of RBC ghost was then dissolved in the same volume of phosphate buffer containing 3% v/v Triton-X100 and incubated on ice for 20 minutes, followed by centrifugation at 20,000 g at 4^{o}C. The supernatant containing soluble band 3 was isolated from the pellet, which contained the insoluble band 3. The pellet was resuspended in phosphate buffer with 3% v/v Triton-X100 and centrifuged again at 20,000 g at 4^{o}C. The supernatant was discarded, and the pellet was resuspended in 10 µl of phosphate buffer. Both soluble and insoluble band 3 were denatured at 95^{o}C, and loaded onto SDS-PAGE. Western blotting was then carried out and analysed as described in section 2.3.3.

2.2.8 *Ex vivo* haemolysis and phosphatidylserine (PS) exposure assays

The susceptibility of RBCs to haemolysis was assessed by first incubating whole mouse blood at room temperature for up to 72 hours, with timepoints at 0, 3, 6, 12, 24, 48 and 72 hours of incubation. For each timepoint, 2 µl of whole blood was resuspended in 200 µl of MT-PBS and centrifuged at 800 g for 3 minutes. 100 µl of the supernatant was taken and the absorbance at 540 nm was measured as an indicator of haemolysis. The percentage of haemolysis was calculated from the absorbance value, with haemolysis in pure water considered as 100% lysis and baseline haemolysis at 0 hour.

The PS exposure was measured by incubating 1.5 µl of the whole blood in 100 µl of Annexin V binding buffer containing 5 µl of Annexin V- Fluorescein isothiocyanate (FITC) for 30 minutes at

room temperature. 400 µl of Annexin V binding buffer was further added into the samples before analysing on BD LSRFortessa (BD Biosciences, Franklin Lakes, NJ) as described in Section 2.4.5.

2.3 Molecular Biology Techniques

2.3.1 Whole exome sequencing

DNA from two G2 mice carrying the abnormal red blood cell parameters (MCV <48fl) were extracted with Qiagen DNeasy blood and tissue kit (Qiagen, Venlo, Netherlands) for exome sequencing as previous described [401]. Briefly, at least 10 μg of DNA was prepared for exome enrichment with Agilent Sure select kit paired-end genomic library from Illumina (San Diego, CA), followed by high throughput sequencing using a HiSeq 2000 platform. The bioinformatics analysis was conducted by Dr Denis Bauer according to the variant filtering method previously described by Bauer, et al. [402]. Briefly, to avoid the variant loss due to algorithm bias, four variant calling pipelines were created from the raw sequencing data. The sequencing reads were mapped using BWA [403] V0.61 or BOWTIE2 [404] onto the mouse genome (mm9/NCBI37), followed by variant calling using SAMTOOLS [405] V0.1.19 or GATK UnifiedGenotyper [406]. All resulting variants were first annotated using GATK and variants from Sanger's The Mouse Genomes Project, followed by filtering using python scripts to retain true (identified in more than one pipeline) and exclusive variants. Private variants that were shared between the two mutants but not with other mice from isogenic background or previously described ENU mutants were functionally annotated using ANNOVAR [407]. Private non-synonymous exonic and intronic variants within 20 bp from the exon spicing sites were retained as potential candidate ENU mutations.

2.3.2 Genotyping

For routine genotyping of experimental mice, DNA was extracted from mouse tails using Qiagen DNeasy blood and tissue kit. Purified DNA was amplified through PCR using primers listed below. Either GoTaq® DNA polymerase or AmpliTaq® DNA Polymerase were used for all PCR reactions, which was conducted using following conditions:

Temperature (°C)	Time (m:ss)	Number of cycles
95	1:00	1
95	0:30	35
57	0:30	
72	0:40	
72	5:00	1

The PCR products were examined using agarose gel electrophoresis for quality control, followed by purification using either Wizard® SV Gel and PCR Clean-Up System (Promega, Madison, WI) or treatment with ExoSap digestion, where 0.025 µl Exonuclease I (New England Biolabs, Ipswich, MA), 0.25 µl of shrimp alkaline phosphatase (New England Biolabs, Ipswich, MA) and 9.725 µl water was added and incubated at 37°C for 30 minutes. Purified PCR products were then sent for Sanger sequencing by Australian Genome Research Facility (AGRF, WEHI, Melbourne) or to Biomolecular Resource Facility (BRF, ANU, Canberra). Logarithm of odds (LOD) score was calculated based on the number of mice that segregated with the candidate mutations.

Primers for MRI61689 mutation:

Amplicon	Forward	Reverse
Acp5	CAGAAGGATGCCTTTGGGTA	ACCAGCGCTTGGAGATCTTA
Kcnk1	GGGCCTTTTCCTCCTTACAGA	CAGGAAACGGTGACAAATCC
Epas1	GGAAGCCAGAACTTCGATGA	GTAGTGTTCCCTGGGGTGT
Picalm	TCACTGAATGTAATTGGGATATCAT	CACCCTCTCTTCACTTTTGTG
Socs6	CCGCTTTGTTATCCGTCAGT	TGGCAGCAAAGACTTCAATG
Ank-1	TCCCTGGCTTAAAGTTGGTG	CTCTCCCTTAGCTGCATTCC

Primers for MRI95845 mutation:

Amplicon	Forward	Reverse
Snai2	CATCTGCAGACCCACTCTGA	TGGTTGGTAAGCACATGAGAA
Tbc1d23	CACCCCCTTTTTGGTTTCTT	ACGTGCACATCGACTAACCA
Pnpla6	AGGCTGAGGAAGTGTGCCTA	AACTAGCTGGGCTTTGGTCA
Zglp1	CTGGCCTTTGACTTCTGACC	CCTCACAAGGTGGCTGTTTC
Ank-1	CTCCAAGTGAGAGGGTTTGC	GATGGCACACAGTCAGACCA

Primers for MRI96570 mutation:

Amplicon	Forward	Reverse
Fat4	CGCATCCCTTCATACAACCT	ACACCCCACTCACGTAGCTC
Rhcg	TGAGGAATGAGGGAGAAAGG	CCAATATGGCAGCCCTCTAA
Plxnb3	TACCCGATCAATCCAGAAGG	TTCTGAATGTGCAGGGTCAC
Ank-1	TGTGCAGGCATTTCTACATGA	ACTCTCTGGGTAGACCCCGT

Primers for TAR3.5 mouse strain:

Forward: 5'- GTGACAACCTGGCAAAGTGA-3'

Reverse: 5'-ACACCAACACTGGGAGAAGG-3'

2.3.3 RNA extraction, cDNA synthesis, qPCR and cDNA sequencing

RNA was isolated from embryonic livers of E14 embryos using Qiagen RNeasy kit (Qiagen, Venlo, Netherlands), followed by cDNA synthesis using Transcriptor High Fidelity cDNA Synthesis Kit (Roche, Basel, Switzerland). Quantitative PCR was carried out on ViiA™ 7 Real-Time PCR System (Thermo Scientific, Waltham, MA). The $\Delta\Delta C_T$ method was used to determine the cDNA levels of *Ank-1* and the housekeeping gene β-actin and expressed as a fold-change of the mutants to the wild-type. The primers used for *Ank-1* gene spanned exon 2 to 4:

Ank-1-F: 5'-TAACCAGAACGGGTTGAACG-3';

Ank-1-R: 5'-TGTTCCCCTTCTTGGTTGTC-3'

β-Actin-F: 5'- TTCTTTGCAGCTCCTTCGTTGCCG-3';

β-Actin-R: 5'- TGGATGCGTACGTACATGGCTGGG-3'

To characterise the effect of the MRI61689 mutation, cDNA was amplified through PCR using two primers set were design as shown below: Primer set 1 was designed to amplify the wild-type *Ank-1* transcript, whereas primer set 2 was designed to only amplify the predicted mutant transcript with the 11 bp insertion. Amplified PCR products were analysed using agarose gel electrophoresis and each band was purified and sequenced as described previously.

Primer set 1: Forward: ATGCAGAGTCGGTACAAGGC; Reverse: CCGTTCGAGCTGACCTCATT

Primer set 2: Forward: CCTGGGGAACAAGTTTCTTT; Reverse: GTGCAAGGGGCTGTATCCTA

2.3.4 SDS-PAGE, Coomassie staining, Western and proteomic analysis

RBC ghosts (prepared as described in Section 2.2.7) or whole blood lysates were denatured in SDS-PAGE loading buffer (0.0625M Tris pH 6.8, 2% SDS, 10% glycerol, 0.1 M DTT, 0.01% bromophenol blue) at 95°C for 5 minutes before loading onto a Mini-PROTEAN® TGX™ Precast Gels (Bio-Rad, Hercules, CA). The gels were then either stained with Coomassie blue solution (45% v/v methanol, 7% v/v acetic acid, 0.25% w/v Brilliant Blue G) overnight or transferred to a nitrocellulose membrane.

For proteomic analysis of *Ank-1*$^{(MRI95845/MRI95845)}$ and wild-type erythrocytes, each lane of Coomassie-stained gel was cut into pieces and destained and washed with 50% v/v acetonitrile / 50 mM ammonium bicarbonate at 37^{o}C for 15 minutes four times. The pieces were then dried and sent to Australian Proteome Analysis Facility (APAF) for protein alkylation and reduction, trypsin digestion and analysis on a mass spectrometer.

Western blotting was carried out using these primary antibodies: anti-alpha 1 spectrin (clone 17C7) at 1:1000 dilution, anti-beta 1 spectrin (clone 4C3) at 1:1000 dilution (Abcam, Cambridge, UK), anti-N-terminal Ank-1 "p89" (1:1000 dilution), anti-Band 3 (1:5000 dilution) and anti-protein 4.2 (1:4000 dilution) (kind gifts from Connie Birkenmeier, Jackson Laboratory, US). Housekeeping gene GAPDH or β-actin were detected either using anti-GAPDH (clone 6C5) at 1:1000 dilution (Merck Millipore, Darmstadt, Germany), or anti- β-actin (ab8227) (Abcam, Cambridge, UK) at 1:1000 dilution, respectively. Each primary antibody was detected with the appropriate horseradish peroxidase (HRP)-conjugated secondary antibody at 1:5000 dilution from 1 mg/ml stocks. The blots were visualised using ImageQuant LAS 4000 (GE Healthcare Life Sciences, Arlington Heights, IL), and quantified using ImageJ software [408].

2.4 Malaria Infection-related Techniques

2.4.1 Malaria infection

250 µl of thawed *P. chabaudi adami DS* infected blood was injected into the intraperitoneal cavity of a C57BL/6 donor mouse. When the donor mouse reached 1-10% parasite load (parasitaemia), the mouse was euthanised and blood was collected through cardiac puncture. The parasitised blood was diluted in Krebs' buffered saline with 0.2% glucose as described previously [409]. Each experimental mouse was infected with either $1x10^4$ (low dose) or $1x10^7$ (high dose) parasites intraperitoneally. Each mouse was then monitored daily until they started exhibiting symptoms, in which they were monitored four times daily according to the parameters described below. Each parameter was scored 0 to 3 according to the severity of the symptoms, where a score of 3 in any parameters denotes immediate euthanisation of mice. The parasitaemia of these mice were monitored either using light microscopy or flow cytometry.

Parameters to monitor	Score (0-3)
Coat	1 – Rough coat 2 – Unkempt coat, thin body, wounds present 3 – Discoloured, skin discharge
Activity	1 – Isolated, abnormal posture 2 – Huddled/inactive OR overactive 3 – Declining or seizuring
Movement	1 – Slightly uncoordinated/ abnormal 2 – Uncoordinated, walking on toes, reluctant to move 3 – Staggering, paralysis, limb dragging
Eating/drinking	1 – Increased/decreased for 24 hrs 2 – Increased/decreased for 48 hrs 3 – Increased/decreased >48 hours. Obese*
Dehydration	1 – Skin less elastic 2 – Skin tents 3 – Skin tents, eyes sunken
Blood in faeces/urine	1 – Moist faeces 2 – Diarrhoea or dry faeces, abnormal urine (volume/colour) 3 – Uncontrolled diarrhoea, blood in faeces. Nil urine or incontinent
Body weight	1 – Reduced growth 2 – Weight loss >15% 3 – Weight loss >10% over short period or >20% over time

2.4.2 Light microscopy

Blood was collected from mouse tail and smeared onto a glass slide to make a thin blood film. The slides were then briefly fixed in methanol for one minute and air-dried before being stained in a 10% Giemsa solution (Sigma-Aldrich, St Louis, MO) at pH 7.4 for 10 minutes. The slides were examined under a light microscope with the 100x objective with immersion oil, and at least 300 RBCs were counted. Infected RBCs were counted as a proportion to total RBCs, and expressed as percentage parasitaemia.

2.4.3 Terminal deoxynucleotidyl transferase dUTP nick end labelling (TUNEL) staining

3µl of infected blood containing 1-10% parasitaemia were collected during trophozoite stage and fixed in 1 in 4 diluted BD Cytofix™ Fixation Buffer (BD Biosciences, Franklin Lakes, NJ) at 4°C for at least 24 hours until they were needed. Each sample was then washed twice with MT-PBS, and adhered to a glass slide pre-coated with 0.1% polyethylenimine (PEI) for 10 minutes at room temperature. The excess cells were washed off with the wash solution from APO-BrdU TUNEL assay kit (Thermo Scientific, Waltham, MA) and incubated overnight at room temperature with TUNEL labelling solution (1 mM Cobalt Chloride, 25 mM Tris-HCl pH 6.6, 200 mM sodium cacodylate, 0.25 mg/ml BSA, 60uM BrdUTP, 15 U Terminal transferase). The slides were washed three times with rinse buffer from APO-BrdU TUNEL assay kit, followed by staining with 50 µg/ml of anti-BrdU-Biotin antibody (Novus Biologicals, Littleton, CO) in MT-PBT (MT-PBS, 0.5% BSA, 0.05% Triton X-100) for 1 hour. The slides were then washed three times with MT-PBT, followed by probing with 2 µg/ml Alexa Fluor® 594 conjugated streptavidin (Thermo Scientific, Waltham, MA). Next, they were washed three times with MT-PBS and mounted with SlowFade® Gold antifade reagent with DAPI (Thermo Scientific, Waltham, MA) and sealed. When the slides were dried, they were examined using Axioplan 2 fluorescence light microscope (Carl Zeiss, Oberkochen, Germany) between 60x to 100x magnification. At least 100 DAPI-positive cells were

counted, and each was graded as either positive or negative for TUNEL staining, as an indication of DNA fragmentation.

2.4.4 *In vivo* erythrocyte tracking (IVET) assay

The IVET assay was carried out as previously described by Lelliott, et al. [410]. Briefly, 1.5 to 2 ml of whole blood was collected from multiple wild-type and mutant mice via cardiac puncture. The bloods were then stained with either 10 µg/ml of Atto 633 or 125 µg/ml of EZ-Link™ Sulfo-NHS-LC-Biotin (Biotin) (Thermo Scientific, Waltham, MA) for 45 minutes at room temperature, followed by washing three times with MT-PBS. The labelled blood was then mixed in two different dye combinations to correct for any dye effects. $1x10^9$ erythrocytes were injected intravenously into infected wild-type mice at 1-5% parasitaemia during schizogony stage, usually 8-10 days post-infection with $1x10^4$ parasites. Blood samples were collected at 30 minutes, 3 hours, 12 hours, 20 hours and 36 hours after injection. The ratio of infected labelled erythrocytes was determined using flow cytometry, as an indication of the relative susceptibility of RBC to malaria infections. The proportion of labelled blood populations was also tracked over time to determine the clearance of these RBCs from the circulation.

2.4.5 Flow cytometric analysis of blood samples

For RBC lifetime assays, 2 µl of whole blood samples were stained with 2 µg/ml streptavidin-PE-Cy7, 1 µg/ml anti-CD71-allophycocyanin (APC) (clone R17217), 1 µg/ml anti-CD45–APC eFluor 780 (clone 30-F11) (eBioscience, San Diego, CA), 4 µM Hoechst 33342 (Sigma-Aldrich, St Louis, MO) and 12 µM JC-1 (Thermo Scientific, Waltham, MA) in MTRC. The samples were washed once with MTRC and further stained with 2 µg/ml streptavidin-PE-Cy7 to capture all biotin-labelled

cells. Immediately prior to analysing on flow cytometer, 5 µl of 123count eBeads (eBioscience, San Diego, CA) was added to determine the relative anaemic levels.

For both malaria infections and IVET assay, 2 µl of whole blood samples was stained with 2 µg/ml streptavidin-PE-Cy7 (only for experiments with biotinylated erythrocytes), 1 µg/ml anti-CD45–allophycocyanin (APC)–eFluor 780 (clone 30-F11), 1 µg/ml anti-CD71 (TFR1)–PerCP–eFluor 710 (clone R17217) (eBioscience, San Diego, CA), 4 µM Hoechst 33342 (Sigma-Aldrich, St Louis, MO) and 12 µM JC-1 (Thermo Scientific, Waltham, MA) in MTRC.

All samples analysed through flow cytometry were performed on BD LSRFortessa (BD Biosciences, Franklin Lakes, NJ), where 100,000 to 2,000,000 events were collected and visualized on FACSDiva^{TM} and FlowJo software. The RBCs and leukocytes were first selected on forward scatter and side scatter channels (FSC/SSC) signals, followed by gating of single cells based on FSC area to height ratio. RBCs were further isolated by gating on CD71 negative and CD45 negative population, followed by gating on Atto-labelled and Biotin-labelled erythrocytes on appropriate channels (APC for Atto-633, PE for Atto-565 and PE-Cy7 for Biotin). The parasitaemia of each labelled erythrocyte population was determined by gating on Hoechst 33342 positive and JC-1 positive population.

2.5 *In vitro P. falciparum* Culture Techniques

2.5.1 Maintenance of *in vitro P. falciparum* cultures

3D7 strain *P. falciparum* cultures (a gift from R. Anders, La Trobe University, Melbourne, Australia) were maintained in isolated type O+ RBC from the Australian Red Cross under 1% O_2 and 3% CO_2 in Complete Culture Media (CCM) at 37^0C. Parasitaemia levels were monitored using light microscopy every two days and sub-cultured when necessary, usually above 5% parasitaemia. The cultures were maintained up to fifteen passages before being replaced with a new frozen stock.

2.5.2 Isolation of late stage erythrocytic *P. falciparum*

70% Percoll® was first prepared by diluting 100% Percoll® (Sigma-Aldrich, St Louis, MO) with 10x RPMI and Red Cell Wash/Sorbitol (13.3% Sorbitol, 10 mM sodium phosphate, 160 mM NaCl, pH 7.4). Pelleted *P. falciparum* culture was layered gently on top of the Percoll® solution and centrifuged at 3500 rpm (2850 g) for 10 minutes without brakes. The top layer containing late stage *P. falciparum* was collected and washed twice with CCM wash (CCM without serum and Albumax®), and a small RBC smear was made. These cells were examined under light microscopy to determine the proportion of mature trophozoites.

2.5.3 *P. falciparum in vitro* invasion and growth assay

Blood from patients with hereditary spherocytosis was obtained from the Royal North Shore hospital by Dr David Rabbolini with informed consent (HREC 2014/715). The buffy coats were first removed via centrifugation and kept for DNA isolation and genome sequencing using Qiagen DNeasy blood and tissue kit (Qiagen, Venlo, Netherlands) according to the

manufacturer's instructions. The RBCs were collected and washed twice with CCM wash. Previously purified late stage *P. falciparum* was added to the control or patient's blood to give approximately 1% parasitaemia and diluted to 2.5% haematocrit with CCM, followed by distributing into a 24-well plate, 1ml in each well with four replicates. Blood smears were collected from each well every 6-24 hours for three days. The parasitaemia and parasite developmental stages were determined under light microscopy where at least 1,000 RBCs were counted. Alternatively, the samples were fixed with a 1 in 4 dilution of BD Cytofix™ Fixation Buffer (BD Biosciences, Franklin Lakes, NJ) in PBS, and analysed using flow cytometry (Section 2.4.5).

2.6 *In vitro* Expression of Recombinant Proteins

2.6.1 Plasmid design and cloning

Plasmids with inserts containing the cDNA for the human *ANK-1* protein residue 866-1068 (*ANK-1 Zu5*) and fragment containing the cDNA for the human β-spectrin protein residue 1517-1905 (*SPTB-1315*) and β-spectrin protein residue 1517-1905 with D1781R mutation (*SPTB-D1781R*), were purchased from Thermo Scientific. These fragments were amplified using PCR with primers that introduced new restriction sites for cloning into a GST-tag expression plasmid (pGEX-6P-3) (GE Healthcare Life Sciences, Arlington Heights, IL) as described below, and illustrated in Figure 2.1:

ANK-1 Zu5: BamHI and Xhol restriction sites

Forward: 5'-CTGATTGGATCCATGCCTGAGACAGTGGTGA-3'

Reverse: 5'-GGACATCTCGAGGTTACCGTGACATGATCACG-3'

SPTB-1315 and *SPTB-D1781R*: BamHI and Xhol restriction sites

Forward: 5'-GACTGTGGATCCATGAAGAAGAACCAGACACTG-3'

Reverse: 5'-GTAATACTCGAGTTAGAATTTATCCGCCGTG-3'

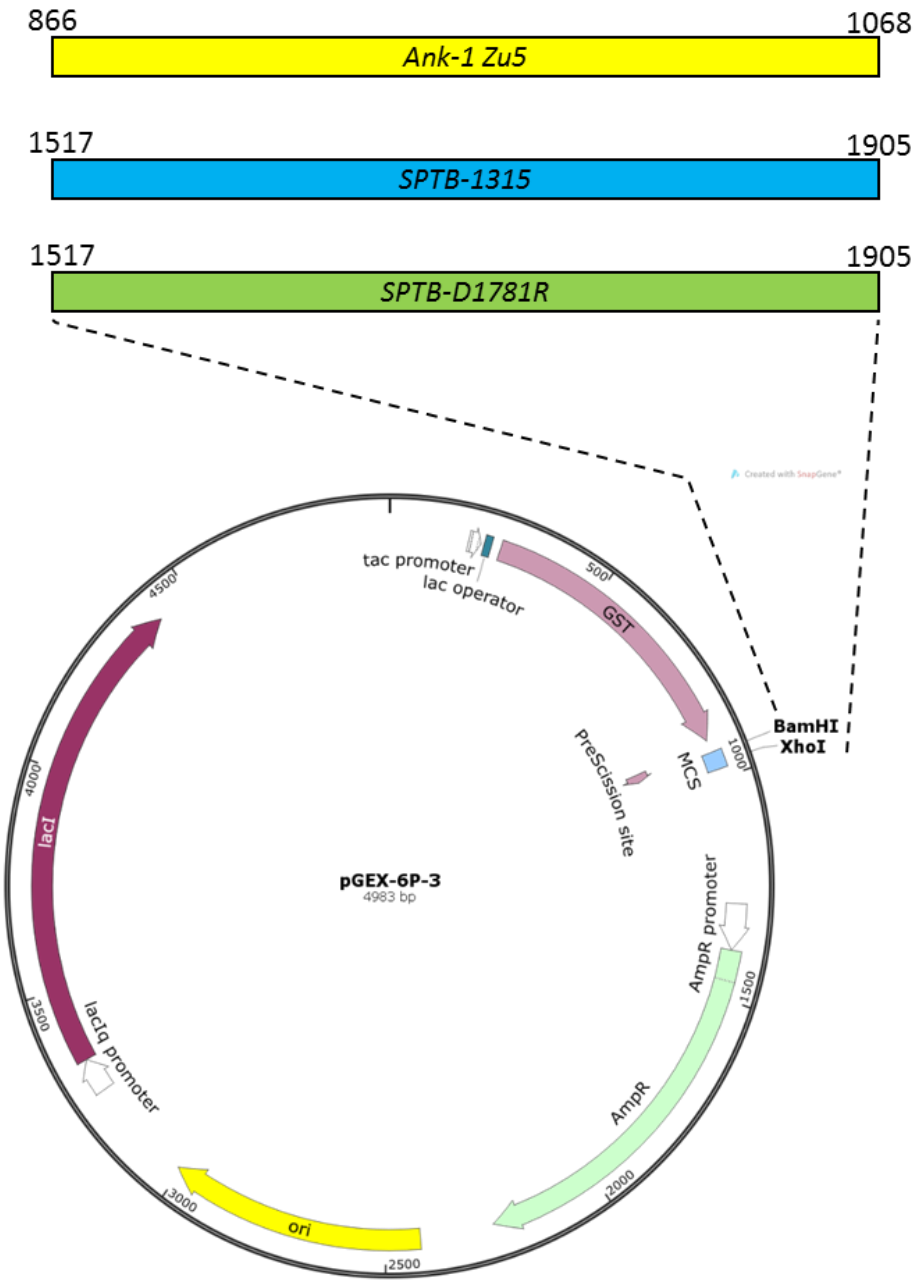

Figure 2.1: The plasmid map of GST-tagged proteins. The schematic diagram of pGEX-6P-3 showing the location and their associated restriction sites of *ANK-1_Zu5, SPTB-1315* and *SPTB-D1781R* inserts with their residue position in the native proteins.

For the His-tag expression plasmid, DNA fragments containing cDNA for the human β-spectrin protein residue 1583-1905 (*SPTB-1315*) and the mutated version (*SPTB-D1781R*) were inserted into 6xHis-tag expression plasmid (pRSET-A) and purchased from Thermo Scientific (Figure 2.2a).

The cDNA *ANK-1* protein residue 911-1068 (*ANK-1 Zu5*) were amplified with primers listed as below to introduce restriction sites for cloning into the pRSET-A plasmid backbone (Figure 2.2b):

ANK-1 Zu5: BamHI and HinDIII restriction sites into pRSET-A plasmid (for residues 911-1068)

Forward: 5'-CTGATTGGATCCACAGGGTTTCTGGTGAGC-3'

Reverse: 5'-GTAACTAAGCTT TTACCGTGACATGATCACG-3'

a)

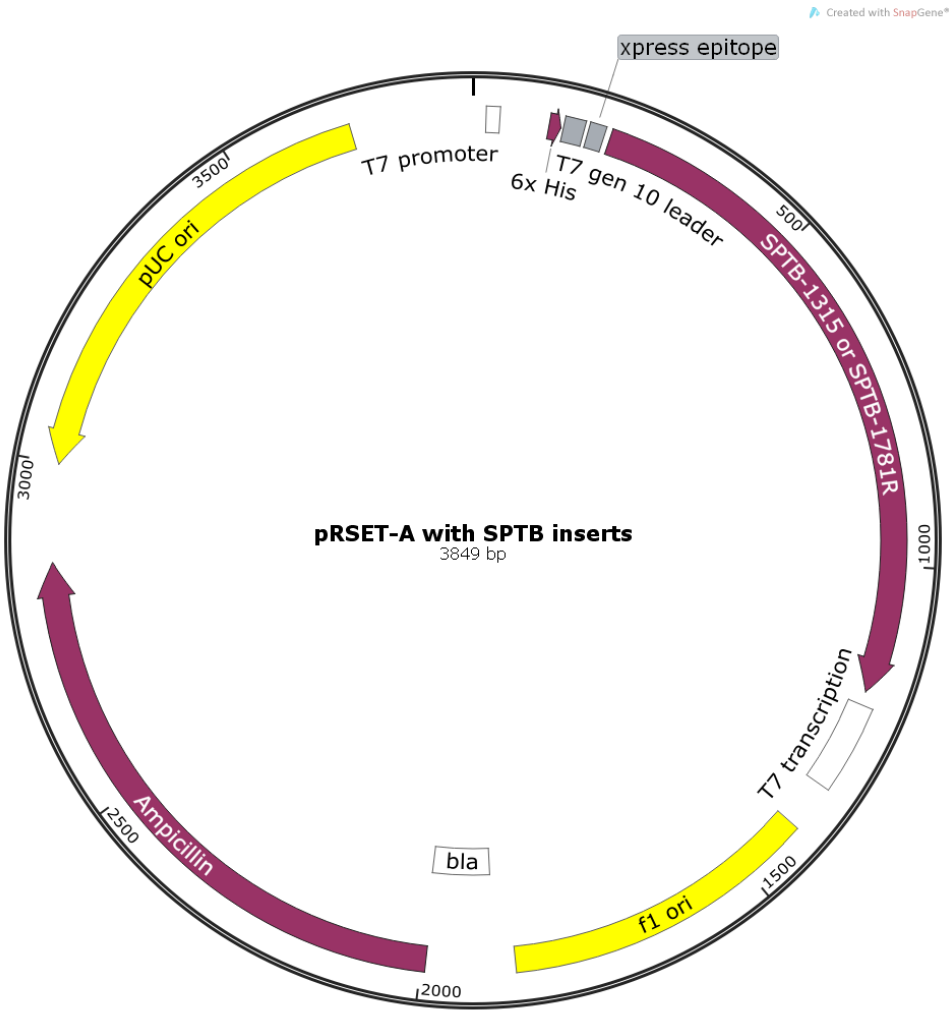

b)

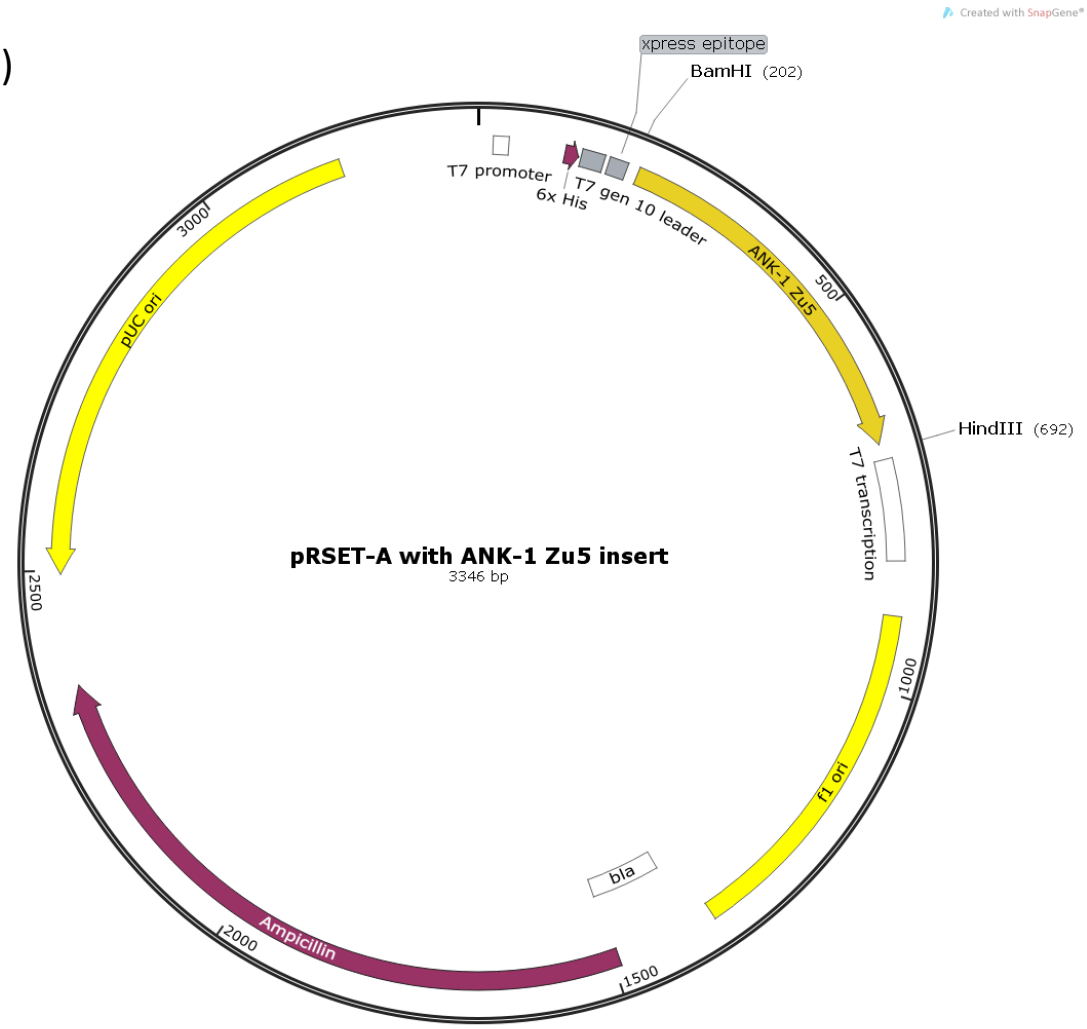

Figure 2.2: The plasmid maps of 6xHis-tagged proteins. The schematic diagram of pRSET-A plasmid with *SPTB-1315* or *SPTB-D1781R* inserts as purchased (a), and the cloned *ANK-1 Zu5* insert using BamHI and HinDIII restriction sites (b).

The PCR products were purified with Wizard® SV Gel and PCR Clean-Up System (Promega, Madison, WI) and restriction digested with appropriate enzymes according to the manufacturer's instructions (New England Biolabs, Ipswich, MA). The expression constructs were also restriction digested. The digested constructs and PCR products were then gel purified using QIAquick® Gel Extraction Kit (Qiagen, Venlo, Netherlands). The purified fragments were

ligated into the constructs using T4 DNA ligase (New England Biolabs, Ipswich, MA) in a 1:3 construct to fragments ratio overnight at 4°C according to the manufacturer's instructions.

2.6.2 Transformation of competent *Escherichia coli* (*E. coli*)

50-100 ng purified or ligated plasmid DNA was added into 30-50 µl of MAX Efficiency® DH5α™ Competent Cells (Thermo Scientific, Waltham, MA) or competent BL21 and incubated on ice for at least 30 minutes. It was then heat-shocked in water bath at 42^0C for 45 seconds and immediately cooled on ice for 2-5 minutes. 500-1000µl of lysogeny broth (LB) or Super Optimal Broth with Catabolite repression (SOC medium) (Thermo Scientific, Waltham, MA) was then added and incubated at 37^0C with shaking for 60-90 minutes. 200 µl of the culture was spread on an LB agar plate containing 100 µg/ml ampicillin. The plates were incubated overnight at 37^0C and the transformed colonies were isolated and amplified. The plasmid DNA from each amplified colony was extracted using PureLink® Quick Plasmid Miniprep Kit (Thermo Scientific, Waltham, MA), and PCR was conducted as described in Section 2.3.2, using the primers described below. Frozen stocks were prepared for long-term storage by adding 50% sterile glycerol with the culture in 1 to 1 ratio and stored at -80°C.

pGEX-6P-3 *SPTB-1315* and *SPTB-D1781R* primer sets:

A) Forward: 5'-ATATAGCATGGCCTTTGCAG-3'; Reverse: 5'-GATGATCTGTTCCCCCTCAG-3'

B) Forward: 5'-TGTGATGCTGAAGCGACATT-3'; Reverse: 5'-GGCACCCGTGTAGAAGTAGC-3'

C) Forward: 5'-ATCGCCCAGTGGAAGGAC-3'; Reverse: 5'-TCAGAGGTTTTCACCGTCATC-3'

pGEX-6P-3 *ANK-1 Zu5* primer sets:

A) Forward: 5'-GCGACCATCCTCCAAAATC-3'; Reverse: 5'-CTCCTGTGCTCCTTCCACAC-3'

B) Forward: 5'-GCCAGCAGGATCATAGCACT-3'; Reverse: 5'-GACAAGCTGTGACCGTCTCC-3'

For pRSET-A *ANK-1 Zu5*, genotyping was carried out using the same primers in Section 2.6.1.

2.6.3 Heterologous protein expression

A starter culture was first grown overnight from frozen stock in 5 ml of LB with 100µg/ml ampicillin (LB-A). The culture was then diluted to 250 ml with LB-A and incubated at 37^0C with shaking until the OD_{600} reached 0.5-1.0. 1 mM of Isopropyl β-D-1-thiogalactopyranoside (IPTG) was added to the culture to induce protein expression for 4 hours. The culture was centrifuged and the pellet was stored at -80^0C until needed.

For ANK-1 Zu5 protein expression at 16^0C, the culture was instead cooled on ice in a 4^0C room for an hour before adding 1 mM IPTG. The culture was then incubated at 16^0C for at least 16 hours before being harvested as described above.

2.6.4 Protein purification

For purification of GST-tagged proteins, frozen pellets were first resuspended in 20 ml PBS, followed by lysing with a French press. The lysates were then centrifuged at 20,000 g for 20 minutes at 4^0C and the supernatant was collected. The supernatant was loaded onto a 5 ml GSTrap HP column (GE Healthcare Life Sciences, Arlington Heights, IL) and purified via syringes according to the manufacturer's instructions. The proteins could either be treated with PreScission Protease (GE Healthcare Life Sciences, Arlington Heights, IL) before elution or eluted with GST-tag attached.

For His-tagged SPTB-1315 and SPTB-D1781R purification, the frozen pellets were first resuspended in 5 ml of lysis buffer (20mM sodium phosphate pH 8.0, 1 mg/ml lysozyme and protease inhibitor) and sonicated with 1 minute pulses (1 minute on, 1 minute off) for 5 times on ice. The lysates were then centrifuged at 20,000 g for 20 minutes at 4^0C and the supernatant

was collected. The supernatant was then diluted to 40 ml with 20 mM sodium phosphate pH 8.0 and loaded onto a High Performance Liquid Chromatography (HPLC) with 1 ml HiTrap™ Chelating column loaded with 0.25 M nickel sulphate (GE Healthcare Life Sciences, Arlington Heights, IL). The column was first washed with 30 mM imidazole for 20 minutes before eluting with 200 mM imidazole.

For His-tagged ANK-1 Zu5 purification, the frozen pellet were resuspended in 5 ml lysis buffer with 8 M urea, followed by sonication and centrifugation as described for His-tagged Sptb1315 purification. The supernatant was loaded onto HPLC as described above, followed by dialysis with Pur-A-Lyzer™ Midi Dialysis Kit with 3.5kDa cutoff (Sigma-Aldrich, St Louis, MO) to remove urea (and equilibrated with 1 M NaCl when stated). The proteins were then eluted with stepwise with up to 200-500 mM imidazole.

All fractions were analysed on SDS-PAGE, Coomassie and western blot to determine the presence and amount of purified protein.

2.6.5 Protein binding assay

The protein interaction was carried out on Biacore 2000 (GE Healthcare Life Sciences, Arlington Heights, IL) with the help of Dr Ante Jerkovic. Briefly, the purified GST-tagged SPTB-1315 and SPTB-D1781R and GST-cleaved ANK-1 Zu5 were first dialysed into Biacore Running Buffer. The Sensor Chip CM5 (GE Healthcare Life Sciences, Arlington Heights, IL) were purchased and coated with anti-GST antibody (Abcam, Cambridge, UK) according to the manufacturer's instructions, followed by the loading of GST-tagged SPTB-1315 and SPTB-D1781R proteins into two different chambers as the ligand for the binding assay. The binding assay was carried out as described by Ipsaro, et al. [396], where 0, 0.62, 1.25, 2.5, 5, 10, 20 µg/ml of GST-cleaved ANK-1 Zu5 were injected as analyte and the responses were recorded.

2.7 Statistical Analysis

The LOD score method coupled with Bonferroni correction was used to determine the causative mutation for ENU-treated mouse strains. All data sets were tested for normality using Shapiro-Wilk Normality Test (http://sdittami.altervista.org/shapirotest/ShapiroTest.html) [411]. The statistical significance of the malaria survival was tested using the Log-Rank test. The statistical significance of parasite infection was determined via the statmod software package for R (http://bioinf.wehi.edu.au/software/compareCurves) using the 'compareGrowthCurves' function with 10,000 permutation, followed by adjustments for multiple testing. The statistical significance for the ratios of IVET assays was determined using the one sample t-test with hypothetical mean of 1. For the rest of the results, statistical significance was determined using two-tailed Students t-tests, either through direct comparison or on the area under curves, with $P<0.05$ being statistically significant.

2.8 Recipes

MT-PBS (Mouse-tonicity phosphate buffered saline)

150mM NaCl

16mM Na_2HPO_4

4mM NaH_2PO4

Adjusted to pH 7.4

Annexin V Binding Buffer

150mM NaCl

10mM HEPES

25mM $CaCl_2$

CCM (Complete Culture Media)

500ml Roswell Park Memorial Institute (RPMI) medium

1.6% GlutaMAX™ Supplement

0.2% Albumax®

4% pooled human serum

10mM D-Glucose

25µg/ml gentamycin

6mM HEPES

0.2mM hypoxanthine

Red Cell Wash/Sorbitol

13.3% Sorbitol

10mM sodium phosphate

160mM NaCl

Adjusted to pH 7.4 and filter sterilise

MTRC (Mouse-tonicity Ringer's complete solution)

154mM NaCl

5.6mM KCl

1mM $MgCl_2$

2.2mM $CaCl_2$

10mM glucose

20mM HEPES

0.5% BSA

4mM EDTA

Adjusted to pH 7.4 and filter sterilise

Biacore Running Buffer

0.01 M HEPES pH 7.4

0.15 M NaCl

3 mM EDTA

0.005% v/v Surfactant P20

CHAPTER 3

ENU-INDUCED ANKYRIN-1 MUTATION MRI61689

3.1 Introduction

Malaria is a mosquito-borne disease caused by the protozoan *Plasmodium*, responsible for many deaths every year, mostly children [14]. In endemic regions with limited healthcare access, host genetics is one of the major determinants of malaria susceptibility and survival [89,94,97]. This is evident from the distributions of various genetic polymorphisms in humans, such as Duffy antigen negativity and sickle cell trait, which coincide with malaria distribution [97,158,160]. It is thought that these genetic polymorphisms confer protection against malaria, thus providing a survival advantage in the face of malaria-induced mortality [186,209].

In addition, these polymorphisms also provide crucial insights into host-parasite interactions. *Plasmodium* relies on a favourable host environment in order to thrive, many erythrocyte-related polymorphisms have been discovered that interfere with parasite survival thus contributing to malaria resistance. These include polymorphisms that affect the cytoskeleton of erythrocytes, such as Southeast Asian Ovalocytosis (SAO), hereditary elliptocytosis (HE) and spherocytosis (HS) [182,183,185,188,193]. Several hypotheses have been proposed for the mechanisms by which they confer malaria protection, including reduced erythrocyte invasion, intra-erythrocytic growth and cytoadherence [186,191-193,232,256,257,282]. However, due to the heterogeneity of the manifestation of these disorders in the human population, contradicting evidences for resistance mechanisms has often been presented. A study done by Facer [193] showed that only patients carrying certain spectrin mutations have impaired parasite invasion of red blood cells (RBC), but not others that also exhibited HE symptoms. A similar observation was reported by Chishti, et al. [192], where individuals with defective protein 4.1 exhibited intra-erythrocytic growth inhibition, but not those with glycophorin C defects, despite the fact that both defects gave rise to HE. These differences in malaria resistance mechanisms remained largely unexplored, and further studies in this aspect would potentially provide useful insight into host-parasite interactions.

The RBC cytoskeletal protein ankyrin-1 (ANK-1), is a 210kDa protein responsible for connecting the spectrin network with the RBC membrane through interactions with band 3, protein 4.2 and the Rhesus complex [393,412,413]. Spherocytosis is a genetic disorder where RBCs are abnormally small and are known as spherocytes. ANK-1 mutations account for more than 50% of human HS cases [201]. However, similar to SAO and HE, HS is a heterogeneous disorder where the symptoms vary greatly depending on the mutations. The disorder can range from asymptomatic through to severe anaemia requiring splenectomy [414]. Despite a possible association with malaria, HS is actually common in Northern European and Japanese populations with frequency of about 1 in 2000 individuals [196-198,415], but much rarer in other populations [194]. Nevertheless, several *in vitro* and *in vivo* studies have repeatedly reported association between HS and malaria resistance, and several mechanisms have been suggested. An *in vitro* study done by Schulman, et al. [191] using RBCs from HS patients suggested that parasite invasion and growth in these erythrocytes was impaired. This is further supported by studies done in mice with ankyrin-1 mutations. Both *Ank-1*$^{(nb/nb)}$ and *Ank-1* $^{(MRI23420/+)}$ have shown inhibited intra-erythrocytic growth and erythrocyte invasion possibly due to spectrin and ankyrin deficiency, respectively [189,204]. On the other hand, another mutation described by Rank, et al. [190], *Ank-1*$^{1674/+}$, parasite invasion appeared to be normal in these erythrocytes. Instead, increased erythrocyte fragility was proposed as a contributing factor for increased malaria resistance [190]. Taking these observations together, it is possible that disruption to erythrocyte cytoskeletons can mediate multiple mechanisms of resistance.

In a large phenotypic N-ethyl-N-nitrosourea (ENU) mutagenesis screen, using either abnormal red cells or resistance to malaria as to the screened phenotypes, we identified many novel mutations that give rise to RBC abnormalities and consequently malaria resistance in mice. As part of the discovery process for HDT candidate gene for malaria, I further characterised these genes and examined the role they played during malaria infections. It is reported here an ENU-induced mutation in the ankyrin-1 gene (*Ank-1*$^{(MRI61689)}$) which was found to exhibit a HS-like

phenotype, with significantly lower RBC volumes, increased osmotic fragility and decreased deformability. *Ank-1*$^{(MRI61689)}$ also confers resistance towards *Plasmodium chabaudi adami* infection in mice, and *Ank-1*$^{(MRI61689/+)}$ mice were shown to show both reduced merozoite invasion and increased RBC clearance, possibly as a consequence of reduced red blood cell deformability.

This work has previously been published and presented here as a direct excerpt from: Huang, H. M., D. C. Bauer, P. M. Lelliott, A. Greth, B. J. McMorran, S. J. Foote and G. Burgio (2016). "A novel ENU-induced ankyrin-1 mutation impairs parasite invasion and increases erythrocyte clearance during malaria infection in mice." *Sci Rep* **6**: 37197. This work investigated the effect of MRI61689 mutation on the manifestation of HS-like phenotypes, as well as highlighting the complex roles of ankyrin-1 in mediating malaria resistance.

3.2 Results

3.2.1 The MRI61689 mutation gives rise to a hereditary spherocytosis-like phenotype

To identify genes associated with malaria susceptibility, ENU-treated male B6.BKS (D)-Lepr^{db}/J mice (G0) was crossed with isogenic female mice to produce G1 progeny with random point mutations across the genome. Genes affecting RBCs are hypothesised to be associated with malaria protection, therefore, a haematological screening was performed on these G1 mice and those exhibiting abnormal blood parameters were selected for further studies. The G1 mouse carrying the MRI61689 mutation was initially identified from an unrelated ENU suppressor screen for the recessive mutation db/db. The G1 MRI61689 exhibited abnormal blood parameters on an ADVIA haematological analyser, with reduced mean corpuscular volume (MCV) of 48.6fl compared to the background of 53.3±0.5fl. The MCV value from the B6.BKS (D)-Lepr^{db}/J background is comparable to C57BL/6 mice. The G1 founder mouse was crossed with B6.BKS (D)-Lepr^{db}/J to produce G2 mice where approximately half of the animals exhibited an abnormal phenotype (Table 3.1). The affected G2 progeny, which were obligate heterozygotes for the ENU-induced mutation, showed reduction in MCV (46.1±0.2fl) compared to unaffected progeny (51.4±0.4fl), lower mean corpuscular haemoglobin (MCH) (13.5±0.1pg compared to 14.6±0.1pg of wild-type), elevated RBC count (11.1±0.1x10^9 cells/ml compared to 10.5±0.1x10^9 cells/ml of wild-type) (Table 3.1). No differences were observed for total haemoglobin (HB), mean corpuscular haemoglobin concentration (MCHC), white blood cell (WBC) count, platelets count (PLT) or reticulocyte percentage (Table 3.1).

Table 3.1: **The complete blood count of *Ank-1*$^{(MRI61689/+)}$ mice.**

	WBC (x10^6 /ml)	RBC (x10^9 /ml)	HGB (g/L)	MCV (fl)	MCH (pg)	MCHC (g/L)	PLT (x10^6 /ml)	% Retics
Wild type	8.7±0.5	10.5±0.1	153.2 ±2.2	51.4±0.4	14.6±0.1	283.6± 2.8	1151± 57	2.69± 0.26
Ank-1$^{(MRI61689/+)}$	11.9± 4.5	11.1±0.1	151.2 ±1.4	46.1±0.2	13.5±0.1	281.4± 9.3	1151± 61	2.24± 0.21
p-values	NS	P<0.01	NS	P<0.001	P<0.001	NS	NS	NS

The haematological parameters of *Ank-1*$^{(MRI61689/+)}$ compared to wild-type mice (n=19-25). WBC = white blood cell count; RBC = red blood cell count; HGB = haemoglobin; MCV = mean corpuscular volume; MCH = mean corpuscular haemoglobin; MCHC = mean corpuscular haemoglobin concentration; PLT = platelet concentration; %Retics = percentage of reticulocytes. P values were calculated using Student's t-tests, and data were presented as mean ± SEM.

However, when two affected mice were intercrossed, a quarter of the pups were found to die within 1 week postnatally, suggesting homozygosity for MRI61689 might be incompatible with life. Blood smears were taken from these pups and compared with the other affected and unaffected mice. The heterozygotes have slightly smaller RBCs but no target cells or spherocytes were observed (Figure 3.1a). Conversely, homozygous mice had significantly smaller RBCs with anisocytosis, fragmented RBCs, acanthocytes and reticulocytosis (Figure 3.1a). Under SEM, RBCs of heterozygous mice seemed to have less distinct discoid shape, but otherwise no distinguishing features were observed. (Figure 3.1b). On the other hand, the RBCs of homozygous mice appeared very deformed, acanthocytic and appeared to lack the discoid shape (Figure 3.1b). When subjected to osmotic stress, RBCs of heterozygous mice showed significantly increased fragility compared to wild-type erythrocytes (with 50% haemolysis at approximately 5.6 g/L compared to 4.5 g/L of wild-type) (Figure 3.1c). The RBC deformability was assessed using an *in vitro* spleen retention assay by filtering RBCs through a layer of beads with varying sizes. This is thought to model splenic filtration *in vivo*, with retention thought to indicate reduced

deformability. As shown in Figure 3.1d, up to 70% of the RBCs from heterozygous MRI61689 mice were retained within the bead layer compared to 3.5% of wild-type RBCs, suggesting a significantly reduced RBC deformability in the presence of this ankyrin-1 mutation.

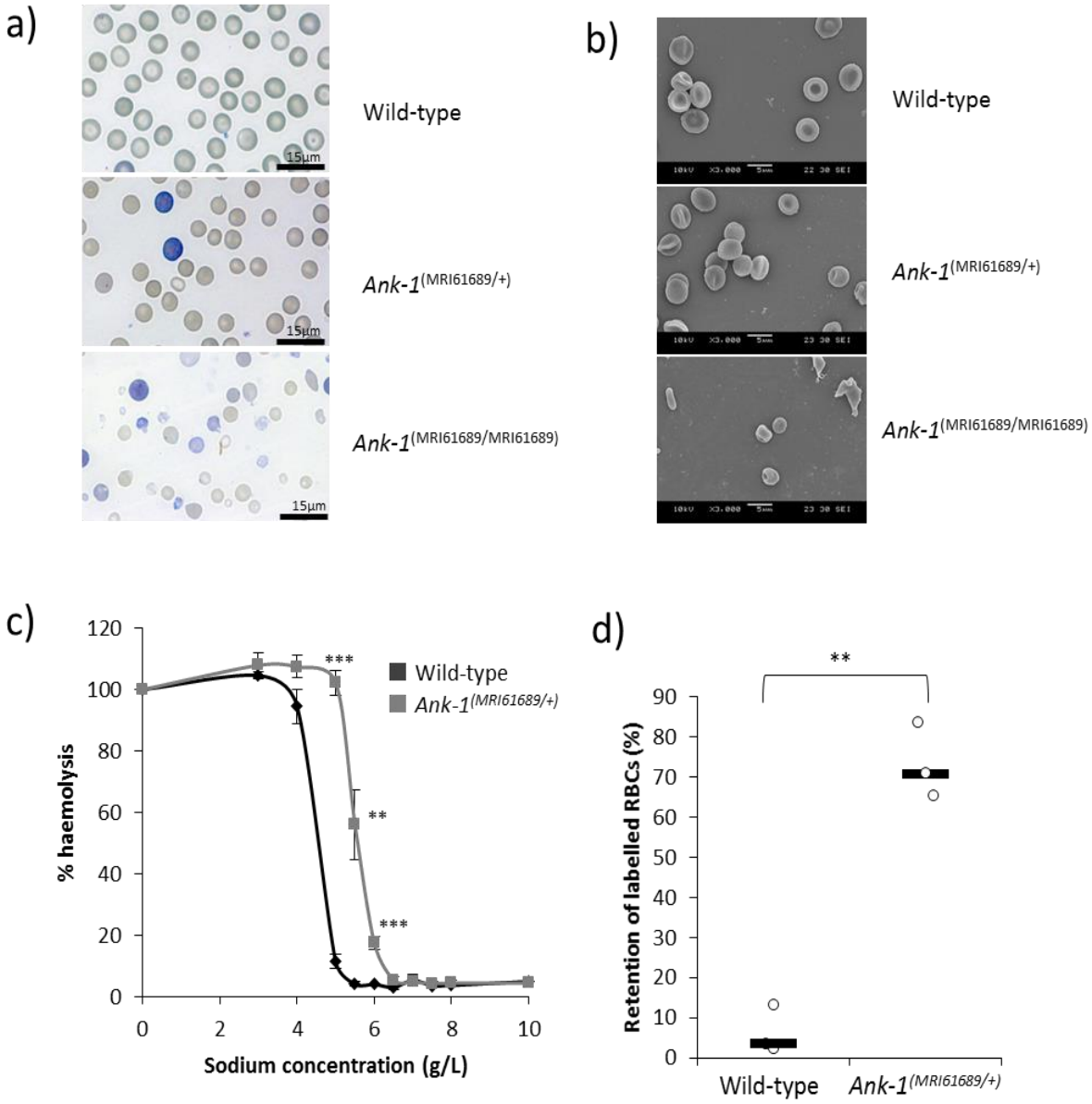

Figure 3.1: The phenotypic characterisation of *Ank-1*$^{(MRI61689/+)}$ mice. The morphology of *Ank-1*$^{(MRI61689/+)}$ and *Ank-1*$^{(MRI61689/MRI61689)}$ erythrocytes under light microscopy with Giemsa stain (a) and scanning electron microscopy (b). The osmotic fragility curve of wild-type and *Ank-1*$^{(MRI61689/+)}$ erythrocytes when subjected to osmotic stress (c) (n=5-7 mice per group). The *in-vitro* spleen retention rate of wild-type and *Ank-1*$^{(MRI61689/+)}$ erythrocytes when passing through filter beds (d) (n=3 mice per group). P values were calculated using parametric Student's t-test. ** indicates P<0.01, *** indicates P<0.001, and all error bars are standard error of mean (SEM).

3.2.2 MRI61689 carries a splice site mutation in Ank-1 gene resulting in an alternative transcript and exon skipping

To identify the causative mutation responsible for this abnormal RBC count, the exomes of 2 heterozygous mice were sequenced. Exome sequencing revealed a number of variants. These were prioritised based on filters as shown in Table 3.2. Through further genotyping using Sanger sequencing, a mutation in *Ank-1* gene was found to correlate with all the affected mice and was proven to segregate perfectly with the reduced MCV for over 3 generations of mouse crosses. The mutation was found in the 17-18 intron of *Ank-1* gene, with T to A transversion 11 base pair upstream of exon 18 (IVS17-11T>A) (Figure 3.2a). This is situated in the ankyrin-repeats domain involved in band 3 binding. It was proposed that the mutation introduced a new acceptor splice site for exon 18, potentially leading to a frameshift mutation.

Table 3.2: The identification of MRI61689 mutation.

Chromosome	Gene name	Location	Reference base	Variant base	Number of mutant mice with mutation	LOD score (Threshold: 2.08)
9	*Acp5*	22129643	C	A	(3/8)	-0.32
8	*Kcnk1*	126025024	C	T	(4/8)	0
17	*Epas1*	86825679	A	T	(0/8)	-2.33
7	*Picalm*	90165538	G	T	(0/8)	-2.33
18	*Socs6*	88869240	A	G	(5/8)	0.32
8	*Ank-1*	23106019	T	A	(8/8)	2.33

Six variants were selected from the exome sequencing, each mutation was sequenced in *Ank-1*$^{(MRI61689/+)}$ mice and the number of mutant mice carrying each mutation was determined and LOD score was calculated based on Chi-squared distribution, with LOD threshold being 2.08, adjusted using Bonferroni's correction (n=8 mice).

To assess this hypothesis, transcript analysis was performed. Embryonic liver RNA was extracted, cDNA was synthesized and PCR-amplified using primers listed in the experimental procedures. Figure 3.2b shows the PCR products of embryonic liver cDNA from non-mutant, *Ank-1*$^{(MRI61689/+)}$ and *Ank-1*$^{(MRI61689/MRI61689)}$ when amplified using primer set 1, which covers exon 17 to 21. Bands of approximately 400bp can be observed in all the genotypes, but *Ank-1*$^{(MRI61689/MRI61689)}$ also exhibited a second smaller product of approximately 300bp length. It is likely that this second band was the product of exon skipping. Sanger sequencing of these PCR products revealed that the 300bp product lacked exon 18, confirming that the exon 18 was skipped, and exon 19 was directly connected to exon 17 during transcription (Figure 3.2c). This transcript is predicted to produce a shortened, in-frame 207kDa ANK-1 protein.

To examine the effect of MRI61689 mutation in heterozygous mice, a primer set containing the predicted acceptor splice site (primer set 2) was designed. Figure 3.2d shows that the mutant transcript is only present in *Ank-1*$^{(MRI61689/+)}$ and *Ank-1*$^{(MRI61689/MRI61689)}$ mice, as predicted. Further Sanger sequencing revealed an insertion of 11bp into the transcript adding an additional donor splicing site and causing a frameshift mutation in the exon that would result in a premature stop codon at amino acid position 724, as illustrated in Figure 3.2e, thus giving rise to a truncated protein of 78.5kDa. Therefore, the homozygous mice exhibit a mutation at 11 bp upstream of the exon 18 donor splicing site resulting in two alternative transcripts: the skipping of exon 18 and an 11bp insertion and creation of an additional donor splicing site leading to frameshift mutation that would result in a premature stop codon and a truncated protein.

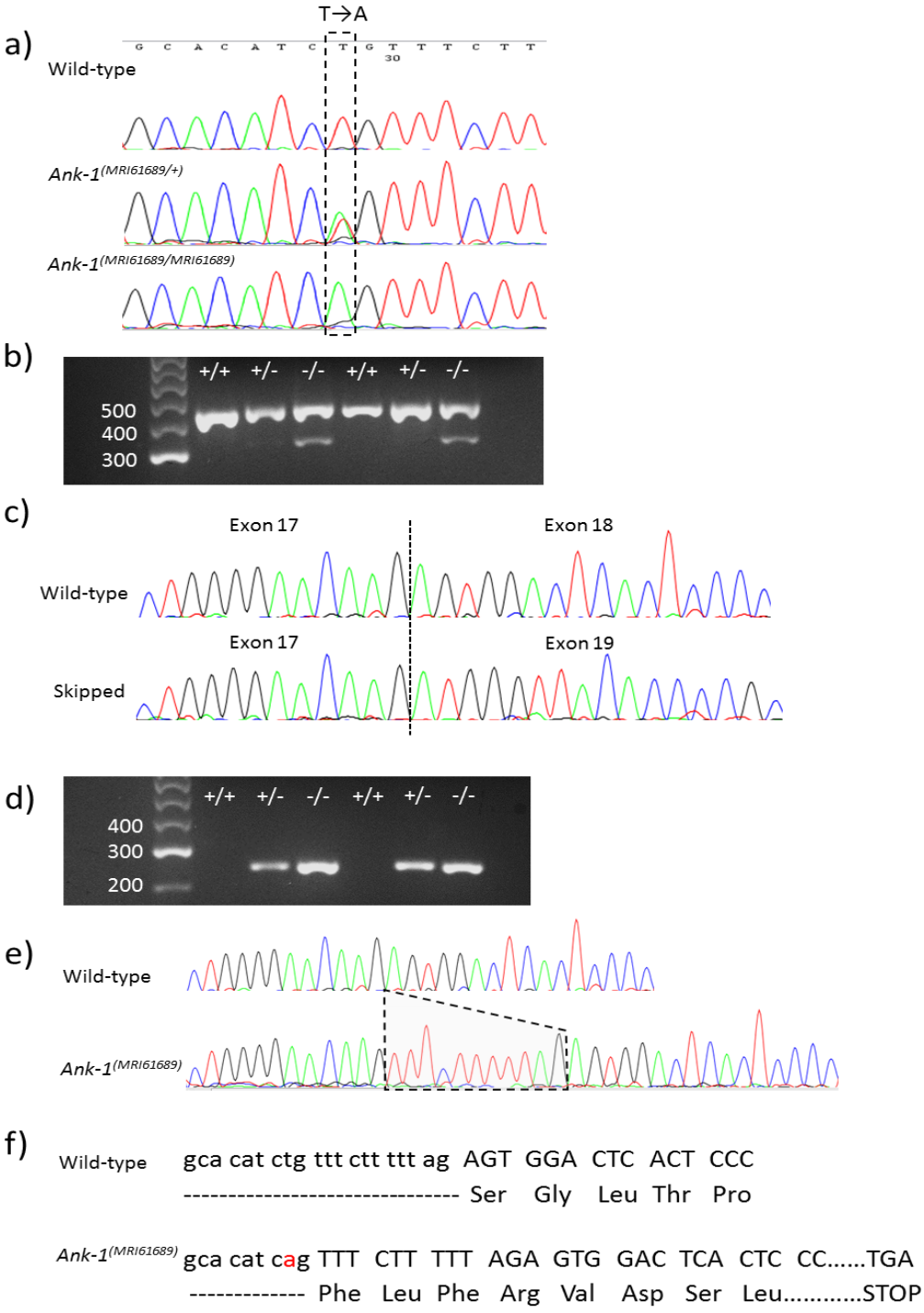

Figure 3.2: The identification of *Ank-1*$^{(MRI61689)}$ mutation and its effects on transcription. The sequencing of *Ank-1*$^{(MRI61689)}$ mutation, showing a T to A transversion (a). Gel electrophoresis of amplified cDNA product from wild-type, *Ank-1*$^{(MRI61689/+)}$ and *Ank-1*$^{(MRI61689/MRI61689)}$ embryonic livers with primers that spanned the exon 17 to 21 of ankyrin-1 cDNA (primer set 1) (b). The sequencing results of both bands, showing exon skipping in the abnormal transcript of *Ank-1*$^{(MRI61689/MRI61689)}$ embryonic liver (c). Gel electrophoresis of amplified cDNA product from wild-type, *Ank-1*$^{(MRI61689/+)}$ and *Ank-1*$^{(MRI61689/MRI61689)}$ embryonic livers with primers that contained the predicted 11bp insertion (primer set 2) (d). Sequencing result showing an 11bp insertion between exon 17 and 18 cDNA of the *Ank-1*$^{(MRI61689)}$ transcript (e). The predicted effect of the insertion on the translation of ankyrin-1, showing a frameshift and a premature chain termination (f).

This mutation was likely to reduce the *Ank*-1 expression levels. Therefore, this hypothesis was assessed by examining the gene expression levels of *Ank-1* in embryonic liver using qPCR at mRNA level and Western blotting at protein level in mature RBCs. As shown in Figure 3.3a, *Ank-1* mRNA levels in both *Ank-1*$^{(MRI61689/+)}$ and *Ank-1*$^{(MRI61689/MRI61689)}$ E14 embryonic livers were significantly reduced, up to 60% and 80% reduction compared to the wild-type, respectively, which supported our hypothesis. However, no significant reduction in the full length ANK-1 (210kDa) protein levels was observed in both Coomassie staining and Western blotting (Figure 3.3b-d). No truncated form of ANK-1 (78.5kDa) was observed in *Ank-1*$^{(MRI61689/+)}$ erythrocytes. Furthermore, no reduction was observed for the protein levels of other cytoskeletal proteins, including band 3, protein 4.2, alpha- and beta-spectrin (Figure 3.3b and c, Supp. Figure 3.1). This suggested that erythrocyte protein levels might be compensated by the WT allele in *Ank-1*$^{(MRI61689/+)}$ mice, and the reduction in *Ank-1* mRNA levels did not seem to affect the protein levels.

3.2.3 *Ank-1*$^{(MRI61689/+)}$ mice are resistant to *Plasmodium chabaudi* infection

It was hypothesised that the *Ank-1*$^{(MRI61689)}$ mutation would confer malaria resistance. The malaria susceptibility of *Ank-1*$^{(MRI61689/+)}$ mice was examined by injecting a lethal dose of *Plasmodium chabaudi adami DS*, a murine strain of malaria that models the *Plasmodium falciparum* erythrocytic stage [416], which invades erythrocytes of all ages. The *Ank-1*$^{(MRI61689/+)}$ mice exhibited significantly lower peak parasitaemia, with only approximately 13% parasitaemia compared to 52% parasitaemia of wild-type (Figure 3.4a) but no delay in the appearance of parasites was observed. In addition, *Ank-1*$^{(MRI61689/+)}$ have a significantly increased survival rate, where all the *Ank-1*$^{(MRI61689/+)}$ mice survived the infection (Figure 3.4b) compared to the 16% survival of wild-type mice. Since *Ank-1*$^{(MRI61689)}$ directly affects the red cell (cytoskeletal protein), the malaria resistance was likely due to a RBC-autonomous effect.

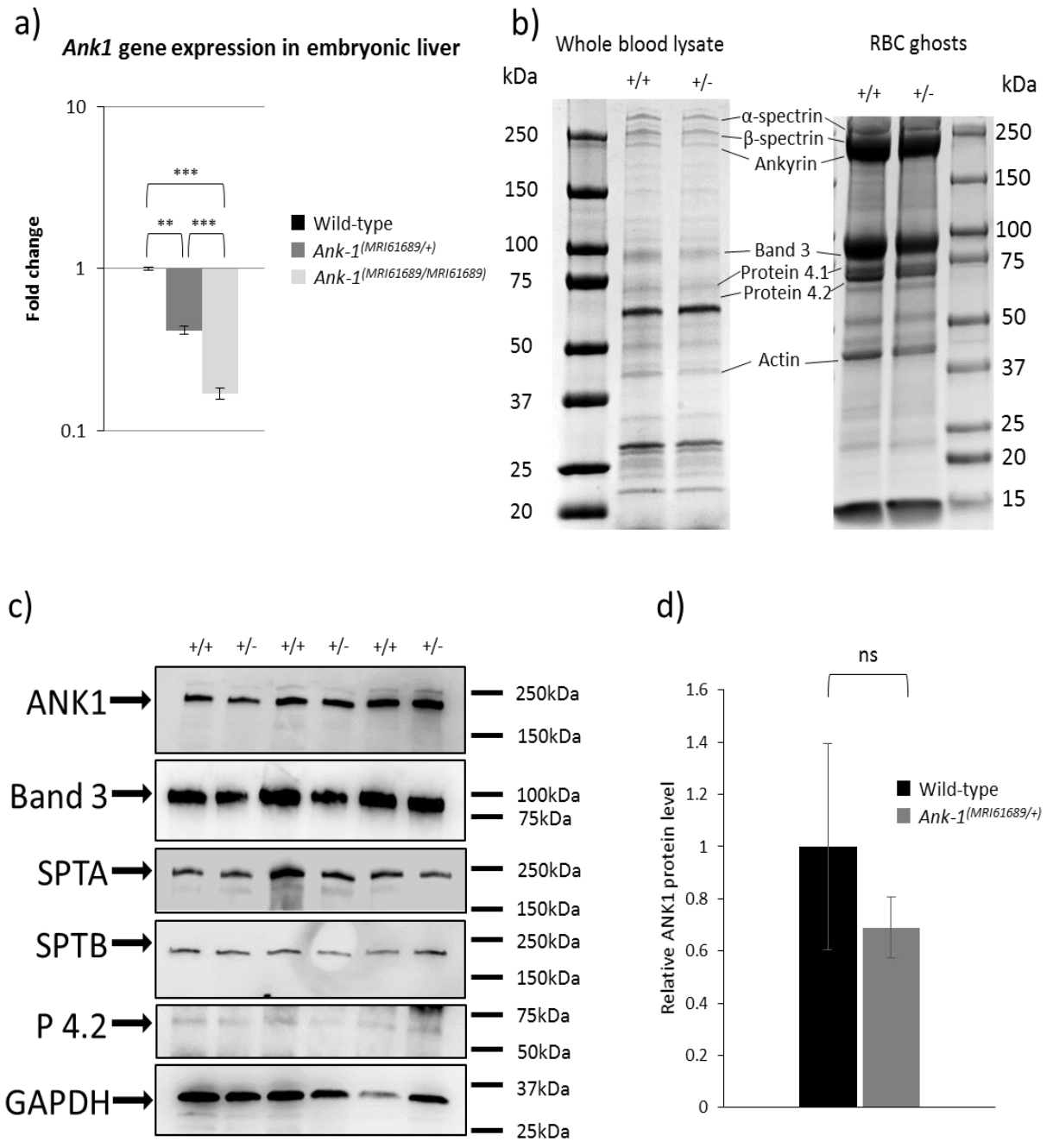

Figure 3.3: The effect of *Ank-1*$^{(MRI61689)}$ mutation on the *Ank-1* expression. Quantitative PCR showing the ankyrin-1 mRNA levels in both *Ank-1*$^{(MRI61689/+)}$ and *Ank-1*$^{(MRI61689/MRI61689)}$ embryonic liver (a). The protein levels of various cytoskeletal proteins examined with Coomassie (b). Representative Western blot images for ankyrin-1 (ANK1), Band 3, alpha-spectrin (SPTA), beta-spectrin (SPTB), protein 4.2 (P 4.2) and Glyceraldehyde 3-phosphate dehydrogenase (GAPDH) housekeeping gene in RBC membrane(c). The quantitative analysis of ankyrin-1 (d) (n=3 replicates per group). P values were calculated using Student's t-test. **P<0.01, ***P<0.001, error bars indicate SEM.

Therefore, three mechanisms of *P. chabaudi* resistance in *Ank-1*$^{(MRI61689/+)}$ mice were postulated. Firstly, the maturation of parasite inside the *Ank-1*$^{(MRI61689/+)}$ erythrocytes could be impaired leading to reduced growth and death of parasites [189]. Secondly, the *Ank-1*$^{(MRI61689/+)}$ erythrocytes might be resistant to merozoite invasion, which resulted in reduced parasitaemia and delayed course of infection [257]. Finally, the infected *Ank-1*$^{(MRI61689/+)}$ erythrocytes might more prone to destruction during the course of infection (increased clearance), thus posing a challenge for the parasite to establish a successful infection [205].

3.2.4 *Ank-1*$^{(MRI61689)}$ does not impair the intra-erythrocytic growth of *P. chabaudi*

To elucidate the possible mechanisms of resistance, the effect of the *Ank-1*$^{(MRI61689/+)}$ mutation on parasite intra-erythrocytic growth was investigated using the TUNEL assay at 1-10% parasitaemia. TUNEL detects DNA fragmentation, a marker for apoptosis or necrosis. In conjunction with a DNA fluorescent dye, DAPI, it is possible to detect dying parasites in the erythrocytes (Figure 3.4c) [189,417]. The TUNEL-positivity of *P. chabaudi* in *Ank-1*$^{(MRI61689/+)}$ erythrocytes was measured during the late trophozoite stage of the infections, which was the portion of the parasite lifecycle affected by the *Ank1* mutation in the *Ank-1*$^{(MRI23420/+)}$ line. As shown in Figure 3.4d, no differences was observed in the percentage of TUNEL-positive parasites in both wild-type and *Ank-1*$^{(MRI61689/+)}$ erythrocytes (24.7 ± 2.3% in *Ank-1*$^{(MRI61689/+)}$ mice compared to 29.5 ± 2.9% in wild-type). This indicated that *Ank-1*$^{(MRI61689)}$ did not impair parasite intra-erythrocytic growth.

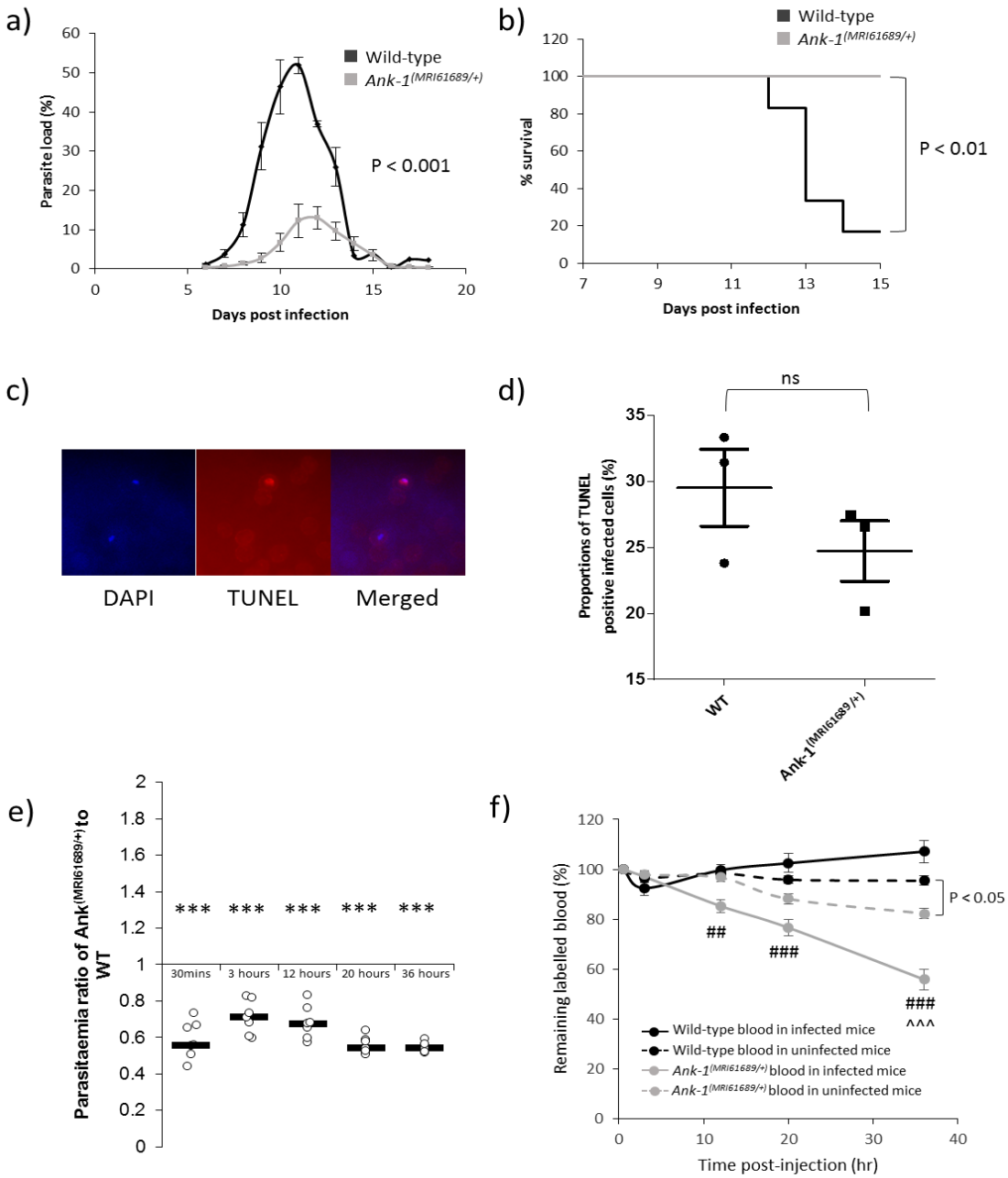

Figure 3.4: The response of *Ank-1*$^{(MRI61689/+)}$ mice to malaria infection. The parasite load of wild-type and *Ank-1*$^{(MRI61689/+)}$ mice when infected with 1x10^4 *P. chabaudi* (a) and the associated survival curve (b). Parasite intra-erythrocytic growth was assessed through TUNEL assay at 1-10% parasitaemia during late trophozoite stage, as visualised from immunofluorescent images showing presence of parasites and TUNEL-positive parasites (c). The number of TUNEL-positive parasites in both wild-type and *Ank-1*$^{(MRI61689/+)}$ mice were counted and expressed as a percentage (d) (n=3). For parasite invasion and RBC clearance, The IVET assay was done showing the ratio of infected *Ank-1*$^{(MRI61689/+)}$ to wild-type erythrocytes over 36 hours (e) and the relative number *Ank-1*$^{(MRI61689/+)}$ and wild-type erythrocyte in both infected and uninfected mice (f) during *P. chabaudi* infection (n=7 mice per group). P values for (a) and (b) were calculated using permutation test and Log-Rank test, respectively, p value for (d) - (f) was calculated using Student's t-test, with hypothetical mean of 1 for (e). ** indicates P<0.01, *** indicates P<0.001, ## and ### indicates P<0.01 and P<0.001 respectively when compared to wild-type RBC number in infected mice, whereas ^^^ indicates P<0.001 when compared to *Ank-1*$^{(MRI61689/+)}$ RBC number in uninfected mice. Error bars indicate SEM.

3.2.5 *Ank-1*$^{(MRI61689/+)}$ erythrocyte is resistant to *P. chabaudi* invasion, and have increased clearance from circulation

Erythrocyte invasion and clearance were assessed via an *in vivo* erythrocyte tracking (IVET) assay. Labelled blood of wild-type and *Ank-1*$^{(MRI61689/+)}$ mice were injected into infected wild-type mice during merozoite invasion to examine the ability of *Plasmodium chabaudi* to invade and grow within erythrocytes of both genotypes. The result compared the percentage of parasitized cells of both genotypes and expressed as a ratio of parasitaemia in *Ank-1*$^{(MRI61689/+)}$ RBC to wild-type RBC populations. As shown in Figure 3.4e, lower parasitaemia ratio (approximately 0.55) was observed from 30 minutes after injection with labelled blood, and was consistently lower in *Ank-1*$^{(MRI61689/+)}$ blood over 36 hours post injection, which indicates a lower invasion rate into the *Ank-1*$^{(MRI61689/+)}$ RBCs. Additionally, the remaining proportion of labelled RBCs was also monitored over the course of the assay. A significant reduction of *Ank-1*$^{(MRI61689/+)}$ erythrocytes in infected mice compared to wild-type erythrocytes was observed, with up to a 45% reduction in *Ank-1*$^{(MRI61689/+)}$ RBC number compared with wild-type (Figure 3.4f). On the other hand, a smaller reduction was observed for *Ank-1*$^{(MRI61689/+)}$ erythrocytes compared to wild-type in uninfected mice, suggesting *Ank-1*$^{(MRI61689/+)}$ RBCs are more likely to get cleared from circulation during malaria infection. As the percentage of infected erythrocytes was low (5-20%) (Supp. figure 3.3), this indicates that the majority of the RBCs getting cleared were uninfected RBCs, possibly as a result of bystander effect. This experiment suggested that two possible mechanisms of resistance are both operating to produce the lower parasitaemia and increased survival in *Ank-1*$^{(MRI61689/+)}$ mice, the reduction of parasite invasion and increased clearance of *Ank-1*$^{(MRI61689/+)}$ RBCs.

3.3 Discussion

3.3.1 Summary of findings

A novel mutation in *Ank-1* gene, MRI61689, is reported here to cause a hereditary spherocytosis-like phenotype, with reduced MCV, increased osmotic fragility and reduced deformability. MRI61689 is an intronic mutation between exon 17 and 18 where two possible splice variants could arise, one has an introduced acceptor site resulting a frameshift, whereas the other consists of a skipped exon 18. The *Ank-1* mRNA levels were reduced, but no reduction in protein levels were observed. The predicted truncated form (78.5kDa) was also not observed. *Ank-1*$^{(MRI61689/+)}$ mice also have increased resistance to *Plasmodium chabaudi* infections, and the erythrocyte invasion was impaired but the intra-erythrocytic growth appeared normal. The *Ank-1*$^{(MRI61689/+)}$ RBCs were also more likely to be cleared from circulation during infection, an observation independent of number of parasitized erythrocytes.

3.3.2 *Ank-1*$^{(MRI61689)}$ is unique but comparable to other ankyrin-1 mutations in human and mice

In comparison of *Ank-1*$^{(MRI61689)}$ mice to other previously described *Ank-1* mouse models, they appeared comparable to *Ank-1*$^{(MRI23420)}$ mice, but more severe than *Ank-1*^{1674} and *Ank-1*^{nb} mice. More specifically, most homozygous *Ank-1*$^{(MRI61689)}$ mice died within a week after birth, similar to homozygous *Ank-1*$^{(MRI23420)}$ mice, while homozygous *Ank-1*^{1674} and *Ank-1*^{nb} mice were viable [190,204]. However, no notable differences were observed in heterozygous *Ank-1*^{MRI61689} mice in terms of their RBC microcytosis, morphology and susceptibility to osmotic stress compared to heterozygous *Ank-1*^{1674} and *Ank-1*$^{(MRI23420)}$ mice [189,190]. However, similar to *Ank-1*$^{1674/+}$ mice and unlike *Ank-1*$^{(MRI23420/+)}$ mice, *Ank-1*$^{(MRI61689/+)}$ mice exhibited similar levels of ankyrin-1 and other

RBC cytoskeletal protein to wild-type, which might suggest compensation by the wild-type allele, and thus warrants further studies.

In humans, many *ANK-1* mutations that result in frameshift have been described, most of which situated in the band 3 binding domain towards the N terminus [394,418]. While no *Ank-1*$^{(MRI61689)}$ homologous mutation has been described in humans, a frameshift mutation has been reported to be in the exon 17, called Ankyrin Osaka I, which gave rise to symptomatic HS [418]. Furthermore, exon skipping in human *ANK-1* gene has also been documented. Edelman, et al. [419] reported a HS patient exhibiting a severe ankyrin-deficient HS due to an introduction of a new splice acceptor site for exon 17, known as ankyrin^{Ankara}. Under further examination, this mutation was found to give rise to multiple splice forms, including insertions and skipped exons. Most splice forms with insertion were expected to cause frameshift, potentially leading to premature termination of ankyrin [419]. This finding is in agreement with the observation in *Ank-1*$^{(MRI61689/MRI61689)}$ mice, where frameshift caused by new splice acceptor site, leading to high mortality rate with severe HS-like phenotype in *Ank-1*$^{(MRI61689/MRI61689)}$ mice. It is likely that the surviving *Ank-1*$^{(MRI61689/MRI61689)}$ mice relied on the exon-skipping splice form to produce in-frame functional *Ank-1* proteins. However, further studies are required for support this hypothesis.

3.3.3 Complex mechanisms of *P. chabaudi* resistance mediated by ankyrin-1 mutations

In terms of the response to malaria infection, *Ank-1*$^{(MRI61689/+)}$ mice exhibited similar degree of malaria resistance as *Ank-1*$^{(MRI23420/+)}$ and *Ank-1*$^{1674/+}$ mice, with at least 30-40% reduction in parasitaemia and increased survival [189,190], and unlike *Ank-1*$^{nb/+}$ mice with only 10% reduction [204]. Previous studies suggested the reduction in erythrocyte invasion and intra-erythrocytic growth to be the major resistance mechanisms [189,204]. However, normal parasite invasion was reported in *Ank-1*$^{1674/+}$ mice [190]. As a result, the potential mechanisms of *Ank-1*$^{(MRI61689/+)}$ mice were

explored in this study in attempt to elucidate the complex roles ankyrin-1 plays during malaria infections.

First, *Ank-1*$^{(MRI61689/+)}$ mice exhibit normal parasite intra-erythrocytic growth (Figure 3.4d), in contrast to *Ank-1*$^{(MRI23420/+)}$ mice. TUNEL assay detects the presence of DNA fragmentation which occurs during apoptosis and necrosis [420], indicating dying parasites in RBCs [417]. McMorran, et al. [417] reported TUNEL-positive parasites in C57BL/6 wild-type mice at a level consistent with the observations in this study. On the other hand, Greth, et al. [189] reported a lower TUNEL-positive in their SJL/J wild-type mice, which most likely due to differences in the genetic background of experimental mice. Nevertheless, abnormal parasite morphology was not observed under light microscopy unlike *Ank-1*$^{(MRI23420/+)}$ mice, which support the deductions of parasite death from the TUNEL assays. No difference in gametocyte numbers was observed (Supp. Figure 3.2), indicating gametocytogenesis was not affected. However, the possible growth retardation that might occur in other parasite stages cannot be excluded, which were not tested in this study.

In terms of parasite invasion, *Ank-1*$^{(MRI61689/+)}$ RBCs were found to be more resistant to merozoite invasion as shown in the IVET assay (Figure 3.4e). The *Ank-1*$^{(MRI61689/+)}$ erythrocytes were less infected compared to the wild-type 30 minutes after injection during merozoite invasion, and stayed consistently lower compared to wild-type throughout the erythrocytic cycle. This reduction in invasion has also been observed in *Ank-1*$^{(MRI23420/+)}$ mice [189]. In contrast, Rank, et al. [190] reported no difference in parasite invasion for *Ank-1*$^{1674/+}$ mice, indicating a different effect mediated by *Ank-1*^{1674} mutation compared to *Ank-1*$^{(MRI23420)}$ and *Ank-1*$^{(MRI61689)}$ mutations.

From these comparisons with other ankyrin mouse models, it is evident that RBC cytoskeleton plays an important yet complex role during malaria infections. However, the exact mechanism for each of these different phenotypes for each ankyrin haplotype remains elusive, different ankyrin mutations can exert different effects on the parasites depending on the location of the mutations, giving rise to multiple resistance mechanisms. This hypothesis is also consistent with

the heterogeneous HS symptoms associated with ankyrin mutations, which highlights the complicated interactions between RBC cytoskeletons and malaria parasites.

3.3.4 Increased clearance of uninfected RBCs as a novel resistance mechanisms in *Ank-1*$^{(MRI61689/+)}$ mice

On the other hand, one important observation from the IVET assay is the rapid clearance of *Ank-1*$^{(MRI61689/+)}$ erythrocytes from the circulation within 36 hours post-injection, up to 40% of the initial RBC number (Figure 3.4f). However, at this timepoint the parasitaemia of the host mice was only 5-20% (Supp. Figure 3.3), therefore the rate of RBC clearance cannot be explained by the clearance of parasitized RBCs, instead, it is likely that the majority of the RBCs being cleared were uninfected. In comparison, no loss was observed for wild-type erythrocytes in both infected and uninfected mice. Since, in these experiments both wild-type and *Ank-1*$^{(MRI61689/+)}$ blood were subjected to the same host environment simultaneously, it implies that the clearance of *Ank-1*$^{(MRI61689/+)}$ erythrocytes is cell autonomous, rather than due to other effects of the host animal during infection. This is further supported by the observation that increased *Ank-1*$^{(MRI61689/+)}$ erythrocyte clearance in uninfected mice, indicating that *Ank-1*$^{(MRI61689/+)}$ erythrocytes were predisposed for clearance. This is the first observation of increased, uninfected RBC clearance associated with an ankyrin mutation. Bystander clearance is typically observed in inflammation, such as during sepsis [421], and is thought to cause severe malaria anaemia during malaria infection in humans through the destruction of normal uninfected RBCs [422,423]. It is possible that *Ank-1*$^{(MRI61689)}$ causes a more exaggerated bystander effect during malaria infection, leading to a further reduction of *Ank-1*$^{(MRI61689/+)}$ erythrocyte numbers.

Reduced RBC deformability was proposed to be one of the mechanisms of bystander clearance during malaria anaemia through phagocytosis and splenic filtration [424,425]. From the *in vitro* spleen retention assay (Figure 3.1d), *Ank-1*$^{(MRI61689/+)}$ erythrocytes exhibited reduced

deformability, making them more likely to be retained in the filter layer, which is likely to promote their destruction in *in vivo* settings. Therefore, that *Ank-1*^{MRI61689} mutation was proposed to cause alteration to the erythrocyte, which renders them more likely to be cleared from the circulation.

3.4 Conclusion

In summary, the ENU-induced *Ank-1*^{MRI61689} mutation was reported to cause an HS-like phenotype in mice, and confers significant resistance to *P. chabaudi* infection. *Ank-1*$^{(MRI61689/+)}$ erythrocytes were proposed to be significantly resistant to parasite invasion but appeared to support normal trophozoite development, although it is possible that this mutation might affect growth of other parasite stages. This ankyrin mutation was associated with an increased RBC clearance during malaria infection, which is a novel observation from this study. This study emphasizes the importance of RBC cytoskeletal proteins in mediating multiple complex mechanisms of resistance towards malaria, which provide further insights to the complex interaction between the host and parasites.

3.5 Supplementary Figures

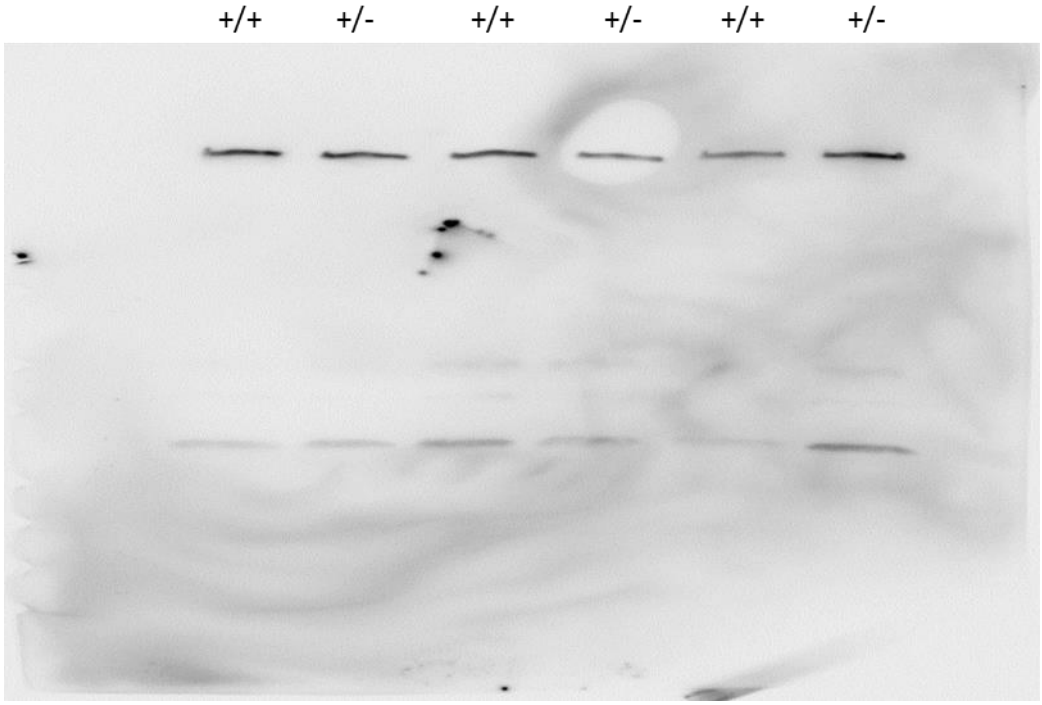

Supplementary Figure 3.1: The full western blot membrane when probed with anti-beta-spectrin antibody. The disparity of band intensity as shown in Figure 3c is due to uneven surface of the membrane rather than post-processing issue.

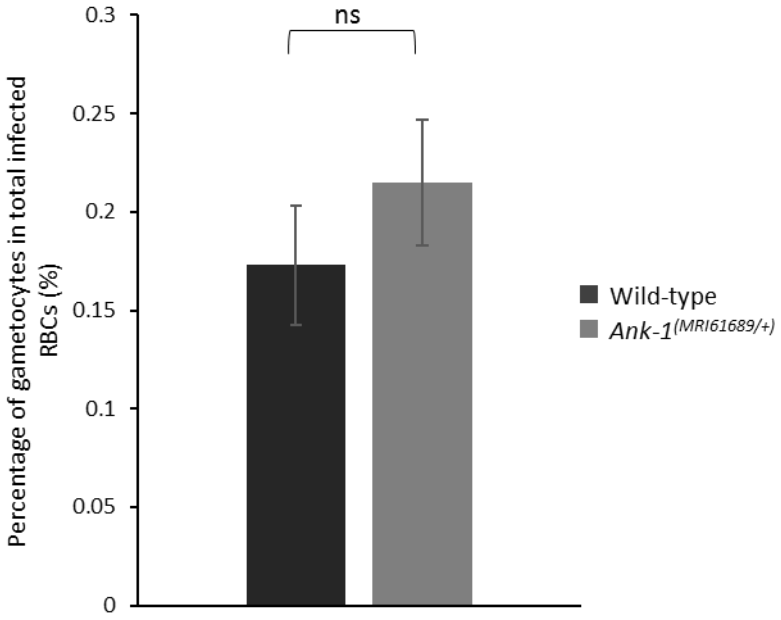

Supplementary Figure 3.2: **The percentage of gametocytes of wild-type and of *Ank-1*$^{(MRI61689/+)}$ mice during malaria infection.** Parasite gametocyte numbers were counted under light microscopy at 15-30% parasitaemia, and the proportion of gametocytes to total infected RBCs were calculated (n=6). P values was calculated using Student's t-test. Error bars indicate SEM.

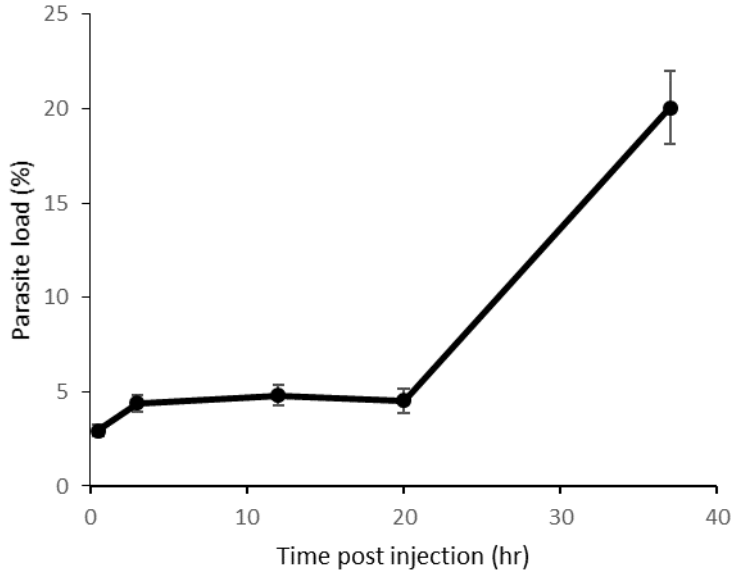

Supplementary Figure 3.3: **The parasite load of the mice during IVET assays.** The parasite load of the host mice during IVET assay (n=7). Error bars indicate SEM.

CHAPTER 4

ENU-INDUCED ANKYRIN-1 MUTATIONS

MRI96570 AND MRI95845

4.1 Introduction

Historically, malarial parasites have been co-evolving with humans for thousands of years and have played a major role in shaping human genetics in malaria endemic regions [94,426]. Indeed, many genetic polymorphisms were selected for as they provide significant survival advantages during malaria infections [94,427], resulting in high frequencies of protective genetic mutations in malaria endemic regions. The majority of them affect the red blood cell, and hence the blood stage of malaria infections [174,427,428].

Interestingly, these genetic mutations or alleles often exhibit varying degrees of malaria protection even if they affect the same gene, which is influenced by the location and the severity of mutations [429,430]. This phenomenon, known as "allelic heterogeneity", is characterised by multiple different phenotypes arising from mutations in a single gene. It has been described for certain genes affecting malaria susceptibility, which is reflected by their geographical distribution within endemic regions [431]. One of the most prominent examples of this is the β-globin gene, which is well known for its two malaria protective alleles – the HbS and HbC in African populations [100,339]. HbC is restricted to West Africa, whereas HbS is widespread throughout Africa, which is thought to be linked to the effectiveness of each allele to confer malaria resistance, and their associated morbidity [432,433]. Studies on these alleles would not only allow a better understanding of host-parasite interactions, but also give us insights into the dynamics of population genetics in malaria endemic regions [431].

However, allelic heterogeneity could also complicate the characterisation of the malaria protective roles of certain genes, often resulting in conflicting evidence from various studies. One example of such polymorphisms is CD36 deficiency, which was originally thought to be protective against malaria, as evidenced by the positive selection in East Asian and African populations [322,434,435]. While some studies reported increased malaria protection [436], others reported no significant associations [324] or even increased susceptibility [322,323]. It is possible that

these contradictive findings are due to confounding factors associated with allelic heterogeneity in CD36 deficiency [429]. This also further emphasises the importance of taking allelic heterogeneity into consideration to enable a better design in future studies involving host genetics in malaria, as well as various infectious diseases.

In contrast, the allelic heterogeneity of genes affecting RBC cytoskeleton in terms of malaria susceptibility is poorly understood. Many of the resulting genetic disorders are heterogeneous, such as hereditary spherocytosis (HS), which is characterised by the formation of "spherocytes", RBCs that exhibit reduced volume due to disruptions in erythrocyte cytoskeletons. HS is caused by mutations in ankyrin, spectrins, band 3 and protein 4.2, with ankyrin mutations contributing to more than 50% of HS cases [195,201,437-439]. HS also exhibits clinical heterogeneity, where the severity depends greatly on the location and the nature of mutations [394]. However, the prevalence of HS in malaria endemic regions is not well studied, where only specific cases were reported [200,440-442]. Nevertheless, *in vivo* and *in vitro* studies have repeatedly suggested an association of HS with increased malaria resistance, and several mechanisms have been proposed, although not all of them were consistent [189-191,204]. Based on these observations, it was hypothesised that the inconsistencies in resistance mechanisms might be due to the allelic heterogeneity of genes associated with HS.

To explore this hypothesis, mouse models carrying two novel N-ethyl-N-nitrosourea (ENU)-induced ankyrin mutations were examined. These two mouse lines, *Ank-1*$^{(MRI96570/+)}$ and *Ank-1*$^{(MRI95845/MRI95845)}$, displayed haematological and clinical features consistent with HS, and a marked resistance to infection by the murine malarial parasite, *P. chabaudi*. Analysis of the underlying mechanism of resistance to infection revealed both common and distinct features between the strains. RBCs from both lines were similarly resistant to merozoite invasion. However, the *Ank-1*$^{(MRI95845/MRI95845)}$ erythrocytes were also more rapidly cleared from circulation during an infection, whereas an impairment in intra-erythrocytic parasite maturation was

observed in the infected *Ank-1*$^{(MRI96570/+)}$ erythrocytes. This study highlights the first report of allelic heterogeneity of *Ank-1* gene in the context of malaria resistance in mouse models.

4.2 Results

4.2.1 MRI96570 and MRI95845 carry mutations in *Ank-1* gene

ENU-treated SJL/J male mice were crossed with wild-type female to produce G1 progeny with random point mutations, which were then subjected to haematological screening to identify genes affecting RBC properties, as potential candidates that might confer malaria protection. G1 mice MRI96570 and MRI95845 were identified from the ENU-dominant screen with mean cellular volume (MCV) three standard deviations below the normal level of the respective parental line - 48.5fl for MRI96570, and 50.6fl for MRI95845, compared to the background of 55.1±1.2fl. Both G1 mice were crossed with wild-type to produce G2 offspring to assess the heritability of the phenotype, where approximately half of the progeny showed reduction in MCV (20 out of 36 MRI96570 mice with 47.2±0.22fl, and 24 out of 45 MRI95845 mice with 47.6±0.24fl), suggesting a dominant mode of inheritance. Two affected MRI96570 and MRI95845 G2 progeny, which also showed a reduction of MCV, were sent for exome sequencing to identify the causative genetic mutations. Unique variants shared between the affected mice were filtered and selected for mice carrying MRI96570 mutation (Table 4.1a) or MRI95845 mutation (Table 4.1b). Each candidate mutation was genotyped by Sanger sequencing and it was found that a mutation in ankyrin-1 (*Ank-1*) was present in all the affected mice (Table 4.1a and b), and co-segregated completely with the reduced MCV phenotype for over three generations of crosses. The MRI96570 mutation is a T to A transversion in exon 34 of *Ank-1* gene (Figure 4.1a), resulting in a premature stop codon at amino acid position 1398, as opposed to the full-length protein of 1907 amino acids. The MRI95845 mutation is a T to A transversion in exon 5

(Figure 4.1b), which is predicted to cause a substitution of tyrosine for asparagine at amino acid residue 149. MRI96570 mutation is situated in the spectrin binding domain, whereas MRI95845 mutation is located in the 4th ankyrin repeat domain (Figure 4.1c). MRI96570 and MRI95845 will be referred as *Ank-1*$^{(MRI96570)}$ and *Ank-1*$^{(MRI95845)}$ respectively, for the rest of the chapter.

Table 4.1: The candidate genes for MRI96570 and MRI95845 mutations.

a)

Chromosome	Gene name	Location	Reference base	Variant base	Number of mutant mice with mutation	LOD score (Threshold: 1.9)
3	*Fat4*	38888347	T	A	0/10	-2.81
7	*Rhcg*	79601661	T	C	0/10	-2.81
8	*Ank1*	23119400	T	A	10/10	2.81
X	*Plxnb3*	73763183	G	T	0/10	-2.81

b)

Chromosome	Gene name	Location	Reference base	Variant base	Number of mutant mice with mutation	LOD score (Threshold: 2.0)
8	*Ank1*	23085597	T	A	10/10	2.81
8	*Pnpla6*	3531116	G	A	8/10	1.24
9	*Zglp1*	21062907	G	A	0/10	-2.81
16	*Snai2*	14708259	A	C	0/10	-2.81
16	*Tbc1d23*	57191544	T	C	0/10	-2.81

Variants from exome sequencing were filtered to exclude strain-specific variants and variants found in other ENU-induced mice. Variants that were shared between the two mice carrying MRI96570 mutation or MRI95845 mutation are shown in (a) and (b), respectively. For each mutation, the candidate genes were Sanger sequenced in effected mice to determine the correlation between the genetic mutations and the phenotype by calculating the LOD score based on Chi-squared distribution. LOD Threshold = 1.9 for MRI96570, 2.0 for MRI95845 (n=

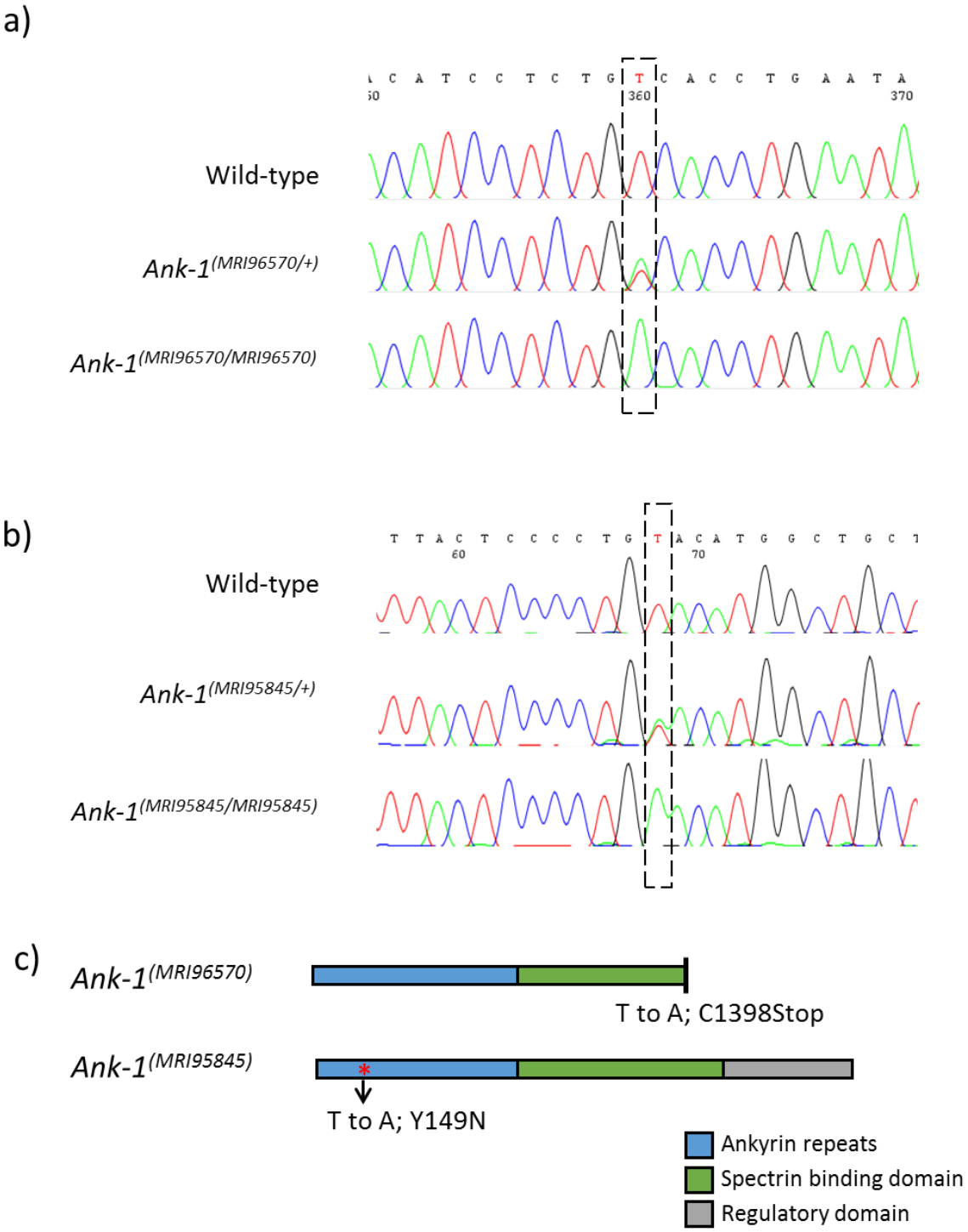

Figure 4.1: The location of *Ank-1*$^{(MRI96570)}$ and *Ank-1*$^{(MRI95845)}$ mutation. Sanger sequencing of mice carrying *Ank-1*$^{(MRI96570)}$ revealed a T to A transversion in exon 34 of *Ank-1* gene, which is predicted to induce a premature stop codon (a). Mice carrying *Ank-1*$^{(MRI95845)}$ mutation were found to have a T to A transversion in exon 5 of *Ank-1* gene, which is predicted to cause a missense mutation from tyrosine to asparagine at residue 149 (b). The schematic diagram showing the location of *Ank-1*$^{(MRI96570)}$ and *Ank-1*$^{(MRI95845)}$ mutations in the ankyrin-1 protein (c).

4.2.2 *Ank-1*$^{(MRI96570)}$ and *Ank-1*$^{(MRI95845)}$ cause HS-like phenotypes

4.2.2.1 Mice carrying Ank-1$^{(MRI96570)}$ *and Ank-1*$^{(MRI95845)}$ *mutation exhibit microcytosis and anisocytosis*

Affected *Ank-1*$^{(MRI96570)}$ and *Ank-1*$^{(MRI95845)}$ G2 progeny showed a significant reduction in MCV and mean cellular haemoglobin (MCH), elevated RBC count and red cell distribution width (RDW) (Table 4.2). When two *Ank-1*$^{(MRI96570/+)}$ or *Ank-1*$^{(MRI95845/+)}$ G2 progeny were intercrossed, *Ank-1*$^{(MRI96570/MRI96570)}$ mice were born with severe jaundice and died within several days from birth (Figure 4.2a), suggesting homozygosity for *Ank-1*$^{(MRI96570)}$ mutation caused lethal anaemia. On the other hand, *Ank-1*$^{(MRI95845/MRI95845)}$ appeared healthy with normal lifespan, but exhibited exaggerated RBC abnormalities compared to *Ank-1*$^{(MRI95845/+)}$ mice, showing further reduction of MCV (43.0±0.1 fl), significantly increased reticulocytosis (5.68±0.43% compared to 2.23±0.26% of wild-type) and lower total haemoglobin level (142.6±1.7 g/L compared to 150.5±0.8 g/L of wild-type) (Table 4.2). However, no significant differences were observed for white blood cell count, platelet count and haemoglobin concentration in each RBC, suggesting that production of leukocytes, platelets and haemoglobin are not affected by both mutations. These findings are consistent with the hallmarks of HS patients.

Table 4.2: The complete blood count of *Ank-1*$^{(MRI96570/+)}$, *Ank-1*$^{(MRI95845/+)}$ and *Ank-1*$^{(MRI95845/MRI95845)}$

	Wild type	*Ank-1*$^{(MRI96570/+)}$	*Ank-1*$^{(MRI95845/+)}$	*Ank-1*$^{(MRI95845/MRI95845)}$
WBC (x10^6 /ml)	11.3±0.3	11.2±0.4	11.9±0.8	12.1±0.8
RBC (x10^9 /ml)	10.1±0.1	11.0±0.1***	10.7±0.1***	10.9±0.1***
HGB (g/L)	150.5±0.8	150.7±1.1	148.8±1.9	142.6±1.7*
MCV (fl)	52.3±0.2	46.9±0.2***	46.6±0.2***	43.0±0.1*** ^
MCH (pg)	14.9±0.1	13.7±0.1***	13.9±0.1***	13.1±0.2*** ^
MCHC (g/L)	285.3±1.2	290.3±1.8	298.3±2.4	294.7±4.0
RDW (%)	14.5±0.1	15.3±0.1***	16.1±0.3***	18.4±0.2*** ^
PLT (x10^6 /ml)	1036±31	1051±34	992±51	1026±53
Retics (%)	2.23±0.26	3.34±0.42	3.33±0.46	5.68±0.43***

The blood parameters were obtained from a haematological analyser ADVIA 120. WBC = white blood cell count; RBC = red blood cell count; HGB = total haemoglobin; MCV = mean corpuscular volume; MCH = mean corpuscular haemoglobin; MCHC = mean corpuscular haemoglobin concentration; RDW = red cell distribution width; PLT = platelet counts; Retics = percentage of reticulocytes, n=23-50. P values were calculated using Student's t-test, with Bonferroni adjusted significance threshold = 0.001852, * P< 0.001, ** P< 1x10^{-5} compared to wild-type mice; whereas ^ P<0.001 compared to *Ank-1*$^{(MRI95845/+)}$ mice.

4.2.2.2 Ank-1$^{(MRI96570)}$ *and Ank-1*$^{(MRI95845)}$ *cause increased RBC osmotic fragility and reduced RBC deformability*

Mice carrying these *Ank-1* mutations were expected to have increased osmotic fragility, as observed in HS patients. As such, the susceptibility of erythrocytes towards osmotic stress was assessed by subjecting the RBCs to various concentration of hypotonic sodium chloride solutions. Both *Ank-1*$^{(MRI96570/+)}$ and *Ank-1*$^{(MRI95845/+)}$ RBCs showed significantly increased fragility, where 50% haemolysis was observed at approximately 5.6 and 5.4 g/L (equivalent to 104mM and 100mM) sodium chloride, respectively, compared to approximately 4.6g/L (84mM) sodium chloride of wild-type (Figure 4.2b). The *Ank-1*$^{(MRI95845/MRI95845)}$ RBCs showed further susceptibility towards osmotic stress, with 50% haemolysis at approximately 6.5 g/L (121mM) sodium chloride concentration.

The mutant RBCs were also predicted to have shorter half-life, which is also one of the symptoms of HS. Therefore, RBC half-life was determined by biotinylating mouse RBCs and tracking the remaining biotinylated RBCs over time. As shown in Figure 4.2c, erythrocytes from *Ank-1*$^{(MRI95845/MRI95845)}$ RBCs have significantly shorter half-life of approximately 9.5 days as opposed to 16 days of wild-type erythrocytes, but no significant difference was observed for erythrocytes from heterozygous mice.

Another feature of HS is the reduced RBC deformability, which was examined using two different analytical techniques: ektacytometry and an *in vitro* spleen retention assay. Ektacytometry measures the flexibility of RBCs when subjected to shear pressure, and expresses as an elongation index, which indicates the deformability of RBCs. The *Ank-1*$^{(MRI96570/+)}$ RBCs showed reduced elongation index compared to wild-type, whereas *Ank-1*$^{(MRI95845/MRI95845)}$ RBCs showed further reduction in elongation index, indicating significant reduction in RBC deformability (Figure 4.2d). In addition, the *in vitro* spleen retention assay was performed by passing the erythrocytes through layer of microbeads of varying sizes, modelling *in vivo* splenic filtration. RBC deformability was assessed by the ability of RBCs to pass through the bead layer. Figure 4.2e showed three independent measurements of RBC deformability via splenic retention assay, comparing between wild-type, *Ank-1*$^{(MRI96570/+)}$, *Ank-1*$^{(MRI95845/+)}$ and *Ank-1*$^{(MRI95845/MRI95845)}$ RBCs. An approximately 70% increased retention for *Ank-1*$^{(MRI96570/+)}$ RBCs was observed compared to wild-type, whereas erythrocytes of *Ank-1*$^{(MRI95845/+)}$ and *Ank-1*$^{(MRI95845/MRI95845)}$ mice showed 86% and 90% increased RBC retention compared to wild-type, respectively. However, no significant difference was observed between *Ank-1*$^{(MRI96570/+)}$ and *Ank-1*$^{(MRI95845/MRI95845)}$ erythrocytes.

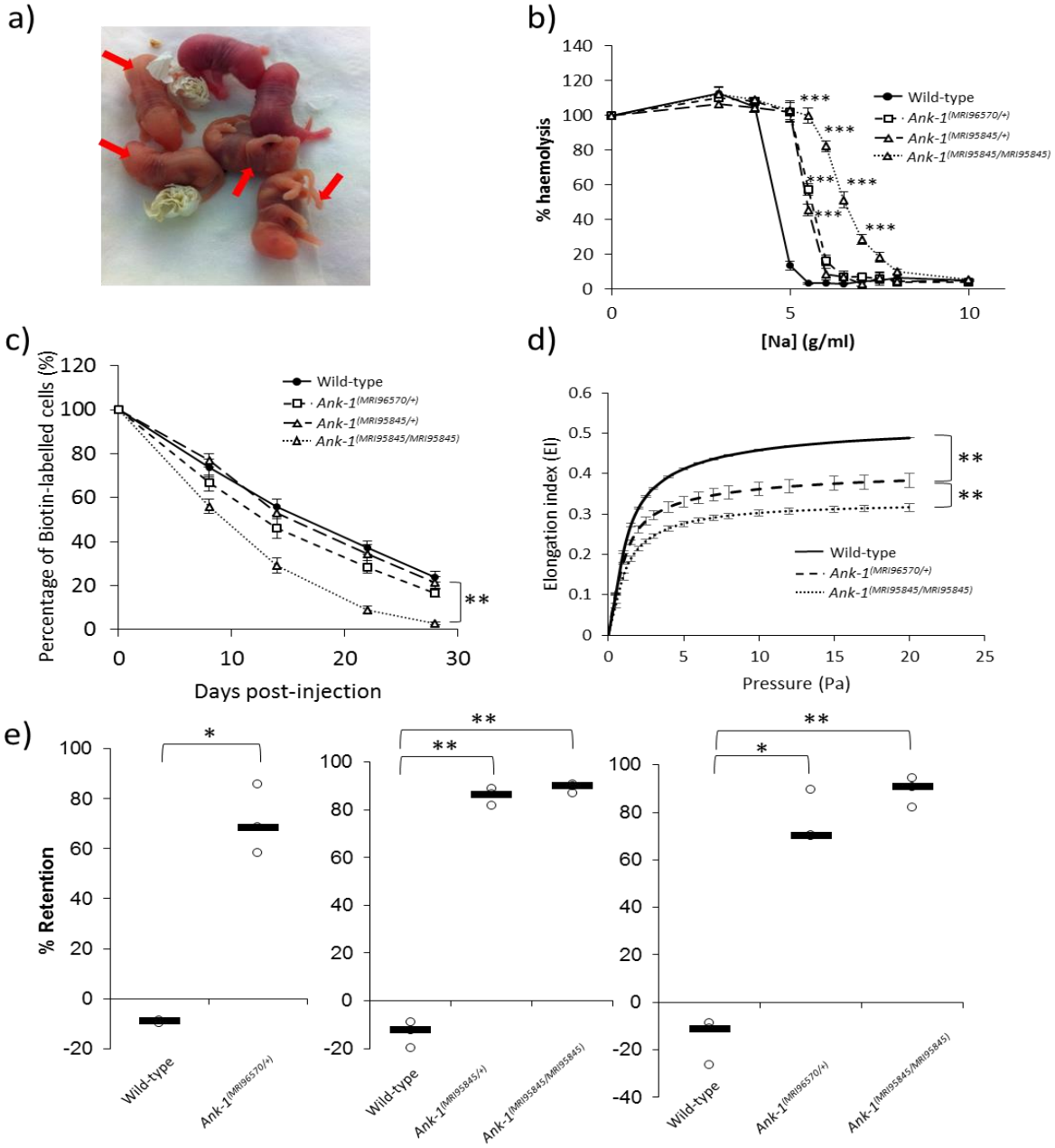

Figure 4.2: The phenotypes of *Ank-1*$^{(MRI96570/+)}$, *Ank-1*$^{(MRI95845/+)}$ and *Ank-1*$^{(MRI95845/MRI95845)}$ mice. The *Ank-1*$^{(MRI96570/MRI96570)}$ pups (indicated by arrows) showed severe jaundice and died within 1 week after birth (a). The osmotic fragility of *Ank-1*$^{(MRI96570/+)}$, *Ank-1*$^{(MRI95845/+)}$ and *Ank-1*$^{(MRI95845/MRI95845)}$ erythrocytes in hypotonic solution from 0-10g/L sodium (n=5 mice) (b). The RBC half-life of *Ank-1*$^{(MRI96570/+)}$, *Ank-1*$^{(MRI95845/+)}$ and *Ank-1*$^{(MRI95845/MRI95845)}$ mice (n=5 mice) (c). The elasticity of *Ank-1*$^{(MRI96570/+)}$ and *Ank-1*$^{(MRI95845/MRI95845)}$ RBCs under shear pressure as measured by ektacytometer (n=3 mice) (d). The proportion of retained *Ank-1*$^{(MRI96570/+)}$, *Ank-1*$^{(MRI95845/+)}$ and *Ank-1*$^{(MRI95845/MRI95845)}$ RBCs when passing through a layer of beads during the *in vitro* spleen retention assay (n=3 mice) (e). P values were calculated using Student's t-tests. * P<0.05, ** P<0.01, *** P<0.001. All error bars indicate standard error of mean (SEM).

4.2.2.3 Ank-1$^{(MRI96570)}$ and Ank-1$^{(MRI95845)}$ caused RBC morphological changes

The morphological changes of erythrocytes as the result of these mutations were examined under a light microscope, as HS patients often exhibit abnormal RBC morphology. As shown in Figure 4.3a, both *Ank-1*$^{(MRI96570/+)}$ and *Ank-1*$^{(MRI95845/+)}$ mice exhibited slight reduction in RBC size, but otherwise no obvious shape differences. *Ank-1*$^{(MRI95845/MRI95845)}$ mice had smaller RBCs and displayed anisocytosis, where RBCs were of unequal sizes. On the other hand, blood smears obtained from jaundiced *Ank-1*$^{(MRI96570/MRI96570)}$ pups showed reticulocytosis, fragmented RBCs and severe anisocytosis. Under scanning electron microscopy (SEM) (Figure 4.3b), the erythrocytes of both *Ank-1*$^{(MRI96570/+)}$ and *Ank-1*$^{(MRI95845/+)}$ mice were slightly smaller and less distinct discocyte-shaped, whereas *Ank-1*$^{(MRI95845/MRI95845)}$ erythrocytes appeared more acanthocytic.

4.2.2.4 Ank-1$^{(MRI96570/+)}$ and Ank-1$^{(MRI95845/MRI95845)}$ erythrocytes exhibit increased susceptibility to haemolysis and higher phosphatidylserine externalisation.

The susceptibility of RBCs *Ank-1*$^{(MRI95845/+)}$ and *Ank-1*$^{(MRI95845/MRI95845)}$ erythrocytes to haemolysis was also examined, which is one of the symptoms of HS [443]. Erythrocytes were incubated *ex vivo* at room temperature, and monitored haemolysis rate. *Ank-1*$^{(MRI95845/MRI95845)}$ RBCs underwent rapid haemolysis after 12 hours, with approximately 31% haemolysis compared to 9% of wild-type erythrocytes (Figure 4.4a). *Ank-1*$^{(MRI96570/+)}$ erythrocytes, on the other hand, only exhibited increased haemolysis after 48 hours of incubation (32% haemolysis compared to 7% of wild-type). These *Ank-1*$^{(MRI96570/+)}$ and *Ank-1*$^{(MRI95845/MRI95845)}$ erythrocytes also exhibited higher Annexin V on flow cytometer regardless of incubation temperature (Figure 4.4b-d), indicating higher phosphatidylserine (PS) externalisation as the result of membrane instability. These results suggested that *Ank-1*$^{(MRI95845/MRI95845)}$ erythrocytes, and to the lesser extent, *Ank-1*$^{(MRI96570/+)}$ erythrocytes, were more susceptible to degradation, and possibly have a more unstable RBC

membrane. The findings so far demonstrated that these *Ank-1* mice exhibit haematological and clinical features consistent with HS.

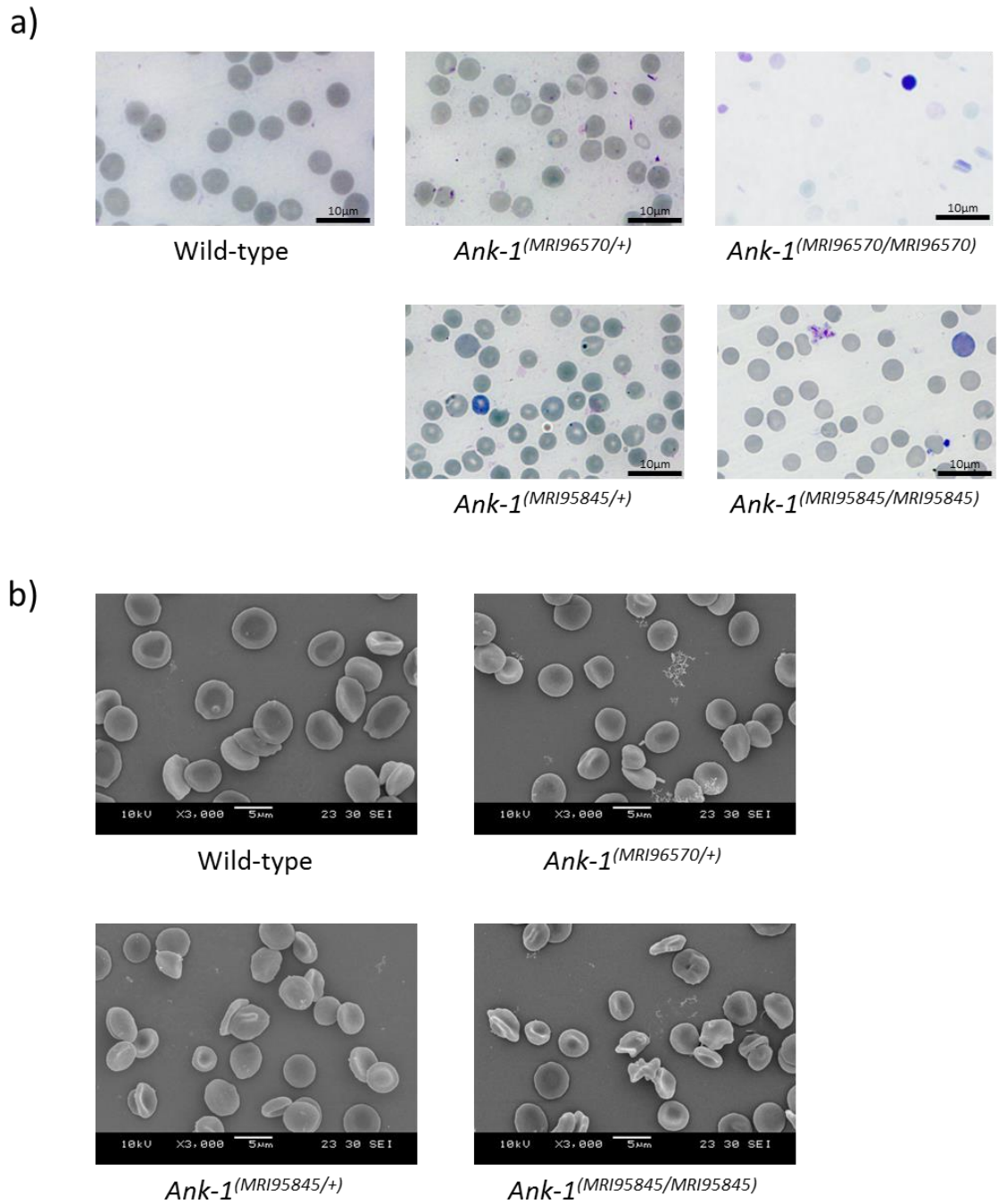

Figure 4.3: The RBC morphology of mice carrying *Ank-1*$^{(MRI96570)}$ or *Ank-1*$^{(MRI95845)}$ mutation. Giemsa-stained blood smears as examined under light microscope at 100x magnification (a). Scanning electron microscopic images showing the RBC shape of *Ank-1*$^{(MRI96570/+)}$, *Ank-1*$^{(MRI95845/+)}$ and *Ank-1*$^{(MRI95845/MRI95845)}$ mice (b).

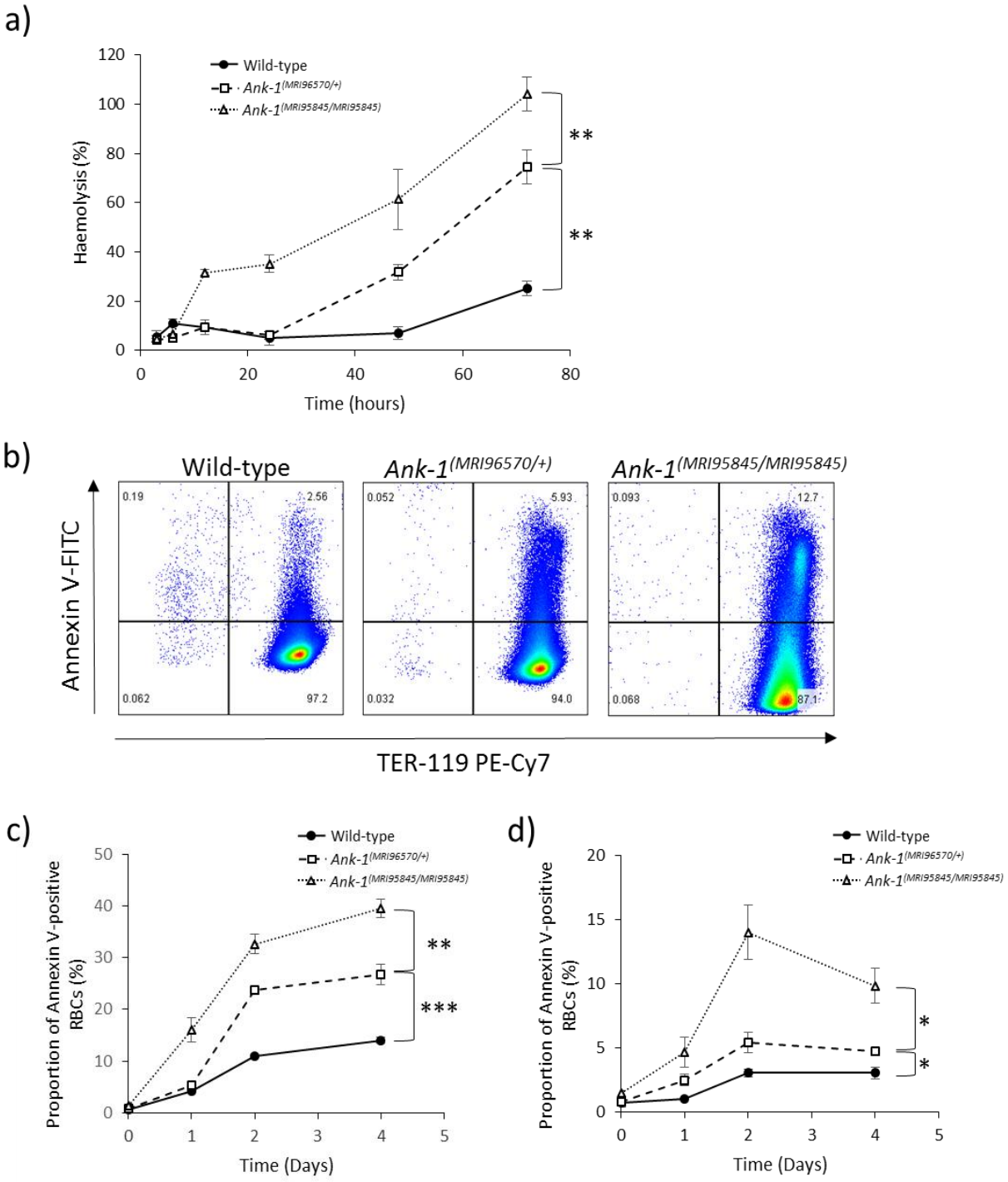

Figure 4.4: The susceptibility of *Ank-1*$^{(MRI96570/+)}$ and *Ank-1*$^{(MRI95845/MRI95845)}$ erythrocytes to haemolysis and eryptosis. The percentage of haemolysis of wild-type, *Ank-1*$^{(MRI96570/+)}$ and *Ank-1*$^{(MRI95845/MRI95845)}$ erythrocytes when incubated *ex vivo* at room temperature (a) (n=3 mice). The exposure of phosphatidylserine (PS) as a marker for eryptosis was measured using FITC-conjugated Annexin V on flow cytometry (b). The proportion of RBCs population positive for Annexin V binding was recorded over 4 days of incubation at room temperature (c) or 4^{o}C (d)(n=3 mice). All experiments were conducted with n=3-5 mice per group and p values were calculated using Student's t-tests. * P<0.05, ** P<0.01, *** P<0.001. Error bars indicate SEM.

4.2.3 *Ank-1*$^{(MRI95845/MRI95845)}$ erythrocytes have disrupted cytoskeletal structure and reduced expression of RBC cytoskeletal proteins

4.2.3.1 Reduced Ank-1 mRNA levels in embryonic livers of mice carrying Ank-1$^{(MRI96570)}$ *and Ank-1*$^{(MRI95845)}$ *mutation*

The effect of these mutations on the *Ank-1* expression levels were also investigated. The *Ank-1* mRNA levels were examined via quantitative PCR on E14 embryonic livers, as it is the major erythropoietic organ during embryo development, and normalised against the wild-type levels. As shown in Figure 4.5a, significant reduction of *Ank-1* mRNA levels was observed in *Ank-1*$^{(MRI96570/+)}$, *Ank-1*$^{(MRI95845/+)}$ and *Ank-1*$^{(MRI95845/MRI95845)}$ embryonic livers (ranging from 0.61 to 0.67 of wild-type levels), whereas *Ank-1*$^{(MRI96570/MRI96570)}$ embryonic liver showed the most reduction (mean of 0.38 of wild-type levels).

4.2.3.2 Expression levels of various RBC cytoskeletal proteins in mice carrying Ank-1$^{(MRI96570)}$ *and Ank-1*$^{(MRI95845)}$ *mutation*

The ANK-1 and other erythrocyte cytoskeletal protein levels were also examined. Coomassie staining and Western blotting of the RBC membrane fractions did not show a significant difference in ANK-1 levels between wild-type, *Ank-1*$^{(MRI96570/+)}$ and *Ank-1*$^{(MRI95845/MRI95845)}$ erythrocytes (Figure 4.5b-d). The predicted truncated ANK-1$^{(MRI96570/+)}$ form (160kDa) was also not evidenced. The levels of other cytoskeletal proteins were also examined to account for possible disruptions to interactions with other binding partners of ankyrin-1. However, no difference was observed for Band 3, α- and β-spectrin, whereas significantly lower protein 4.2 level was observed in *Ank-1*$^{(MRI95845/MRI95845)}$ erythrocytes (Figure 4.5d).

Further characterisation of *Ank-1*$^{(MRI95845/MRI95845)}$ erythrocyte cytoskeletal proteins was performed using liquid chromatography/mass spectrometry (LC/MS) on the RBC membrane. They were first separated on SDS-PAGE, followed by alkylation and trypsin-digestion, before being analysed on LC/MS. Of the protein hits obtained from the mass spectrometry, RBC cytoskeleton-related proteins were selected and examined. Figure 4.5e shows the relative abundance of various RBC cytoskeletal proteins normalised to the total protein content. Significant reduction in ankyrin-1, protein 4.2 and stomatin levels were observed in *Ank-1*$^{(MRI95845/MRI95845)}$ erythrocyte membranes.

4.2.3.3 Ank-1$^{(MRI95845/MRI95845)}$ *erythrocytes exhibit increased band 3 mobility and solubility*

It is likely that *Ank-1*$^{(MRI95845/MRI95845)}$ caused disruption to the RBC cytoskeletons, as evidenced from the reduced amount of various RBC cytoskeletal proteins from previous experiments. In order to support our hypothesis, the band 3 mobility across the RBC membrane was examined as an indicator of disrupted RBC cytoskeleton [444,445]. Erythrocytic band 3 was fluorescently labelled with eosin-5'-maleimide and performed Fluorescence Recovery after Photobleaching (FRAP) on erythrocytes, which involved photobleaching with high-powered laser followed by a recovery period where the fluorescence intensity was recorded. *Ank-1*$^{(MRI95845/MRI95845)}$ RBCs were found to have significantly higher fluorescence recovery compared to wild-type and *Ank-1*$^{(MRI96570/+)}$ RBCs (Figure 4.6a), which suggests a higher band 3 mobility in *Ank-1*$^{(MRI95845/MRI95845)}$ erythrocytes. It was proposed that this was due to an increased amount of band 3 that was not associated with the RBC cytoskeleton, which was assessed by measuring the solubility of band 3 in the presence of detergent. It has been shown that un-bound band 3 is more soluble compared to those interacting with the RBC cytoskeleton [446]. Therefore, it was predicted that *Ank-1*$^{(MRI95845/MRI95845)}$ erythrocytes would have higher amounts of soluble band 3 when treated with detergent, which can be visualised on Western blot, and the relative amount of soluble band 3

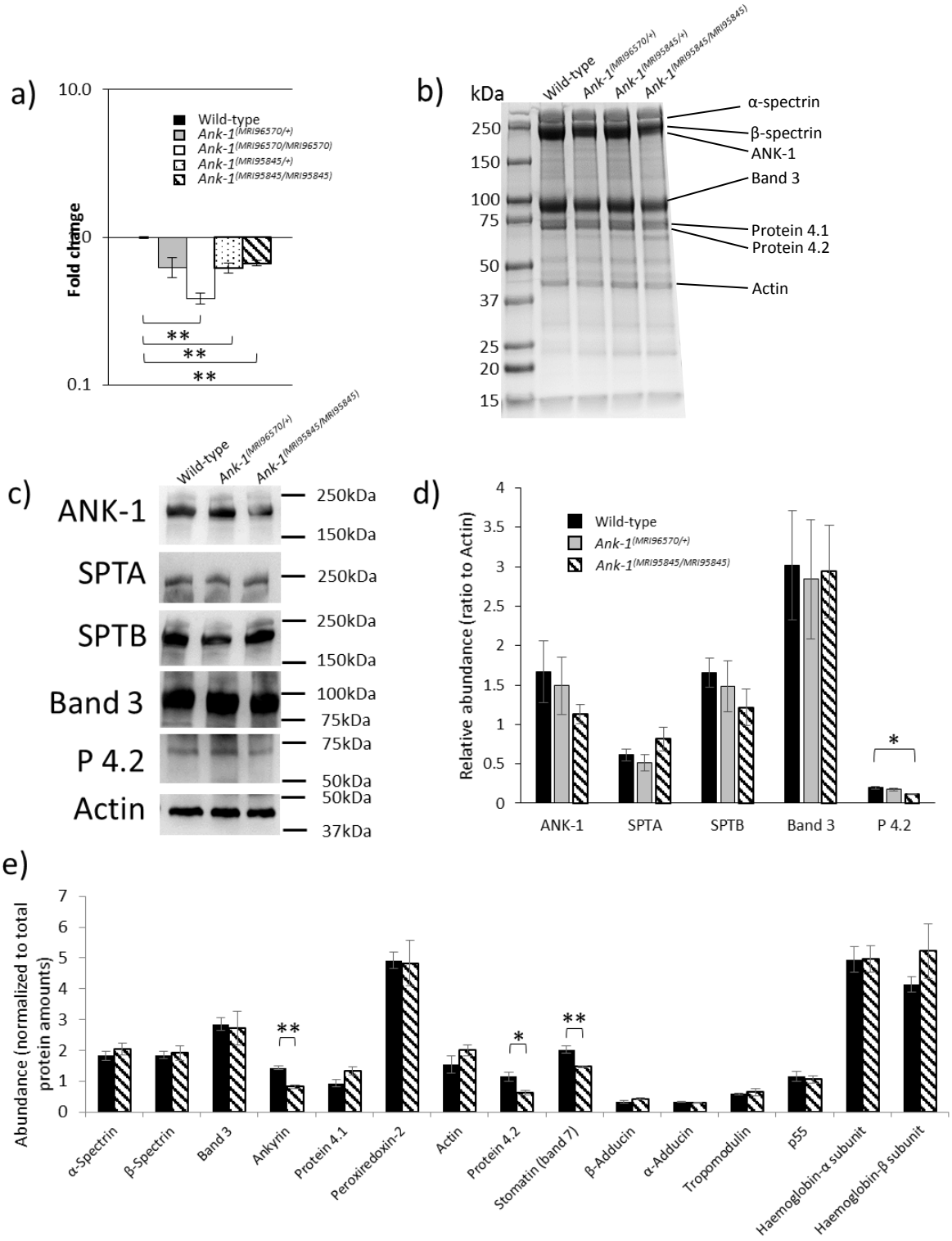

Figure 4.5: The expression of *Ank-1* and other RBC cytoskeletal proteins in mice carrying *Ank-1*$^{(MRI96570)}$ or *Ank-1*$^{(MRI95845)}$ mutation. Quantitative PCR was carried out on E14 embryonic livers to examine *Ank-1* expression levels (n=3 mice) (a). The abundance of ANK-1 and other RBC cytoskeletal protein levels of *Ank-1*$^{(MRI96570/+)}$, *Ank-1*$^{(MRI95845/+)}$ and *Ank-1*$^{(MRI95845/MRI95845)}$ mice as examined via Coomassie (b) and Western blot (c) on membranes of mature RBCs. The relative abundance of various cytoskeletal protein levels calculated from Western blots (n=3 mice) (d). The proteomics results of *Ank-1*$^{(MRI95845/MRI95845)}$ erythrocyte membrane compared to wild-type as measured using LC/MS (n=3 mice) (e). SPTA = α-spectrin, SPTB = β-spectrin, P 4.2 = Protein 4.2. P values were calculated using Student's t-tests. * P<0.05, ** P<0.01. Error bars indicate SEM.

was expressed as a percentage of the total band 3 amount. Indeed, significantly higher proportions of soluble band 3 was observed in *Ank-1*$^{(MRI95845/MRI95845)}$ erythrocytes compared to wild-type and *Ank-1*$^{(MRI96570/+)}$ erythrocytes in three independent replicates of the experiment (Figure 4.6b-c). These results suggested that *Ank-1*$^{(MRI95845/MRI95845)}$ erythrocytes have increased amount of un-associated band 3 in the membrane compared to *Ank-1*$^{(MRI96570/+)}$ erythrocytes, indicating a disrupted RBC cytoskeleton.

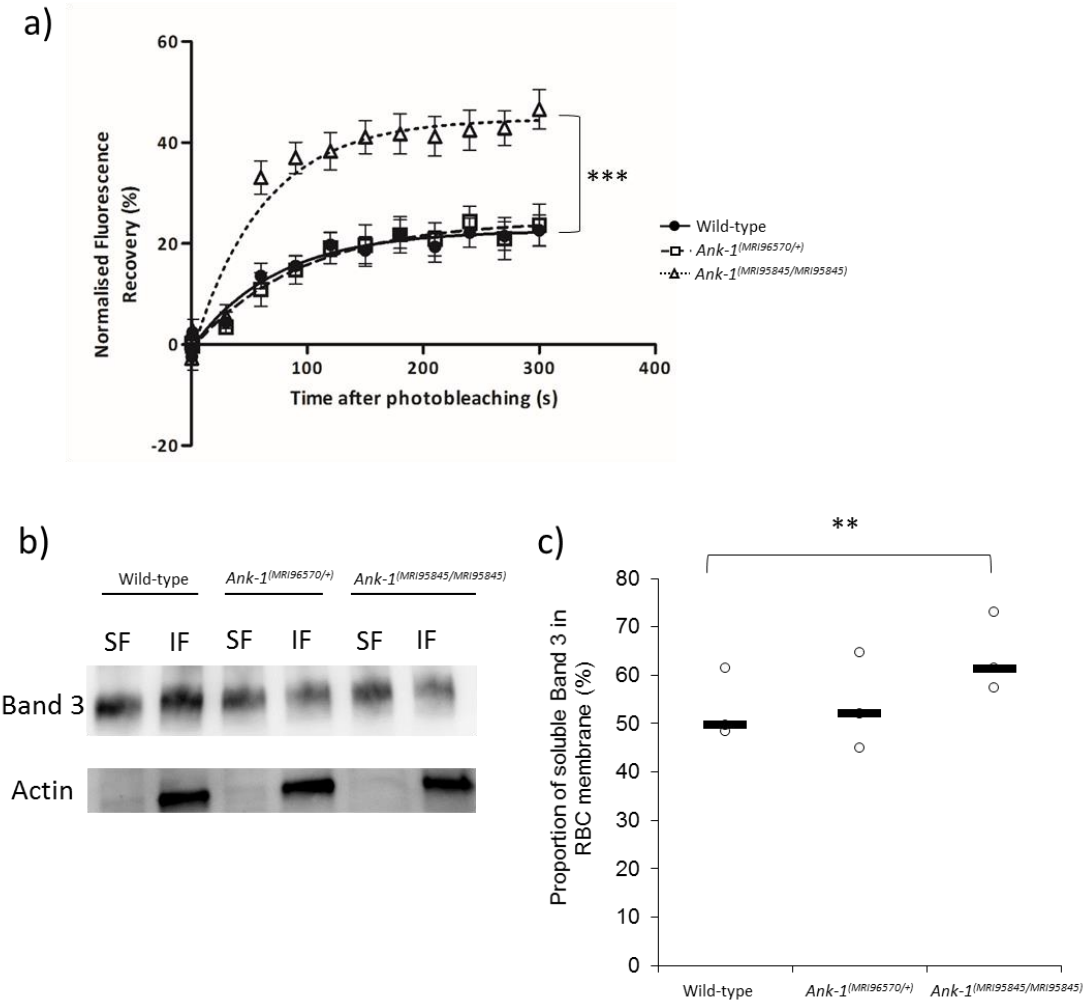

Figure 4.6: The mobility and solubility of band 3 of *Ank-1*$^{(MRI96570/+)}$ and *Ank-1*$^{(MRI95845/MRI95845)}$ erythrocytes. The band 3 mobility on RBC membrane was measured using Fluorescence recovery after Photobleaching (FRAP), showing the recovery rate of fluorescence as a result of Band 3 migration to the bleach spot (n=9-21) (a). The solubility of band 3 of *Ank-1*$^{(MRI96570/+)}$ and *Ank-1*$^{(MRI95845/MRI95845)}$ erythrocytes as determined by comparing the proportion of triton-X100-soluble band 3 to the total band 3 amount in RBC membrane on Western blot (b) (SF= triton-X100-soluble fraction; IF = triton-X100-insoluble fraction), with quantitation as shown in (c) (n=3 mice per group). P-values for (a) were calculated using Student's t-test on the area under curve, whereas paired Student's t-test was used in (b) for three separate replicates of the experiment. ** P< 0.01, *** P<0.001. Error bars indicate SEM.

4.2.4 *Ank-1*$^{(MRI96570)}$ and *Ank-1*$^{(MRI95845)}$ give rise to resistance towards *P. chabaudi* infection

It was proposed that mice carrying these mutations have reduced susceptibility to malaria infection, which was examined by injecting with a lethal dose of *P. chabaudi*, and the percentage of parasitised RBCs (parasitaemia) was recorded. As shown in Figure 4.7a, *Ank-1*$^{(MRI96570/+)}$ and *Ank-1*$^{(MRI95845/+)}$ mice showed significant reduction in peak parasitaemia of approximately 15-20%, while *Ank-1*$^{(MRI95845/MRI95845)}$ mice showed approximately 30% reduction in peak parasitaemia compared to wild-type. *Ank-1*$^{(MRI95845/MRI95845)}$ mice also showed a two-day delay in parasitaemia, peaking on day 12 post-infection rather than day 10 as with wild-type. *Ank-1*$^{(MRI95845/MRI95845)}$ mice also exhibited significantly higher survival rate compared to wild-type during *P. chabaudi* infection, but no significant difference was observed for *Ank-1*$^{(MRI96570/+)}$ and *Ank-1*$^{(MRI95845/+)}$ mice compared to wild-type (Figure 4.7b). Overall, these results suggested that both *Ank-1*$^{(MRI96570/+)}$ and *Ank-1*$^{(MRI95845/+)}$ mice showed moderate resistance, whereas *Ank-1*$^{(MRI95845/MRI95845)}$ mice exhibited significant resistance towards *P. chabaudi* infection in relative to the wild-type mice.

From these results, further investigation on the possible mechanisms of resistance mediated by *Ank-1*$^{(MRI96570)}$ and *Ank-1*$^{(MRI95845)}$ mutations was performed. Three important determinants of parasite growth and survival within the host were examined. Firstly, the ability of parasite to survive within these erythrocytes was studied, since ankyrin-1 mutations have previously been implicated to impair parasite intra-erythrocytic maturation [189]. Secondly, the erythrocyte invasion was assessed as the mutations disrupt erythrocyte cytoskeletal structure, which is important for facilitating efficient erythrocyte invasion [192]. Thirdly, the mutations might result in an improved detection of parasitised RBCs, thus enhancing their removal from circulation during malaria infection. Since *Ank-1*$^{(MRI96570/+)}$ and *Ank-1*$^{(MRI95845/MRI95845)}$ mice exhibited differences in malaria resistance, it was hypothesised that they mediate malaria resistance through different pathways.

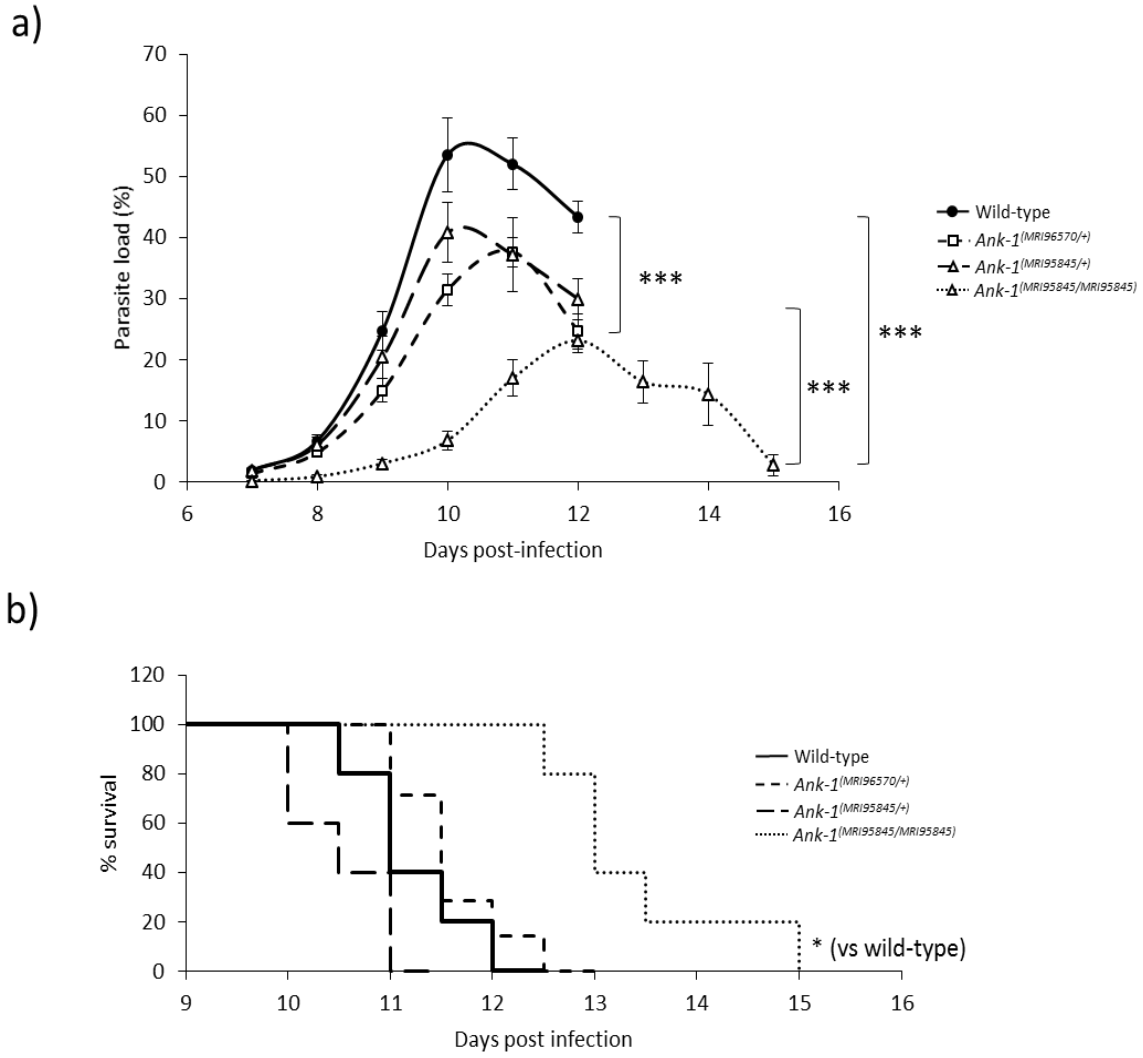

Figure 4.7: The parasitaemia and survival curves of *Ank-1*$^{(MRI96570/+)}$, *Ank-1*$^{(MRI95845/+)}$ and *Ank-1*$^{(MRI95845/MRI95845)}$ mice when challenged with *P. chabaudi*. The parasite load (a) and survival rate (b) of *Ank-1*$^{(MRI96570/+)}$, *Ank-1*$^{(MRI95845/+)}$ and *Ank-1*$^{(MRI95845/MRI95845)}$ mice from day 7 to day 15 post-infection when challenged with 1x10^4 parasite intraperitoneally as determined by light microscopy. (n=9-13 mice each genotype). P values for (a) and (b) were calculated using permutation test and Log-Rank test, respectively.* P<0.05, *** P<0.001. Error bars indicate SEM

4.2.5 *Ank-1*$^{(MRI96570/+)}$ and *Ank-1*$^{(MRI95845/MRI95845)}$ erythrocytes are resistant to merozoite invasion

First, the ability of parasite to invade erythrocytes was assessed via an *in vivo* erythrocyte tracking (IVET) assay. Labelled RBCs from either wild-type, *Ank-1*$^{(MRI96570/+)}$ or *Ank-1*$^{(MRI95845/MRI95845)}$ mice were injected into infected wild-type mice of 1-10% parasitaemia during late schizogony stage and the parasitaemia of each genotype was monitored over 36-40 hours to indicate relative invasion rates. The initial invasion period was expected at 30 minutes to 3 hour timepoints, and the results were expressed as a ratio of parasitised RBCs of either, *Ank-1*$^{(MRI96570/+)}$ to wild-type (Figure 4.8a), *Ank-1*$^{(MRI95845/MRI95845)}$ to wild-type (Figure 4.8b), or *Ank-1*$^{(MRI96570/+)}$ to *Ank-1*$^{(MRI95845/MRI95845)}$ (Figure 4.8c). From Figure 4.8a and 4.8b, *Ank-1*$^{(MRI96570/+)}$ and *Ank-1*$^{(MRI95845/MRI95845)}$ erythrocytes were less parasitised compared to wild-type (0.6-0.7 for *Ank-1*$^{(MRI96570/+)}$ and 0.55-0.8 for *Ank-1*$^{(MRI95845/MRI95845)}$) from 3 hours up to 36 hours post-injection, indicating both *Ank-1*$^{(MRI96570/+)}$ and *Ank-1*$^{(MRI95845/MRI95845)}$ erythrocytes were more resistant to parasite invasion than wild-type. However, no significant differences in parasitaemia ratio were observed at 30 minute timepoint. Furthermore, when the invasion rate of both *Ank-1*$^{(MRI96570/+)}$ and *Ank-1*$^{(MRI95845/MRI95845)}$ erythrocytes were compared in infected wild-type mice (Figure 4.8c), no significant difference in parasitaemia ratio was observed, suggesting a similar invasion rate between the two mutant erythrocytes.

4.2.6 *Ank-1*$^{(MRI96570/+)}$ erythrocytes impair parasite maturation

Second, the parasite intra-erythrocytic maturation was determined through a TUNEL assay, which allows the detection of fragmented DNA in RBCs, as an indication of dying parasites (Figure 4.8d) [417]. Samples were collected from infected mice at 1-10% parasitaemia at both young ring stage and late trophozoite stage, and the proportion of TUNEL-positive infected RBCs were calculated. As seen from Figure 4.8e, more TUNEL-positive parasites were observed within *Ank-1*$^{(MRI96570/+)}$ erythrocytes, in both ring (30.1±3.4% compared to 15.2±3.1% of wild-type) and trophozoite stage (30.8±3.8% compared to 11.7±1.0% of wild-type), whereas no differences were observed for *Ank-1*$^{(MRI95845/+)}$ and *Ank-1*$^{(MRI95845/MRI95845)}$ erythrocytes. This result suggested that the growth of parasites within *Ank-1*$^{(MRI96570/+)}$ erythrocytes was impaired, but was normal in *Ank-1*$^{(MRI95845/+)}$ and *Ank-1*$^{(MRI95845/MRI95845)}$ erythrocytes. This also indicate that *Ank-1*$^{(MRI96570)}$ disrupts parasite maturation, whereas *Ank-1*$^{(MRI95845)}$ seems to support normal parasite growth, although growth inhibition at other stages were not studied.

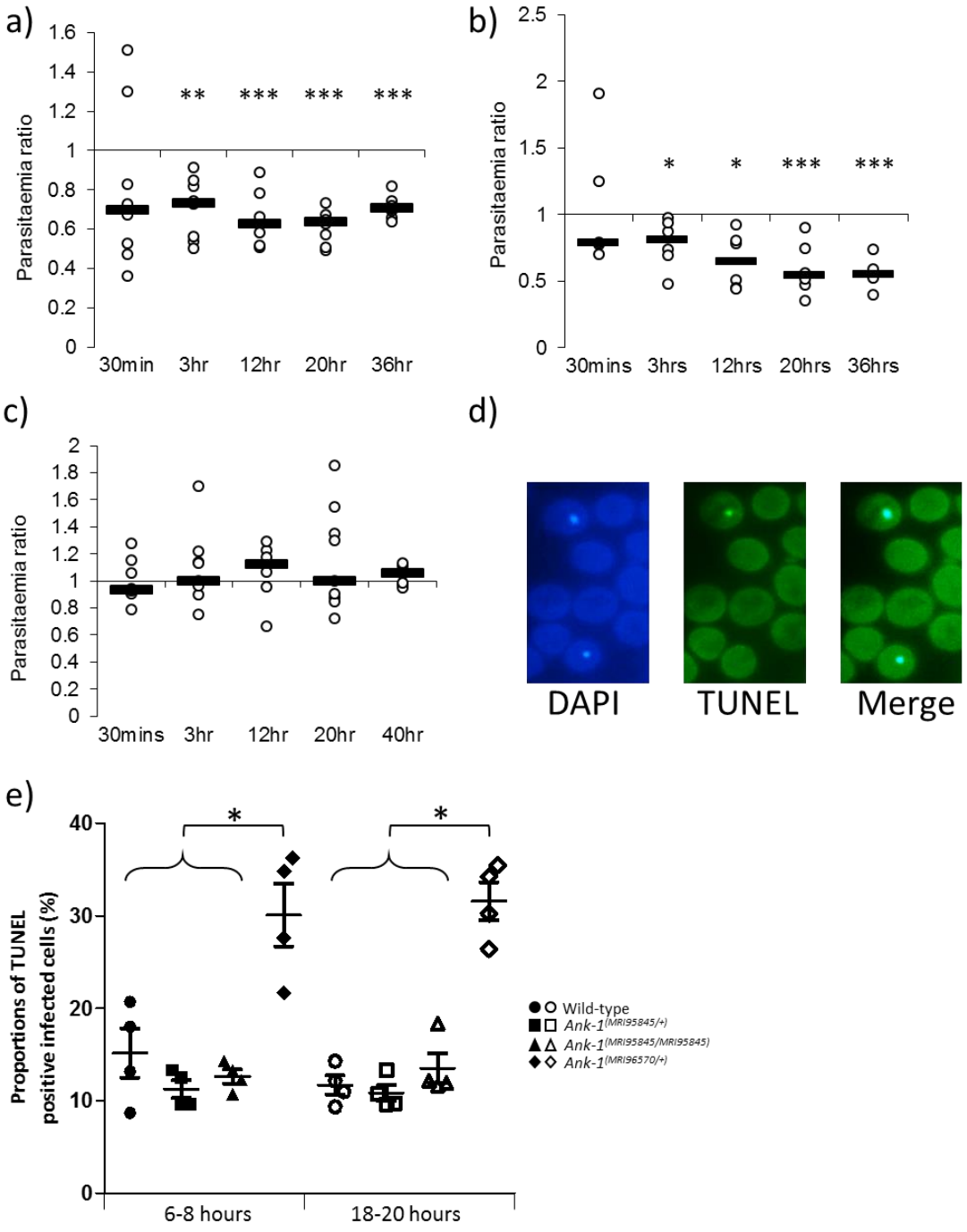

Figure 4.8: The parasite invasion and intra-erythrocytic growth as indicated via IVET and TUNEL assay. The relative invasion efficiency into *Ank-1*$^{(MRI96570/+)}$ and *Ank-1*$^{(MRI95845/MRI95845)}$ erythrocytes was examined through IVET assay, where parasitaemia ratio was calculated from parasite load of either *Ank-1*$^{(MRI96570/+)}$ to wild-type (a), *Ank-1*$^{(MRI95845/MRI95845)}$ to wild-type (b), or *Ank-1*$^{(MRI96570/+)}$ to *Ank-1*$^{(MRI95845/MRI95845)}$ erythrocytes (c) (n=5-7). The parasite growth inhibition was determined via TUNEL assay on infected RBCs (DAPI-positive) as an indicator of apoptotic and necrotic parasites (d). At least 100 infected RBCs was counted and the proportions of TUNEL-positive infected RBCs were calculated for *Ank-1*$^{(MRI96570/+)}$, *Ank-1*$^{(MRI95845/+)}$ and *Ank-1*$^{(MRI95845/MRI95845)}$ mice at 1-5% parasitaemia at ring stage (6-8 hours) and late trophozoite (18-20 hours) stage (n=4) (e). P values were calculated using Student's t-tests. *P<0.05, **P<0.01, ***P<0.001. Error bars indicates SEM.

4.2.7 *Ank-1*$^{(MRI95845/MRI95845)}$ erythrocytes are more likely to get cleared during malaria infections

The proportions of labelled erythrocytes were also monitored during the IVET assays to compare the relative loss of the two labelled RBC populations as the indicator of RBC clearance during malaria infection. No significant reduction in *Ank-1*$^{(MRI96570/+)}$ erythrocyte numbers was observed during IVET assay compared to wild-type (Figure 4.9a). On the other hand, the number of labelled *Ank-1*$^{(MRI95845/MRI95845)}$ erythrocytes decreased significantly compared to wild-type and *Ank-1*$^{(MRI96570/+)}$ erythrocytes (Figure 4.9b and c), with approximately 20% and 50% reduction, respectively. However, the parasitaemia measurements during the IVET assays were approximately 2% to 16-30% (Supp. Figure 1a and b), which did not correlate with the reduction of labelled *Ank-1*$^{(MRI95845/MRI95845)}$ erythrocytes. This suggested an increased bystander clearance rather than clearance of infected *Ank-1*$^{(MRI95845/MRI95845)}$ RBCs. To further investigate this phenomenon, the RBCs of infected mice from each genotype were biotinylated and the RBC half-life was examined without blood transfusion. As shown in Figure 4.9d, the *Ank-1*$^{(MRI96570/+)}$ mice exhibited no significant reduction in RBC numbers, whereas *Ank-1*$^{(MRI95845/MRI95845)}$ mice were found to have significantly shorter half-life of approximately 6 days, which did not correlate with the parasitaemia curve (Supp. Figure 1c). This observation of shorter RBC half-life in infected *Ank-1*$^{(MRI95845/MRI95845)}$ mice is consistent with the increased *Ank-1*$^{(MRI95845/MRI95845)}$ erythrocyte clearance as shown in IVET assays. The *Ank-1*$^{(MRI95845/MRI95845)}$ mice were also found to have increased reticulocytes count early infection compared to wild-type and *Ank-1*$^{(MRI96570/+)}$ mice (Figure 4.9e). Overall, these results indicated that *Ank-1*$^{(MRI95845/MRI95845)}$ erythrocytes have increased clearance and turnover rate and *Ank-1*$^{(MRI95845/MRI95845)}$ mice have increased erythropoiesis during malaria infection, both of which were not evidenced in *Ank-1*$^{(MRI96570/+)}$ mice.

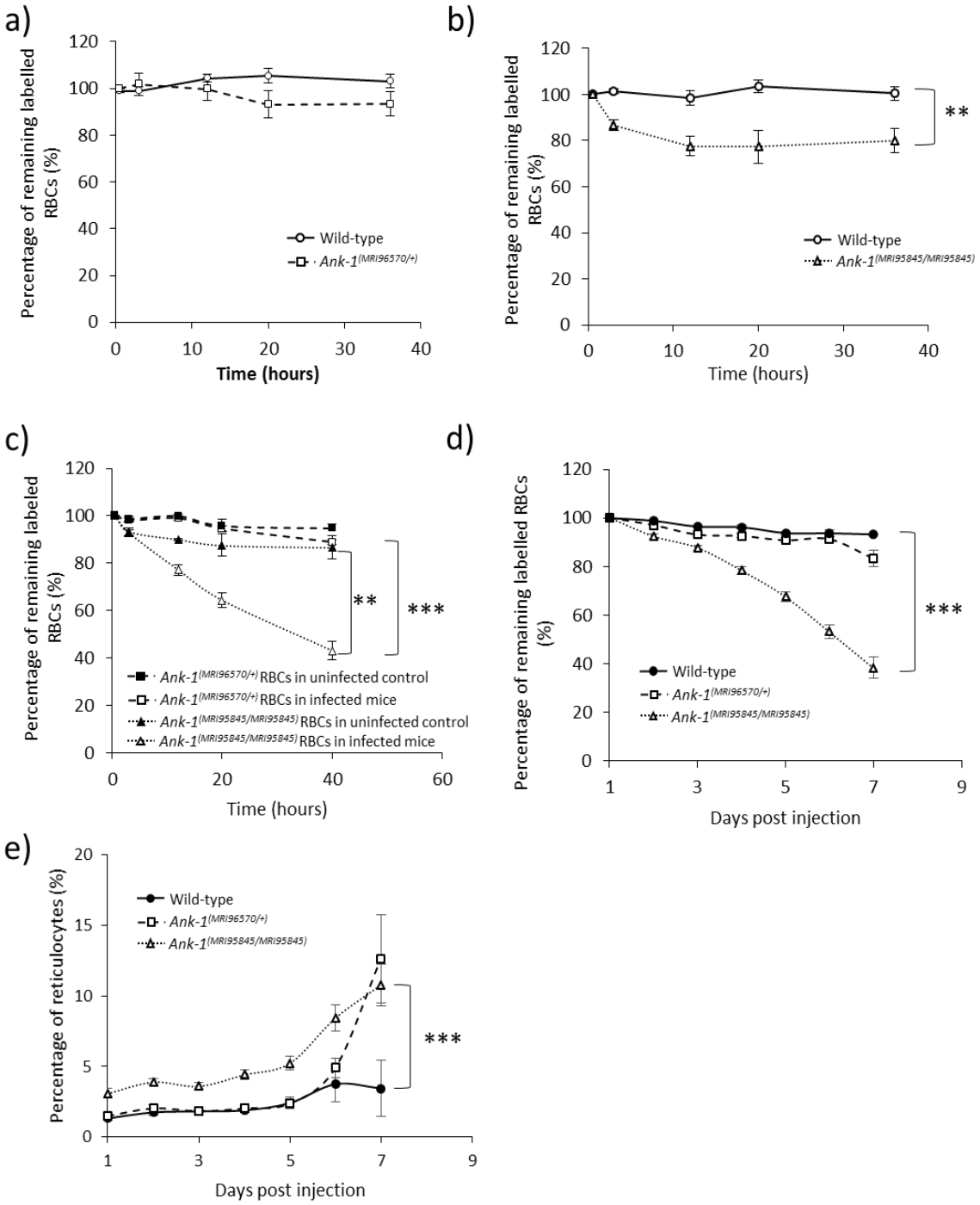

Figure 4.9: The clearance of wild-type, *Ank-1*$^{(MRI96570/+)}$ *Ank-1*$^{(MRI95845/MRI95845)}$ erythrocytes and reticulocytosis during malaria infection. The remaining percentage of labelled RBCs was monitored during the course of IVET assays, comparing between wild-type and *Ank-1*$^{(MRI96570/+)}$ erythrocytes (a), wild-type and *Ank-1*$^{(MRI95845/MRI95845)}$ erythrocytes (b), and *Ank-1*$^{(MRI96570/+)}$ and *Ank-1*$^{(MRI95845/MRI95845)}$ erythrocytes (c) (n=5-7). The half-life of wild-type, *Ank-1*$^{(MRI96570/+)}$ *Ank-1*$^{(MRI95845/MRI95845)}$ erythrocytes during malaria infection as determined by biotinylation of RBCs when parasites were detectable (n=6-7) (d). The reticulocytosis of wild-type, *Ank-1*$^{(MRI96570/+)}$ *Ank-1*$^{(MRI95845/MRI95845)}$ mice during malaria infection as calculated by the proportion of non-biotinylated CD71-positive population (n=6-7) (e). P values were calculated using Student's t-test on the area under curve for each genotype and treatment. ** P<0.01, *** P<0.001. Error bars indicate SEM.

4.2.8 Increased *Ank-1*$^{(MRI95845/MRI95845)}$ erythrocytes clearance during malaria infection is mainly mediated via splenic filtration

Two mechanisms were hypothesised for the increased clearance of *Ank-1*$^{(MRI95845/MRI95845)}$ erythrocytes. First, the *Ank-1*$^{(MRI95845/MRI95845)}$ erythrocytes might be more likely to be detected and cleared by the spleen, and second, the *Ank-1*$^{(MRI95845/MRI95845)}$ erythrocyte clearance might be mediated through the immune system. To determine the role of the spleen in erythrocyte clearance, splenectomised mice were first infected with *P. chabaudi* and infused with labelled wild-type and *Ank-1*$^{(MRI95845/MRI95845)}$ erythrocytes, the proportions of which were monitored over time. As shown in Figure 4.10a, *Ank-1*$^{(MRI95845/MRI95845)}$ erythrocyte numbers are approximately two-fold higher ($P<0.01$) in splenectomised mice compared to non-splenectomised mice. This suggests that the spleen is a major contributor towards *Ank-1*$^{(MRI95845/MRI95845)}$ erythrocyte clearance, although the clearance was not completely abrogated in the absence of the spleen.

4.2.9 Toll-like receptor 4 (TLR4)-mediated pathways play a minor role in *Ank-1*$^{(MRI95845/MRI95845)}$ erythrocytes clearance

As a result, the role of the immune system in the clearance of *Ank-1*$^{(MRI95845/MRI95845)}$ erythrocytes was explored. It is thought that innate immune system requires several days to be activated to eliminate parasitised RBCs [447,448]. Therefore, the activation of the innate immune system was minimised by infecting mice with high dose of *P. chabaudi* ($2x10^7$) and performed an IVET assay two days post-infection. From Figure 4.10b, *Ank-1*$^{(MRI95845/MRI95845)}$ erythrocytes were significantly less parasitised compared to wild-type erythrocytes, in agreement with previous IVET assays. In terms of *Ank-1*$^{(MRI95845/MRI95845)}$ erythrocyte numbers, no significant clearance was observed for up to 15 hours post-injection, indicating a possible delay in *Ank-1*$^{(MRI95845/MRI95845)}$ erythrocyte clearance (Figure 4.10c).

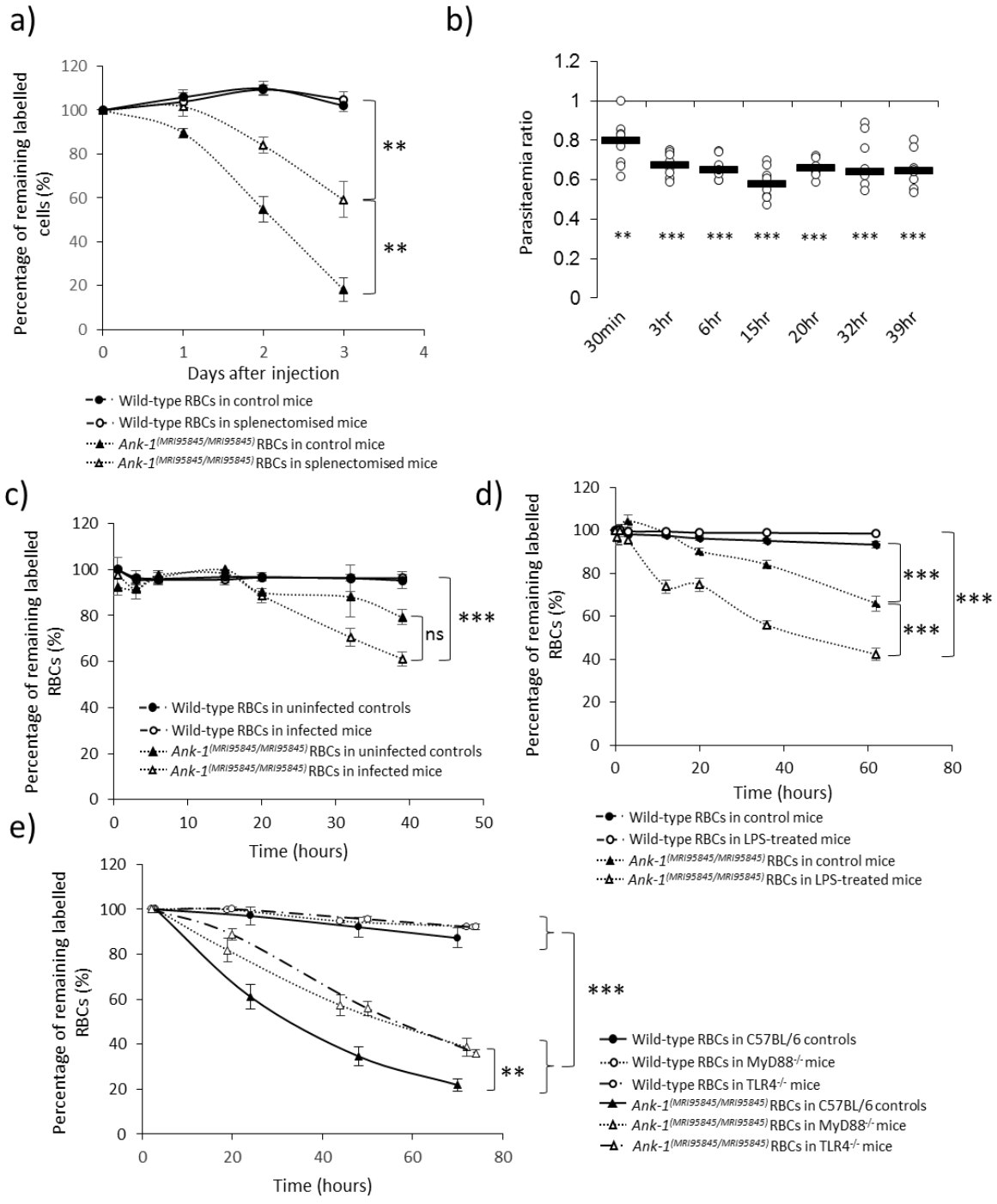

Figure 4.10: The role of splenic filtration and TLR4-mediated clearance in the destruction of *Ank-1*$^{(MRI95845/MRI95845)}$ erythrocytes. The remaining proportion of labelled wild-type and *Ank-1*$^{(MRI95845/MRI95845)}$ erythrocytes in infected splenectomised and control mice over 3 days starting at 1% parasitaemia (n=6) (a). The parasitaemia ratio (b) and the proportion (c) of labelled *Ank-1*$^{(MRI95845/MRI95845)}$ to wild-type erythrocytes in mice infected with high dose ($2x10^7$) of parasites during IVET assay (n=8). The remaining proportion of labelled wild-type and *Ank-1*$^{(MRI95845/MRI95845)}$ erythrocytes in uninfected LPS-treated and control mice over 62 hours (n=6) (d). The proportion of labelled wild-type and *Ank-1*$^{(MRI95845/MRI95845)}$ erythrocytes in uninfected control C57BL/6, MyD88$^{-/-}$ and TLR4$^{-/-}$ mice during IVET assay (n=5-6) (e). P values were calculated using Student's t-test with hypothetical mean of 1 for (b), and on the area under curve for the rest of the figures. ** P<0.01, *** P<0.001. Error bars indicate SEM.

The effect of an activated innate immune system on *Ank-1*$^{(MRI95845/MRI95845)}$ erythrocyte clearance was further studied using lipopolysaccharides (LPS) as the activating agent, which has been shown to activate Toll-like receptor 4 (TLR4) pathway to mediate innate immune responses [449]. Uninfected mice were first injected with labelled blood, followed by LPS injection into the intraperitoneal cavity the following day. Mice treated with LPS showed increased *Ank-1*$^{(MRI95845/MRI95845)}$ erythrocyte clearance compared to control mice, with an additional 20% reduction in *Ank-1*$^{(MRI95845/MRI95845)}$ erythrocyte numbers at 60 hours post-injection (Figure 4.10d), whereas no reduction in numbers was observed for wild-type erythrocytes in both control and LPS-treated mice. These findings suggest a possible LPS-mediated pathway involving TLR4 or other secondary pro-inflammatory pathways, resulting in the activation of the innate immune system for the clearance of *Ank-1*$^{(MRI95845/MRI95845)}$ erythrocytes, although it might also due to other effects LPS has on other aspects of immune system.

As such, this theory was further investigated by monitoring the *Ank-1*$^{(MRI95845/MRI95845)}$ erythrocyte numbers in Myeloid Differentiation Primary Response 88 (MyD88) and TLR4 knockout mice, both of which have previously shown activation by LPS [449]. Figure 4.10e compares the wild-type and *Ank-1*$^{(MRI95845/MRI95845)}$ erythrocyte numbers in C57BL/6 control, with *MyD88*$^{-/-}$ and *TLR4*$^{-/-}$ mice. In agreement with previous findings, the *Ank-1*$^{(MRI95845/MRI95845)}$ erythrocyte number reduced significantly compared to wild-type erythrocytes. Both *MyD88*$^{-/-}$ and *TLR4*$^{-/-}$ mice showed approximately 15% reduction in *Ank-1*$^{(MRI95845/MRI95845)}$ erythrocyte clearance, which is statistically significant. These results suggest that TLR4-MyD88 pathway might not be the major contributor for increased *Ank-1*$^{(MRI95845/MRI95845)}$ erythrocyte clearance.

4.3 Discussion

4.3.1 Summary of findings

In this study, two novel ENU-induced ankyrin-1 mutations in mice were investigated: MRI96570 which carries a nonsense mutation, and MRI95845 which carries a missense mutation. Both mutations resulted in HS-like phenotypes, with a reduction in RBC MCV and MCH, elevated RBC count and increased RBC osmotic fragility. Mice carrying either mutation showed significant resistance towards malaria infections. Although both mutations impair parasite invasion, they also affect other processes related to the survival of the parasites. Increased parasite growth inhibition was observed in *Ank-1*$^{(MRI96570/+)}$ erythrocytes, whereas *Ank-1*$^{(MRI95845/MRI95845)}$ erythrocytes were more likely to be removed from circulation predominantly via splenic filtration.

4.3.2 *Ank-1*$^{(MRI96570)}$ and *Ank-1*$^{(MRI95845)}$ mutations displayed allelic heterogeneity on host mice phenotypes and during malaria infections

Although both *Ank-1* mutations give rise to HS-like phenotype in mice, the severity was notably different. Homozygosity for MRI96570 mutation is lethal, while MRI95845 homozygotes appeared healthy, while both *Ank-1*$^{(MRI96570/+)}$ mice and *Ank-1*$^{(MRI95845/+)}$ mice exhibited HS-phenotypes with similar severity. Unlike the heterozygotes, *Ank-1*$^{(MRI95845/MRI95845)}$ RBCs are more susceptible to haemolysis (Figure 4.4) and a disrupted RBC cytoskeletal structure (Figure 4.6). These findings are consistent with the clinical heterogeneity of HS in human populations, where various *ANK-1* mutations give rise to symptomatic HS [394], and homozygosity for null mutations are usually lethal [450].

While both mutations conferred malaria protection (Figure 4.7) and appeared to impair parasite invasion (Figure 4.8), they also showed some remarkable differences in mediating this resistance.

Parasites in *Ank-1*$^{(MRI96570/+)}$ erythrocytes were more likely to be TUNEL-positive, indicating impaired intra-erythrocytic maturation, which was not observed in *Ank-1*$^{(MRI95845/+)}$ and *Ank-1*$^{(MRI95845/MRI95845)}$ erythrocytes (Figure 4.8b). While it is possible that MRI95845 mutation might affect parasite growth in other stages, MRI95845 appeared to support normal parasite maturation at least in ring and trophozoite stages.

Conversely, *Ank-1*$^{(MRI95845/MRI95845)}$ erythrocytes were more likely to be removed from circulation and possibly increased turnover rate (Figure 4.9c-e), a phenomenon that was not observed in *Ank-1*$^{(MRI96570/+)}$ erythrocytes. This increased removal was most likely due to bystander RBC clearance during infection, since it did not correlate with the parasite load (Supp. Figure 4.1), and only detectable during malaria infection or upon immune system stimulation (Figure 4.10d). The majority of *Ank-1*$^{(MRI95845/MRI95845)}$ erythrocyte clearance was partly mediated by the spleen (Figure 4.10a) and possibly the LPS-TLR4 mediated pathway, to a lesser extent (Figure 4.10d). However, immune activation via other pathways might also contribute to the clearance, which could be explored in further studies. Nevertheless, it is evident from these findings that *Ank-1* gene exhibits allelic heterogeneity in mediating malaria resistance.

4.3.3 Similarities of allelic heterogeneity in *Ank-1* and other malaria susceptibility genes

As evidenced from this study, the protective effect of the *Ank-1* gene against malaria is dependent on the nature and the location of mutations within the gene. Similarly, this allelic heterogeneity is also observed in other malaria susceptibility genes in human populations. For instance, although many G6PD deficiency-causing alleles have been implicated with malaria protection [451,452], the protective effects are often debated, with many studies reporting increased, or no protection, for individuals with certain alleles of G6PD deficiency [121,123,453-456]. This is thought to be due to the phenotypic complexity of G6PD deficiency associated with

malaria susceptibility [430]. Indeed, various G6PD alleles have been shown to cause a reduction of G6PD activity with differing severity, and was proposed to correlate with the malaria protection they conferred [453]. Similarly, *Ank-1* mutations described in this study, as well as other previous mouse studies [189,190,204], exhibit variability in malaria resistance, most likely as the result of allelic heterogeneity.

The heterogeneity in malaria resistance mechanisms of the *Ank-1* gene as observed in this study is comparable to the two prevalent alleles of the β-globin gene – the HbS and HbC, which result from amino acid substitution at position 6 from glutamate to valine, or lysine, respectively. They exhibit some similarities in mediating malaria resistance, including impaired parasite growth [209,211], reduced cytoadherence [210,212,288] and increased erythrocyte clearance [205]. However, HbS erythrocytes were found to be more resistant to all forms of malaria, whereas HbC erythrocytes appeared to be protective against cerebral malaria [432]. This difference in malaria protection was proposed to correlate with distribution of HbS and HbC in Africa [433], further emphasising the importance of allelic heterogeneity in understanding host-parasite interactions.

4.3.4 Allelic heterogeneity of *Ank-1* and its association with malaria

In contrast, due to lack of large scale studies on the HS prevalence in malaria endemic regions, ankyrin has not been associated with malaria protection. Although HS prevalence is more well-characterised in Northern European and Japanese populations, with a prevalence of about 1 in 2000 [196,198,415], one study proposed an increased HS incidence in Algeria of about 1 in 1000 [457], raising the possibility of positive selection of HS by malarial parasites. However, as the result of extreme allelic heterogeneity of HS-causing genes, many alleles do not reach sufficient frequencies [458] or achieve consistent symptoms [459] to be easily associated with malaria protection. In addition, technical difficulties [200], confounding factors from large genetic variation in African populations [460], as well as poor diagnostics and health systems [460], pose significant

challenges for dissecting the connection between HS and malaria. With development of more advanced technologies and better characterisation of the genetic structure of African populations, further studies into the association of HS and malaria could potentially yield beneficial insights into the co-evolutionary relationships between humans and *Plasmodium*.

Nonetheless, previous *in vivo* studies have indicated that *Ank*-1 mutations affect merozoite invasion and maturation [189,204], both of which were also demonstrated in this study. However, this study also describes the first direct *in vivo* observation of different mutations in the *Ank-1* gene mediating two distinct, independent mechanisms of malaria resistance, where one impairs parasite maturation and the other increases RBC clearance. Ankyrin is one of the key proteins involved in RBC remodelling by parasites [236,272,280], and maintaining the structure of RBC cytoskeleton [394,461]. It is possible that this allelic heterogeneity is due to the effect each mutation has on the integrity of RBC cytoskeletal structure, as evidenced by the significantly increased band 3 solubility and mobility caused by *Ank-1*$^{(MRI95845)}$, but not *Ank-1*$^{(MRI96570)}$ mutation (Figure 4.6). This suggests that mutations at different locations of the ankyrin protein might have different effects on the RBCs, consequently impacts the ability of parasites to invade and grow. This hypothesis also agrees with the findings from other *Ank-1* mice from previous studies, as well as *Ank-1*$^{(MRI61689/+)}$ mice from previous chapter, where each mutation exhibited differences in terms of mechanisms of malaria resistance. However the interaction between RBC cytoskeletons and malarial parasites was not directly tested in this study, which is one major limitation of this study. Nevertheless, this could be the basis for further studies, which might explain the differences in the underlying malaria resistance between ankyrin-1 mutations.

4.4 Conclusion

In conclusion, this chapter reported a novel observation where the *Ank-1* gene exhibits phenotypic heterogeneity in mediating malaria resistance mechanisms either via impairing intra-erythrocytic parasite growth, or promoting RBC clearance. Further studies should extend the understanding of the effects of various *Ank-1* mutations on the development of intra-erythrocytic parasites, as well as the association of HS with malaria in human populations. This could provide new insights into the intricate relationships between RBC cytoskeletal structure and parasite interactions. Furthermore, understanding the mechanisms of malaria resistance caused by ankyrin-1 gene enables us to further assess the suitability of ankyrin-1 gene as a HDT target, which is ultimately the goal of this project.

4.5 Supplementary Figures

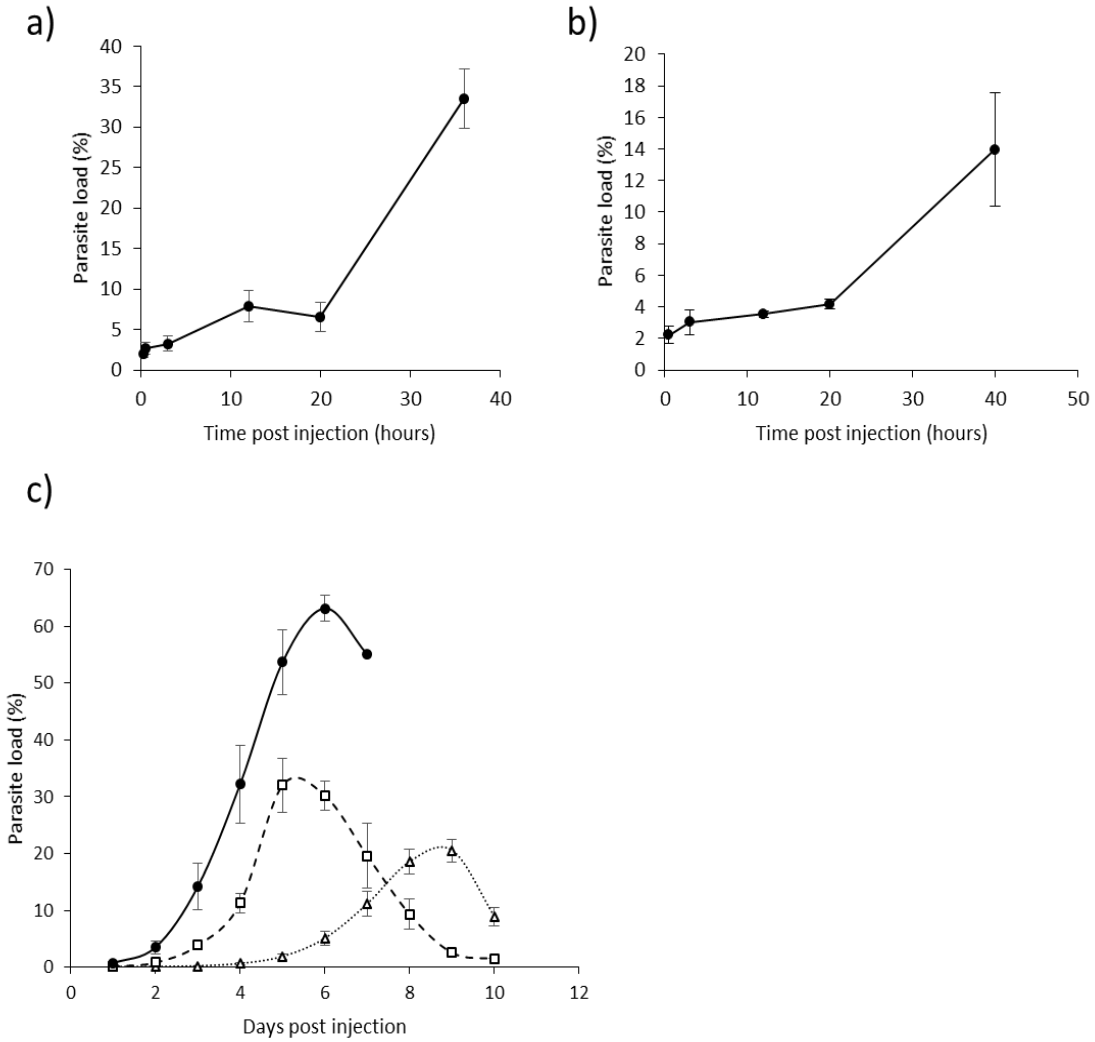

Supplementary Figure 4.1: The parasitaemia of the host mice during IVET assays and half-life assay. The parasitaemia curve of the host mice during IVET assays, when comparing wild-type with *Ank-1*$^{(MRI95845/MRI95845)}$ erythrocytes (a), and *Ank-1*$^{(MRI96570/+)}$ with *Ank-1*$^{(MRI95845/MRI95845)}$ erythrocytes (b) (n=5-7). The parasitaemia curve of wild-type, *Ank-1*$^{(MRI96570/+)}$ and *Ank-1*$^{(MRI95845/MRI95845)}$ mice during RBC half-life assay (n=6-7) (c).

CHAPTER 5

ANKYRIN-1 AS A POTENTIAL HDT CANDIDATE FOR MALARIA

5.1 Introduction

The erythrocytic cytoskeleton is comprised of various interconnecting proteins, such as band 3, ankyrin-1, α- and β-spectrin, protein 4.2 and protein 4.1R, forming a mesh-like network throughout the RBC, which gives rise to the distinct shape and reversible deformability of RBCs to travel through narrow capillaries [462,463]. During malaria infection, the RBC cytoskeleton plays an important role during the development of blood-stage parasites, which includes facilitating the invasion of merozoites [236,464] and the presentation of parasite-derived proteins on RBC surface [272,465]. As such, many genetic mutations affecting RBC cytoskeletal proteins [184,186,260] have been associated with disruptions to these processes, thereby conferring malaria protection.

RBC cytoskeleton consists of two major protein complexes, the ankyrin complex and the actin junctional complex [466]. Ankyrin complex contains several key proteins, such as band 3, ankyrin-1, protein 4.2, β-spectrin and the Rhesus complex [466,467]. In particular, ankyrin-1 is involved in the "anchoring" of spectrin tetramers onto the RBC membrane through interactions with other membrane proteins [468]. Ankyrin-1 contains several important functional domains: an N-terminal domain comprised of ankyrin repeats, a 33-residue motif that interacts with band 3 and protein 4.2; a central spectrin-binding domain; and a C-terminal regulatory domain, which is thought to affect the expression of various isoforms of ankyrin-1 [469-471]. Of particular interest in this chapter is the spectrin-binding domain, which is predicted to confer malaria resistance when disrupted. Detailed studies examining ankyrin-spectrin interactions by others determined the ankyrin-spectrin interactions involved a so-called Zu5 subdomain within the spectrin-binding domain of ankyrin-1 that binds specifically to the spectrin repeat 14 and 15 of β-spectrin [396,472,473], as illustrated in Figure 5.1. Studies by Ipsaro and Mondragon [398] have further isolated the specific amino acid residues crucial in mediating ankyrin-spectrin binding *in vitro*. Through the use of

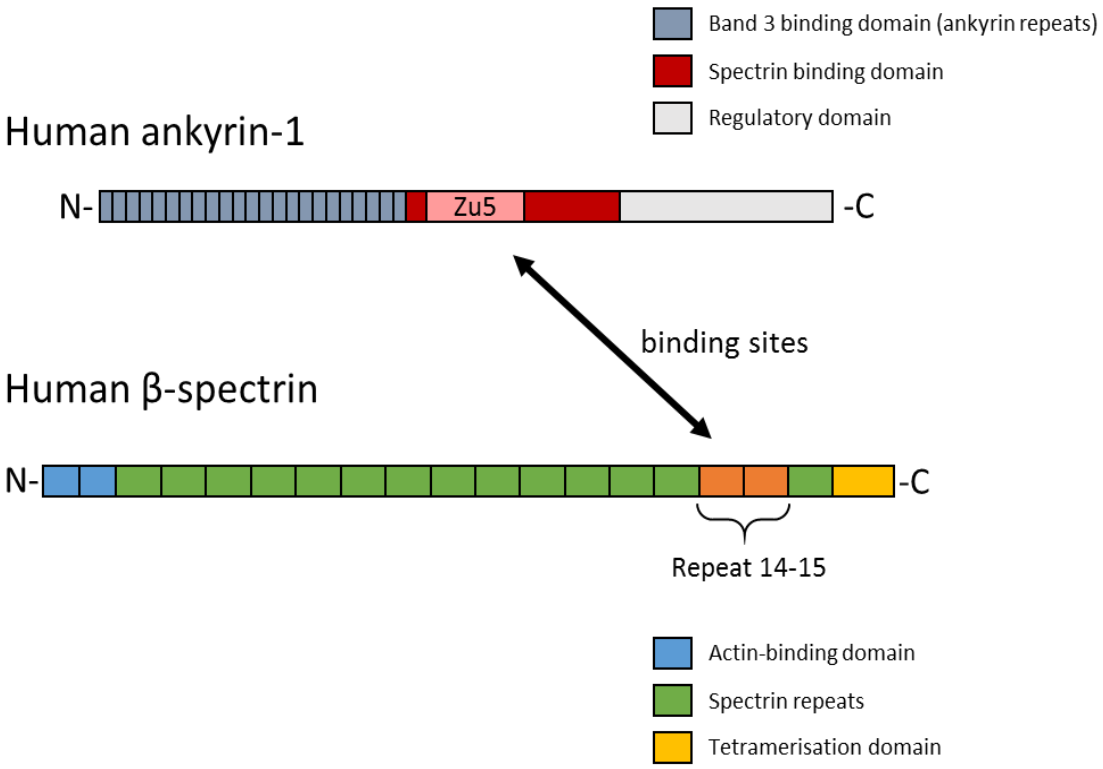

Figure 5.1: Schematic diagram of the interaction between human ankyrin-1 and β-spectrin. The human ankyrin-1 consists of 3 domains, the N-terminal band 3-binding domain with many ankyrin repeats, the central spectrin-binding domain with the Zu5 subdomain and the regulatory domain. The human β-spectrin consists of the N-terminal actin-binding domain, followed by 16 repeats of spectrin and the tetramerisation domain. The binding sites between ankyrin-1 and β-spectrin was localised at the Zu5 subdomain of ankyrin-1, and the spectrin repeat 14 and 15 of β-spectrin, as indicated by the two-headed arrow.

recombinant protein fragments containing the interacting domains of the two proteins, they observed a significantly reduced inter-protein binding interaction when the aspartic acid residue at position 1781 of β-spectrin was substituted with arginine (D1781R) [398].

Mutations in the RBC cytoskeleton proteins are associated with increased malaria resistance, as evidenced from previous *in vitro* [191,192] and *in vivo* [189,190,204] studies, as well as findings from previous chapters. From the findings by Ipsaro and Mondragon [398] and previous data, it is possible that interrupting the ankyrin-spectrin interaction though drugs could induce host resistance towards malaria. Therefore, in order for assess this possibility, a mouse line was created with the D1781R mutation and examined the effects on the erythrocyte and the response to malarial infection, to genetically validate the resulting interruption of ankyrin-

spectrin interaction. It was hypothesised that mice carrying D1781R would exhibit features consistent with an abnormal RBC cytoskeleton and consequently malaria resistance. The result would also indicate the feasibility of targeting ankyrin-spectrin interaction as part of the host-directed therapy (HDT) for malaria. As such, the development of a high-throughput screening (HTS) assay was initiated to enable the identification of small molecules that may disrupt the ankyrin-spectrin interaction, replicating the effect of the D1781R mutation biochemically.

In the context of clinical studies, disruptions to the RBC cytoskeleton are associated with several genetic disorders, such as hereditary spherocytosis (HS) and elliptocytosis (HE). In particular, HS is thought to be a result of the weakening of vertical interactions [474], with ankyrin-1 defect being the most common [201]. Despite many *in vivo* studies implicating the association of HS with malaria resistance [189,190,204], this relationship is not well-defined in clinical settings. Furthermore, as evidenced from the previous chapter, mice with HS-like phenotypes exhibit heterogeneity in mediating malaria resistance. Therefore, it was hypothesised that human HS patients might also exhibit differences in their malaria susceptibility, as a result of allelic heterogeneity in the HS-causing genes. Further studies on the various HS-causing alleles in humans could provide beneficial insights to the roles of specific alleles in conferring malaria protection, which could lead to the discovery of more potential HDT candidates for malaria.

The aim of this chapter is to evaluate the suitability of targeting ankyrin-spectrin interaction as a HDT target, by further investigating the possibility of the D1781R mutation in giving rise to malaria resistance. A mouse strain, TAR3.5, was generated which carries the D1781R mutation in its β-spectrin gene through the CRISPR/Cas9 system. Mice carrying the D1781R mutation was observed to exhibit HS-like phenotype and increased resistance to malaria infections, in agreement with our hypothesis. As a result, pilot studies into characterising the binding kinetics of ankyrin and spectrin were conducted to be used for HTS for HDT drug development. The ability of *P. falciparum* to invade and growth within the RBCs HS patients *in vitro* was assessed, as a further validation of malaria resistance mechanisms observed in mouse models from

previous chapters. The process of carrying out whole genome sequencing is currently underway to identify new HS-causing alleles, which would allow us to associate these alleles with the malaria protection they conferred, as well as determine their potential as HDT candidates. This chapter highlights the potential of targeting RBC cytoskeletal proteins to develop a HDT for malaria, as well as providing more direct evidence for the protective role of HS during malaria infections.

5.2 Results

5.2.1 D1781R mutation causes HS-like phenotypes in mice

D1781R is situated in the 14th spectrin repeat (Figure 5.2a), which is involved in ankyrin binding [396]. The D1781R mutation was introduced into SJL/J mice via the CRISPR/Cas9 system through homologous recombination in the presence of a guide RNA containing the sequence of interest and a single-stranded oligonucleotides containing the D1781R mutation, generating the TAR3.5 mouse strain. Ten days old founder mice were genotyped by Sanger sequencing to reveal a dinucleotide point mutation in exon 34 of *Sptb* gene, with a substitution of GA with CG nucleotides indicating successful editing (Figure 5.2b). TAR3.5 mice heterozygous for D1781R mutation will be referred to as *Sptb*$^{(D1781R/+)}$, whereas homozygotes will be referred to as *Sptb*$^{(D1781R/D1781R)}$. Both *Sptb*$^{(D1781R/+)}$ and *Sptb*$^{(D1781R/D1781R)}$ mice appeared healthy with no signs of morbidity and exhibited a normal lifespan, indicating that the mutation had a minor detrimental effect on the mice.

If the mutation disrupts ankyrin-spectrin binding, as predicted by Ipsaro and Mondragon [398], it was hypothesised to give rise to a HS-like phenotype. As a result, haematological analysis was performed on *Sptb*$^{(D1781R/+)}$ mice. The *Sptb*$^{(D1781R/+)}$ mice exhibited a significant reduction in MCV (49.7±0.4 fl compared to 53.3±0.6 fl of wild-type) and MCH (14.4±0.2 pg compared to 15.1±0.1

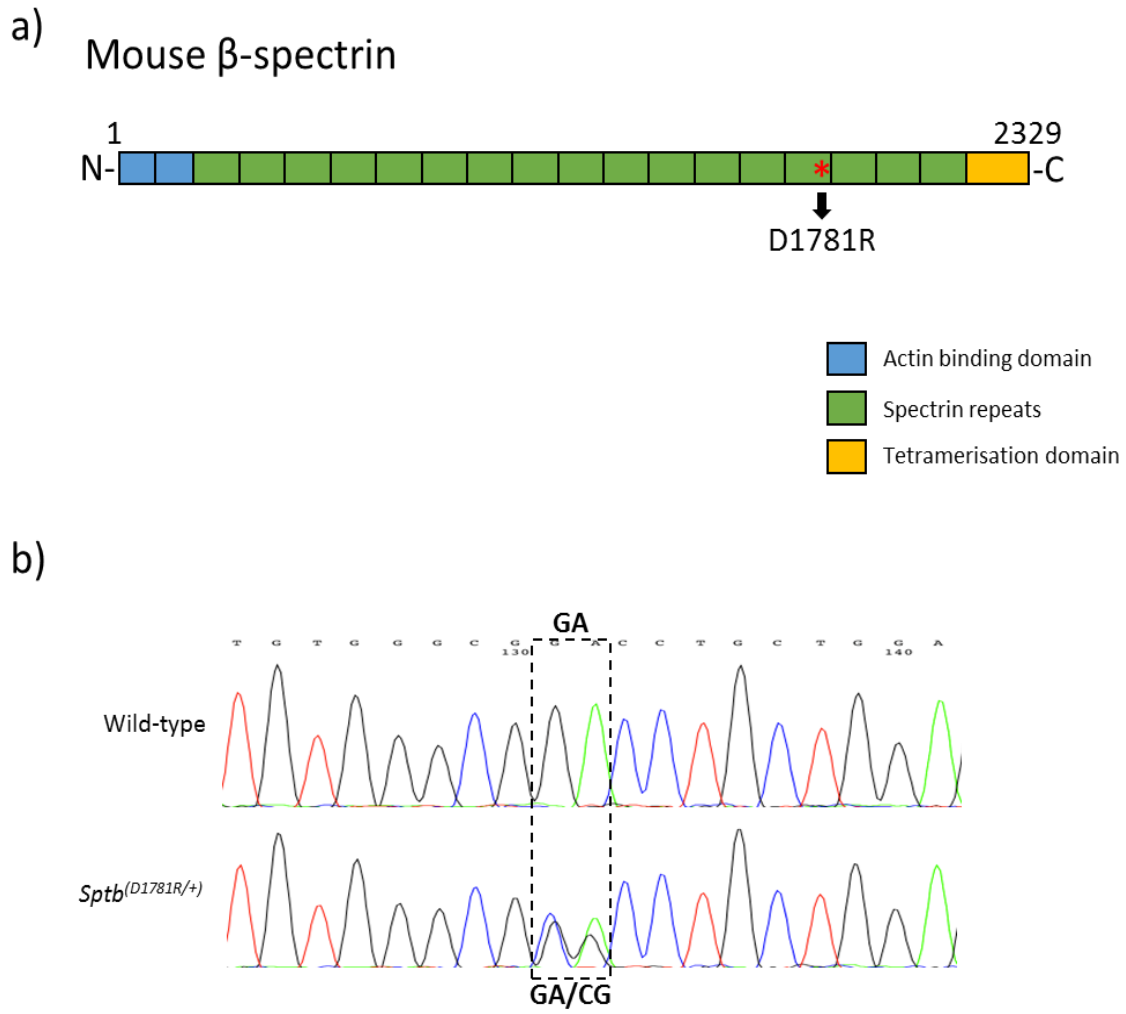

Figure 5.2: The location of D1781R mutation. The predicted effect of D1781R mutation on the SPTB protein, showing an aspartate to arginine substitution at residue 1781 in the 14th repeat of spectrin domain (a). The Sanger sequencing of mice carrying the D1781R mutation in the heterozygous state, showing a dinucleotide mutation from GA to CG (b).

pg of wild-type) (Figure 5.3a-b), suggesting a reduced RBC volume and haemoglobin amount. RBC osmotic fragility was also assessed as part of the diagnosis for HS. As shown in Figure 5.3c, the RBCs of *Sptb*$^{(D1781R/+)}$ mice showed no significant difference compared to wild-type RBCs, however, the RBCs of *Sptb*$^{(D1781R/D1781R)}$ mice exhibited a significant increase in osmotic fragility compared to wild-type RBCs, with 50% lysis at approximately 5.6 g/L sodium chloride concentration, as opposed to 4.4 g/L of wild-type RBCs. These findings indicate that D1781R mutation can give rise to HS-like phenotype in mice.

The disruptive effect of the D1781R mutation was hypothesised to affect the structural integrity of the RBC cytoskeleton. Therefore, the mobility of membrane band 3 was examined as an indication of binding affinity of band 3 with the RBC cytoskeleton, via Fluorescence recovery after photobleaching (FRAP) analysis with fluorescently labelled band 3, and recorded the recovery of fluorescence intensity after photobleaching with high-powered laser. The RBCs from *Sptb*$^{(D1781R/D1781R)}$ mice were specifically examined, as they reflected the full disruptive effect of the mutations. As shown in Figure 5.3d, they exhibited a significantly increased fluorescence recovery, indicating increased band 3 mobility, which supported our hypothesis. It is likely that this disruption would lead to decreased RBC deformability [475]. Therefore, two methods were used to investigate the RBC deformability: Ektacytometry and *in vitro* retention assay though the use of metal beads to model splenic filtration (described by Deplaine, et al. [400]), in which RBC retention indicates reduction in RBC deformability. Firstly, when subjected to shear stress in the ektacytometer, erythrocytes of *Sptb*$^{(D1781R/+)}$ mice exhibited a similar elongation index as wild-type erythrocytes (Figure 5.3e), suggesting no difference in RBC deformability in *Sptb*$^{(D1781R/+)}$ mice, however, *Sptb*$^{(D1781R/D1781R)}$ mice were not analysed due to time constraints. For the *in vitro* retention assay, *Sptb*$^{(D1781R/+)}$ erythrocytes showed significantly increased retention in the bead layer, whereas the *Sptb*$^{(D1781R/D1781R)}$ erythrocytes showed a further increased retention (Figure 5.3f). These findings suggest a reduction in RBC deformability in *Sptb*$^{(D1781R/+)}$ and *Sptb*$^{(D1781R/D1781R)}$ mice.

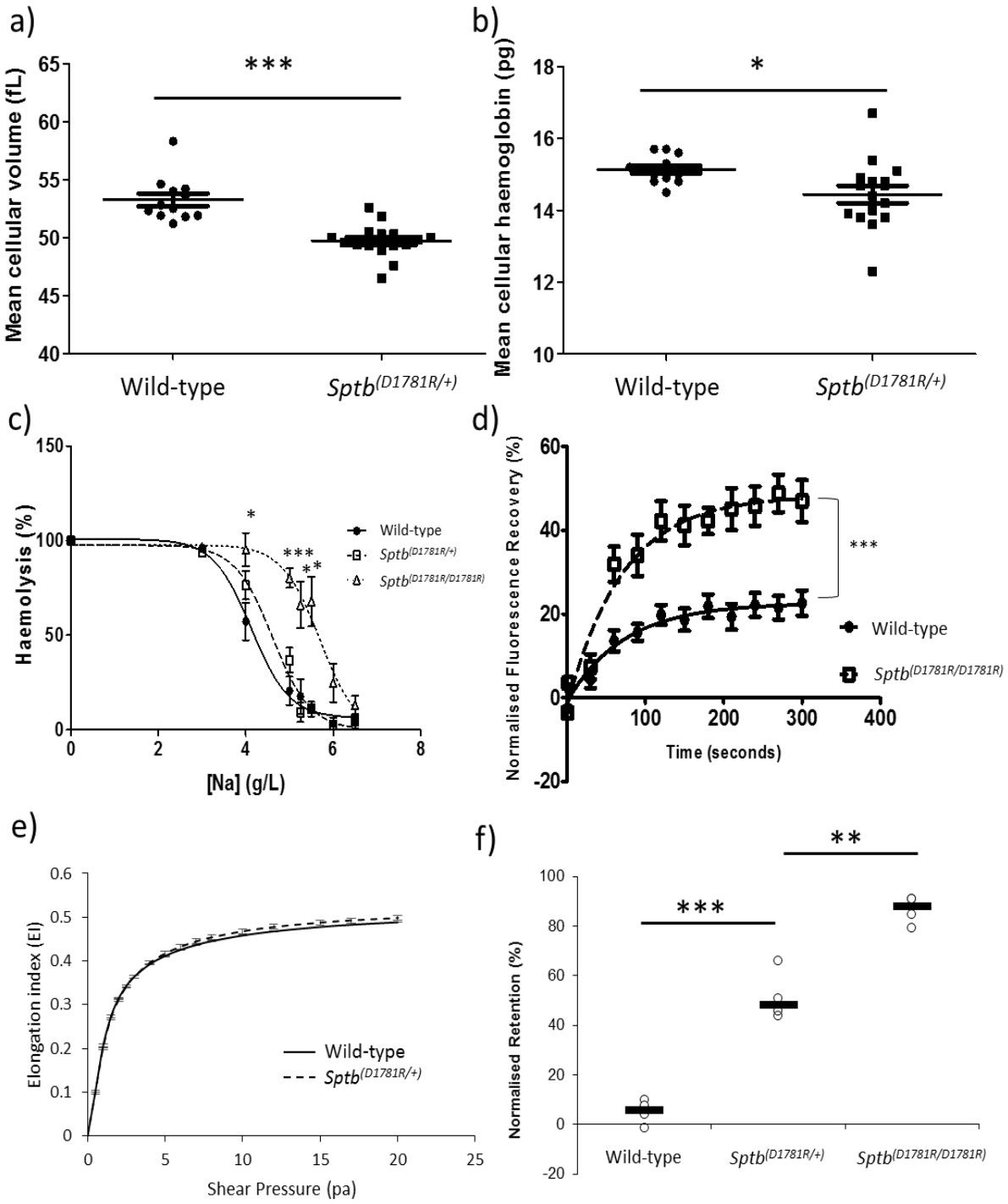

Figure 5.3: The phenotypic characterisation of D1781R mice. The RBC mean cellular volume (MCV) (a) and the mean cellular haemoglobin (b) of wild-type and *Sptb*$^{(D1781R/+)}$ mice. The RBC osmotic fragility of wild-type, *Sptb*$^{(D1781R/+)}$ and *Sptb*$^{(D1781R/D1781R)}$ mice (c) (n=4). Membrane band 3 mobility of wild-type and *Sptb*$^{(D1781R/D1781R)}$ erythrocytes as measured via FRAP assay (n=15-17) (d). The RBC deformability was measured by ektacytometry (n=3) (e) and *in vitro* spleen retention assay (n=4) (f). All p values were calculated using parametric Student's t-test. Specifically, p-value for (d) was calculated on the area under curves. * P<0.05, ** P<0.01, *** P<0.001. Error bars indicate SEM.

5.2.2 D1781R mutation confer malaria resistance in mice, and inhibit merozoite invasion

To test if the D1781R mutation confers malaria resistance, both *Sptb*$^{(D1781R/+)}$ and *Sptb*$^{(D1781R/D1781R)}$ mice were challenged with *P. chabaudi adami DS* and recorded the parasite load and survival rate over time. Approximately 60% of the *Sptb*$^{(D1781R/D1781R)}$ mice survived the challenge, whereas none of the wild-type littermates survived ($p<0.01$). Comparing between these two genotypes, there was also a significant reduction in peak parasitaemia (28% compared with 57% of wild-type; $p<0.01$) and a three-day delay before this was reached in the homozygotes (Figures 5.4a and 5.4b). On the other hand, the *Sptb*$^{(D1781R/+)}$ mice exhibited a less pronounced increase in survival and reduction in parasitaemia compared to wild-type, although these differences are not statistically significant ($P=0.09$).

The mechanisms for the resistance to malaria infection observed in the *Sptb*$^{(D1781R/D1781R)}$ mice were investigated. An IVET assay was performed to assess the ability of parasites to invade mutant erythrocytes and the RBC clearance rate during malaria infection. The parasitaemia of both genotypes of RBCs were compared and expressed as a ratio to indicate the relative susceptibility towards merozoite invasion. The ratio of infected mutant (*Sptb*$^{(D1781R/D1781R)}$) versus wild type erythrocytes infected with *P. chabaudi* parasites was significantly less than one, from one hour until 32 hours after the labelled red cells were injected into an infected wild-type recipient mouse with 2-9% initial parasitaemia (Figure 5.4c). This suggested that mutant RBC were more resistant than their wild type counterparts to merozoite invasion. The proportions of labelled wild-type and *Sptb*$^{(D1781R/D1781R)}$ RBCs remained similar during the examined period of infection (Figure 5.4d), suggesting no significant difference clearance of *Sptb*$^{(D1781R/D1781R)}$ erythrocytes. To further verify this observation, the RBC half-life was monitored in infected wild-type and *Sptb*$^{(D1781R/D1781R)}$ mice. The RBCs of *Sptb*$^{(D1781R/D1781R)}$ mice exhibited modest but a statistically significant reduction in RBC half-life of about 10% compared to wild-type mice

(Figure 5.4e), thus unlikely to be a major contributor to the malaria resistance, although the exact mechanisms remained to be explored. Overall, these results suggested that impaired merozoite invasion is likely to be the major underlying resistance mechanisms of *Sptb*$^{(D1781R/D1781R)}$ mice.

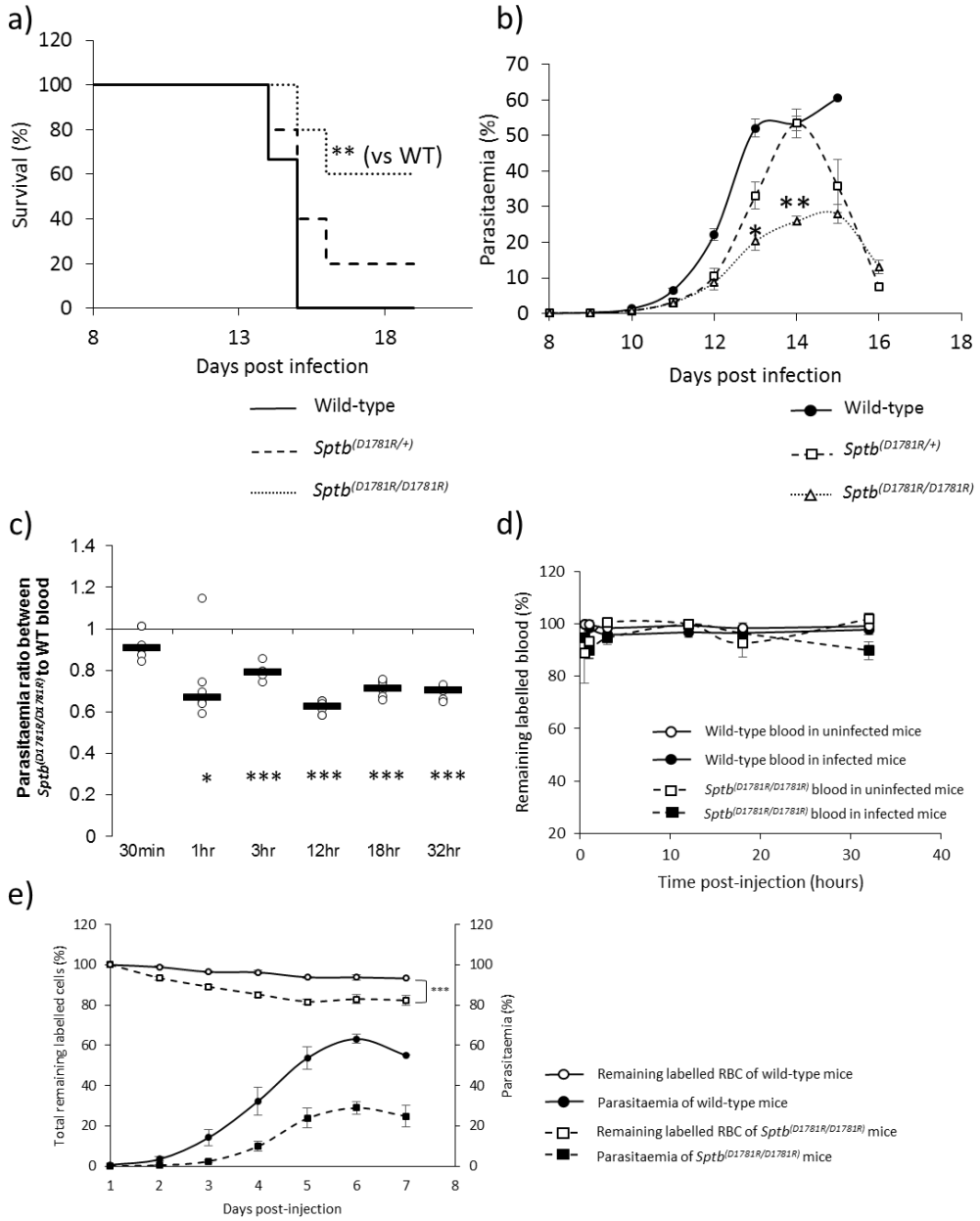

Figure 5.4: The effect of D1781R mutation during malaria infections. The survival rate (a) and the parasite load (b) of wild-type, *Sptb*$^{(D1781R/+)}$ and *Sptb*$^{(D1781R/D1781R)}$ mice when challenged with 1x10^4 *P. chabaudi*. The parasitaemia ratio of *Sptb*$^{(D1781R/D1781R)}$ to wild-type erythrocytes as measured by IVET assay (c), and the percentage of remaining labelled erythrocytes (d) over 36 hours post-injection (n=5). The RBC half-life of *Sptb*$^{(D1781R/D1781R)}$ mice during malaria infection, in conjunction with the parasitaemia curve (e) (n=5). P values for (a) were calculated using Log-Rank test; for (b), (d) and (e), p values were calculated on the area under curves using Student's t-test; while for (c), p values were obtained using Student's t-test with hypothetical mean of 1. * P<0.05, **P<0.01, ***P<0.001. Error bars indicate SEM.

5.2.3 Expression and purification of recombinant ankyrin and spectrin protein fragments

Following the validation of malaria protection conferred by D1781R mutation, the development of an assay for the HTS was initiated to identify potential drug molecules to interrupt ankyrin-spectrin interactions, as a possible HDT drug for malaria treatment. A heterologous expression of recombinant protein fragments containing the binding site of ankyrin (*ANK-1 Zu5*; residues 911 to 1068) and β-spectrin (*SPTB-1315*; residues 1583 to 1905), and the β-spectrin fragment with the D1781R mutation (*SPTB-D1781R)* was performed in *E. coli*. These fragments were first expressed in a GST-tag expression plasmid (pGEX-6P-3), and purified on a GST affinity column (Supp. Figure 5.1a-b).

However, the ANK-1 Zu5 protein exhibited low solubility and stability, where more than 50% of the ANK-1 Zu5 protein were found in the insoluble fraction after protein expression, and some soluble protein precipitated after purification. The preliminary binding assay was carried out on the Biacore 2000, which showed a reduced binding of SPTB-D1781R fragment with the ANK-1 fragment, compared to the SPTB-1315 fragment (Supp. Figure 5.1c), which is possibly consistent with the previous study [398].

As a result, GST tags were replaced with 6X histidine (His) tags (Figure 5.5a) to improve the solubility of these protein fragments by reducing steric interference during protein folding. The protein fragments were purified on high performance liquid chromatography (HPLC) on a nickel affinity column (HiTrap Chelating HP). For SPTB-1315 and SPTB-D1781R protein fragments, the chromatograms of the purification, as well as the analysis of each fraction via Coomassie staining and Western blotting with anti-6XHis antibody were illustrated in Figure 5.5b. This result indicates the successful purification of His-tagged spectrin fragments, as evidenced from the presence of expected size on SDS-PAGE and presence of 6xHis tags on a Western blot. Similarly for ANK-1 Zu5 purification, the fractions from purification as indicated

by the arrows were analysed using Coomassie staining and Western blotting (Figure 5.5c). The presence of His-tagged ANK-1 Zu5 protein fragments were verified based on the expected size on SDS-PAGE, as well as the presence of His-tags when probed with anti-6xHis antibody on Western blot. However, due to time constraints, further protein purifications and binding assays were not conducted.

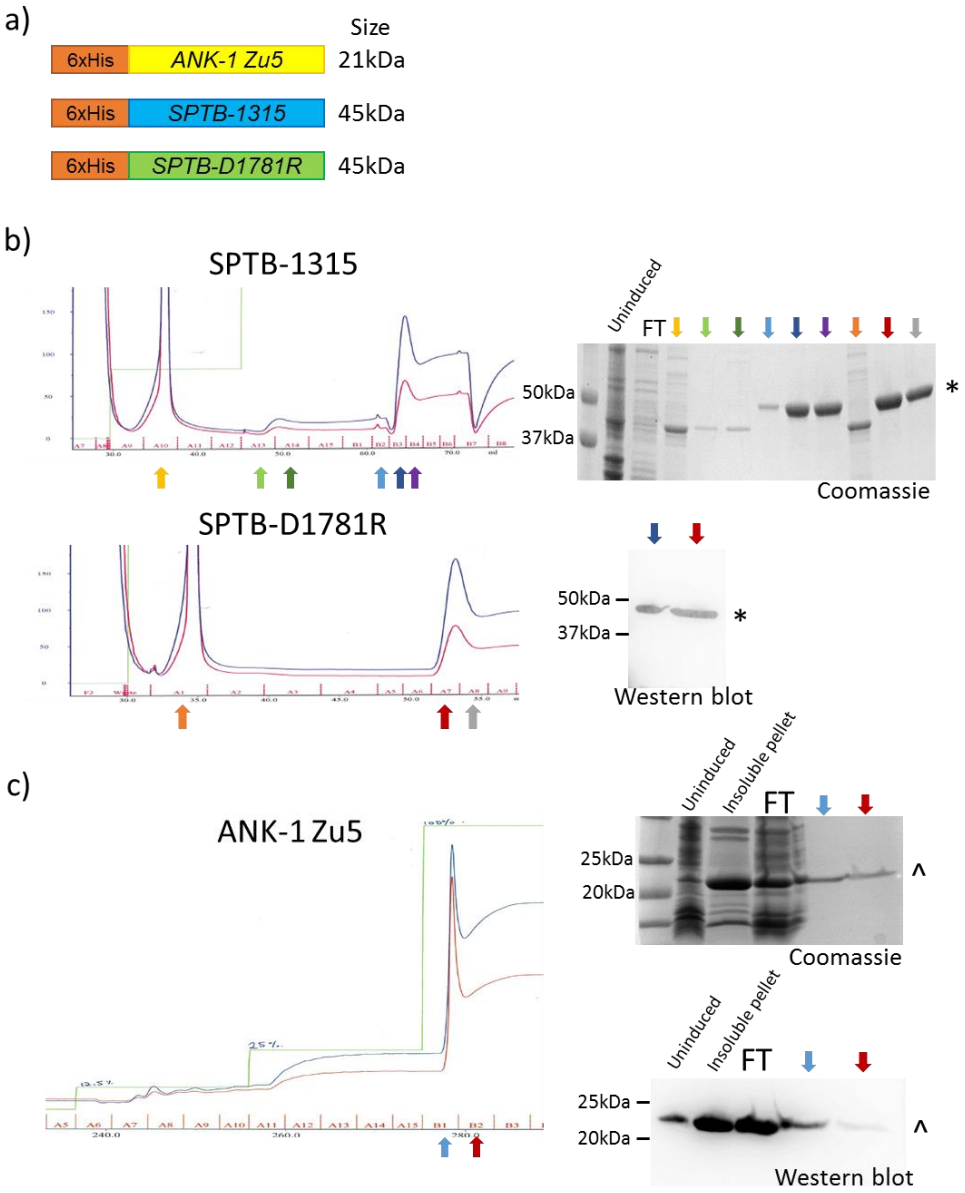

Figure 5.5: The purification of 6xHis-tagged recombinant GST-tagged ANK-1 and SPTB binding fragments. The schematic diagram and predicted protein sizes of 6xHis-tagged ankyrin Zu5 domain (ANK-1 Zu5), beta spectrin repeat 13 to 15 (SPTB-1315) and beta spectrin repeat 13 to 15 carrying D1781R mutation (SPTB-D1781R) (a). The HPLC chromatograms of SPTB-1315 and D1781R purification (b); and ANK-1 Zu5 purification (c), where each coloured arrow indicates fraction analysed via Coomassie staining or Western blotting using Anti-6xHis antibody. FT= flow through during purification, * indicates the presence of SPTB proteins fragments, ^ indicates the presence of ANK protein fragments.

5.2.4 Erythrocytes from HS patients are resistant to parasite invasion

Based on the findings above, it is likely that mutations that disrupt RBC cytoskeleton which give rise to genetic disorders such as HS could be targeted for HDT development against malaria. As such, it is of our interest to identify more HS-causing alleles as potential HDT candidates, as well as verifying our proposed malaria resistance mechanisms as seen in ENU-mice from previous chapters. With the collaboration of Dr David Rabbolini from the Royal North Shore Hospital, blood samples were obtained from human patients which had been diagnosed with symptomatic HS and monitored periodically. Under light microscopy, the RBCs of HS patients appeared echinocytic, anisocytic and some exhibited loss of central pallor (Figure 5.6a). The RBCs of HS patients also appeared more likely to undergo haemolysis compared to control RBCs. To assess their susceptibility towards *P. falciparum*, an *in vitro* parasite invasion and growth assay was conducted on the RBCs of four HS patients (A-D). Some purified trophozoites stage parasites was first inoculated with either control or HS erythrocytes to give an approximately 1% starting parasitaemia and measured the parasite load and developmental stages in these RBCs. As shown in Figure 5.6b, RBCs from all four HS patients exhibited a significant reduction in parasitaemia at 12 hours post-inoculation, suggesting a significant reduction in the invasion rate of *P. falciparum* into these RBCs. However, these spherocytes exhibit constant parasitaemia and similar proportion of parasite stages compared to control RBCs throughout the cycle, possibly indicating normal parasite maturation within these RBCs from HS patients, although further investigation is required.

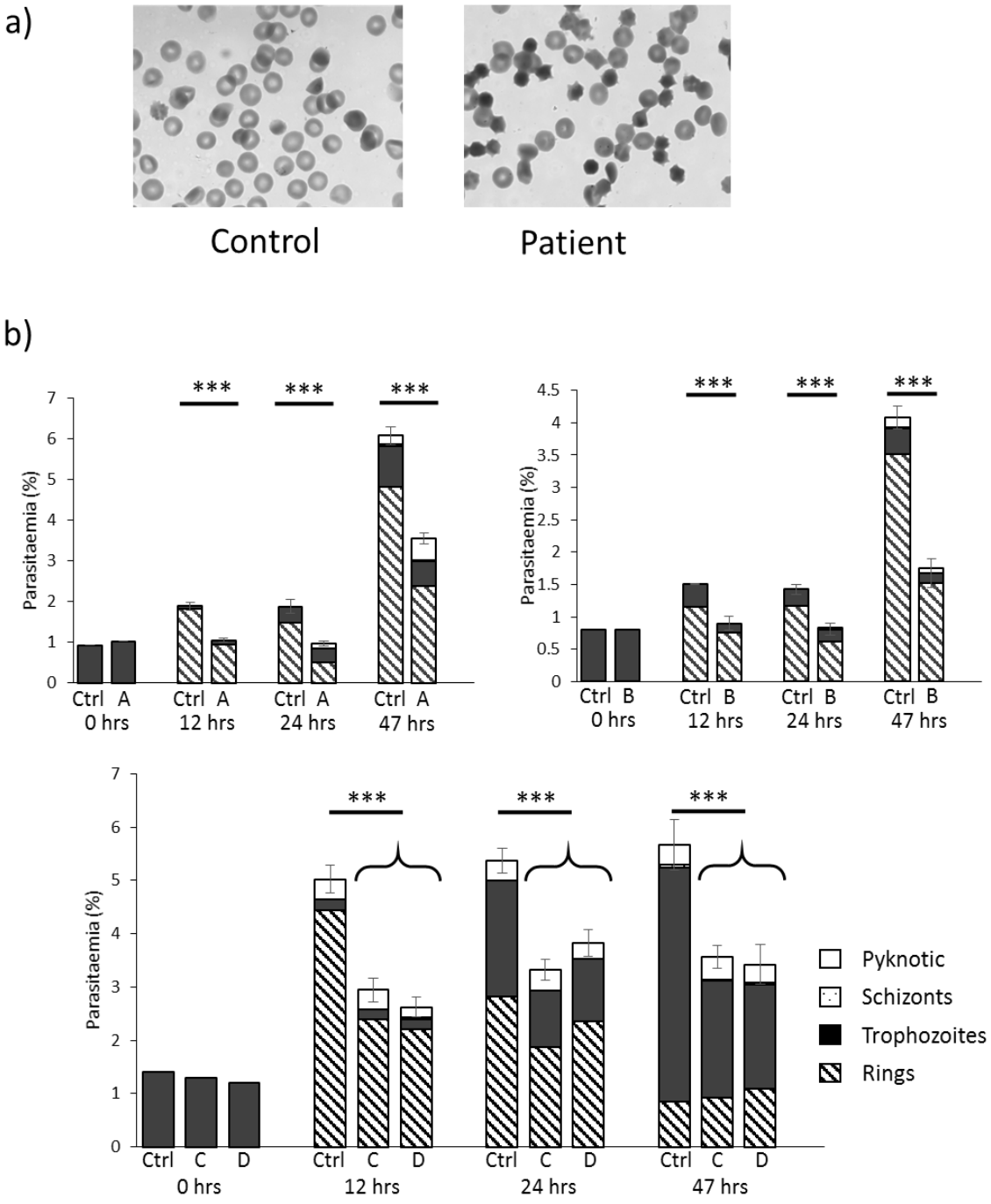

Figure 5.6: The RBC morphology and *P. falciparum* susceptibility of HS patients. The RBC morphology of the HS patient compared to the healthy control in *in vitro P. falciparum* culture (a). The parasitaemia and the stages of *P. falciparum* (3D7 strain) in control and HS (A-D) erythrocytes up to 47 hours, starting with approximately 1% mature trophozoites, each with 4 technical replicates (b). P values were calculated using Student's t-tests. *** P<0.001. Error bars indicate SEM.

5.3 Discussion

5.3.1 Summary of findings

In this chapter, a CRISPR/Cas9 generated mouse strain with a D1781R substitution in the β-spectrin gene was reported to exhibit HS-like phenotype and resistance to malaria, thus providing a genetic validation for the disruptive effect of D1781R. The development of HTS assay for disrupting ankyrin-spectrin interaction was also initiated to look for potential HDT drug candidates. Finally, an *in vitro P. falciparum* invasion and growth assay was performed on RBCs of HS patients to verify our previous observations of reduced invasion and growth of malarial parasites in mouse models.

5.3.2 The genetic validation of D1781R disruptive effect for HDT development

With better characterisation of various protein-protein interactions (PPI) and technological advances, drug inhibition for PPI is one of the emerging areas of research in the past decade [476]. Many studies have been conducted with the aim of identifying PPI inhibitors for various cancers or inflammatory diseases (reviewed by Arkin, et al. [477]). Notably, the BCL-family, which is involved in apoptosis, has been one of the targets for PPI inhibition to treat cancers [478,479], with several potential inhibitors having progressed into clinical trials [480-482], highlighting the realities of using PPI as drug targets. However, many challenges still remain, such as the lack of defined binding sites in many PPI and the low inherent hit rate from HTS [483]. Nevertheless, with the discovery of critical binding residues of ankyrin-spectrin interactions [398], it is possible to target this PPI for malaria HDT development, providing that it could be verified *in vivo*.

The genetic validation of the D1781R disruptive effect described in this study enabled further investigations into developing a HTS for discovering potential drugs that interrupt ankyrin-spectrin binding. One important observation is that these mice did not exhibit any signs of

morbidity and survived well into adulthood, indicating minimal toxicity associated with the D1781R mutation. In the context of malaria infections, the D1781R mutation appeared to confer significant malaria protection to the host mice without detrimental effects, unlike many protective genetic polymorphisms in humans, which are often accompanied with fitness cost. These observations also further suggested that interruption of ankyrin-spectrin interaction is unlikely to result in morbidity, which presents an attractive target for HDT development.

As such, the characterisation of the binding kinetics of ankyrin-spectrin interaction was carried out for HTS development. However, the poor solubility and stability of ANK-1 Zu5 protein fragment posed a significant technical challenge to the study, possibly due to misfolding during protein expression. Therefore, further optimisation of the expression or purification is required, either by slowing protein expression or using additives to improve the protein stability after purification. Nevertheless, our preliminary result on the ankyrin-spectrin binding appeared consistent with the observation by Ipsaro and Mondragon [398] (Supp. Figure 5.1c), which could be further investigated in future studies.

5.3.3 Identification of more potential HDT candidates via studies on HS patients

The genetic validation of the D1781R mutation also presented the prospect of discovering other alleles as suitable HDT targets. Disruptions to the ankyrin-spectrin interaction is likely to manifest as HS in human populations, since it is part of vertical interactions of RBC cytoskeleton. Therefore, with collaboration with local hospitals, HS patients were recruited and their susceptibility to malarial parasites and causative mutations were characterised. As reported in this study, the RBCs of all four HS patients examined in this study exhibited significant resistance towards merozoite invasion (Figure 5.6b), indicating each patient allele could be a potential HDT candidate. Although the causative mutations still remained to be identified, it is possible that these alleles would affect various areas of RBC cytoskeleton, not just restricted to ankyrin-

spectrin interactions, due to the heterogeneous nature of HS. This would reveal other RBC cytoskeletal interactions as potential drug targets, such as protein 4.2-band 3 interactions, which would increase the likelihood of successful malaria HDT developments.

Furthermore, despite the strong association of HS and malaria as implicated in many *in vivo* studies, evidence from *in vitro* and epidemiological association studies on the relationship of HS with malaria have been lacking, with only a few studies being reported [191,457]. Observations from this study would consolidate with the existing evidence on the malaria protective effect in humans, allowing further examination on the possible resistance mechanisms conferred by HS. Coupled with the genetic information of these HS patients, it is possible to infer the effect of each HS-causing allele on the parasite survival, as the result of HS heterogeneity in conferring malaria resistance. Further studies would provide a better understanding of crucial cytoskeletal components that are essential for parasite development.

5.4 Conclusion

In conclusion, this study demonstrated the genetic verification of the importance of β-spectrin D1781 residue *in vivo*, which could potentially be mimicked using drugs for malaria HDT development. In addition, the potential protective roles of HS against malaria in humans were explored *in vitro*, which would provide additional insights to host-parasite interaction, and possibly identify more suitable HDT targets for malaria. With sufficient timeframe, this study could potentially yield valuable evidence on the possibility of translating *in vivo* studies into clinical settings.

5.5 Supplementary Figures

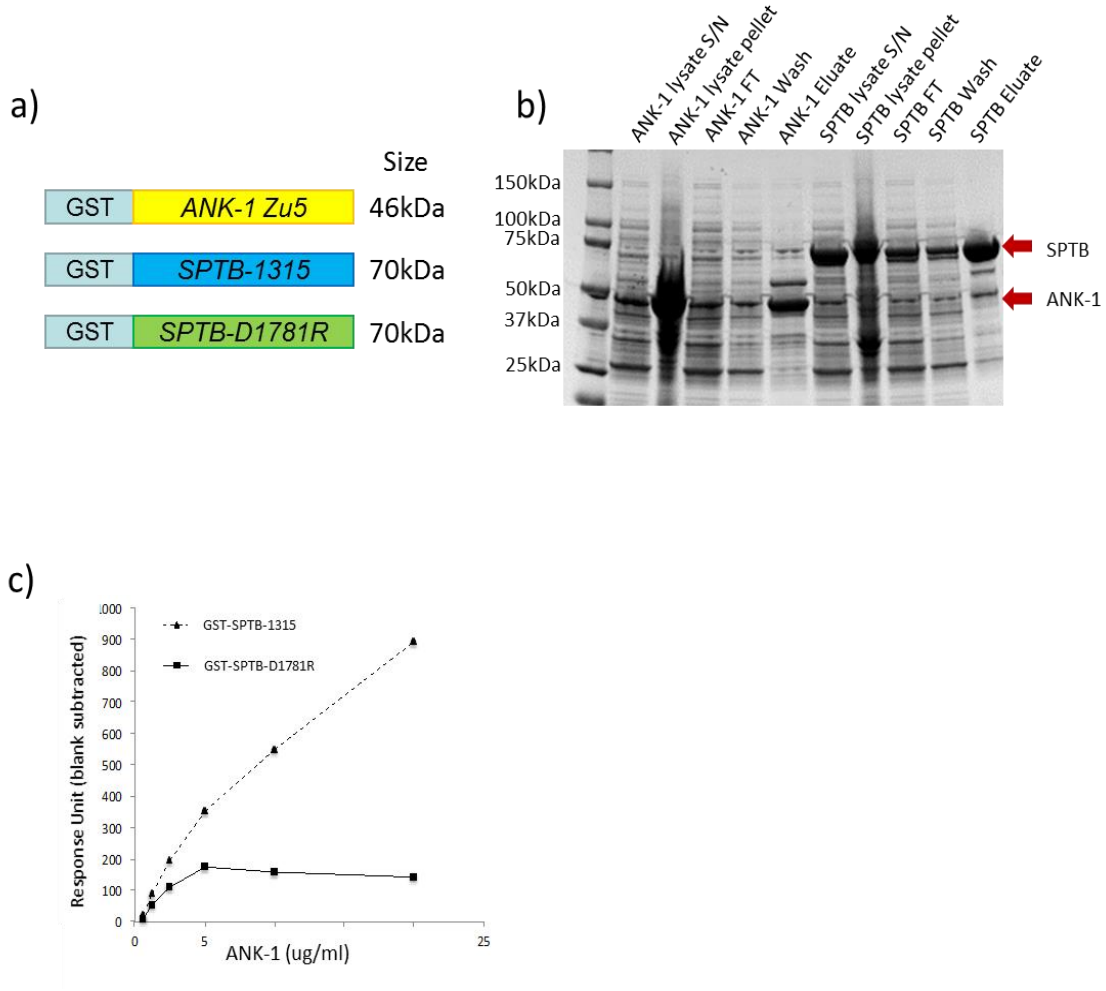

Supplementary Figure 5.1: The purification and interaction of recombinant GST-tagged ANK-1 and SPTB binding fragments. The schematic diagram and predicted protein sizes of GST-tagged ankyrin Zu5 domain (ANK-1 Zu5), beta spectrin repeat 13 to 15 (SPTB-1315) and beta spectrin repeat 13 to 15 carrying D1781R mutation (SPTB-D1781R) (a). The purification process of ANK-1 Zu5 and SPTB fragments using GST-Trap column (b), where S/N = supernatant, FT = flow through, and the expected size of ANK-1 and SPTB fragments are indicated by the red arrows. The preliminary result of ANK-1 and SPTB binding as determined via Biacore 2000, using a chip coated with biotinylated SPTB fragments and variable concentration of cleaved ANK fragments (d) (n=1).

CHAPTER 6

GENERAL DISCUSSION AND CONCLUSION

Plasmodium infections have been a major driver of the evolution of human genetics for thousands of years, as evidenced by the large number of genetic polymorphisms associated with malaria protection in populations of malaria endemic regions [427,484]. These genetic polymorphisms reveal host-parasite interactions that are crucial for parasite survival, allowing the identification of potential drug targets for malaria treatments, as well as providing potential solutions to the emergence of multidrug-resistant malarial parasites. One such approach is to target host proteins or pathways essential to parasite survival to mediate the killing of parasites, mimicking the protective effect of human genetic polymorphisms, known as host-directed therapy (HDT). It is hypothesised that since HDT targets are not under the influence of parasite genetics, the parasites unlikely to overcome these host protection though mutations. As a result, it is proposed that HDT would be more resilient to parasite resistance, potentially providing a useful adjuvant to be used with the current combination chemotherapy for malaria. HDT could also prevent the establishment of infections, allowing it to be a prophylactic therapy for malaria. However, one of the biggest drawbacks for HDT is potential toxicity as a result of inhibition of host proteins. Therefore, it is important to have a full understanding of the biology of the potential HDT targets to ensure the safety of administering HDT drugs for malaria treatment.

This project was conducted with the goals of identifying novel mutations in host genes through an ENU mutagenesis screen in mice that provide protection against a malarial infection, understanding the mechanisms of malaria protection, and determining the suitability of these genes as drug targets for HDT development. RBC cytoskeletal proteins were identified in this screen to be potential HDT targets for further investigation. In particular, this study revolved around one RBC cytoskeletal protein, ankyrin-1 (*Ank-1*), which was previously identified to give rise to a HS-like phenotype and confer malaria resistance in mice [189]. This study aimed to extend the understanding of the underlying malaria resistance mechanisms in mice carrying ankyrin-1 mutations, as well as exploring the possibility of targeting ankyrin-1 for malaria HDT development.

Although *Ank-1* has been repeatedly implicated to confer malaria resistance, the underlying mechanisms were not always clear. Previous studies have suggested that ankyrin-1 mutations mediate malaria resistance by reducing erythrocyte invasion and impairing intra-erythrocytic parasite maturation [189,204], however, some studies reported the absence of such effects [190]. With further investigation on another ankyrin-1 mutation, *Ank-1*$^{(MRI61689)}$, a novel malaria resistance mechanism via increased RBC bystander clearance was discovered, where uninfected RBC are more likely to be removed from the circulation, resulting in an overall increased RBC turnover rate, thus possibly impairing the establishment of malaria infections. It is interesting to note that it appeared to support normal intra-erythrocytic parasite maturation, in contrast with previous studies on *Ank-1*$^{(MRI23420/+)}$ and *Ank-1*$^{(nb/nb)}$ mice [189,204]. However, rather than portraying these as contradicting evidences, it was proposed that these differences were due to the ability of ankyrin-1 to mediate multiple resistance mechanisms, ranging from impairing merozoite invasion, inhibiting intra-erythrocytic maturation and mediating the senescence of RBCs, adding a level of complexity in characterising the protective roles of ankyrin-1. It was hypothesised that the various ankyrin-1 mutations can exert different effects on the parasites depending on the location of the mutations, although the exact mechanism of each mutant allele remains to be investigated.

To further support our hypothesis, two different ankyrin-1 mutations were examined, *Ank-1*$^{(MRI96570)}$ and *Ank-1*$^{(MRI95845)}$, and compared them in terms of their effect on RBCs and their protective mechanisms against malaria. Results shows that ankyrin-1 can mediates two distinctly different malaria resistance mechanisms depending on the mutations. While both mutations impaired merozoite invasion, *Ank-1*$^{(MRI96570)}$ inhibited the maturation of parasites, whereas *Ank-1*$^{(MRI95845)}$ caused a rapid RBC clearance during malaria infections. Although further examinations of each resistance mechanism were not performed, this difference in resistance mechanisms is likely due to the various effects each ankyrin-1 mutation had on the RBC cytoskeleton. *Ank-1*$^{(MRI95845/MRI95845)}$ erythrocytes, possibly similar to *Ank-1*$^{(MRI61689/+)}$ erythrocytes,

could be inherently more susceptible to clearance. This is evidenced by significantly reduced deformability, increased susceptibility towards haemolysis and band 3 mobility, which is thought to be due to the disrupted RBC cytoskeleton resulting in the dissociation of band 3 from the cytoskeletal protein complexes [349]. Alternatively, it could be the result of expression of pro-phagocytic signals on the surface of these RBCs, such as increased PS exposure or band 3 aggregation, which requires further investigation. On the other hand, the underlying mechanisms of parasite growth arrest mediated by *Ank-1*$^{(MRI96570)}$ was less clear, but it could be due to the disruption to the RBC remodelling process during parasite growth, since intra-erythrocytic parasites require interactions with the RBC cytoskeleton for the expression of parasite-derived proteins on the RBC surface [272]. When comparing these mutations with the *Ank-1*$^{(MRI61689)}$ and those in previous studies [189,204], it is implied that all *Ank*-1 mutations are associated with impaired merozoite invasion, while the additional resistance mechanisms are dependent on the location and nature of *Ank-1* mutations, although the exact relationship between genotype and phenotype remains elusive. As a result, the future work for this aspect of the study lies in obtaining direct evidence on the effects of diverse causative ankyrin-1 mutations on the RBC cytoskeletal structure, as well as examining the sequestration of RBC in various organs, through super resolution microscopy and intra-vital imaging techniques, to further support our current findings. Nevertheless, this is the first direct description of the allelic heterogeneity in the ankyrin-1 gene. This also suggests that RBC cytoskeleton is important for multiple aspects of the erythrocytic stage of malarial parasites, potentially poses a significant challenge for the parasites to overcome, thus presents a promising target for malaria HDT development.

In addition, both ankyrin-1 mutations showed differences in the severity of HS-like phenotypes in mice, consistent with the observations in human population studies [394]. Since HS is a heterogeneous disorder, the manifestation of HS symptoms is dependent on the nature of the causative mutations [394]. Indeed, most symptomatic HS due to ankyrin-1 mutations in humans

are caused by nonsense, insertion and deletion mutations, inferring that some missense mutations might be asymptomatic, and hence, have not been identified.

While the association of ankyrin-1 mutations with HS symptoms is well-established in human populations, it is not yet described in terms of malaria resistance. This is most likely due to the lack of detailed association studies between HS and malaria, which is further compounded by co-occurrence of other malaria susceptibility genes, poor healthcare systems and the limited technical capabilities of current technologies [200,460]. Nevertheless, it is reasonable to expect the allelic heterogeneity of ankyrin-1 mutations to have a malaria protective role in human populations, similar to the observations in mouse models. This hypothesis is further supported by the similar phenomenon observed in other malaria susceptibility genes, such as the β-globin gene, and disorders including G6PD deficiency [430,432]. Perhaps the most striking example of this is the β-globin gene, where the HbS and HbC alleles exhibit different geographical distributions throughout Africa based on their genotype-dependent malarial protective effects [432,433]; while heterozygosity for HbS provides significant malaria protection, it is only homozygosity which is significantly protective for HbC. This also provides insights to the evolutionary history between human and *Plasmodium*. Although it was predicted that ankyrin-1 alleles that give rise to symptomatic HS would also confer malaria resistance, it is unknown if the alleles that cause mild or asymptomatic HS would also exhibit malaria protection. Therefore, it is of interest to characterise these asymptomatic HS alleles, which could lead to identification of potential HDT targets with significant malaria protection while exhibiting minimal side-effects.

Although there is still much to learn on the association of HS and malaria, it is evident that disruptions to the RBC cytoskeletal structure leads to malaria protection, as observed in other RBC disorders such as SAO and HE [188,260]. With better understanding of the interactions between the RBC cytoskeleton and parasites, it is possible to mimic the disruptive effects of HS to confer malaria resistance, which raised the possibility of using ankyrin-1 and its related binding partners as HDT candidates for malaria. One such protein is β-spectrin (*Sptb)*, which interacts with

ankyrin-1 via the 14th and 15th spectrin motifs [396]. Similar to ankyrin-1, β-spectrin mutations were also associated with increased malaria resistance in both human and mice [191,194,257], thus presenting a likely target for HDT development as well. Furthermore, the recent identification of binding residues of ankyrin-1 with β-spectrin [398] allowed us to explore the prospect of interrupting the ankyrin-spectrin interaction using small molecules to confer malaria protection in host RBCs.

The genetic validation of ankyrin-spectrin interaction described in this study provided a promising indication for the feasibility of using such interaction for HDT development. Although further verification on the exact disruptive effect is needed, we expect to identify drug candidates which could interrupt ankyrin-spectrin interaction *in vitro*. With further optimisation, such drugs would also interrupt ankyrin-spectrin interactions *in vivo*, which would disrupt the RBC cytoskeleton structure and consequently impair parasite survival, similar to observations on *Sptb*$^{(D1781R)}$ mice, although the exact effect of such drugs on parasites requires further characterisation. Furthermore, the interruption of ankyrin-spectrin interactions was expected to have minor toxicity on the host, as evidenced from the lack of apparent morbidity of *Sptb*$^{(D1781R)}$ mice, however, other potential toxic effects of these drugs cannot be excluded, which is an important factor to consider for therapeutic targets. It is speculated that these drugs could be used in conjunction with the current chemotherapies for malaria, as a preventative to drug-resistant parasites. However, it is unknown whether such drugs would be ideal as malaria prophylactics, since the roles of ankyrin-1 during the establishment of liver stage infections were not explored.

The study on *Sptb*$^{(D1781R)}$ mice also led us to investigate other areas of the RBC cytoskeletal structure as attractive targets for HDT development. Therefore, the malaria susceptibility of HS patients was assessed in an attempt to identify protective alleles as potential HDT candidates. Results so far indicated that all of them displayed reduced merozoite invasion, but the causative mutations remain to be identified. Despite this, it is expected that all of them would exhibit

different causative alleles due to the heterogeneous nature of HS, which might reveal interesting roles of other parts of the RBC cytoskeleton in malaria infections, such as band 3-protein 4.2-ankyrin interactions, as well as their suitability as HDT candidates.

Altogether, this thesis demonstrated the importance of the RBC cytoskeleton in the survival of blood stage malaria parasites. The RBC cytoskeleton exhibits complex interactions during various parasite processes. This is evidenced by the specific disruptive effects, which are observed to be dependent on the nature and location of mutations, giving rise to multiple mechanisms of malaria resistance. This study also highlighted the possibility of developing HDT revolving around the interactions between RBC cytoskeletal proteins, which might fill certain niches that current antimalarials could not, by providing a theoretically resistance-proof treatment for malaria. Coupled with the naturally rapid turnover rate of RBCs and the specificity of such drugs to RBC cytoskeletons, such HDTs might contribute significantly to the current malaria treatments.

In the context of human populations, this thesis first consolidates the heterogeneous nature of HS, as seen with the varying severity of HS-like phenotypes of ankyrin-1 mice. This is consistent with what is observed in human populations, emphasising the robustness of using mouse models to mimic human RBC disorders. This study also uncovered the possible allelic heterogeneity of HS in mediating malaria resistance. While such phenomenon still remains to be discovered in human populations, it is reasonable to expect that different HS-causing mutations would result in various degrees of malaria protection, perhaps similar to G6PD deficiency, where each geographical region exhibits a predominant allele responsible for malaria protection, enabling further investigations into the evolutionary relationship of human and *Plasmodium*.

In order to achieve these goals, further studies should revolve around characterising the exact effects of ankyrin-1 mutations on the RBC cytoskeletal structure, which potentially provide

direct evidence for the disruptive effects of ankyrin-1 mutations on the RBC cytoskeleton. Through the use of super-resolution microscopy, the RBC cytoskeletal network lattice of mice carrying ankyrin-1 mutations could be resolved, potentially providing explanations for the underlying heterogeneous phenotype of ankyrin-1 mutations. This would also indicate whether the disrupted RBC cytoskeleton is crucial in mediating malaria resistance, addressing one of the important knowledge gaps in this study. In addition, further examination of the binding kinetics of ankyrin-spectrin interaction should be conducted as the first step towards HDT development for malaria, since it is required for the downstream HTS assay to identify potential drug candidates. Further genomic sequencing and *in vitro* studies on the erythrocytes of HS patients should also be performed in order to identify other potential HDT candidates within the RBC cytoskeleton.

Nevertheless, this thesis extended our understanding of the relationship between the RBC cytoskeleton and malarial parasites, as well as opening up new opportunities for further studies. With the correct tools and more advanced technologies, future research could broaden our knowledge on host-parasite interactions and population genetics, perhaps even discover new therapeutic approaches for malaria.

REFERENCES

1 (WHO), W. H. O. *World Malaria Report 2015*. (World Health Organisation (WHO), 2015).

2 O'Meara, W. P. *et al.* Effect of a fall in malaria transmission on morbidity and mortality in Kilifi, Kenya. *Lancet* **372**, 1555-1562, doi:10.1016/S0140-6736(08)61655-4 (2008).

3 Nyarango, P. M. *et al.* A steep decline of malaria morbidity and mortality trends in Eritrea between 2000 and 2004: the effect of combination of control methods. *Malar J* **5**, 33, doi:10.1186/1475-2875-5-33 (2006).

4 Otten, M. *et al.* Initial evidence of reduction of malaria cases and deaths in Rwanda and Ethiopia due to rapid scale-up of malaria prevention and treatment. *Malar J* **8**, 14, doi:10.1186/1475-2875-8-14 (2009).

5 Jagannathan, P. *et al.* Increasing incidence of malaria in children despite insecticide-treated bed nets and prompt anti-malarial therapy in Tororo, Uganda. *Malar J* **11**, 435, doi:10.1186/1475-2875-11-435 (2012).

6 Guerra, C. A. *et al.* The limits and intensity of *Plasmodium falciparum* transmission: implications for malaria control and elimination worldwide. *PLoS Med* **5**, e38, doi:10.1371/journal.pmed.0050038 (2008).

7 Gething, P. W. *et al.* A new world malaria map: *Plasmodium falciparum* endemicity in 2010. *Malar J* **10**, 378, doi:10.1186/1475-2875-10-378 (2011).

8 Meis, J. F., Verhave, J. P., Jap, P. H. & Meuwissen, J. H. An ultrastructural study on the role of Kupffer cells in the process of infection by *Plasmodium berghei* sporozoites in rats. *Parasitology* **86 (Pt 2)**, 231-242 (1983).

9 Hermsen, C. C. *et al.* Testing vaccines in human experimental malaria: statistical analysis of parasitemia measured by a quantitative real-time polymerase chain reaction. *Am J Trop Med Hyg* **71**, 196-201 (2004).

10 Eichner, M. *et al.* Genesis, sequestration and survival of *Plasmodium falciparum* gametocytes: parameter estimates from fitting a model to malariatherapy data. *Trans R Soc Trop Med Hyg* **95**, 497-501 (2001).

11 Kwiatkowski, D. & Nowak, M. Periodic and chaotic host-parasite interactions in human malaria. *Proc Natl Acad Sci U S A* **88**, 5111-5113 (1991).

12 (WHO), W. H. O. in *Guidelines for the Treatment of Malaria.* Ch. Annex 6, (World Health Organization, 2015).

13 Eisele, T. P. & Steketee, R. W. African malaria control programs deliver ITNs and achieve what the clinical trials predicted. *PLoS Med* **8**, e1001088, doi:10.1371/journal.pmed.1001088 (2011).

14 W.H.O. *World Malaria Report 2015*. (World Health Organisation (WHO), 2015).

15 Lindblade, K. A. *et al.* A cohort study of the effectiveness of insecticide-treated bed nets to prevent malaria in an area of moderate pyrethroid resistance, Malawi. *Malaria Journal* **14**, 1-15, doi:10.1186/s12936-015-0554-1 (2015).

16 Stewart, T. & Marchand, R. Factors that affect the success and failure of Insecticide Treated Net Programs for malaria control in SE Asia and the Western Pacific. *Geneva: World Health Organization*, 1-36 (2003).

17 Smithuis, F. M. *et al.* The effect of insecticide-treated bed nets on the incidence and prevalence of malaria in children in an area of unstable seasonal transmission in western Myanmar. *Malaria Journal* **12**, 1-15, doi:10.1186/1475-2875-12-363 (2013).

18 Graves, P. & Gelband, H. Vaccines for preventing malaria (SPf66). *The Cochrane database of systematic reviews*, CD005966, doi:10.1002/14651858.CD005966 (2006).

19 Horii, T. *et al.* Evidences of protection against blood-stage infection of *Plasmodium falciparum* by the novel protein vaccine SE36. *Parasitology international* **59**, 380-386, doi:10.1016/j.parint.2010.05.002 (2010).

20 Olugbile, S. *et al.* Vaccine potentials of an intrinsically unstructured fragment derived from the blood stage-associated *Plasmodium falciparum* protein PFF0165c. *Infect Immun* **77**, 5701-5709, doi:10.1128/IAI.00652-09 (2009).

21 Tamminga, C. *et al.* Human adenovirus 5-vectored *Plasmodium falciparum* NMRC-M3V-Ad-PfCA vaccine encoding CSP and AMA1 is safe, well-tolerated and immunogenic but does not protect against controlled human malaria infection. *Human vaccines & immunotherapeutics* **9**, 2165-2177, doi:10.4161/hv.24941 (2013).

22 Stoute, J. A. *et al.* A preliminary evaluation of a recombinant circumsporozoite protein vaccine against *Plasmodium falciparum* malaria. RTS,S Malaria Vaccine Evaluation Group. *N Engl J Med* **336**, 86-91, doi:10.1056/NEJM199701093360202 (1997).

23 Rts, S. C. T. P. Efficacy and safety of RTS,S/AS01 malaria vaccine with or without a booster dose in infants and children in Africa: final results of a phase 3, individually randomised, controlled trial. *Lancet* **386**, 31-45, doi:10.1016/S0140-6736(15)60721-8 (2015).

24 Rts, S. C. T. P. Efficacy and safety of the RTS,S/AS01 malaria vaccine during 18 months after vaccination: a phase 3 randomized, controlled trial in children and young infants at 11 African sites. *PLoS Med* **11**, e1001685, doi:10.1371/journal.pmed.1001685 (2014).

25 Hoffman, S. L. *et al.* Protection of humans against malaria by immunization with radiation-attenuated *Plasmodium falciparum* sporozoites. *J Infect Dis* **185**, 1155-1164, doi:10.1086/339409 (2002).

26 Hoffman, S. L. *et al.* Development of a metabolically active, non-replicating sporozoite vaccine to prevent *Plasmodium falciparum* malaria. *Human vaccines* **6**, 97-106 (2010).

27 Epstein, J. E. *et al.* Live attenuated malaria vaccine designed to protect through hepatic CD8(+) T cell immunity. *Science* **334**, 475-480, doi:10.1126/science.1211548 (2011).

28 Seder, R. A. *et al.* Protection against malaria by intravenous immunization with a nonreplicating sporozoite vaccine. *Science* **341**, 1359-1365, doi:10.1126/science.1241800 (2013).

29 Li, Y. & Wu, Y. L. An over four millennium story behind qinghaosu (artemisinin)--a fantastic antimalarial drug from a traditional chinese herb. *Curr Med Chem* **10**, 2197-2230 (2003).

30 Petersen, I., Eastman, R. & Lanzer, M. Drug-resistant malaria: molecular mechanisms and implications for public health. *FEBS Lett* **585**, 1551-1562, doi:10.1016/j.febslet.2011.04.042 (2011).

31 Na-Bangchang, K. & Karbwang, J. Current status of malaria chemotherapy and the role of pharmacology in antimalarial drug research and development. *Fundamental & clinical pharmacology* **23**, 387-409, doi:10.1111/j.1472-8206.2009.00709.x (2009).

32 in *Guidelines for the Treatment of Malaria WHO Guidelines Approved by the Guidelines Review Committee* (World Health Organisation, 2015).

33 Coatney, G. R. Pitfalls in a discovery: the chronicle of chloroquine. *Am J Trop Med Hyg* **12**, 121-128 (1963).

34 Payne, D. Spread of chloroquine resistance in *Plasmodium falciparum*. *Parasitol Today* **3**, 241-246 (1987).

35 Wellems, T. E. & Plowe, C. V. Chloroquine-resistant malaria. *J Infect Dis* **184**, 770-776, doi:10.1086/322858 (2001).

36 Rosenthal, P. J. & Meshnick, S. R. Hemoglobin catabolism and iron utilization by malaria parasites. *Mol Biochem Parasitol* **83**, 131-139 (1996).

37 Dorn, A. *et al.* An assessment of drug-haematin binding as a mechanism for inhibition of haematin polymerisation by quinoline antimalarials. *Biochemical pharmacology* **55**, 727-736 (1998).

38 Zhang, J., Krugliak, M. & Ginsburg, H. The fate of ferriprotorphyrin IX in malaria infected erythrocytes in conjunction with the mode of action of antimalarial drugs. *Mol Biochem Parasitol* **99**, 129-141 (1999).

39 Sullivan, D. J., Jr., Gluzman, I. Y., Russell, D. G. & Goldberg, D. E. On the molecular mechanism of chloroquine's antimalarial action. *Proc Natl Acad Sci U S A* **93**, 11865-11870 (1996).

40 Pagola, S., Stephens, P. W., Bohle, D. S., Kosar, A. D. & Madsen, S. K. The structure of malaria pigment beta-haematin. *Nature* **404**, 307-310, doi:10.1038/35005132 (2000).

41 Verdier, F., Le Bras, J., Clavier, F., Hatin, I. & Blayo, M. C. Chloroquine uptake by *Plasmodium falciparum*-infected human erythrocytes during in vitro culture and its relationship to chloroquine resistance. *Antimicrob Agents Chemother* **27**, 561-564 (1985).

42 Sidhu, A. B., Verdier-Pinard, D. & Fidock, D. A. Chloroquine resistance in *Plasmodium falciparum* malaria parasites conferred by *pfcrt* mutations. *Science* **298**, 210-213, doi:10.1126/science.1074045 (2002).

43 Barnes, D. A., Foote, S. J., Galatis, D., Kemp, D. J. & Cowman, A. F. Selection for high-level chloroquine resistance results in deamplification of the *pfmdr1* gene and increased sensitivity to mefloquine in *Plasmodium falciparum*. *EMBO J* **11**, 3067-3075 (1992).

44 Fidock, D. A. *et al.* Mutations in the *P. falciparum* digestive vacuole transmembrane protein *Pf*CRT and evidence for their role in chloroquine resistance. *Mol Cell* **6**, 861-871 (2000).

45 Lehane, A. M. & Kirk, K. Chloroquine resistance-conferring mutations in *pfcrt* give rise to a chloroquine-associated H+ leak from the malaria parasite's digestive vacuole. *Antimicrob Agents Chemother* **52**, 4374-4380, doi:10.1128/AAC.00666-08 (2008).

46 Koenderink, J. B., Kavishe, R. A., Rijpma, S. R. & Russel, F. G. The ABCs of multidrug resistance in malaria. *Trends Parasitol* **26**, 440-446, doi:10.1016/j.pt.2010.05.002 (2010).

47 Sanchez, C. P., Rotmann, A., Stein, W. D. & Lanzer, M. Polymorphisms within PfMDR1 alter the substrate specificity for anti-malarial drugs in *Plasmodium falciparum*. *Mol Microbiol* **70**, 786-798, doi:10.1111/j.1365-2958.2008.06413.x (2008).

48 Reed, M. B., Saliba, K. J., Caruana, S. R., Kirk, K. & Cowman, A. F. Pgh1 modulates sensitivity and resistance to multiple antimalarials in *Plasmodium falciparum*. *Nature* **403**, 906-909, doi:10.1038/35002615 (2000).

49 Foote, S. J. *et al.* Several alleles of the multidrug-resistance gene are closely linked to chloroquine resistance in *Plasmodium falciparum*. *Nature* **345**, 255-258, doi:10.1038/345255a0 (1990).

50 Sibley, C. H. *et al.* Pyrimethamine-sulfadoxine resistance in *Plasmodium falciparum*: what next? *Trends Parasitol* **17**, 582-588 (2001).

51 Hyde, J. E. Exploring the folate pathway in *Plasmodium falciparum*. *Acta tropica* **94**, 191-206, doi:10.1016/j.actatropica.2005.04.002 (2005).

52 Cowman, A. F., Morry, M. J., Biggs, B. A., Cross, G. A. & Foote, S. J. Amino acid changes linked to pyrimethamine resistance in the dihydrofolate reductase-thymidylate synthase gene of *Plasmodium falciparum*. *Proc Natl Acad Sci U S A* **85**, 9109-9113 (1988).

53 Roper, C. *et al.* Intercontinental spread of pyrimethamine-resistant malaria. *Science* **305**, 1124, doi:10.1126/science.1098876 (2004).

54 Roper, C. *et al.* Antifolate antimalarial resistance in southeast Africa: a population-based analysis. *Lancet* **361**, 1174-1181, doi:10.1016/S0140-6736(03)12951-0 (2003).

55 Kublin, J. G. *et al.* Molecular markers for failure of sulfadoxine-pyrimethamine and chlorproguanil-dapsone treatment of *Plasmodium falciparum* malaria. *J Infect Dis* **185**, 380-388, doi:10.1086/338566 (2002).

56 Wernsdorfer, W. H. & Noedl, H. Molecular markers for drug resistance in malaria: use in treatment, diagnosis and epidemiology. *Current opinion in infectious diseases* **16**, 553-558, doi:10.1097/01.qco.0000104295.87920.fd (2003).

57 Urdaneta, L., Plowe, C., Goldman, I. & Lal, A. A. Point mutations in dihydrofolate reductase and dihydropteroate synthase genes of *Plasmodium falciparum* isolates from Venezuela. *Am J Trop Med Hyg* **61**, 457-462 (1999).

58 Yuthavong, Y. *et al.* Malarial (*Plasmodium falciparum*) dihydrofolate reductase-thymidylate synthase: structural basis for antifolate resistance and development of effective inhibitors. *Parasitology* **130**, 249-259 (2005).

59 Lell, B. & Kremsner, P. G. Clindamycin as an antimalarial drug: review of clinical trials. *Antimicrob Agents Chemother* **46**, 2315-2320 (2002).

60 Gaillard, T., Madamet, M. & Pradines, B. Tetracyclines in malaria. *Malar J* **14**, 445, doi:10.1186/s12936-015-0980-0 (2015).

61 Prapunwattana, P., O'Sullivan, W. J. & Yuthavong, Y. Depression of *Plasmodium falciparum* dihydroorotate dehydrogenase activity in in vitro culture by tetracycline. *Mol Biochem Parasitol* **27**, 119-124 (1988).

62 Budimulja, A. S., Syafruddin, Tapchaisri, P., Wilairat, P. & Marzuki, S. The sensitivity of *Plasmodium* protein synthesis to prokaryotic ribosomal inhibitors. *Mol Biochem Parasitol* **84**, 137-141 (1997).

63 Dahl, E. L. *et al.* Tetracyclines specifically target the apicoplast of the malaria parasite *Plasmodium falciparum*. *Antimicrob Agents Chemother* **50**, 3124-3131, doi:10.1128/AAC.00394-06 (2006).

64 Yeh, E. & DeRisi, J. L. Chemical rescue of malaria parasites lacking an apicoplast defines organelle function in blood-stage *Plasmodium falciparum*. *PLoS Biol* **9**, e1001138, doi:10.1371/journal.pbio.1001138 (2011).

65 Rieckmann, K. H. *et al.* Recent military experience with malaria chemoprophylaxis. *The Medical journal of Australia* **158**, 446-449 (1993).

66 Orlandi-Pradines, E. *et al.* Antibody responses to several malaria pre-erythrocytic antigens as a marker of malaria exposure among travelers. *Am J Trop Med Hyg* **74**, 979-985 (2006).

67 Tan, K. R. *et al.* Doxycycline for malaria chemoprophylaxis and treatment: report from the CDC expert meeting on malaria chemoprophylaxis. *Am J Trop Med Hyg* **84**, 517-531, doi:10.4269/ajtmh.2011.10-0285 (2011).

68 Briolant, S., Wurtz, N., Zettor, A., Rogier, C. & Pradines, B. Susceptibility of *Plasmodium falciparum* isolates to doxycycline is associated with *pftetQ* sequence polymorphisms and *pftetQ* and *pfmdt* copy numbers. *J Infect Dis* **201**, 153-159, doi:10.1086/648594 (2010).

69 Gaillard, T. *et al. PftetQ* and *pfmdt* copy numbers as predictive molecular markers of decreased ex vivo doxycycline susceptibility in imported *Plasmodium falciparum* malaria. *Malar J* **12**, 414, doi:10.1186/1475-2875-12-414 (2013).

70 Klayman, D. L. Qinghaosu (artemisinin): an antimalarial drug from China. *Science* **228**, 1049-1055 (1985).

71 Price, R. N. *et al.* Effects of artemisinin derivatives on malaria transmissibility. *Lancet* **347**, 1654-1658 (1996).

72 Skinner, T. S., Manning, L. S., Johnston, W. A. & Davis, T. M. In vitro stage-specific sensitivity of *Plasmodium falciparum* to quinine and artemisinin drugs. *Int J Parasitol* **26**, 519-525 (1996).

73 Xie, S. C. *et al.* Haemoglobin degradation underpins the sensitivity of early ring stage *Plasmodium falciparum* to artemisinins. *J Cell Sci* **129**, 406-416, doi:10.1242/jcs.178830 (2016).

74 Haynes, R. K. & Vonwiller, S. C. The behaviour of qinghaosu (artemisinin) in the presence of heme iron(II) and (III). *Tetrahedron Letters* **37**, 253-256, doi:http://dx.doi.org/10.1016/0040-4039(95)02141-8 (1996).

75 Meshnick, S. R. Artemisinin: mechanisms of action, resistance and toxicity. *Int J Parasitol* **32**, 1655-1660 (2002).

76 Jones-Brando, L., D'Angelo, J., Posner, G. H. & Yolken, R. In vitro inhibition of Toxoplasma gondii by four new derivatives of artemisinin. *Antimicrob Agents Chemother* **50**, 4206-4208, doi:10.1128/aac.00793-06 (2006).

77 Loup, C., Lelievre, J., Benoit-Vical, F. & Meunier, B. Trioxaquines and heme-artemisinin adducts inhibit the in vitro formation of hemozoin better than chloroquine. *Antimicrob Agents Chemother* **51**, 3768-3770, doi:10.1128/aac.00239-07 (2007).

78 Kannan, R., Sahal, D. & Chauhan, V. S. Heme-artemisinin adducts are crucial mediators of the ability of artemisinin to inhibit heme polymerization. *Chemistry & biology* **9**, 321-332 (2002).

79 Haynes, R. K. *et al.* Artemisinin antimalarials do not inhibit hemozoin formation. *Antimicrob Agents Chemother* **47**, 1175 (2003).

80 Eckstein-Ludwig, U. *et al.* Artemisinins target the SERCA of *Plasmodium falciparum*. *Nature* **424**, 957-961, doi:10.1038/nature01813 (2003).

81 Uhlemann, A. C. *et al.* A single amino acid residue can determine the sensitivity of SERCAs to artemisinins. *Nature structural & molecular biology* **12**, 628-629, doi:10.1038/nsmb947 (2005).

82 Cui, L. *et al.* Lack of association of the S769N mutation in *Plasmodium falciparum* SERCA (PfATP6) with resistance to artemisinins. *Antimicrob Agents Chemother* **56**, 2546-2552, doi:10.1128/AAC.05943-11 (2012).

83 Noedl, H. *et al.* Evidence of Artemisinin-Resistant Malaria in Western Cambodia. *New England Journal of Medicine* **359**, 2619-2620, doi:doi:10.1056/NEJMc0805011 (2008).

84 Dondorp, A. M. *et al.* Artemisinin Resistance in *Plasmodium falciparum* Malaria. *New England Journal of Medicine* **361**, 455-467, doi:doi:10.1056/NEJMoa0808859 (2009).

85 Ariey, F. *et al.* A molecular marker of artemisinin-resistant *Plasmodium falciparum* malaria. *Nature* **505**, 50-55, doi:10.1038/nature12876 (2014).

86 Straimer, J. *et al.* Drug resistance. K13-propeller mutations confer artemisinin resistance in *Plasmodium falciparum* clinical isolates. *Science* **347**, 428-431, doi:10.1126/science.1260867 (2015).

87 Mbengue, A. *et al.* A molecular mechanism of artemisinin resistance in *Plasmodium falciparum* malaria. *Nature* **520**, 683-687, doi:10.1038/nature14412 (2015).

88 Mok, S. *et al.* Population transcriptomics of human malaria parasites reveals the mechanism of artemisinin resistance. *Science* **347**, 431-435, doi:10.1126/science.1260403 (2015).

89 Carter, R. & Mendis, K. N. Evolutionary and historical aspects of the burden of malaria. *Clin Microbiol Rev* **15**, 564-594 (2002).

90 Miller, L. H., Mason, S. J., Dvorak, J. A., McGinniss, M. H. & Rothman, I. K. Erythrocyte receptors for (*Plasmodium knowlesi*) malaria: Duffy blood group determinants. *Science* **189**, 561-563 (1975).

91 Barnwell, J. W., Nichols, M. E. & Rubinstein, P. In vitro evaluation of the role of the Duffy blood group in erythrocyte invasion by *Plasmodium vivax*. *J Exp Med* **169**, 1795-1802 (1989).

92 Allison, A. C. Protection afforded by sickle-cell trait against subtertian malareal infection. *British medical journal* **1**, 290-294 (1954).

93 Bienzle, U., Ayeni, O., Lucas, A. O. & Luzzatto, L. Glucose-6-phosphate dehydrogenase and malaria. Greater resistance of females heterozygous for enzyme deficiency and of males with non-deficient variant. *Lancet* **1**, 107-110 (1972).

94 Kwiatkowski, D. P. How malaria has affected the human genome and what human genetics can teach us about malaria. *Am J Hum Genet* **77**, 171-192 (2005).

95 Haldane, J. B. S. Disease and Evolution. *Ricerca Science Supplement* **19**, 68-76 (1949).

96 Ashley-Koch, A., Yang, Q. & Olney, R. S. Sickle hemoglobin (HbS) allele and sickle cell disease: a HuGE review. *American journal of epidemiology* **151**, 839-845 (2000).

97 Piel, F. B. *et al.* Global distribution of the sickle cell gene and geographical confirmation of the malaria hypothesis. *Nature communications* **1**, 104, doi:10.1038/ncomms1104 (2010).

98 Williams, T. N. & Weatherall, D. J. World distribution, population genetics, and health burden of the hemoglobinopathies. *Cold Spring Harbor perspectives in medicine* **2**, a011692, doi:10.1101/cshperspect.a011692 (2012).

99 Ackerman, H. *et al.* A comparison of case-control and family-based association methods: the example of sickle-cell and malaria. *Ann Hum Genet* **69**, 559-565, doi:10.1111/j.1529-8817.2005.00180.x (2005).

100 May, J. *et al.* Hemoglobin variants and disease manifestations in severe *falciparum* malaria. *Jama* **297**, 2220-2226, doi:10.1001/jama.297.20.2220 (2007).

101 Diallo, D. A. *et al.* A comparison of anemia in hemoglobin C and normal hemoglobin A children with *Plasmodium falciparum* malaria. *Acta tropica* **90**, 295-299, doi:10.1016/j.actatropica.2004.02.005 (2004).

102 Agarwal, A. *et al.* Hemoglobin C associated with protection from severe malaria in the Dogon of Mali, a West African population with a low prevalence of hemoglobin S. *Blood* **96**, 2358-2363 (2000).

103 Rihet, P., Flori, L., Tall, F., Traore, A. S. & Fumoux, F. Hemoglobin C is associated with reduced *Plasmodium falciparum* parasitemia and low risk of mild malaria attack. *Hum Mol Genet* **13**, 1-6, doi:10.1093/hmg/ddh002 (2004).

104 Modiano, D. *et al.* Haemoglobin C protects against clinical *Plasmodium falciparum* malaria. *Nature* **414**, 305-308, doi:10.1038/35104556 (2001).

105 Mockenhaupt, F. P. *et al.* Hemoglobin C and resistance to severe malaria in Ghanaian children. *J Infect Dis* **190**, 1006-1009, doi:10.1086/422847 (2004).

106 Flatz, G. Hemoglobin E: Distribution and population dynamics. *Humangenetik* **3**, 189-234, doi:10.1007/bf00273124.

107 Vichinsky, E. Hemoglobin E Syndromes. *ASH Education Program Book* **2007**, 79-83, doi:10.1182/asheducation-2007.1.79 (2007).

108 Hutagalung, R. *et al.* Influence of hemoglobin E trait on the severity of *falciparum* malaria. *J Infect Dis* **179**, 283-286, doi:10.1086/314561 (1999).

109 Chotivanich, K. *et al.* Hemoglobin E: a balanced polymorphism protective against high parasitemias and thus severe P falciparum malaria. *Blood* **100**, 1172-1176 (2002).

110 O'Donnell, A. *et al.* Interaction of malaria with a common form of severe thalassemia in an Asian population. *Proc Natl Acad Sci U S A* **106**, 18716-18721, doi:10.1073/pnas.0910142106 (2009).

111 Weatherall, D. J. Phenotype-genotype relationships in monogenic disease: lessons from the thalassaemias. *Nat Rev Genet* **2**, 245-255 (2001).

112 Williams, T. N. *et al.* High incidence of malaria in alpha-thalassaemic children. *Nature* **383**, 522-525, doi:10.1038/383522a0 (1996).

113 Allen, S. J. *et al.* alpha+-Thalassemia protects children against disease caused by other infections as well as malaria. *Proc Natl Acad Sci U S A* **94**, 14736-14741 (1997).

114 Udomsangpetch, R. *et al.* Alteration in cytoadherence and rosetting of *Plasmodium falciparum*-infected thalassemic red blood cells. *Blood* **82**, 3752-3759 (1993).

115 Beutler, E. Glucose-6-phosphate dehydrogenase deficiency: a historical perspective. *Blood* **111**, 16-24 (2007).

116 Beutler, E. & Duparc, S. Glucose-6-phosphate dehydrogenase deficiency and antimalarial drug development. *Am J Trop Med Hyg* **77** (2007).

117 Howes, R. E. *et al.* Spatial distribution of G6PD deficiency variants across malaria-endemic regions. *Malaria Journal* **12**, 1-15, doi:10.1186/1475-2875-12-418 (2013).

118 Howes, R. E., Battle, K. E., Satyagraha, A. W., Baird, J. K. & Hay, S. I. G6PD deficiency: Global distribution, genetic variants and primaquine therapy. *Adv Parasitol* **81**, doi:10.1016/b978-0-12-407826-0.00004-7 (2013).

119 Khim, N. *et al.* G6PD deficiency in *Plasmodium falciparum* and *Plasmodium vivax* malaria-infected Cambodian patients. *Malar J* **12**, 171, doi:10.1186/1475-2875-12-171 (2013).

120 Shah, S. S. *et al.* Heterogeneous alleles comprising G6PD deficiency trait in West Africa exert contrasting effects on two major clinical presentations of severe malaria. *Malaria Journal* **15**, 1-8, doi:10.1186/s12936-015-1045-0 (2016).

121 Guindo, A., Fairhurst, R. M., Doumbo, O. K., Wellems, T. E. & Diallo, D. A. X-Linked G6PD Deficiency Protects Hemizygous Males but Not Heterozygous Females against Severe Malaria. *PLoS Medicine* **4**, e66, doi:10.1371/journal.pmed.0040066 (2007).

122 Sirugo, G. Reassessing an old claim: Natural selection of hemizygotes and heterozygotes for G6PD deficiency in Africa by resistance to severe malaria. *American Journal of Hematology* **88**, 436-436, doi:10.1002/ajh.23424 (2013).

123 Ruwende, C. *et al.* Natural selection of hemi- and heterozygotes for G6PD deficiency in Africa by resistance to severe malaria. *Nature.* **376**, doi:10.1038/376246a0 (1995).

124 Mohrenweiser, H. W. Functional hemizygosity in the human genome: direct estimate from twelve erythrocyte enzyme loci. *Human Genetics* **77**, 241-245, doi:10.1007/bf00284477 (1987).

125 Beutler, E. & Gelbart, T. Estimating the prevalence of pyruvate kinase deficiency from the gene frequency in the general white population. *Blood* **95**, 3585-3588 (2000).

126 Min-Oo, G. *et al.* Pyruvate kinase deficiency in mice protects against malaria. *Nat Genet* **35**, 357-362, doi:10.1038/ng1260 (2003).

127 Durand, P. M. & Coetzer, T. L. Pyruvate kinase deficiency protects against malaria in humans. *Haematologica* **93**, 939-940 (2008).

128 Ayi, K. *et al.* Pyruvate kinase deficiency and malaria. *N Engl J Med* **358**, 1805-1810, doi:10.1056/NEJMoa072464 (2008).

129 Cao, K. *et al.* Analysis of the frequencies of HLA-A, B, and C alleles and haplotypes in the five major ethnic groups of the United States reveals high levels of diversity in these loci and contrasting distribution patterns in these populations. *Human immunology* **62**, 1009-1030 (2001).

130 Garamszegi, L. Z. Global distribution of malaria-resistant MHC-HLA alleles: the number and frequencies of alleles and malaria risk. *Malaria Journal* **13**, 1-9, doi:10.1186/1475-2875-13-349 (2014).

131 Garamszegi, L. Z., De Groot, N. G. & Bontrop, R. E. Correlated evolution of nucleotide substitution rates and allelic variation in Mhc-DRB lineages of primates. *BMC Evol Biol* **9**, doi:10.1186/1471-2148-9-73 (2009).

132 Hill, A. V. *et al.* Common west African HLA antigens are associated with protection from severe malaria. *Nature* **352**, 595-600 (1991).

133 Osafo-Addo, A. D. *et al.* HLA-DRB1*04 allele is associated with severe malaria in northern Ghana. *Am J Trop Med Hyg* **78**, 251-255 (2008).

134 Lyke, K. E. *et al.* Association of HLA alleles with *Plasmodium falciparum* severity in Malian children. *Tissue Antigens* **77**, doi:10.1111/j.1399-0039.2011.01661.x (2011).

135 Hananantachai, H. *et al.* Polymorphisms of the HLA-B and HLA-DRB1 genes in Thai malaria patients. *Japanese journal of infectious diseases* **58**, 25-28 (2005).

136 Gichohi-Wainaina, W. N. *et al.* Tumour necrosis factor allele variants and their association with the occurrence and severity of malaria in African children: a longitudinal study. *Malaria Journal* **14**, 1-11, doi:10.1186/s12936-015-0767-3 (2015).

137 Aidoo, M. *et al.* Tumor necrosis factor-alpha promoter variant 2 (TNF2) is associated with pre-term delivery, infant mortality, and malaria morbidity in western Kenya: Asembo Bay Cohort Project IX. *Genet Epidemiol* **21**, doi:10.1002/gepi.1029 (2001).

138 Ubalee, R. *et al.* Strong association of a tumor necrosis factor-alpha promoter allele with cerebral malaria in Myanmar. *Tissue Antigens* **58**, 407-410 (2001).

139 Moore, J. M., Nahlen, B. L., Misore, A., Lal, A. A. & Udhayakumar, V. Immunity to placental malaria. I. Elevated production of interferon-gamma by placental blood mononuclear cells is associated with protection in an area with high transmission of malaria. *J Infect Dis* **179**, 1218-1225, doi:10.1086/314737 (1999).

140 Cabantous, S. *et al.* Evidence that interferon-gamma plays a protective role during cerebral malaria. *J Infect Dis* **192**, 854-860, doi:10.1086/432484 (2005).

141 Gyan, B. *et al.* Polymorphisms in interleukin-1beta and interleukin-1 receptor antagonist genes and malaria in Ghanaian children. *Scand J Immunol* **56**, 619-622 (2002).

142 Ouma, C. *et al.* Polymorphic Variability in the Interleukin (IL)-1β Promoter Conditions Susceptibility to Severe Malarial Anemia and Functional Changes in IL-1β Production. *Journal of Infectious Diseases* **198**, 1219-1226, doi:10.1086/592055 (2008).

143 Gyan, B. A. *et al.* Allelic polymorphisms in the repeat and promoter regions of the interleukin-4 gene and malaria severity in Ghanaian children. *Clin Exp Immunol* **138**, 145-150, doi:10.1111/j.1365-2249.2004.02590.x (2004).

144 Zhang, G. *et al.* Interleukin-10 (IL-10) Polymorphisms Are Associated with IL-10 Production and Clinical Malaria in Young Children. *Infection and Immunity* **80**, 2316-2322, doi:10.1128/iai.00261-12 (2012).

145 Gandhi, M. Complement receptor 1 and the molecular pathogenesis of malaria. *Indian Journal of Human Genetics* **13**, 39-47, doi:10.4103/0971-6866.34704 (2007).

146 Stoute, J. A. Complement receptor 1 and malaria. *Cell Microbiol* **13**, 1441-1450, doi:10.1111/j.1462-5822.2011.01648.x (2011).

147 Panda, A. K. *et al.* Complement Receptor 1 Variants Confer Protection from Severe Malaria in Odisha, India. *PLoS ONE* **7**, e49420, doi:10.1371/journal.pone.0049420 (2012).

148 Cockburn, I. A. *et al.* A human complement receptor 1 polymorphism that reduces *Plasmodium falciparum* rosetting confers protection against severe malaria. *Proceedings of the National Academy of Sciences of the United States of America* **101**, 272-277, doi:10.1073/pnas.0305306101 (2004).

149 Spadafora, C. *et al.* Complement receptor 1 is a sialic acid-independent erythrocyte receptor of *Plasmodium falciparum*. *PLoS Pathog* **6**, e1000968, doi:10.1371/journal.ppat.1000968 (2010).

150 Bredt, D. S. & Snyder, S. H. Nitric oxide: a physiologic messenger molecule. *Annual review of biochemistry* **63**, 175-195, doi:10.1146/annurev.bi.63.070194.001135 (1994).

151 Boutlis, C. S. *et al.* Nitric oxide production and mononuclear cell nitric oxide synthase activity in malaria-tolerant Papuan adults. *Infect Immun* **71**, 3682-3689 (2003).

152 Gramaglia, I. *et al.* Low nitric oxide bioavailability contributes to the genesis of experimental cerebral malaria. *Nat Med* **12**, 1417-1422, doi:10.1038/nm1499 (2006).

153 Ong, P. K. *et al.* Nitric Oxide Synthase Dysfunction Contributes to Impaired Cerebroarteriolar Reactivity in Experimental Cerebral Malaria. *PLoS Pathog* **9**, e1003444, doi:10.1371/journal.ppat.1003444 (2013).

154 Kun, J. F. *et al.* Polymorphism in promoter region of inducible nitric oxide synthase gene and protection against malaria. *Lancet* **351**, 265-266, doi:10.1016/s0140-6736(05)78273-8 (1998).

155 Burgner, D. *et al.* Inducible nitric oxide synthase polymorphism and fatal cerebral malaria. *The Lancet* **352**, 1193-1194, doi:10.1016/S0140-6736(05)60531-4 (1998).

156 Levesque, M. C. *et al.* Malaria severity and human nitric oxide synthase type 2 (NOS2) promoter haplotypes. *Human genetics* **127**, 163-182, doi:10.1007/s00439-009-0753-3 (2010).

157 Szabo, M. C., Soo, K. S., Zlotnik, A. & Schall, T. J. Chemokine class differences in binding to the Duffy antigen-erythrocyte chemokine receptor. *J Biol Chem* **270**, 25348-25351 (1995).

158 Miller , L. H., Mason , S. J., Clyde , D. F. & McGinniss , M. H. The Resistance Factor to *Plasmodium vivax* in Blacks. *New England Journal of Medicine* **295**, 302-304, doi:doi:10.1056/NEJM197608052950602 (1976).

159 Sanger, R., Race, R. R. & Jack, J. The Duffy blood groups of New York negroes: the phenotype Fy (a-b-). *Br J Haematol* **1**, 370-374 (1955).

160 Zimmerman, P. A. *et al.* Emergence of FY*A(null) in a Plasmodium vivax-endemic region of Papua New Guinea. *Proc Natl Acad Sci U S A* **96**, 13973-13977 (1999).

161 Culleton, R. L. *et al.* Failure to detect *Plasmodium vivax* in West and Central Africa by PCR species typing. *Malaria Journal* **7**, 1-8, doi:10.1186/1475-2875-7-174 (2008).

162 Miller, L. H., Mason, S. J., Dvorak, J. A., McGinniss, M. H. & Rothman, I. K. Erythrocyte receptors for (Plasmodium knowlesi) malaria: Duffy blood group determinants. *Science* **189**, doi:10.1126/science.1145213 (1975).

163 Haynes, J. D. *et al.* Receptor-like specificity of a *Plasmodium knowlesi* malarial protein that binds to Duffy antigen ligands on erythrocytes. *J Exp Med* **167**, 1873-1881 (1988).

164 Mason, S. J., Miller, L. H., Shiroishi, T., Dvorak, J. A. & McGinniss, M. H. The Duffy blood group determinants: their role in the susceptibility of human and animal erythrocytes to *Plasmodium knowles*i malaria. *Br J Haematol* **36**, 327-335 (1977).

165 Woldearegai, T. G., Kremsner, P. G., Kun, J. F. & Mordmuller, B. *Plasmodium vivax* malaria in Duffy-negative individuals from Ethiopia. *Trans R Soc Trop Med Hyg* **107**, 328-331, doi:10.1093/trstmh/trt016 (2013).

166 Ménard, D. *et al. Plasmodium vivax* clinical malaria is commonly observed in Duffy-negative Malagasy people. *Proceedings of the National Academy of Sciences* **107**, 5967-5971, doi:10.1073/pnas.0912496107 (2010).

167 Mendes, C. *et al.* Duffy Negative Antigen Is No Longer a Barrier to *Plasmodium vivax* ? Molecular Evidences from the African West Coast (Angola and Equatorial Guinea). *PLoS Negl Trop Dis* **5**, e1192, doi:10.1371/journal.pntd.0001192 (2011).

168 Cavasini, C. E. *et al. Plasmodium vivax* infection among Duffy antigen-negative individuals from the Brazilian Amazon region: an exception? *Trans R Soc Trop Med Hyg* **101**, 1042-1044, doi:10.1016/j.trstmh.2007.04.011 (2007).

169 Ngassa Mbenda, H. G. & Das, A. Molecular evidence of *Plasmodium vivax* mono and mixed malaria parasite infections in Duffy-negative native Cameroonians. *PLoS One* **9**, e103262, doi:10.1371/journal.pone.0103262 (2014).

170 Menard, D. *et al.* Whole genome sequencing of field isolates reveals a common duplication of the Duffy binding protein gene in Malagasy *Plasmodium vivax* strains. *PLoS Negl Trop Dis* **7**, e2489, doi:10.1371/journal.pntd.0002489 (2013).

171 Roubinet, F. *et al.* Evolution of the O alleles of the human ABO blood group gene. *Transfusion* **44**, 707-715, doi:10.1111/j.1537-2995.2004.03346.x (2004).

172 Cserti, C. M. & Dzik, W. H. The ABO blood group system and *Plasmodium falciparum* malaria. *Blood* **110**, 2250-2258, doi:10.1182/blood-2007-03-077602 (2007).

173 Pathirana, S. L. *et al.* ABO-blood-group types and protection against severe, *Plasmodium falciparum* malaria. *Ann Trop Med Parasitol* **99**, 119-124, doi:10.1179/136485905x19946 (2005).

174 Lell, B. *et al.* The role of red blood cell polymorphisms in resistance and susceptibility to malaria. *Clinical infectious diseases : an official publication of the Infectious Diseases Society of America* **28**, 794-799, doi:10.1086/515193 (1999).

175 Fischer, P. R. & Boone, P. Short report: severe malaria associated with blood group. *Am J Trop Med Hyg* **58**, 122-123 (1998).

176 Giblett, E. R., Motusky, A. G. & Fraser, G. R. Population genetic studies in the Congo. IV. Haptoglobin and transferrin serum groups in the Congo and in other African population.s. *American Journal of Human Genetics* **18**, 553-558 (1966).

177 Patel, S. S. *et al.* The association of the glycophorin C exon 3 deletion with ovalocytosis and malaria susceptibility in the Wosera, Papua New Guinea. *Blood* **98**, 3489-3491 (2001).

178 Maier, A. G. *et al. Plasmodium falciparum* erythrocyte invasion through glycophorin C and selection for Gerbich negativity in human populations. *Nat Med* **9**, 87-92 (2003).

179 Mayer, D. C. *et al.* Glycophorin B is the erythrocyte receptor of *Plasmodium falciparum* erythrocyte-binding ligand, EBL-1. *Proc Natl Acad Sci U S A* **106**, 5348-5352, doi:10.1073/pnas.0900878106 (2009).

180 Tavul, L. *et al.* Glycophorin C delta(exon3) is not associated with protection against severe anaemia in Papua New Guinea. *Papua and New Guinea medical journal* **51**, 149-154 (2008).

181 Crosnier, C. *et al.* Basigin is a receptor essential for erythrocyte invasion by *Plasmodium falciparum*. *Nature* **480**, 534-537, doi:10.1038/nature10606 (2011).

182 Jarolim, P. *et al.* Deletion in erythrocyte band 3 gene in malaria-resistant Southeast Asian ovalocytosis. *Proceedings of the National Academy of Sciences of the United States of America* **88**, 11022-11026 (1991).

183 Mgone, C. S. *et al.* Occurrence of the erythrocyte band 3 (AE1) gene deletion in relation to malaria endemicity in Papua New Guinea. *Trans R Soc Trop Med Hyg* **90**, 228-231 (1996).

184 Amato, D. & Booth, P. B. Hereditary ovalocytosis in Melanesians. *Papua and New Guinea medical journal* **20**, 26-32 (1977).

185 Genton, B. *et al.* Ovalocytosis and cerebral malaria. *Nature* **378**, 564-565, doi:10.1038/378564a0 (1995).

186 Allen, S. J. *et al.* Prevention of cerebral malaria in children in Papua New Guinea by southeast Asian ovalocytosis band 3. *Am J Trop Med Hyg* **60**, 1056-1060 (1999).

187 Rosanas-Urgell, A. *et al.* Reduced Risk of *Plasmodium vivax* Malaria in Papua New Guinean Children with Southeast Asian Ovalocytosis in Two Cohorts and a Case-Control Study. *PLoS Med* **9**, e1001305, doi:10.1371/journal.pmed.1001305 (2012).

188 Lecomte, M. C. *et al.* Hereditary elliptocytosis in West Africa: frequency and repartition of spectrin variants. *C R Acad Sci III* **306**, 43-46 (1988).

189 Greth, A. *et al.* A novel ENU-mutation in ankyrin-1 disrupts malaria parasite maturation in red blood cells of mice. *PLoS One* **7**, e38999, doi:10.1371/journal.pone.0038999 (2012).

190 Rank, G. *et al.* Novel roles for erythroid Ankyrin-1 revealed through an ENU-induced null mouse mutant. *Blood* **113**, 3352-3362, doi:10.1182/blood-2008-08-172841 (2009).

191 Schulman, S. *et al.* Growth of *Plasmodium falciparum* in human erythrocytes containing abnormal membrane proteins. *Proc Natl Acad Sci U S A* **87**, 7339-7343 (1990).

192 Chishti, A. H., Palek, J., Fisher, D., Maalouf, G. J. & Liu, S. C. Reduced invasion and growth of *Plasmodium falciparum* into elliptocytic red blood cells with a combined deficiency of protein 4.1, glycophorin C, and p55. *Blood* **87**, 3462-3469 (1996).

193 Facer, C. A. Erythrocytes carrying mutations in spectrin and protein 4.1 show differing sensitivities to invasion by *Plasmodium falciparum*. *Parasitol Res* **81**, 52-57 (1995).

194 Glele-Kakai, C. *et al.* Epidemiological studies of spectrin mutations related to hereditary elliptocytosis and spectrin polymorphisms in Benin. *Br J Haematol* **95**, 57-66 (1996).

195 Gallagher, P. G. & Forget, B. G. Hematologically Important Mutations: Spectrin and Ankyrin Variants in Hereditary Spherocytosis. *Blood Cells, Molecules, and Diseases* **24**, 539-543, doi:10.1006/bcmd.1998.0217 (1998).

196 Godal, H. C. & Heisto, H. High prevalence of increased osmotic fragility of red blood cells among Norwegian blood donors. *Scandinavian journal of haematology* **27**, 30-34 (1981).

197 Jensson, O., Jonasson, J. L. & Magnusson, S. Studies on herediatary spherocytosis in Iceland. *Acta medica Scandinavica* **201**, 187-195 (1977).

198 Eber, S. W., Pekrun, A., Neufeldt, A. & Schroter, W. Prevalence of increased osmotic fragility of erythrocytes in German blood donors: screening using a modified glycerol lysis test. *Annals of hematology* **64**, 88-92 (1992).

199 Bolton-Maggs, P. H. *et al.* Guidelines for the diagnosis and management of hereditary spherocytosis. *Br J Haematol* **126**, 455-474, doi:10.1111/j.1365-2141.2004.05052.x (2004).

200 Sangerman, J. *et al.* Ankyrin-linked hereditary spherocytosis in an African-American kindred. *Am J Hematol* **83**, 789-794, doi:10.1002/ajh.21254 (2008).

201 Eber, S. W. *et al.* Ankyrin-1 mutations are a major cause of dominant and recessive hereditary spherocytosis. *Nat Genet* **13**, 214-218, doi:10.1038/ng0696-214 (1996).

202 Savvides, P., Shalev, O., John, K. M. & Lux, S. E. Combined spectrin and ankyrin deficiency is common in autosomal dominant hereditary spherocytosis. *Blood* **82**, 2953-2960 (1993).

203 Da Costa, L., Galimand, J., Fenneteau, O. & Mohandas, N. Hereditary spherocytosis, elliptocytosis, and other red cell membrane disorders. *Blood Reviews* **27**, 167-178, doi:http://dx.doi.org/10.1016/j.blre.2013.04.003 (2013).

204 Shear, H. L., Roth, E. F., Jr., Ng, C. & Nagel, R. L. Resistance to malaria in ankyrin and spectrin deficient mice. *Br J Haematol* **78**, 555-560 (1991).

205 Ayi, K., Turrini, F., Piga, A. & Arese, P. Enhanced phagocytosis of ring-parasitized mutant erythrocytes: a common mechanism that may explain protection against *falciparum* malaria in sickle trait and beta-thalassemia trait. *Blood* **104**, 3364-3371, doi:10.1182/blood-2003-11-3820 (2004).

206 Pasvol, G., Weatherall, D. J. & Wilson, R. J. Cellular mechanism for the protective effect of haemoglobin S against *P. falciparum* malaria. *Nature.* **274**, doi:10.1038/274701a0 (1978).

207 Friedman, M. Erythrocytic mechanism of sickle cell resistance to malaria. *Proc Natl Acad Sci.* **75**, doi:10.1073/pnas.75.4.1994 (1978).

208 Chaves, M. A., Leonart, M. S. & do Nascimento, A. J. Oxidative process in erythrocytes of individuals with hemoglobin S. *Hematology (Amsterdam, Netherlands)* **13**, 187-192, doi:10.1179/102453308x343356 (2008).

209 Cyrklaff, M. *et al.* Hemoglobins S and C interfere with actin remodeling in *Plasmodium falciparum*-infected erythrocytes. *Science* **334**, 1283-1286, doi:10.1126/science.1213775 (2011).

210 Fairhurst, R. M. *et al.* Abnormal display of PfEMP-1 on erythrocytes carrying haemoglobin C may protect against malaria. *Nature* **435**, 1117-1121, doi:10.1038/nature03631 (2005).

211 Fairhurst, R. M., Fujioka, H., Hayton, K., Collins, K. F. & Wellems, T. E. Aberrant development of *Plasmodium falciparum* in hemoglobin CC red cells: implications for the malaria protective effect of the homozygous state. *Blood* **101**, 3309-3315, doi:10.1182/blood-2002-10-3105 (2003).

212 Fairhurst, R. M., Bess, C. D. & Krause, M. A. Abnormal PfEMP1/knob display on *Plasmodium falciparum*-infected erythrocytes containing hemoglobin variants: fresh insights into malaria pathogenesis and protection. *Microbes and Infection / Institut Pasteur* **14**, 851-862, doi:10.1016/j.micinf.2012.05.006 (2012).

213 Vernes, A. J., Haynes, J. D., Tang, D. B., Dutoit, E. & Diggs, C. L. Decreased growth of *Plasmodium falciparum* in red cells containing haemoglobin E, a role for oxidative stress, and a sero-epidemiological correlation. *Trans R Soc Trop Med Hyg* **80**, 642-648 (1986).

214 Brockelman, C. R., Wongsattayanont, B., Tan-ariya, P. & Fucharoen, S. Thalassemic erythrocytes inhibit in vitro growth of *Plasmodium falciparum*. *Journal of Clinical Microbiology* **25**, 56-60 (1987).

215 Krause, M. A. *et al.* alpha-Thalassemia impairs the cytoadherence of *Plasmodium falciparum*-infected erythrocytes. *PLoS One* **7**, e37214, doi:10.1371/journal.pone.0037214 (2012).

216 Lang, K. S. *et al.* Enhanced erythrocyte apoptosis in sickle cell anemia, thalassemia and glucose-6-phosphate dehydrogenase deficiency. *Cellular physiology and biochemistry : international journal of experimental cellular physiology, biochemistry, and pharmacology* **12**, 365-372 (2002).

217 Pattanapanyasat, K. *et al.* Impairment of *Plasmodium falciparum* growth in thalassemic red blood cells: further evidence by using biotin labeling and flow cytometry. *Blood* **93**, 3116-3119 (1999).

218 Luzzatto, L., Usanga, F. A. & Reddy, S. Glucose-6-phosphate dehydrogenase deficient red cells: resistance to infection by malarial parasites. *Science.* **164**, doi:10.1126/science.164.3881.839 (1969).

219 Usanga, E. A. & Luzzatto, L. Adaptation of *Plasmodium falciparum* to glucose 6-phosphate dehydrogenase-deficient host red cells by production of parasite-encoded enzyme. *Nature* **313**, 793-795 (1985).

220 Cappadoro, M. *et al.* Early phagocytosis of glucose-6-phosphate dehydrogenase (G6PD)-deficient erythrocytes parasitized by Plasmodium falciparum may explain malaria protection in G6PD deficiency. *Blood.* **92** (1998).

221 Arese, P., Turrini, F. & Schwarzer, E. Band 3/Complement-mediated Recognition and Removal of Normally Senescent and Pathological Human Erythrocytes. *Cellular Physiology and Biochemistry* **16**, 133-146 (2005).

222 Ayi, K., Liles, W. C., Gros, P. & Kain, K. C. Adenosine Triphosphate Depletion of Erythrocytes Simulates the Phenotype Associated with Pyruvate Kinase Deficiency and Confers Protection against *Plasmodium falciparum In Vitro*. *Journal of Infectious Diseases* **200**, 1289-1299, doi:10.1086/605843 (2009).

223 Tham, W. H. *et al.* Complement receptor 1 is the host erythrocyte receptor for *Plasmodium falciparum* PfRh4 invasion ligand. *Proc Natl Acad Sci U S A* **107**, 17327-17332, doi:10.1073/pnas.1008151107 (2010).

224 Rowe, J. A. *et al.* Mapping of the region of complement receptor (CR) 1 required for *Plasmodium falciparum* rosetting and demonstration of the importance of CR1 in rosetting in field isolates. *J Immunol* **165**, 6341-6346 (2000).

225 Michon, P., Fraser, T. & Adams, J. H. Naturally acquired and vaccine-elicited antibodies block erythrocyte cytoadherence of the *Plasmodium vivax* Duffy binding protein. *Infect Immun* **68**, 3164-3171 (2000).

226 Wertheimer, S. P. & Barnwell, J. W. *Plasmodium vivax* interaction with the human Duffy blood group glycoprotein: identification of a parasite receptor-like protein. *Exp Parasitol* **69**, 340-350 (1989).

227 Barragan, A., Kremsner, P. G., Wahlgren, M. & Carlson, J. Blood Group A Antigen Is a Coreceptor in *Plasmodium falciparum* Rosetting. *Infection and Immunity* **68**, 2971-2975, doi:10.1128/iai.68.5.2971-2975.2000 (2000).

228 Miller, L. H. *et al.* Evidence for differences in erythrocyte surface receptors for the malarial parasites, *Plasmodium falciparum* and *Plasmodium knowlesi*. *The Journal of Experimental Medicine* **146**, 277-281, doi:10.1084/jem.146.1.277 (1977).

229 Facer, C. A. Merozoites of *P. falciparum* require glycophorin for invasion into red cells. *Bull Soc Pathol Exot Filiales* **76**, 463-469 (1983).

230 Li, X. *et al.* Identification of a specific region of *Plasmodium falciparum* EBL-1 that binds to host receptor glycophorin B and inhibits merozoite invasion in human red blood cells. *Mol Biochem Parasitol* **183**, 23-31, doi:10.1016/j.molbiopara.2012.01.002 (2012).

231 Jiang, L., Duriseti, S., Sun, P. & Miller, L. H. Molecular basis of binding of the *Plasmodium falciparum* receptor BAEBL to erythrocyte receptor glycophorin C. *Mol Biochem Parasitol* **168**, 49-54, doi:10.1016/j.molbiopara.2009.06.006 (2009).

232 Cortes, A., Benet, A., Cooke, B. M., Barnwell, J. W. & Reeder, J. C. Ability of *Plasmodium falciparum* to invade Southeast Asian ovalocytes varies between parasite lines. *Blood* **104**, 2961-2966, doi:10.1182/blood-2004-06-2136 2004-06-2136 (2004).

233 Abkarian, M., Massiera, G., Berry, L., Roques, M. & Braun-Breton, C. A novel mechanism for egress of malarial parasites from red blood cells. *Blood* **117**, 4118-4124, doi:10.1182/blood-2010-08-299883 (2011).

234 Sturm, A. *et al.* Manipulation of host hepatocytes by the malaria parasite for delivery into liver sinusoids. *Science* **313**, 1287-1290, doi:10.1126/science.1129720 (2006).

235 Bannister, L. H. & Dluzewski, A. R. The ultrastructure of red cell invasion in malaria infections: a review. *Blood cells* **16**, 257-292; discussion 293-257 (1990).

236 Zuccala, E. S. & Baum, J. Cytoskeletal and membrane remodelling during malaria parasite invasion of the human erythrocyte. *Br J Haematol* **154**, 680-689, doi:10.1111/j.1365-2141.2011.08766.x (2011).

237 Keeley, A. & Soldati, D. The glideosome: a molecular machine powering motility and host-cell invasion by Apicomplexa. *Trends Cell Biol* **14**, 528-532, doi:10.1016/j.tcb.2004.08.002 (2004).

238 Gilson, P. R. & Crabb, B. S. Morphology and kinetics of the three distinct phases of red blood cell invasion by *Plasmodium falciparum* merozoites. *International Journal for Parasitology* **39**, 91-96, doi:http://dx.doi.org/10.1016/j.ijpara.2008.09.007 (2009).

239 Chitnis, C. E., Chaudhuri, A., Horuk, R., Pogo, A. O. & Miller, L. H. The domain on the Duffy blood group antigen for binding *Plasmodium vivax* and *P. knowlesi* malarial parasites to erythrocytes. *J Exp Med* **184**, 1531-1536 (1996).

240 Ranjan, A. & Chitnis, C. E. Mapping regions containing binding residues within functional domains of *Plasmodium vivax* and *Plasmodium knowlesi* erythrocyte-binding proteins. *Proc Natl Acad Sci U S A* **96**, 14067-14072 (1999).

241 Zakeri, S., Babaeekhou, L., Mehrizi, A. A., Abbasi, M. & Djadid, N. D. Antibody Responses and Avidity of Naturally Acquired Anti-*Plasmodium vivax* Duffy Binding Protein (PvDBP) Antibodies in Individuals from an Area with Unstable Malaria Transmission. *The American Journal of Tropical Medicine and Hygiene* **84**, 944-950, doi:10.4269/ajtmh.2011.11-0001 (2011).

242 Miller, L. H., Baruch, D. I., Marsh, K. & Doumbo, O. K. The pathogenic basis of malaria. *Nature* **415**, 673-679 (2002).

243 Lopaticki, S. *et al.* Reticulocyte and erythrocyte binding-like proteins function cooperatively in invasion of human erythrocytes by malaria parasites. *Infect Immun* **79**, 1107-1117, doi:10.1128/iai.01021-10 (2011).

244 Tham, W.-H., Healer, J. & Cowman, A. F. Erythrocyte and reticulocyte binding-like proteins of *Plasmodium falciparum*. *Trends in Parasitology* **28**, 23-30, doi:http://dx.doi.org/10.1016/j.pt.2011.10.002 (2012).

245 Hadley, T. J. *et al. Falciparum* malaria parasites invade erythrocytes that lack glycophorin A and B (MkMk). Strain differences indicate receptor heterogeneity and two pathways for invasion. *Journal of Clinical Investigation* **80**, 1190-1193 (1987).

246 Duraisingh, M. T. *et al.* Phenotypic variation of Plasmodium falciparum merozoite proteins directs receptor targeting for invasion of human erythrocytes. *Embo J* **22**, 1047-1057 (2003).

247 Otsuki, H. *et al.* Single amino acid substitution in *Plasmodium yoelii* erythrocyte ligand determines its localization and controls parasite virulence. *Proceedings of the National Academy of Sciences of the United States of America* **106**, 7167-7172, doi:10.1073/pnas.0811313106 (2009).

248 Tolia, N. H., Enemark, E. J., Sim, B. K. & Joshua-Tor, L. Structural basis for the EBA-175 erythrocyte invasion pathway of the malaria parasite *Plasmodium falciparum*. *Cell* **122**, 183-193 (2005).

249 Salinas, N. D., Paing, M. M. & Tolia, N. H. Critical glycosylated residues in exon three of erythrocyte glycophorin A engage *Plasmodium falciparum* EBA-175 and define receptor specificity. *mBio* **5**, e01606-01614, doi:10.1128/mBio.01606-14 (2014).

250 Tham, W. H. *et al. Plasmodium falciparum* uses a key functional site in complement receptor type-1 for invasion of human erythrocytes. *Blood* **118**, 1923-1933, doi:10.1182/blood-2011-03-341305 (2011).

251 Douglas, A. D. *et al.* Neutralization of *Plasmodium falciparum* merozoites by antibodies against PfRH5. *J Immunol* **192**, 245-258, doi:10.4049/jimmunol.1302045 (2014).

252 Wright, K. E. *et al.* Structure of malaria invasion protein RH5 with erythrocyte basigin and blocking antibodies. *Nature* **515**, 427-430, doi:10.1038/nature13715 (2014).

253 Zenonos, Z. A. *et al.* Basigin is a druggable target for host-oriented antimalarial interventions. *J Exp Med* **212**, 1145-1151, doi:10.1084/jem.20150032 (2015).

254 Egan, E. S. *et al.* A forward genetic screen identifies erythrocyte CD55 as essential for *Plasmodium falciparum* invasion. *Science* **348**, 711-714, doi:10.1126/science.aaa3526 (2015).

255 Gwamaka, M., Fried, M., Domingo, G. & Duffy, P. E. Early and extensive CD55 loss from red blood cells supports a causal role in malarial anaemia. *Malaria Journal* **10**, 386, doi:10.1186/1475-2875-10-386 (2011).

256 Kidson, C., Lamont, G., Saul, A. & Nurse, G. T. Ovalocytic erythrocytes from Melanesians are resistant to invasion by malaria parasites in culture. *Proceedings of the National Academy of Sciences of the United States of America* **78**, 5829-5832 (1981).

257 Hadley, T. *et al.* Resistance of Melanesian elliptocytes (ovalocytes) to invasion by *Plasmodium knowlesi* and *Plasmodium falciparum* malaria parasites in vitro. *J Clin Invest* **71**, 780-782 (1983).

258 Miller, L. H. *et al.* A monoclonal antibody to rhesus erythrocyte band 3 inhibits invasion by malaria (*Plasmodium knowlesi*) merozoites. *J Clin Invest* **72**, 1357-1364, doi:10.1172/jci111092 (1983).

259 Mohandas, N., Lie-Injo, L. E., Friedman, M. & Mak, J. W. Rigid membranes of Malayan ovalocytes: a likely genetic barrier against malaria. *Blood* **63**, 1385-1392 (1984).

260 Bunyaratvej, A., Butthep, P., Kaewkettong, P. & Yuthavong, Y. Malaria protection in hereditary ovalocytosis: relation to red cell deformability, red cell parameters and degree of ovalocytosis. *Southeast Asian J Trop Med Public Health* **28 Suppl 3**, 38-42 (1997).

261 Baldwin, M. R., Li, X., Hanada, T., Liu, S.-C. & Chishti, A. H. Merozoite surface protein 1 recognition of host glycophorin A mediates malaria parasite invasion of red blood cells. *Blood* **125**, 2704-2711, doi:10.1182/blood-2014-11-611707 (2015).

262 Goldberg, D. E., Slater, A. F., Cerami, A. & Henderson, G. B. Hemoglobin degradation in the malaria parasite *Plasmodium falciparum*: an ordered process in a unique organelle. *Proceedings of the National Academy of Sciences of the United States of America* **87**, 2931-2935 (1990).

263 Pandey, A. V. *et al.* Hemozoin formation in malaria: a two-step process involving histidine-rich proteins and lipids. *Biochemical and Biophysical Research Communications* **308**, 736-743, doi:http://dx.doi.org/10.1016/S0006-291X(03)01465-7 (2003).

264 Staines, H. M., Rae, C. & Kirk, K. Increased permeability of the malaria-infected erythrocyte to organic cations. *Biochimica et Biophysica Acta (BBA) - Biomembranes* **1463**, 88-98, doi:http://dx.doi.org/10.1016/S0005-2736(99)00187-X (2000).

265 Ginsburg, H. & Stein, W. D. The New Permeability Pathways Induced by the Malaria Parasite in the Membrane of the Infected Erythrocyte: Comparison of Results Using Different Experimental Techniques. *The Journal of Membrane Biology* **197**, 113-134, doi:10.1007/s00232-003-0646-7 (2004).

266 Elsworth, B. *et al.* PTEX is an essential nexus for protein export in malaria parasites. *Nature* **511**, 587-591, doi:10.1038/nature13555 (2014).

267 de Koning-Ward, T. F. *et al.* A newly discovered protein export machine in malaria parasites. *Nature* **459**, 945-949, doi:10.1038/nature08104 (2009).

268 Marti, M., Good, R. T., Rug, M., Knuepfer, E. & Cowman, A. F. Targeting malaria virulence and remodeling proteins to the host erythrocyte. *Science* **306**, 1930-1933, doi:10.1126/science.1102452 (2004).

269 Hiller, N. L. *et al.* A host-targeting signal in virulence proteins reveals a secretome in malarial infection. *Science* **306**, 1934-1937, doi:10.1126/science.1102737 (2004).

270 Heiber, A. *et al.* Identification of new PNEPs indicates a substantial non-PEXEL exportome and underpins common features in *Plasmodium falciparum* protein export. *PLoS Pathog* **9**, e1003546, doi:10.1371/journal.ppat.1003546 (2013).

271 Mundwiler-Pachlatko, E. & Beck, H.-P. Maurer's clefts, the enigma of *Plasmodium falciparum*. *Proceedings of the National Academy of Sciences of the United States of America* **110**, 19987-19994, doi:10.1073/pnas.1309247110 (2013).

272 Maier, A. G., Cooke, B. M., Cowman, A. F. & Tilley, L. Malaria parasite proteins that remodel the host erythrocyte. *Nat Rev Micro* **7**, 341-354, doi:http://www.nature.com/nrmicro/journal/v7/n5/suppinfo/nrmicro2110_S1.html (2009).

273 Sicard, A. *et al.* Activation of a PAK-MEK signalling pathway in malaria parasite-infected erythrocytes. *Cell Microbiol* **13**, 836-845, doi:10.1111/j.1462-5822.2011.01582.x (2011).

274 Bonday, Z. Q., Dhanasekaran, S., Rangarajan, P. N. & Padmanaban, G. Import of host delta-aminolevulinate dehydratase into the malarial parasite: identification of a new drug target. *Nat Med* **6**, 898-903, doi:10.1038/78659 (2000).

275 Varadharajan, S., Sagar, B. C., Rangarajan, P. N. & Padmanaban, G. Localization of ferrochelatase in *Plasmodium falciparum*. *Biochemical Journal* **384**, 429-436 (2004).

276 Fairfield, A., Meshnick, S. & Eaton, J. Malaria parasites adopt host cell superoxide dismutase. *Science* **221**, 764-766, doi:10.1126/science.6348944 (1983).

277 Koncarevic, S. *et al.* The malarial parasite *Plasmodium falciparum* imports the human protein peroxiredoxin 2 for peroxide detoxification. *Proceedings of the National Academy of Sciences* **106**, 13323-13328, doi:10.1073/pnas.0905387106 (2009).

278 Pantaleo, A. *et al.* Analysis of changes in tyrosine and serine phosphorylation of red cell membrane proteins induced by *P. falciparum* growth. *Proteomics* **10**, 3469-3479, doi:10.1002/pmic.201000269 (2010).

279 Millholland, M. G. *et al.* The malaria parasite progressively dismantles the host erythrocyte cytoskeleton for efficient egress. *Molecular & cellular proteomics : MCP* **10**, M111.010678, doi:10.1074/mcp.M111.010678 (2011).

280 Hanspal, M., Dua, M., Takakuwa, Y., Chishti, A. H. & Mizuno, A. *Plasmodium falciparum* cysteine protease falcipain-2 cleaves erythrocyte membrane skeletal proteins at late stages of parasite development. *Presented in part in abstract form at the 43rd Annual Meeting of the American Society of Hematology, Orlando, FL, 2001.* **100**, 1048-1054, doi:10.1182/blood-2002-01-0101 (2002).

281 Le Bonniec, S. *et al.* Plasmepsin II, an Acidic Hemoglobinase from the *Plasmodium falciparum* Food Vacuole, Is Active at Neutral pH on the Host Erythrocyte Membrane Skeleton. *Journal of Biological Chemistry* **274**, 14218-14223, doi:10.1074/jbc.274.20.14218 (1999).

282 Dua, M., Raphael, P., Sijwali, P. S., Rosenthal, P. J. & Hanspal, M. Recombinant falcipain-2 cleaves erythrocyte membrane ankyrin and protein 4.1. *Mol Biochem Parasitol* **116**, 95-99 (2001).

283 Chandramohanadas, R. *et al.* Apicomplexan parasites co-opt host calpains to facilitate their escape from infected cells. *science* **324**, 794-797 (2009).

284 LaMonte, G. *et al.* Translocation of sickle cell erythrocyte microRNAs into *Plasmodium falciparum* inhibits parasite translation and contributes to malaria resistance. *Cell host & microbe* **12**, 187-199, doi:10.1016/j.chom.2012.06.007 (2012).

285 Friedman, M. J., Roth, E. F., Nagel, R. L. & Trager, W. The Role of Hemoglobins C, S, and NBalt in the Inhibition of Malaria Parasite Development in Vitro. *The American Journal of Tropical Medicine and Hygiene* **28**, 777-780 (1979).

286 Hebbel, R. P. Beyond hemoglobin polymerization: the red blood cell membrane and sickle disease pathophysiology. *Blood* **77**, 214-237 (1991).

287 Yuthavong, Y., Butthep, P., Bunyaratvej, A., Fucharoen, S. & Khusmith, S. Impaired parasite growth and increased susceptibility to phagocytosis of *Plasmodium falciparum* infected alpha-thalassemia or hemoglobin Constant Spring red blood cells. *American journal of clinical pathology* **89**, 521-525 (1988).

288 Carlson, J., Nash, G. B., Gabutti, V., al Yaman, F. & Wahlgren, M. Natural protection against severe *Plasmodium falciparum* malaria due to impaired rosette formation. *Blood.* **84** (1994).

289 Nagel, R. L. Innate resistance to malaria: the intraerythrocytic cycle. *Blood Cells* **16**, 321-339; discussion 340-329 (1990).

290 Tishkoff, S. A. *et al.* Haplotype diversity and linkage disequilibrium at human G6PD: recent origin of alleles that confer malarial resistance. *Science.* **293**, doi:10.1126/science.1061573 (2001).

291 Miller, J., Golenser, J., Spira, D. T. & Kosower, N. S. *Plasmodium falciparum*: thiol status and growth in normal and glucose-6-phosphate dehydrogenase deficient human erythrocytes. *Exp Parasitol* **57**, 239-247 (1984).

292 Roth, E. F., Raventos-Suarez, C., Rinaldi, A. & Nagel, R. L. Glucose-6-phosphate dehydrogenase deficiency inhibits in vitro growth of *Plasmodium falciparum*. *Proc Natl Acad Sci USA* **80**, doi:10.1073/pnas.80.1.298 (1983).

293 Roth, E. F., Jr., Schulman, S., Vanderberg, J. & Olson, J. Pathways for the reduction of oxidized glutathione in the *Plasmodium falciparum*-infected erythrocyte: can parasite enzymes replace host red cell glucose-6-phosphate dehydrogenase? *Blood* **67**, 827-830 (1986).

294 Roth, E. F., Jr., Ruprecht, R. M., Schulman, S., Vanderberg, J. & Olson, J. A. Ribose metabolism and nucleic acid synthesis in normal and glucose-6-phosphate dehydrogenase-deficient human erythrocytes infected with *Plasmodium falciparum*. *J Clin Invest* **77**, 1129-1135, doi:10.1172/jci112412 (1986).

295 Weng, H. *et al.* Interaction of *Plasmodium falciparum* knob-associated histidine-rich protein (KAHRP) with erythrocyte ankyrin R is required for its attachment to the erythrocyte membrane. *Biochimica et biophysica acta* **1838**, 185-192, doi:10.1016/j.bbamem.2013.09.014 (2014).

296 Magowan, C. *et al. Plasmodium falciparum* histidine-rich protein 1 associates with the band 3 binding domain of ankyrin in the infected red cell membrane. *Biochim Biophys Acta* **1502**, 461-470 (2000).

297 Crabb, B. S. *et al.* Targeted gene disruption shows that knobs enable malaria-infected red cells to cytoadhere under physiological shear stress. *Cell* **89**, 287-296 (1997).

298 Horrocks, P. *et al.* PfEMP1 expression is reduced on the surface of knobless *Plasmodium falciparum* infected erythrocytes. *J Cell Sci* **118**, 2507-2518, doi:10.1242/jcs.02381 (2005).

299 Téllez, M.-d.-M., Matesanz, F. & Alcina, A. The C-terminal domain of the *Plasmodium falciparum* acyl-CoA synthetases PfACS1 and PfACS3 functions as ligand for ankyrin. *Molecular and Biochemical Parasitology* **129**, 191-198, doi:http://dx.doi.org/10.1016/S0166-6851(03)00123-3 (2003).

300 Matesanz, F., Duran-Chica, I. & Alcina, A. The cloning and expression of Pfacs1, a *Plasmodium falciparum* fatty acyl coenzyme A synthetase-1 targeted to the host erythrocyte cytoplasm. *Journal of molecular biology* **291**, 59-70, doi:10.1006/jmbi.1999.2964 (1999).

301 Dhawan, S., Dua, M., Chishti, A. H. & Hanspal, M. Ankyrin peptide blocks falcipain-2-mediated malaria parasite release from red blood cells. *J Biol Chem* **278**, 30180-30186, doi:10.1074/jbc.M305132200 (2003).

302 Mebius, R. E. & Kraal, G. Structure and function of the spleen. *Nat Rev Immunol* **5**, 606-616 (2005).

303 Weiss, L. Mechanisms of splenic control of murine malaria: cellular reactions of the spleen in lethal (strain 17XL) *Plasmodium yoelii* malaria in BALB/c mice, and the consequences of pre-infective splenectomy. *Am J Trop Med Hyg* **41**, 144-160 (1989).

304 Winkel, K. D. & Good, M. F. Inability of *Plasmodium vinckei*-immune spleen cells to transfer protection to recipient mice exposed to vaccine 'vectors' or heterologous species of plasmodium. *Parasite Immunol* **13**, 517-530 (1991).

305 Villeval, J. L., Lew, A. & Metcalf, D. Changes in hemopoietic and regulator levels in mice during fatal or nonfatal malarial infections. *Experimental Parasitology* **71**, 364-374, doi:http://dx.doi.org/10.1016/0014-4894(90)90062-H (1990).

306 Cranston, H. A. *et al. Plasmodium falciparum* maturation abolishes physiologic red cell deformability. *Science* **223**, 400-403 (1984).

307 Ho, M. *et al.* Splenic Fc receptor function in host defense and anemia in acute *Plasmodium falciparum* malaria. *Journal of Infectious Diseases* **161**, 555-561 (1990).

308 Nagayasu, E. *et al.* CR1 density polymorphism on erythrocytes of *falciparum* malaria patients in Thailand. *Am J Trop Med Hyg* **64**, 1-5 (2001).

309 Rowe, J. A., Moulds, J. M., Newbold, C. I. & Miller, L. H. *P. falciparum* rosetting mediated by a parasite-variant erythrocyte membrane protein and complement-receptor 1. *Nature* **388**, 292-295, doi:10.1038/40888 (1997).

310 Chen, Q. *et al.* Identification of *Plasmodium falciparum* erythrocyte membrane protein 1 (PfEMP1) as the rosetting ligand of the malaria parasite *P. falciparum*. *J Exp Med* **187**, 15-23 (1998).

311 Moulds, J. M. *et al.* Identification of the Kna/Knb polymorphism and a method for Knops genotyping. *Transfusion* **44**, 164-169 (2004).

312 Moulds, J. M. *et al.* Identification of complement receptor one (CR1) polymorphisms in west Africa. *Genes Immun* **1**, 325-329, doi:10.1038/sj.gene.6363676 (2000).

313 Rowe, J. A. *et al.* Blood group O protects against severe *Plasmodium falciparum* malaria through the mechanism of reduced rosetting. *Proceedings of the National Academy of Sciences* **104**, 17471-17476, doi:10.1073/pnas.0705390104 (2007).

314 Febbraio, M., Hajjar, D. P. & Silverstein, R. L. CD36: a class B scavenger receptor involved in angiogenesis, atherosclerosis, inflammation, and lipid metabolism. *J Clin Invest* **108**, 785-791, doi:10.1172/jci14006 (2001).

315 Combes, V., Coltel, N., Faille, D., Wassmer, S. C. & Grau, G. E. Cerebral malaria: role of microparticles and platelets in alterations of the blood-brain barrier. *Int J Parasitol* **36**, 541-546, doi:10.1016/j.ijpara.2006.02.005 (2006).

316 Rowe, J. A., Claessens, A., Corrigan, R. A. & Arman, M. Adhesion of *Plasmodium falciparum*-infected erythrocytes to human cells: molecular mechanisms and therapeutic implications. *Expert Reviews in Molecular Medicine* **11**, e16, doi:10.1017/S1462399409001082 (2009).

317 Wassmer, S. C. *et al.* Platelets reorient *Plasmodium falciparum*-infected erythrocyte cytoadhesion to activated endothelial cells. *J Infect Dis* **189**, 180-189, doi:10.1086/380761 (2004).

318 Pain, A. *et al.* Platelet-mediated clumping of *Plasmodium falciparum*-infected erythrocytes is a common adhesive phenotype and is associated with severe malaria. *Proc Natl Acad Sci U S A* **98**, 1805-1810, doi:10.1073/pnas.98.4.1805 (2001).

319 Chattopadhyay, R., Taneja, T., Chakrabarti, K., Pillai, C. R. & Chitnis, C. E. Molecular analysis of the cytoadherence phenotype of a *Plasmodium falciparum* field isolate that binds intercellular adhesion molecule-1. *Mol Biochem Parasitol* **133**, 255-265 (2004).

320 Berendt, A. R., Simmons, D. L., Tansey, J., Newbold, C. I. & Marsh, K. Intercellular adhesion molecule-1 is an endothelial cell adhesion receptor for *Plasmodium falciparum*. *Nature* **341**, 57-59, doi:10.1038/341057a0 (1989).

321 McCormick, C. J., Craig, A., Roberts, D., Newbold, C. I. & Berendt, A. R. Intercellular adhesion molecule-1 and CD36 synergize to mediate adherence of *Plasmodium falciparum*-infected erythrocytes to cultured human microvascular endothelial cells. *J Clin Invest* **100**, 2521-2529, doi:10.1172/jci119794 (1997).

322 Aitman, T. J. *et al.* Malaria susceptibility and CD36 mutation. *Nature* **405**, 1015-1016, doi:10.1038/35016636 (2000).

323 Ayodo, G. *et al.* Combining evidence of natural selection with association analysis increases power to detect malaria-resistance variants. *Am J Hum Genet* **81**, 234-242, doi:10.1086/519221 (2007).

324 Amodu, O. K. *et al. Plasmodium falciparum* malaria in south-west Nigerian children: is the polymorphism of ICAM-1 and E-selectin genes contributing to the clinical severity of malaria? *Acta tropica* **95**, 248-255, doi:10.1016/j.actatropica.2005.05.011 (2005).

325 Fry, A. E. *et al.* Variation in the ICAM1 gene is not associated with severe malaria phenotypes. *Genes and immunity* **9**, 462-469, doi:10.1038/gene.2008.38 (2008).

326 Bellamy, R., Kwiatkowski, D. & Hill, A. V. Absence of an association between intercellular adhesion molecule 1, complement receptor 1 and interleukin 1 receptor antagonist gene polymorphisms and severe malaria in a West African population. *Trans R Soc Trop Med Hyg* **92**, 312-316 (1998).

327 Cserti-Gazdewich, C. M. *et al.* Combined measurement of soluble and cellular ICAM-1 among children with *Plasmodium falciparum* malaria in Uganda. *Malaria Journal* **9**, 1-10, doi:10.1186/1475-2875-9-233 (2010).

328 Omi, K. *et al.* CD36 polymorphism is associated with protection from cerebral malaria. *Am J Hum Genet* **72**, 364-374, doi:10.1086/346091 (2003).

329 Chilongola, J., Balthazary, S., Mpina, M., Mhando, M. & Mbugi, E. CD36 deficiency protects against malarial anaemia in children by reducing *Plasmodium falciparum*-infected red blood cell adherence to vascular endothelium. *Trop Med Int Health* 14, 810-816, doi:10.1111/j.1365-3156.2009.02298.x (2009).

330 Kun, J. F. et al. Association of the ICAM-1Kilifi mutation with protection against severe malaria in Lambarene, Gabon. Am J Trop Med Hyg 61, 776-779 (1999).

331 Cabrera, A., Neculai, D. & Kain, K. C. CD36 and malaria: friends or foes? A decade of data provides some answers. Trends Parasitol 30, 436-444, doi:10.1016/j.pt.2014.07.006 (2014).

332 Turner, L. et al. Severe malaria is associated with parasite binding to endothelial protein C receptor. Nature 498, 502-505, doi:10.1038/nature12216 (2013).

333 Moxon, C. A. et al. Loss of endothelial protein C receptors links coagulation and inflammation to parasite sequestration in cerebral malaria in African children. Blood 122, 842-851, doi:10.1182/blood-2013-03-490219 (2013).

334 Moxon, C. et al. Role of sequestration-induced loss of protein C receptors in coagulation and inflammation in cerebral malaria. The Lancet 383, S75, doi:10.1016/S0140-6736(14)60338-X (2014).

335 Hansson, H. H. et al. Haplotypes of the endothelial protein C receptor (EPCR) gene are not associated with severe malaria in Tanzania. Malaria Journal 14, 1-9, doi:10.1186/s12936-015-1007-6 (2015).

336 Naka, I., Patarapotikul, J., Hananantachai, H., Imai, H. & Ohashi, J. Association of the endothelial protein C receptor (PROCR) rs867186-G allele with protection from severe malaria. Malar J 13, doi:10.1186/1475-2875-13-105 (2014).

337 Schuldt, K. et al. Endothelial protein C receptor gene variants not associated with severe malaria in ghanaian children. PLoS One 9, doi:10.1371/journal.pone.0115770 (2014).

338 Cholera, R. et al. Impaired cytoadherence of Plasmodium falciparum-infected erythrocytes containing sickle hemoglobin. Proc Natl Acad Sci USA 105, doi:10.1073/pnas.0711401105 (2008).

339 Kilian, N. et al. Hemoglobin S and C affect protein export in Plasmodium falciparum-infected erythrocytes. Biology Open 4, 400-410, doi:10.1242/bio.201410942 (2015).

340 Lang, K. S. et al. Cation channels trigger apoptotic death of erythrocytes. Cell death and differentiation 10, 249-256, doi:10.1038/sj.cdd.4401144 (2003).

341 Boas, F. E., Forman, L. & Beutler, E. Phosphatidylserine exposure and red cell viability in red cell aging and in hemolytic anemia. Proc Natl Acad Sci U S A 95, 3077-3081 (1998).

342 Fadok, V. A. et al. A receptor for phosphatidylserine-specific clearance of apoptotic cells. Nature 405, 85-90, doi:10.1038/35011084 (2000).

343 Li, M. O., Sarkisian, M. R., Mehal, W. Z., Rakic, P. & Flavell, R. A. Phosphatidylserine receptor is required for clearance of apoptotic cells. Science 302, 1560-1563, doi:10.1126/science.1087621 (2003).

344 Kobayashi, N. et al. TIM-1 and TIM-4 glycoproteins bind phosphatidylserine and mediate uptake of apoptotic cells. Immunity 27, 927-940, doi:10.1016/j.immuni.2007.11.011 (2007).

345 Rachmilewitz, E. A. Formation of hemichromes from oxidized hemoglobin subunits. Annals of the New York Academy of Sciences 165, 171-184 (1969).

346 Kannan, R., Labotka, R. & Low, P. S. Isolation and characterization of the hemichrome-stabilized membrane protein aggregates from sickle erythrocytes. Major site of autologous antibody binding. J Biol Chem 263, 13766-13773 (1988).

347 Low, P. S., Waugh, S. M., Zinke, K. & Drenckhahn, D. The role of hemoglobin denaturation and band 3 clustering in red blood cell aging. Science 227, 531-533 (1985).

348 Mannu, F. et al. Role of hemichrome binding to erythrocyte membrane in the generation of band-3 alterations in beta-thalassemia intermedia erythrocytes. Blood 86, 2014-2020 (1995).

349 Ferru, E. et al. Regulation of membrane-cytoskeletal interactions by tyrosine phosphorylation of erythrocyte band 3. Blood 117, 5998-6006, doi:10.1182/blood-2010-11-317024 (2011).

350 Cappellini, M. D. et al. Metabolic indicators of oxidative stress correlate with haemichrome attachment to membrane, band 3 aggregation and erythrophagocytosis in beta-thalassaemia intermedia. Br J Haematol 104, 504-512 (1999).

351 Lutz, H. U. et al. Naturally occurring anti-band-3 antibodies and complement together mediate phagocytosis of oxidatively stressed human erythrocytes. Proc Natl Acad Sci U S A 84, 7368-7372 (1987).

352 Oldenborg, P. A. et al. Role of CD47 as a marker of self on red blood cells. Science 288, 2051-2054 (2000).

353 Ishikawa-Sekigami, T. et al. SHPS-1 promotes the survival of circulating erythrocytes through inhibition of phagocytosis by splenic macrophages. Blood 107, 341-348, doi:10.1182/blood-2005-05-1896 (2006).

354 Fossati-Jimack, L. et al. Selective increase of autoimmune epitope expression on aged erythrocytes in mice: implications in anti-erythrocyte autoimmune responses. Journal of autoimmunity 18, 17-25, doi:10.1006/jaut.2001.0563 (2002).

355 Anniss, A. M. & Sparrow, R. L. Expression of CD47 (integrin-associated protein) decreases on red blood cells during storage. Transfusion and apheresis science : official journal of the World Apheresis Association : official journal of the European Society for Haemapheresis 27, 233-238 (2002).

356 de Back, D. Z., Kostova, E. B., van Kraaij, M., van den Berg, T. K. & van Bruggen, R. Of macrophages and red blood cells; a complex love story. Frontiers in Physiology 5, 9, doi:10.3389/fphys.2014.00009 (2014).

357 Burger, P., Hilarius-Stokman, P., de Korte, D., van den Berg, T. K. & van Bruggen, R. CD47 functions as a molecular switch for erythrocyte phagocytosis. Blood 119, 5512-5521, doi:10.1182/blood-2011-10-386805 (2012).

358 Duranton, C. et al. Electrophysiological properties of the Plasmodium falciparum-induced cation conductance of human erythrocytes. Cellular physiology and biochemistry : international journal of experimental cellular physiology, biochemistry, and pharmacology 13, 189-198, doi:72421 (2003).

359 Huber, S. M., Duranton, C. & Lang, F. in International Review of Cytology Vol. Volume 246 59-134 (Academic Press, 2005).

360 Sherman, I. W., Eda, S. & Winograd, E. Cytoadherence and sequestration in Plasmodium falciparum: defining the ties that bind. Microbes Infect 5, doi:10.1016/s1286-4579(03)00162-x (2003).

361 Eda, S. & Sherman, I. W. Cytoadherence of malaria-infected red blood cells involves exposure of phosphatidylserine. Cellular physiology and biochemistry : international journal of experimental cellular physiology, biochemistry, and pharmacology 12, 373-384 (2002).

362 Banerjee, R., Khandelwal, S., Kozakai, Y., Sahu, B. & Kumar, S. CD47 regulates the phagocytic clearance and replication of the Plasmodium yoelii malaria parasite. Proceedings of the National Academy of Sciences 112, 3062-3067, doi:10.1073/pnas.1418144112 (2015).

363 Scherf, A., Lopez-Rubio, J. J. & Riviere, L. Antigenic variation in Plasmodium falciparum. Annu Rev Microbiol 62, 445-470, doi:10.1146/annurev.micro.61.080706.093134 (2008).

364 Pasternak, N. D. & Dzikowski, R. PfEMP1: An antigen that plays a key role in the pathogenicity and immune evasion of the malaria parasite Plasmodium falciparum. The

International Journal of Biochemistry & Cell Biology 41, 1463-1466, doi:http://dx.doi.org/10.1016/j.biocel.2008.12.012 (2009).

365 de Jong, K. et al. Short survival of phosphatidylserine-exposing red blood cells in murine sickle cell anemia. Blood 98, 1577-1584 (2001).

366 Kuypers, F. A. et al. Membrane phospholipid asymmetry in human thalassemia. Blood 91, 3044-3051 (1998).

367 Lew, V. L. & Bookchin, R. M. Ion transport pathology in the mechanism of sickle cell dehydration. Physiological reviews 85, 179-200, doi:10.1152/physrev.00052.2003 (2005).

368 Luzzi, G., Merry, A., Newbold, C., Marsh, K. & Pasvol, G. Protection by α-thalassaemia against Plasmodium falciparum malaria: modified surface antigen expression rather than impaired growth or cytoadherence. Immunology letters 30, 233-240 (1991).

369 Zumla, A. et al. Host-directed therapies for infectious diseases: current status, recent progress, and future prospects. The Lancet Infectious Diseases 16, e47-e63, doi:http://dx.doi.org/10.1016/S1473-3099(16)00078-5 (2016).

370 Manchanda, V., Sanchaita, S. & Singh, N. P. Multidrug Resistant Acinetobacter. Journal of Global Infectious Diseases 2, 291-304, doi:10.4103/0974-777X.68538 (2010).

371 Caminero, J. A., Sotgiu, G., Zumla, A. & Migliori, G. B. Best drug treatment for multidrug-resistant and extensively drug-resistant tuberculosis. The Lancet Infectious Diseases 10, 621-629, doi:http://dx.doi.org/10.1016/S1473-3099(10)70139-0 (2010).

372 Wongsrichanalai, C., Pickard, A. L., Wernsdorfer, W. H. & Meshnick, S. R. Epidemiology of drug-resistant malaria. The Lancet infectious diseases 2, 209-218 (2002).

373 Reeves, P. M. et al. Disabling poxvirus pathogenesis by inhibition of Abl-family tyrosine kinases. Nat Med 11, 731-739, doi:10.1038/nm1265 (2005).

374 Hartmann, J. T., Haap, M., Kopp, H.-G. & Lipp, H.-P. Tyrosine Kinase Inhibitors - A Review on Pharmacology, Metabolism and Side Effects. Current Drug Metabolism 10, 470-481, doi:10.2174/138920009788897975 (2009).

375 Robert, C. et al. Cutaneous side-effects of kinase inhibitors and blocking antibodies. The lancet oncology 6, 491-500 (2005).

376 Collier, M. A. et al. Delivery of host cell-directed therapeutics for intracellular pathogen clearance. Expert review of anti-infective therapy 11, 1225-1235, doi:10.1586/14787210.2013.845524 (2013).

377 Tobin, D. M. Host-Directed Therapies for Tuberculosis. Cold Spring Harbor perspectives in medicine 5, doi:10.1101/cshperspect.a021196 (2015).

378 Matalon, S., Rasmussen, T. A. & Dinarello, C. A. Histone deacetylase inhibitors for purging HIV-1 from the latent reservoir. Mol Med 17, 466-472, doi:10.2119/molmed.2011.00076 (2011).

379 Krishnan, M. N. & Garcia-Blanco, M. A. Targeting host factors to treat West Nile and dengue viral infections. Viruses 6, 683-708, doi:10.3390/v6020683 (2014).

380 Sakurai, Y. et al. Ebola virus. Two-pore channels control Ebola virus host cell entry and are drug targets for disease treatment. Science 347, 995-998, doi:10.1126/science.1258758 (2015).

381 Chaurasia, M. et al. Chondroitin nanocapsules enhanced doxorubicin induced apoptosis against leishmaniasis via Th1 immune response. International journal of biological macromolecules 79, 27-36, doi:10.1016/j.ijbiomac.2015.04.043 (2015).

382 Mayer-Barber, K. D. et al. Host-directed therapy of tuberculosis based on interleukin-1 and type I interferon crosstalk. Nature 511, 99-103, doi:10.1038/nature13489 (2014).

383 Newton, R. Molecular mechanisms of glucocorticoid action: what is important? Thorax 55, 603-613, doi:10.1136/thorax.55.7.603 (2000).

384 Critchley, J. A., Young, F., Orton, L. & Garner, P. Corticosteroids for prevention of mortality in people with tuberculosis: a systematic review and meta-analysis. The Lancet. Infectious diseases 13, 223-237, doi:10.1016/s1473-3099(12)70321-3 (2013).

385 Singhal, A. et al. Metformin as adjunct antituberculosis therapy. Science Translational Medicine 6, 263ra159-263ra159, doi:10.1126/scitranslmed.3009885 (2014).

386 Pearce, E. L. et al. Enhancing CD8 T-cell memory by modulating fatty acid metabolism. Nature 460, 103-107, doi:10.1038/nature08097 (2009).

387 Piot, P., Muyembe, J.-J. & Edmunds, W. J. Ebola in west Africa: from disease outbreak to humanitarian crisis. The Lancet Infectious Diseases 14, 1034-1035, doi:http://dx.doi.org/10.1016/S1473-3099(14)70956-9 (2014).

388 Fedson, D. S., Jacobson, J. R., Rordam, O. M. & Opal, S. M. Treating the Host Response to Ebola Virus Disease with Generic Statins and Angiotensin Receptor Blockers. mBio 6, e00716-00715, doi:10.1128/mBio.00716-15 (2015).

389 Fedson, D. S. & Rordam, O. M. Treating Ebola patients: a 'bottom up' approach using generic statins and angiotensin receptor blockers. International journal of infectious diseases : IJID : official publication of the International Society for Infectious Diseases 36, 80-84, doi:10.1016/j.ijid.2015.04.019 (2015).

390 Geisbert, T. W. et al. Treatment of Ebola virus infection with a recombinant inhibitor of factor VIIa/tissue factor: a study in rhesus monkeys. Lancet 362, 1953-1958, doi:10.1016/s0140-6736(03)15012-x (2003).

391 Kennedy, S. P., Warren, S. L., Forget, B. G. & Morrow, J. S. Ankyrin binds to the 15th repetitive unit of erythroid and nonerythroid beta-spectrin. J Cell Biol 115, 267-277 (1991).

392 Chang, S. H. & Low, P. S. Identification of a critical ankyrin-binding loop on the cytoplasmic domain of erythrocyte membrane band 3 by crystal structure analysis and site-directed mutagenesis. J Biol Chem 278, 6879-6884, doi:10.1074/jbc.M211137200 (2003).

393 Su, Y. et al. Associations of protein 4.2 with band 3 and ankyrin. Molecular and cellular biochemistry 289, 159-166, doi:10.1007/s11010-006-9159-x (2006).

394 Gallagher, P. G. Hematologically important mutations: ankyrin variants in hereditary spherocytosis. Blood Cells Mol Dis 35, 345-347, doi:10.1016/j.bcmd.2005.08.008 (2005).

395 Stabach, P. R. et al. The structure of the ankyrin-binding site of beta-spectrin reveals how tandem spectrin-repeats generate unique ligand-binding properties. Blood 113, 5377-5384, doi:10.1182/blood-2008-10-184291 (2009).

396 Ipsaro, J. J., Huang, L., Gutierrez, L. & MacDonald, R. I. Molecular epitopes of the ankyrin-spectrin interaction. Biochemistry 47, 7452-7464, doi:10.1021/bi702525z (2008).

397 Ipsaro, J. J., Huang, L. & Mondragon, A. Structures of the spectrin-ankyrin interaction binding domains. Blood 113, 5385-5393, doi:10.1182/blood-2008-10-184358 (2009).

398 Ipsaro, J. J. & Mondragon, A. Structural basis for spectrin recognition by ankyrin. Blood 115, 4093-4101, doi:10.1182/blood-2009-11-255604 (2010).

399 Ran, F. A. et al. Double Nicking by RNA-Guided CRISPR Cas9 for Enhanced Genome Editing Specificity. Cell 154, 1380-1389, doi:10.1016/j.cell.2013.08.021 (2013).

400 Deplaine, G. et al. The sensing of poorly deformable red blood cells by the human spleen can be mimicked in vitro. Blood 117, e88-95, doi:10.1182/blood-2010-10-312801 (2011).

401 Hortle, E. et al. Adenosine monophosphate deaminase 3 activation shortens erythrocyte half-life and provides malaria resistance in mice. Blood, doi:10.1182/blood-2015-09-666834 (2016).

402 Bauer, D. C., McMorran, B. J., Foote, S. J. & Burgio, G. Genome-wide analysis of chemically induced mutations in mouse in phenotype-driven screens. BMC Genomics 16, 1-8, doi:10.1186/s12864-015-2073-4 (2015).

403 Li, H. & Durbin, R. Fast and accurate short read alignment with Burrows-Wheeler transform. Bioinformatics 25, 1754-1760, doi:10.1093/bioinformatics/btp324 (2009).

404 Langmead, B. & Salzberg, S. L. Fast gapped-read alignment with Bowtie 2. Nature methods 9, 357-359, doi:10.1038/nmeth.1923 (2012).

405 Li, H. et al. The Sequence Alignment/Map format and SAMtools. Bioinformatics 25, 2078-2079, doi:10.1093/bioinformatics/btp352 (2009).

406 McKenna, A. et al. The Genome Analysis Toolkit: a MapReduce framework for analyzing next-generation DNA sequencing data. Genome research 20, 1297-1303, doi:10.1101/gr.107524.110 (2010).

407 Wang, K., Li, M. & Hakonarson, H. ANNOVAR: functional annotation of genetic variants from high-throughput sequencing data. Nucleic Acids Research 38, e164-e164, doi:10.1093/nar/gkq603 (2010).

408 Schneider, C. A., Rasband, W. S. & Eliceiri, K. W. NIH Image to ImageJ: 25 years of image analysis. Nat Meth 9, 671-675 (2012).

409 Jarra, W. & Brown, K. Protective immunity to malaria: studies with cloned lines of Plasmodium chabaudi and P. berghei in CBA/Ca mice. I. The effectiveness and inter‐ and intra‐species specificity of immunity induced by infection. Parasite immunology 7, 595-606 (1985).

410 Lelliott, P. M., Lampkin, S., McMorran, B. J., Foote, S. J. & Burgio, G. A flow cytometric assay to quantify invasion of red blood cells by rodent Plasmodium parasites in vivo. Malar J 13, 100, doi:10.1186/1475-2875-13-100 (2014).

411 Shapiro, S. S. & Wilk, M. B. An analysis of variance test for normality (complete samples)†. Biometrika 52, 591-611, doi:10.1093/biomet/52.3-4.591 (1965).

412 Nicolas, V. et al. Rh-RhAG/Ankyrin-R, a New Interaction Site between the Membrane Bilayer and the Red Cell Skeleton, Is Impaired by Rhnull-associated Mutation. Journal of Biological Chemistry 278, 25526-25533, doi:10.1074/jbc.M302816200 (2003).

413 Grey, J. L., Kodippili, G. C., Simon, K. & Low, P. S. Identification of contact sites between ankyrin and band 3 in the human erythrocyte membrane. Biochemistry 51, 6838-6846, doi:10.1021/bi300693k (2012).

414 Casale, M. & Perrotta, S. Splenectomy for hereditary spherocytosis: complete, partial or not at all? Expert review of hematology 4, 627-635, doi:10.1586/ehm.11.51 (2011).

415 Yawata, Y. et al. Characteristic features of the genotype and phenotype of hereditary spherocytosis in the Japanese population. Int J Hematol 71, 118-135 (2000).

416 Stephens, R., Culleton, R. L. & Lamb, T. J. The contribution of Plasmodium chabaudi to our understanding of malaria. Trends in Parasitology 28, 73-82, doi:10.1016/j.pt.2011.10.006 (2012).

417 McMorran, B. J. et al. Platelets Kill Intraerythrocytic Malarial Parasites and Mediate Survival to Infection. Science 323, 797-800, doi:10.1126/science.1166296 (2009).

418 Nakanishi, H., Kanzaki, A., Yawata, A., Yamada, O. & Yawata, Y. Ankyrin gene mutations in japanese patients with hereditary spherocytosis. Int J Hematol 73, 54-63 (2001).

419 Edelman, E. J., Maksimova, Y., Duru, F., Altay, C. & Gallagher, P. G. A complex splicing defect associated with homozygous ankyrin-deficient hereditary spherocytosis. Blood 109, 5491-5493, doi:10.1182/blood-2006-09-046573 (2007).

420 Kyrylkova, K., Kyryachenko, S., Leid, M. & Kioussi, C. Detection of apoptosis by TUNEL assay. Methods Mol Biol 887, 41-47, doi:10.1007/978-1-61779-860-3_5 (2012).

421 Straat, M., van Bruggen, R., de Korte, D. & Juffermans, N. P. Red blood cell clearance in inflammation. Transfusion medicine and hemotherapy : offizielles Organ der Deutschen Gesellschaft fur Transfusionsmedizin und Immunhamatologie 39, 353-361, doi:10.1159/000342229 (2012).

422 Jakeman, G., Saul, A., Hogarth, W. & Collins, W. Anaemia of acute malaria infections in non-immune patients primarily results from destruction of uninfected erythrocytes. Parasitology 119, 127-133 (1999).

423 Lamikanra, A. A. et al. Malarial anemia: of mice and men. Blood 110, 18-28 (2007).

424 Dondorp, A. M. et al. Prognostic significance of reduced red blood cell deformability in severe falciparum malaria. Am J Trop Med Hyg 57, 507-511 (1997).

425 Dondorp, A. et al. The role of reduced red cell deformability in the pathogenesis of severe falciparum malaria and its restoration by blood transfusion. Transactions of the Royal Society of Tropical Medicine and Hygiene 96, 282-286 (2002).

426 Hedrick, P. W. Resistance to malaria in humans: the impact of strong, recent selection. Malaria Journal 11, 349, doi:10.1186/1475-2875-11-349 (2012).

427 Williams, T. N. Red blood cell defects and malaria. Mol Biochem Parasitol 149, 121-127, doi:10.1016/j.molbiopara.2006.05.007 (2006).

428 Williams, T. N. Human red blood cell polymorphisms and malaria. Curr Opin Microbiol 9, 388-394, doi:10.1016/j.mib.2006.06.009 (2006).

429 Fry, A. E. et al. Positive selection of a CD36 nonsense variant in sub-Saharan Africa, but no association with severe malaria phenotypes. Hum Mol Genet 18, 2683-2692, doi:10.1093/hmg/ddp192 (2009).

430 Clark, T. et al. Allelic heterogeneity of G6PD deficiency in West Africa and severe malaria susceptibility. Eur J Hum Genet. 17, doi:10.1038/ejhg.2009.8 (2009).

431 Bauduer, F. Red cell polymorphisms and malaria: an evolutionary approach. Bulletins et mémoires de la Société d'anthropologie de Paris 25, 55-64, doi:10.1007/s13219-012-0060-8 (2013).

432 Kreuels, B. et al. Differing effects of HbS and HbC traits on uncomplicated falciparum malaria, anemia, and child growth. Blood 115, 4551-4558 (2010).

433 Gonçalves, B. P., Gupta, S. & Penman, B. S. Sickle haemoglobin, haemoglobin C and malaria mortality feedbacks. Malaria Journal 15, 26, doi:10.1186/s12936-015-1077-5 (2016).

434 Curtis, B. R. & Aster, R. H. Incidence of the Nak(a)-negative platelet phenotype in African Americans is similar to that of Asians. Transfusion 36, 331-334, doi:10.1046/j.1537-2995.1996.36496226147.x (1996).

435 Urwijitaroon, Y., Barusrux, S., Romphruk, A. & Puapairoj, C. Frequency of human platelet antigens among blood donors in northeastern Thailand. Transfusion 35, 868-870 (1995).

436 Pain, A. et al. A non-sense mutation in Cd36 gene is associated with protection from severe malaria. Lancet 357, 1502-1503, doi:10.1016/s0140-6736(00)04662-6 (2001).

437 Jarolim, P. et al. Characterization of 13 novel band 3 gene defects in hereditary spherocytosis with band 3 deficiency. Blood 88, 4366-4374 (1996).

438 Takaoka, Y. et al. A novel mutation in the erythrocyte protein 4.2 gene of Japanese patients with hereditary spherocytosis (protein 4.2 Fukuoka). Br J Haematol 88, 527-533 (1994).

439 Matsuda, M., Hatano, N., Ideguchi, H., Takahira, H. & Fukumaki, Y. A novel mutation causing an aberrant splicing in the protein 4.2 gene associated with hereditary spherocytosis (protein 4.2Notame). Hum Mol Genet 4, 1187-1191 (1995).

440 Spector, I. & Metz, J. A Bantu family with hereditary spherocytosis. S Afr Med J 37, 211-213 (1963).

441 Hassan, A., Babadoko, A. A., Isa, A. H. & Abunimye, P. Hereditary spherocytosis in a 27-year-old woman: case report. Annals of African medicine 8, 61-63 (2009).

442 Ustun, C. et al. Interaction of sickle cell trait with hereditary spherocytosis: splenic infarcts and sequestration. Acta Haematol 109, 46-49, doi:67273 (2003).

443 Iolascon, A. & Avvisati, R. A. Genotype/phenotype correlation in hereditary spherocytosis. Haematologica 93, 1283-1288, doi:10.3324/haematol.13344 (2008).

444 Kodippili, G. C. et al. Imaging of the diffusion of single band 3 molecules on normal and mutant erythrocytes. Blood 113, 6237-6245, doi:10.1182/blood-2009-02-205450 (2009).

445 Cho, M. R., Eber, S. W., Liu, S.-C., Lux, S. E. & Golan, D. E. Regulation of Band 3 Rotational Mobility by Ankyrin in Intact Human Red Cells. Biochemistry 37, 17828-17835, doi:10.1021/bi981825c (1998).

446 Mohamed, A. H. & Steck, T. L. Band 3 tyrosine kinase. Association with the human erythrocyte membrane. J Biol Chem 261, 2804-2809 (1986).

447 Langhorne, J., Quin, S. J. & Sanni, L. A. Mouse models of blood-stage malaria infections: immune responses and cytokines involved in protection and pathology. Chemical immunology 80, 204-228 (2002).

448 Stevenson, M. M. & Riley, E. M. Innate immunity to malaria. Nat Rev Immunol 4, 169-180 (2004).

449 Lu, Y. C., Yeh, W. C. & Ohashi, P. S. LPS/TLR4 signal transduction pathway. Cytokine 42, 145-151, doi:10.1016/j.cyto.2008.01.006 (2008).

450 Eber, S. & Lux, S. E. Hereditary spherocytosis--defects in proteins that connect the membrane skeleton to the lipid bilayer. Semin Hematol 41, 118-141 (2004).

451 Ruwende, C. & Hill, A. Glucose-6-phosphate dehydrogenase deficiency and malaria. Journal of molecular medicine (Berlin, Germany) 76, 581-588 (1998).

452 Mason, P. J., Bautista, J. M. & Gilsanz, F. G6PD deficiency: the genotype-phenotype association. Blood Rev. 21, doi:10.1016/j.blre.2007.05.002 (2007).

453 Manjurano, A. et al. African glucose-6-phosphate dehydrogenase alleles associated with protection from severe malaria in heterozygous females in Tanzania. PLoS Genet. 11, doi:10.1371/journal.pgen.1004960 (2015).

454 Sirugo, G. et al. G6PD A- deficiency and severe malaria in The Gambia: heterozygote advantage and possible homozygote disadvantage. Am J Trop Med Hyg. 90, doi:10.4269/ajtmh.13-0622 (2014).

455 Toure, O. et al. Candidate polymorphisms and severe malaria in a Malian population. PLoS One 7, e43987, doi:10.1371/journal.pone.0043987 (2012).

456 Martin, S. K. et al. Severe malaria and glucose-6-phosphate-dehydrogenase deficiency: a reappraisal of the malaria/G-6-P.D. hypothesis. Lancet. 1, doi:10.1016/s0140-6736(79)90946-2 (1979).

457 Zerhouni, F., Guetarni, D., Henni, T. & Colonna, P. Occurrence and characteristics of hereditary spherocytosis in Algeria. European journal of haematology 47, 42-47 (1991).

458 Kavallaris, M., Ng, D. & Byrne, F. Cytoskeleton and Human Disease. (Springer, 2012).

459 Shah, S. & Vega, R. Hereditary Spherocytosis. Pediatrics in Review 25, 168-172, doi:10.1542/pir.25-5-168 (2004).

460 A global network for investigating the genomic epidemiology of malaria. Nature 456, 732-737 (2008).

461 Miraglia del Giudice, E., Iolascon, A., Pinto, L., Nobili, B. & Perrotta, S. Erythrocyte membrane protein alterations underlying clinical heterogeneity in hereditary spherocytosis. Br J Haematol 88, 52-55 (1994).

462 Mohandas, N. & Gallagher, P. G. Red cell membrane: past, present, and future. Blood 112, 3939-3948, doi:10.1182/blood-2008-07-161166 (2008).

463 Mohandas, N. & Evans, E. Mechanical properties of the red cell membrane in relation to molecular structure and genetic defects. Annu Rev Biophys Biomol Struct 23, 787-818, doi:10.1146/annurev.bb.23.060194.004035 (1994).

464 Cowman, A. F. & Crabb, B. S. Invasion of red blood cells by malaria parasites. Cell 124, 755-766 (2006).

465 Ho, M. & White, N. J. Molecular mechanisms of cytoadherence in malaria. The American journal of physiology 276, C1231-1242 (1999).

466 Bennett, V. & Baines, A. J. Spectrin and Ankyrin-Based Pathways: Metazoan Inventions for Integrating Cells Into Tissues. Physiological reviews 81, 1353-1392 (2001).

467 Dhermy, D., Schrevel, J. & Lecomte, M. C. Spectrin-based skeleton in red blood cells and malaria. Curr Opin Hematol 14, 198-202, doi:10.1097/MOH.0b013e3280d21afd (2007).

468 Peters, L. & Lux, S. in Seminars in hematology. 85.

469 Davis, J. Q. & Bennett, V. The anion exchanger and Na+ K (+)-ATPase interact with distinct sites on ankyrin in in vitro assays. Journal of Biological Chemistry 265, 17252-17256 (1990).

470 Hall, T. & Bennett, V. Regulatory domains of erythrocyte ankyrin. Journal of Biological Chemistry 262, 10537-10545 (1987).

471 Bennett, V. Purification of an active proteolytic fragment of the membrane attachment site for human erythrocyte spectrin. Journal of Biological Chemistry 253, 2292-2299 (1978).

472 Yasunaga, M., Ipsaro, J. J. & Mondragón, A. Structurally similar but functionally diverse ZU5 domains in human erythrocyte ankyrin. Journal of molecular biology 417, 336-350, doi:10.1016/j.jmb.2012.01.041 (2012).

473 Mohler, P. J., Yoon, W. & Bennett, V. Ankyrin-B targets beta2-spectrin to an intracellular compartment in neonatal cardiomyocytes. J Biol Chem 279, 40185-40193, doi:10.1074/jbc.M406018200 (2004).

474 Delaunay, J. The molecular basis of hereditary red cell membrane disorders. Blood reviews 21, 1-20 (2007).

475 Nakashima, K. & Beutler, E. Erythrocyte cellular and membrane deformability in hereditary spherocytosis. Blood 53, 481-485 (1979).

476 Mullard, A. Protein–protein interaction inhibitors get into the groove. Nat Rev Drug Discov 11, 173-175 (2012).

477 Arkin, M. R., Tang, Y. & Wells, J. A. Small-molecule inhibitors of protein-protein interactions: progressing towards the reality. Chemistry & biology 21, 1102-1114, doi:10.1016/j.chembiol.2014.09.001 (2014).

478 Arkin, M. R. & Wells, J. A. Small-molecule inhibitors of protein-protein interactions: progressing towards the dream. Nat Rev Drug Discov 3, 301-317, doi:10.1038/nrd1343 (2004).

479 Lessene, G. et al. Structure-guided design of a selective BCL-X(L) inhibitor. Nature chemical biology 9, 390-397, doi:10.1038/nchembio.1246 (2013).

480 Tse, C. et al. ABT-263: a potent and orally bioavailable Bcl-2 family inhibitor. Cancer research 68, 3421-3428, doi:10.1158/0008-5472.can-07-5836 (2008).

481 Roberts, A. W. et al. Substantial susceptibility of chronic lymphocytic leukemia to BCL2 inhibition: results of a phase I study of navitoclax in patients with relapsed or refractory disease. Journal of clinical oncology : official journal of the American Society of Clinical Oncology 30, 488-496, doi:10.1200/jco.2011.34.7898 (2012).

482 Souers, A. J. et al. ABT-199, a potent and selective BCL-2 inhibitor, achieves antitumor activity while sparing platelets. Nat Med 19, 202-208, doi:10.1038/nm.3048 (2013).

483 Scott, D. E., Bayly, A. R., Abell, C. & Skidmore, J. Small molecules, big targets: drug discovery faces the protein-protein interaction challenge. Nat Rev Drug Discov 15, 533-550, doi:10.1038/nrd.2016.29 (2016).

484 Lopez, C., Saravia, C., Gomez, A., Hoebeke, J. & Patarroyo, M. A. Mechanisms of genetically-based resistance to malaria. Gene 467, 1-12, doi:10.1016/j.gene.2010.07.008 (2010).